Supporting information for

Phosphasalen group IV metal complexes: Synthesis, Characterisation and Ring Opening Polymerisation of Lactide

Adrien Normand,[a] Raluca Malacea-Kabbara,[a] Rosita Lapenta,[c] Aymeric Dajnak,[a]
Philippe Richard,[a] Hélène Cattey,[a] Anaëlle Bolley,[c] Alfonso Grassi,[d]
Stefano Milione,[d] Audrey Auffrant,*[b]Samuel Dagorne*[c] and Pierre Le Gendre*

[a]*Institut de Chimie Moléculaire de l'Université de Bourgogne (ICMUB), Université de Bourgogne Franche-Comté (UMR-CNRS 6302), 9, av. A. Savary, 21078 Dijon, France.*
[b]*Laboratoire de Chimie Moléculaire, CNRS UMR 9168, École Polytechnique, Institut Polytechnique de Paris, 91128 Palaiseau, France*
[c]*Institut de Chimie de Strasbourg (UMR-CNRS 7177), Université de Strasbourg*
[d]*Dipartimento di Chimica e Biologia, Universita degli Studi di Salerno, via Giovanni Paolo II, 132-84084 Fisciano (SA), Italy*

Contents

Ring nomenclature: the positions of carbon and hydrogen atoms in the aromatic rings were labelled according to Figure S1. Where applicable, the phenyl rings of the diphenylphosphino moiety are differentiated in chiral compounds (PPh^1, PPh^2).

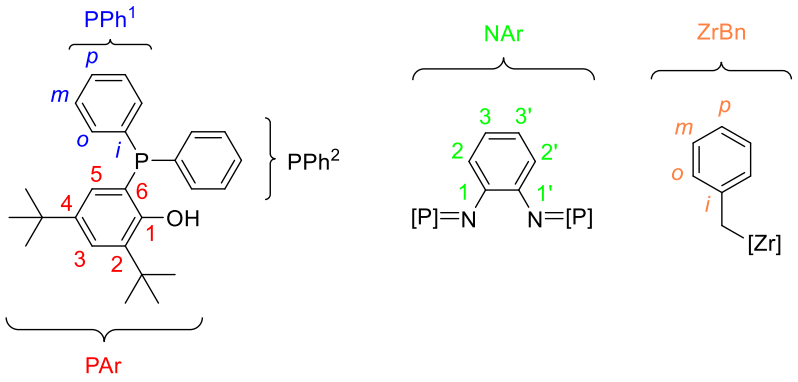

Figure S1

Synthesis of the proligand $1aH_2$

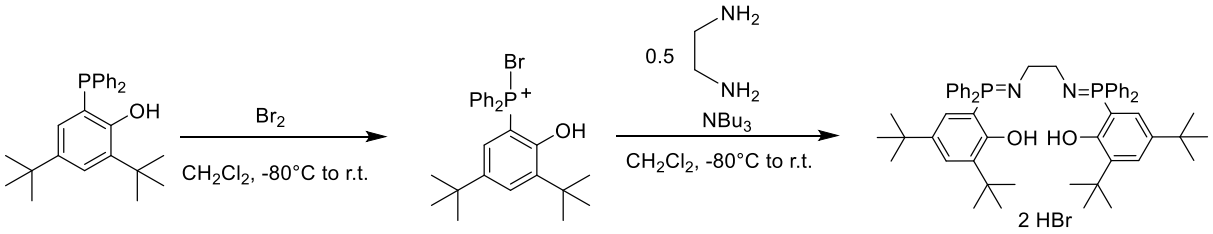

$1aH_2$.2HBr (4.57g, 65%)

2-(diphenylphosphino)-4,6-di(tert-butyl)phenol (5.249 g, 13.4 mmol) was dissolved in dichloromethane (200 mL) and cooled to -80°C under agitation. Bromine (0.69 mL, 13.4 mmol) was added to the solution and the mixture was stirred for 30 min at -80°C. Ethylenediamine (0.45 mL, 6.7 mmol) and tributylamine (3.16 mL, 13.4 mmol) were added by syringe. After 5 hrs reaction at -80°C, the mixture was filtered through a plug of diatomaceous earth, and the solid residue was washed with dichloromethane (3 x 100 mL). The volatiles were removed under vacuum. The yellow residue was suspended in THF (100 mL), and a white solid was filtered. After washing with THF (3 x 50 mL) and diethyl ether (50 mL), **1a.2HBr** was obtained as a white powder (4.57 g, 65%). The ^1H and $^{31}P\{^1H\}$ NMR spectra were identical to those of previously reported material.[1]

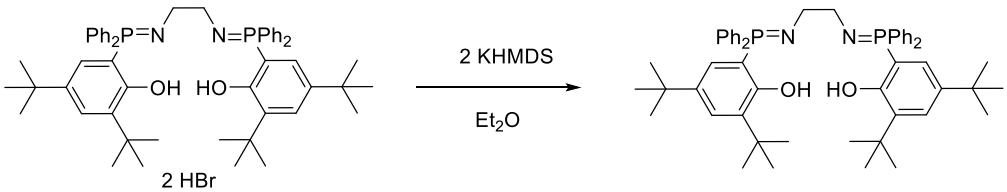

$1aH_2$.2HBr **$1aH_2$** *(2.415 g, 63%)*

1a.2HBr (4.57g, 4.6mmol) was suspended in diethyl ether (75 mL) and KHMDS (1.82 g, 9.16 mmol, 2 equiv) was dissolved separately in diethyl ether (75 mL). The KHMDS solution was added to **1a.2HBr** and the mixture was stirred at room temperature for 3 hrs. The reaction mixture was filtered through diatomaceous earth, and the solid residue was washed with diethyl ether (15 mL). The volatiles were

[1] T.-P.-A. Cao, A. Buchard, X. F. Le Goff, A. Auffrant and C. K. Williams, *Inorg. Chem.*, 2012, **51**, 2157-2169.

removed under vacuum, and the residue was suspended in pentane (100 mL) for 1h. After filtration, **1a** was obtained as a white powder containing 5 % of hexamethyldisilazane (2.415 g, 63% yield).

Elemental Analysis: calculated for $C_{54}H_{66}N_2O_2P_2$: C, 77.48; H, 7.95; N, 3.35. Found: C, 77.35; H, 7.80; N, 3.68.

^{1}H NMR (600 MHz, C_6D_6, 300 K): δ = 8.63 (s, 2H, OH), 7.75-7.70 (m, 10H, *o/m/p* of PPh_2 overlapping with *H*3 of PAr), 7.04-6.93 (m, 12H, *o/m/p* of PPh_2), 6.52 (d, $^3J_{PH}$ = 15.1 Hz, 2H, *H*5 of PAr), 3.22 (m, 4H, NCH_2), 1.78 (s, 18H, CH_3 of ^{t}Bu^2), 1.23 (s, 18H, CH_3 of ^{t}Bu^4).

^{13}C{^{1}H} NMR (150 MHz, C_6D_6, 300 K): δ = 174.7 (m, *C*1 of PAr), 140.9 (m, *C*2 of PAr), 133.1 (m, *o/m/p* of PPh_2), 131.7 (m, *o/m/p* of PPh_2 overlapping with *C*4 of PAr), 130.4 (s, *C*3 of PAr), ca 128.5 (m, *i*-PPh_2 overlapping with C_6D_6 signal), 128.4 (m, *C*5 of PAr overlapping with *o/m/p* of PPh_2), 100.5 (d, $^1J_{CP}$ = 109.4 Hz, *C*6 of PAr), 43.1 (s, CH_2 of NCH_2), 35.8 (s, *C* of ^{t}Bu^2), 34.2 (s, *C* of ^{t}Bu^4) 31.8 (s, CH_3 of ^{t}Bu^4), 29.7 (s, CH_3 of ^{t}Bu^2).

^{31}P{^{1}H} NMR (243 MHz, C_6D_6, 300 K): δ = 42.7 ($\nu_{1/2}$ = 9 Hz).

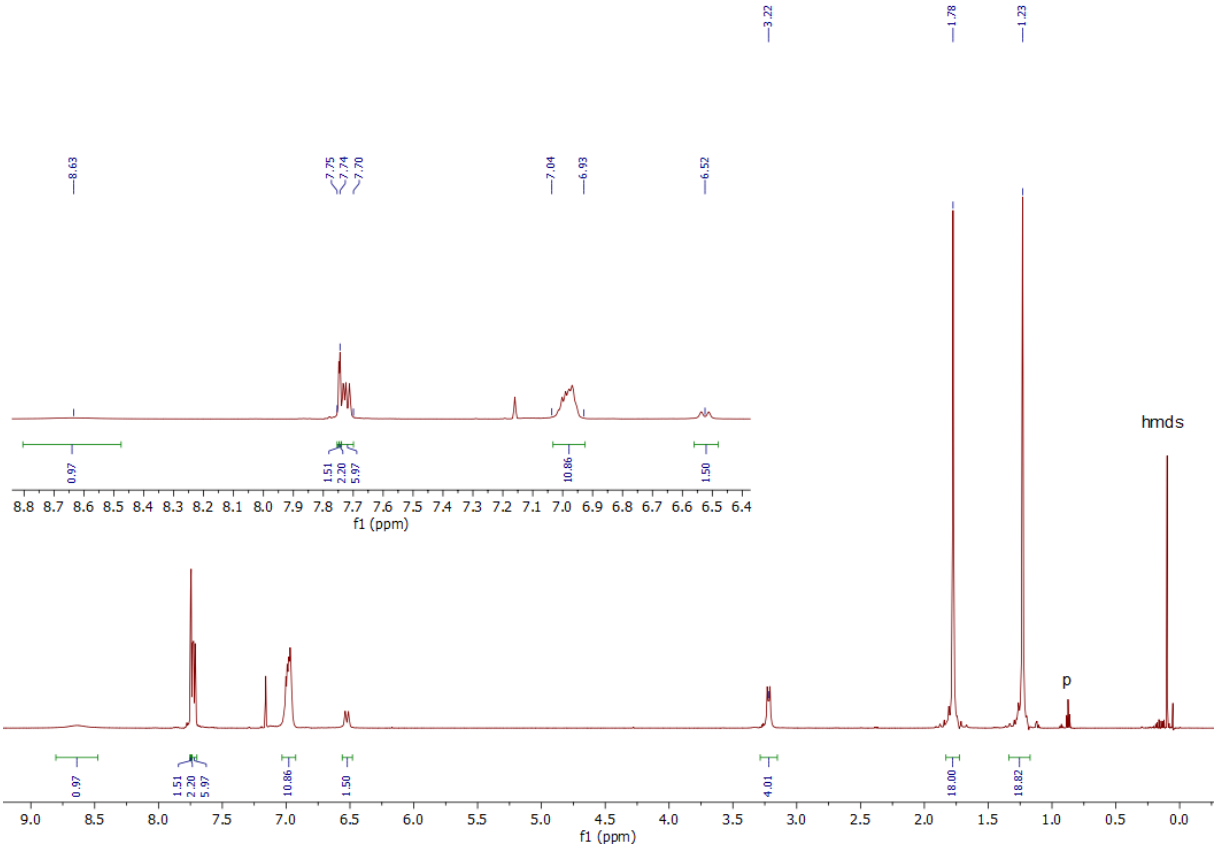

Figure S2: ^{1}H NMR (600 MHz, C_6D_6, 300 K)(p: pentane ; hmds: hexamethyldisilazane) of 1aH_2

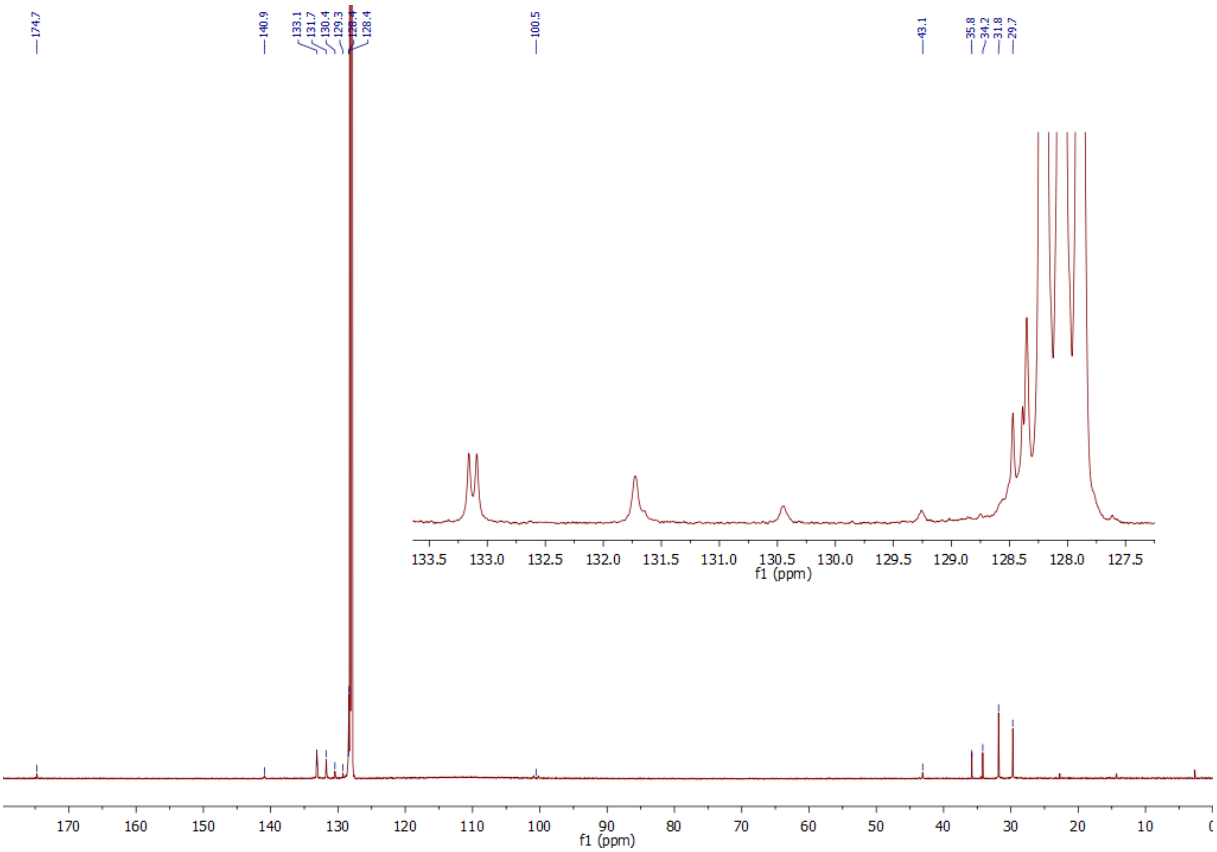

Figure S3: $^{13}C\{^{1}H\}$ NMR (150 MHz, C_6D_6, 300 K) of $1aH_2$

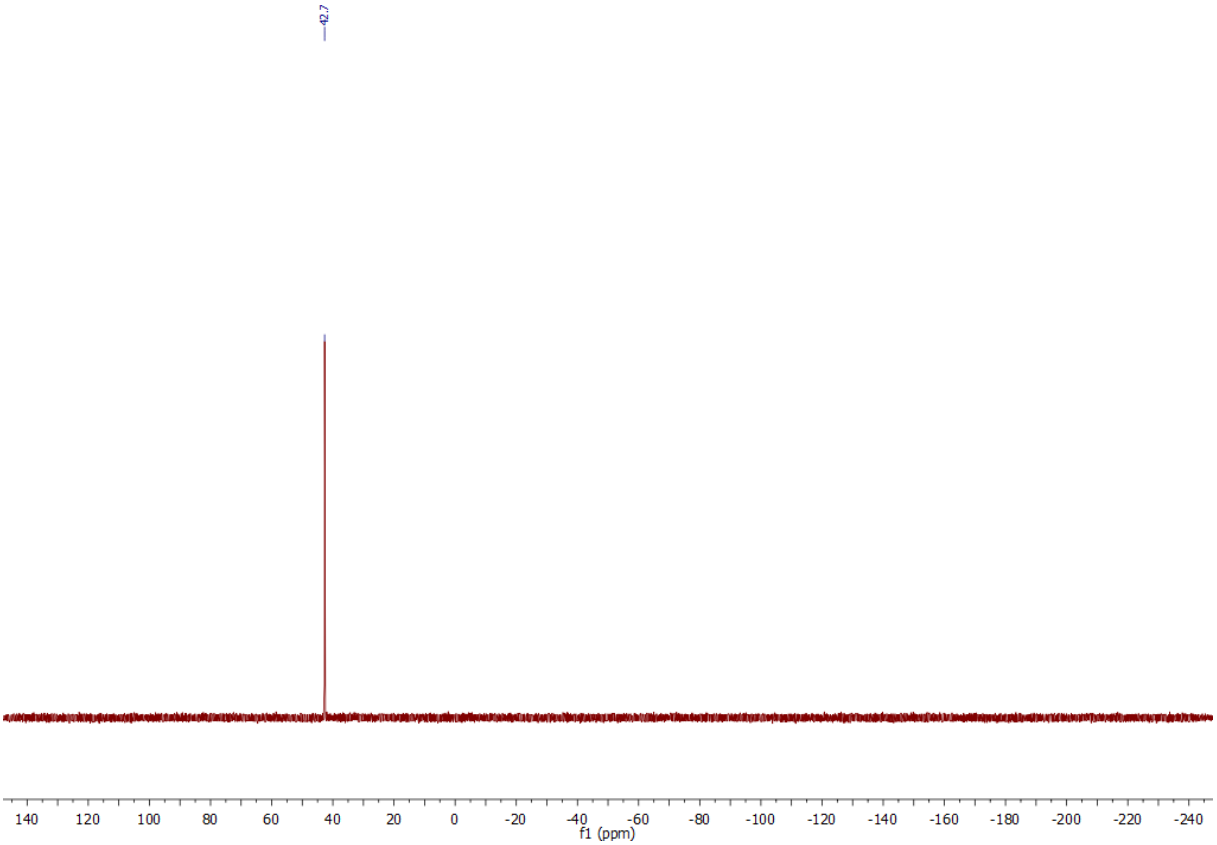

Figure S4: $^{31}P\{^{1}H\}$ NMR (243 MHz, C_6D_6, 300 K) of $1aH_2$

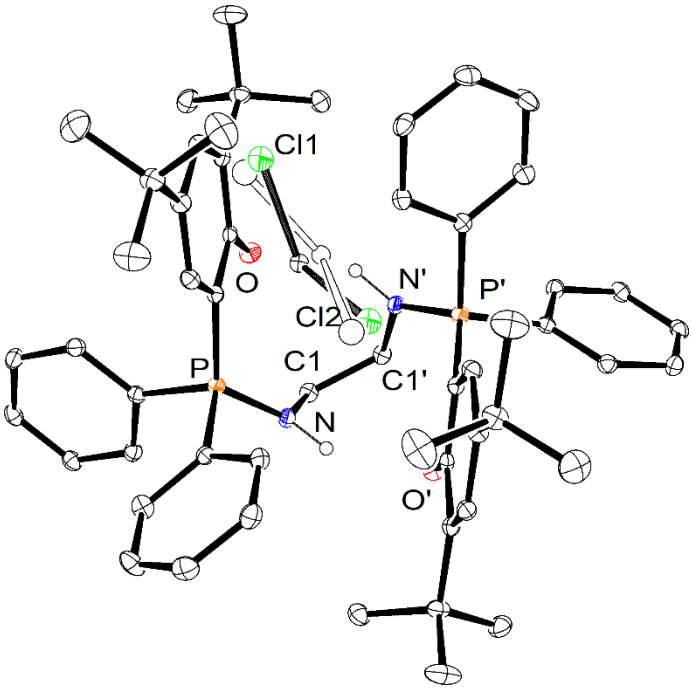

Figure S5: Crystal structure of $1aH_2$. Primed atoms :1-x, y, 1.5-z

Table S1: Crystal data and structure refinement of $1aH_2$

Identification code	1aH2
Internal reference	ral211116_0m
Moiety formula	$C_{54}H_{66}N_2O_2P_2$, 0.1(CH_2Cl_2)
Formula weight	845.52
Temperature/K	110
Crystal system	monoclinic
Space group	C2/c
a/Å	16.866(18)
b/Å	13.874(14)
c/Å	20.49(2)
α/°	90
β/°	92.56(3)
γ/°	90
Volume/Å^3	4790(9)
Z	4
ρ_{calc}g/cm^3	1.172
μ/mm^{-1}	0.144
F(000)	1817.0
Crystal size/mm^3	0.1 × 0.1 × 0.1
Radiation	MoKα (λ = 0.71073)
2Θ range for data collection/°	3.98 to 50
Index ranges	-20 ≤ h ≤ 20, -16 ≤ k ≤ 16, -15 ≤ l ≤ 24
Reflections collected	28200
Independent reflections	4189 [R_{int} = 0.1124, R_{sigma} = 0.0795]
Data/restraints/parameters	4189/0/285
Goodness-of-fit on F^2	1.009

Final R indexes [I>=2σ (I)]	R_1 = 0.0484, wR_2 = 0.0970
Final R indexes [all data]	R_1 = 0.1045, wR_2 = 0.1176
Largest diff. peak/hole / e Å^{-3}	0.27/-0.34
CCDC	1978293

Special refinement details for $1aH_2$

A disordered dichloromethane solvent molecule was localized close to a C2 symmetry axis. Despite a very partial occupation (m=0.1), this molecule was included in the model as a rigid group. The rather high value of R_{int} is mainly due to the low intensities observed at high theta angles.

Synthesis of the proligand $1bH_2$

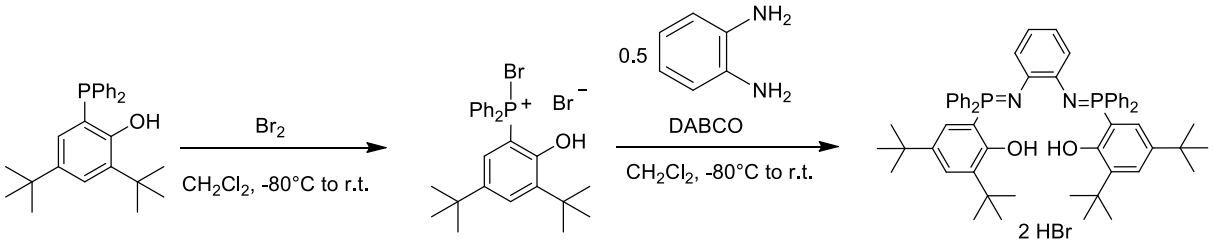

$1bH_2$.2HBr (5.3 g, 80%)

2-(diphenylphosphino)-4,6-di(tert-butyl)phenol (5 g, 12.82mmol) was dissolved in dichloromethane (200 mL) and cooled to -80°C under agitation. Bromine (0.66 mL, 12.82 mmol) was added to the solution and the mixture was stirred for 30 min at -80°C. After stirring another 30 min at room temperature, the solution cooled again at -80°C and DABCO (718 mg, 6.41 mmol) was added followed by a solution of phenylenediamine (692 mg, 6.41 mmol) in 20 mL of dichloromethane. The reaction was stirred 14 hrs at room temperature and then the solvent was removed to give a white precipitate. 100 mL of THF were added and the white suspension was filtered through a plug of diatomaceous earth, and the solid residue was washed with THF (3 x 10 mL). After removing the THF under vacuum, the residue was suspended in diethyl ether (100 mL) and further filtered to give **$1bH_2$.2HBr** as a white powder (5.3 g, 80%). The ^{1}H and ^{31}P{^{1}H} NMR spectra were identical to those of previously reported material.[2]

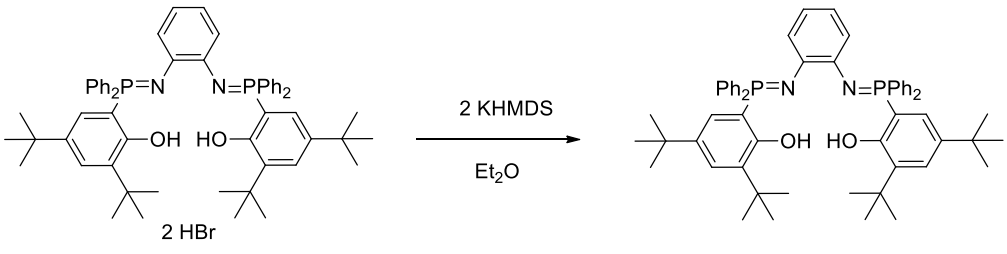

$1bH_2$.2HBr **$1bH_2$** *(1.2 g, 68%)*

$1bH_2$.2HBr (2.1 g, 2 mmol) was suspended in diethyl ether (25 mL) and KHMDS (400 mg, 4 mmol 2 equiv) was added. After stirring at room temperature for 14 hrs, the reaction mixture was filtered through diatomaceous earth and the solid residue was washed with diethyl ether (15 mL).

[2] C. Bakewell, T.-P.-A. Cao, X. F. Le Goff, N. J. Long, A. Auffrant and C. K. Williams, *Organometallics*, 2013, **32**, 1475-1483.

Dichloromethane (30 mL) was added on the remaining solid and further filtrate. After removing the dichloromethane under vacuum, **1bH₂** was obtained as a yellow powder (1.2 g, 68% yield).

NMR characterisation and EA of **1bH₂** have been performed on a sample prepared according to the following procedure which does not require the use of KHMDS in the last step (The ^{1}H and $^{31}P\{^{1}H\}$ NMR spectra of the compounds prepared according to one or the other procedures are identical).

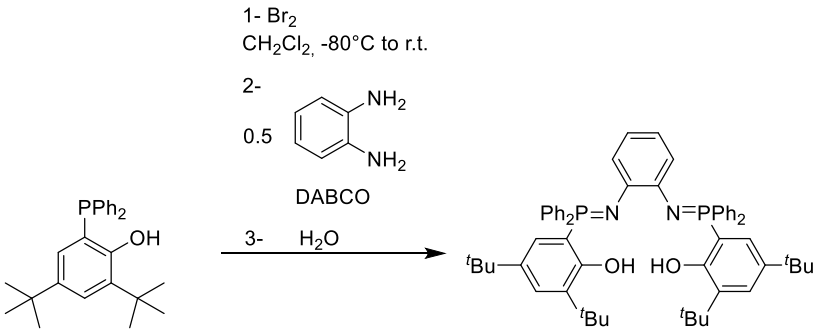

1bH₂ *(3.63 g, 53%)*

2, 4-Di-*tert*-butyl-6-(diphenylphosphino) phenol (7.85 g, 20.1 mmol) was dissolved in dichloromethane (250 mL) and cooled to -80 °C under agitation. Bromine (1.07 mL, 20.1 mmol) was added to the solution and the reaction mixture was stirred for 2h30 at -80 °C. A dichloromethane solution (40 mL) of DABCO and *o*-phenylenediamine was then added to the reaction mixture. The resulting mixture was stirred for 18 hrs, during which it warmed up to room temperature. The reaction mixture was filtered and the filtrate was washed with water (5 x 200 mL) until the aqueous phase reached pH = 4. The combined aqueous phases were extracted with dichloromethane (200 mL). Toluene (100 mL) was added to the combined organic phases and the volatiles were evaporated with a rotary evaporator. A brown powder was obtained, which was further freed from water by azeotropic distillation with 2 x 50 mL of toluene. The crude product was suspended in diethyl ether (25 mL), filtered and washed with diethyl ether (3 x 25 mL) and dried under vacuum to give ligand **1b** as a yellow powder (3.63 g, 53 % yield).

Elemental Analysis: calculated for $C_{58}H_{66}N_2O_2P_2$: C, 78.70; H, 7.52; N, 3.16. Found: C, 78.79; H, 7.42; N, 3.03.

^{1}H NMR (500 MHz, C_6D_6, 300 K): δ = 15.78 (bs, 2H, O*H*), 7.93 (m, 8H, *o* of PPh_2), 7.56 (s, 2H, *H*3 of PAr), 7.13 (dd, $^{3}J_{PH}$ = 16.6 Hz, $^{4}J_{HH}$ = 2.4 Hz, 2H, *H*5 of PAr overlapping with NMR solvent residual protic signal), 7.03-6.96 (m, 10H, *m* and *p* of PPh_2), 6.82 (m, 2H, *H*2 of NAr), 6.64 (m, 2H, *H*3 of NAr), 1.45 (s, 18H, CH_3 of $^{t}Bu^{2}$), 1.17 (s, 18H, CH_3 of $^{t}Bu^{4}$).

$^{13}C\{^{1}H\}$ NMR (126 MHz, C_6D_6, 300 K): δ = 163.6 (s, *C*1 of PAr), 142.8 (dd, $^{3}J_{CP}$ = 17.3 Hz, $^{2}J_{CP}$ = 3.4 Hz *C*1 of NAr), 138.2-138.1 (m, overlapping *C*2/*C*4 of PAr), 133.1 (d, $^{2}J_{CP}$ = 10.0 Hz, *o* of PPh_2), 132.2 (d, $^{1}J_{CP}$ = 82.3 Hz, *i* of PPh_2), 131.4 (s, *p* of PPh_2), 128.4 (d, $^{3}J_{CP}$ = 11.7 Hz, *m* of PPh_2), 127.8 (s, *p* of PAr overlapping with C_6D_6 signal, visible in DEPT 90), 126.1 (d, $^{2}J_{CP}$ = 13.8 Hz, *C*5 of PAr), 121.7 (d, $^{3}J_{CP}$ = 8.2 Hz, *C*2 of NAr), 119.8 (s, *C*3 of NAr), 106.7 (d, $^{1}J_{CP}$ = 128.1 Hz, *C*6 of PAr), 35.4 (s, *C* of $^{t}Bu^{2}$), 34.0 (s, *C* of $^{t}Bu^{4}$), 31.3 (s, *C*H_3 of $^{t}Bu^{4}$), 29.7 (s, *C*H_3 of $^{t}Bu^{2}$).

$^{31}P\{^{1}H\}$ NMR (202 MHz, C_6D_6, 300 K): δ = 18.1 ($\nu_{1/2}$ ≈ 6 Hz).

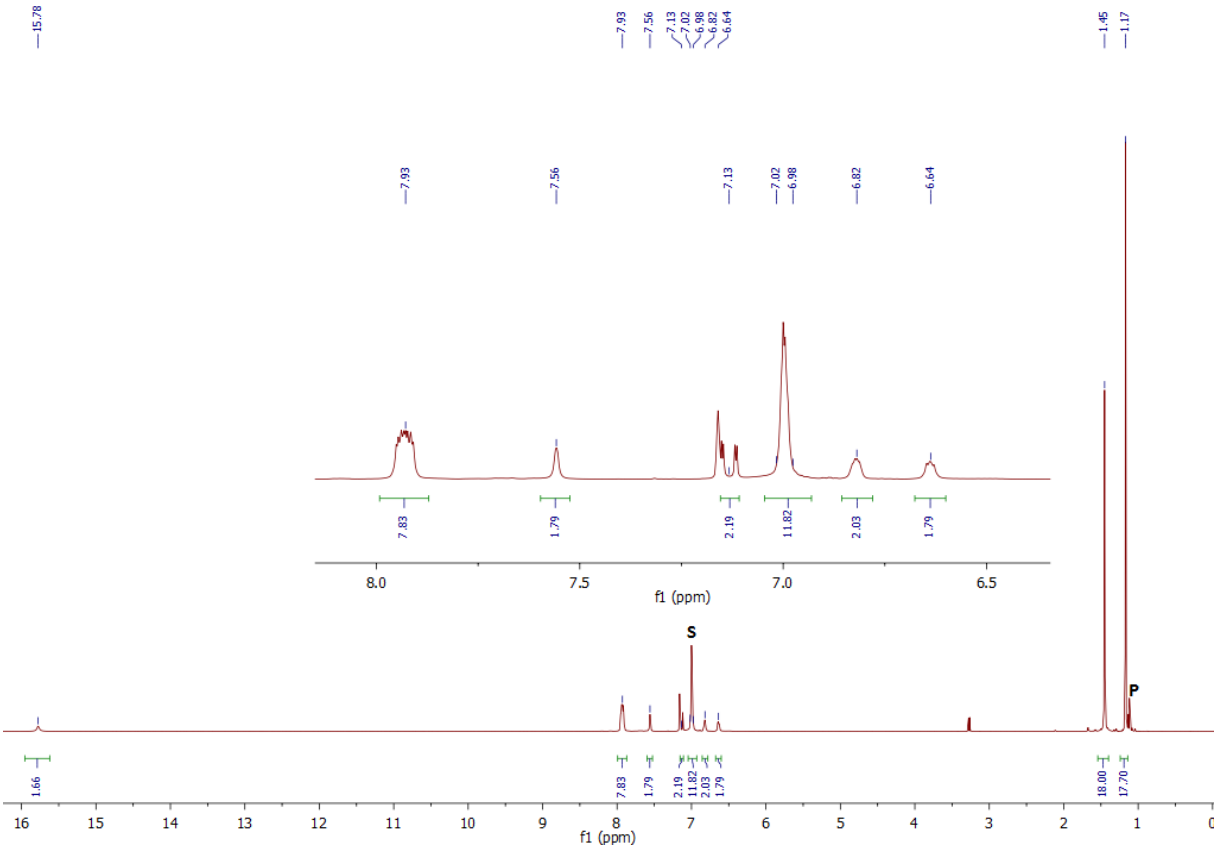

Figure S6: ^{1}H NMR (500 MHz, C_6D_6, 300 K)(p: pentane; s: solvent) of 1bH_2

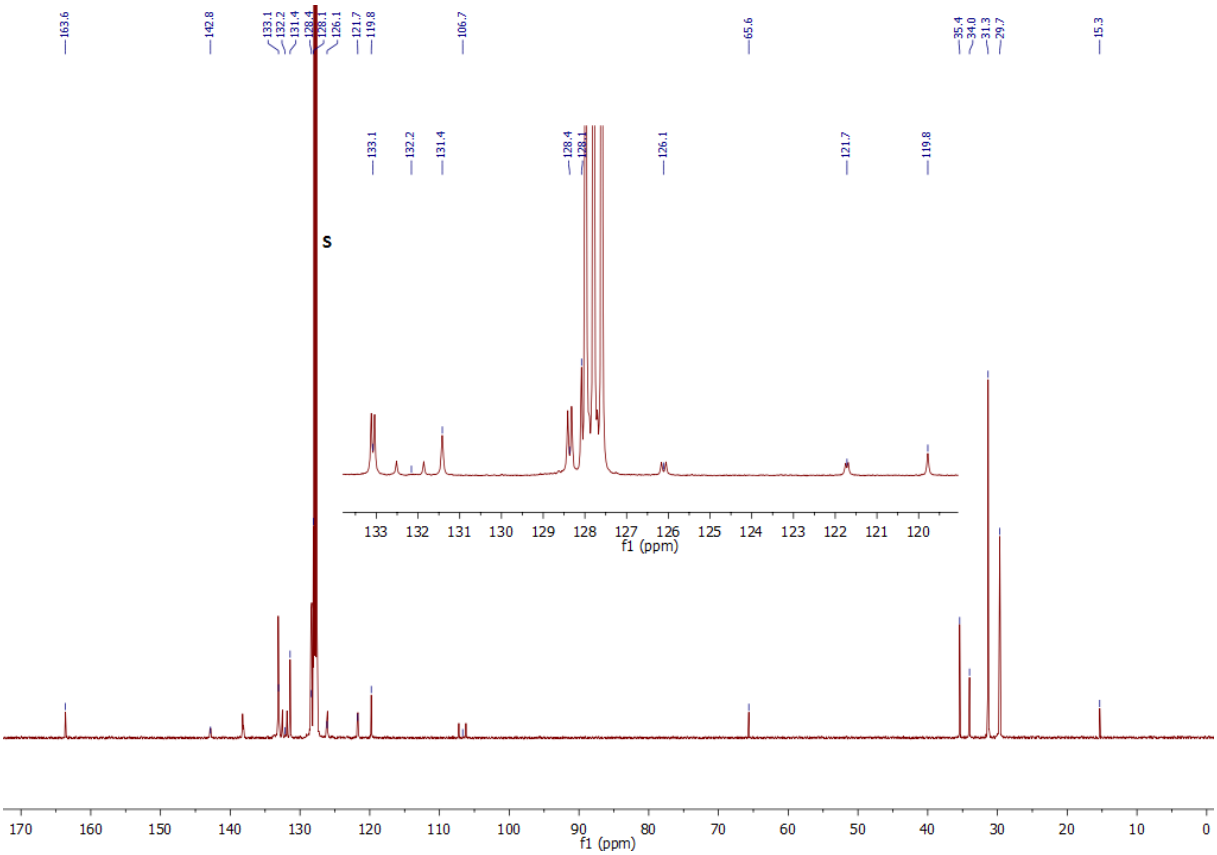

Figure S7: $^{13}C\{^{1}H\}$ NMR (126 MHz, C_6D_6, 300 K)(s: solvent) of 1bH_2

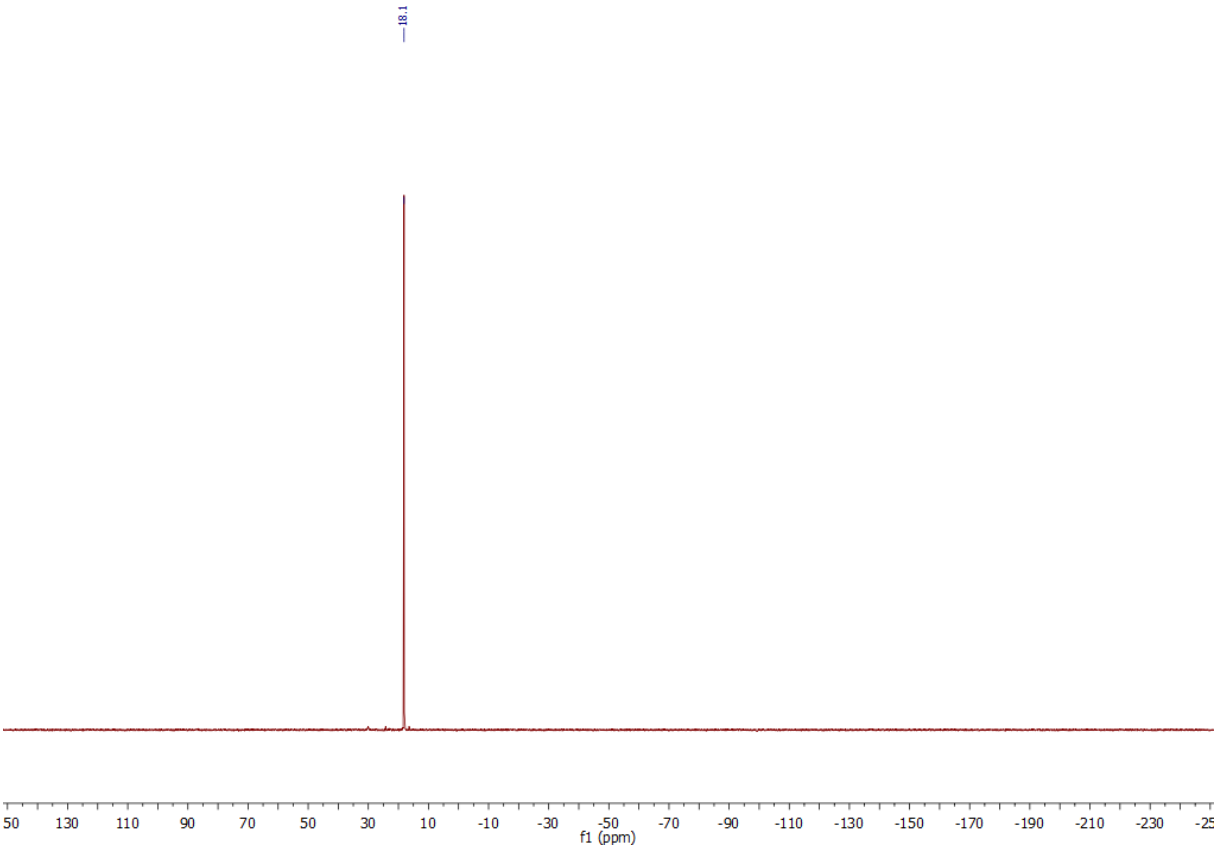

Figure S8: $^{31}P\{^{1}H\}$ NMR (202 MHz, C_6D_6, 300 K) of $1bH_2$

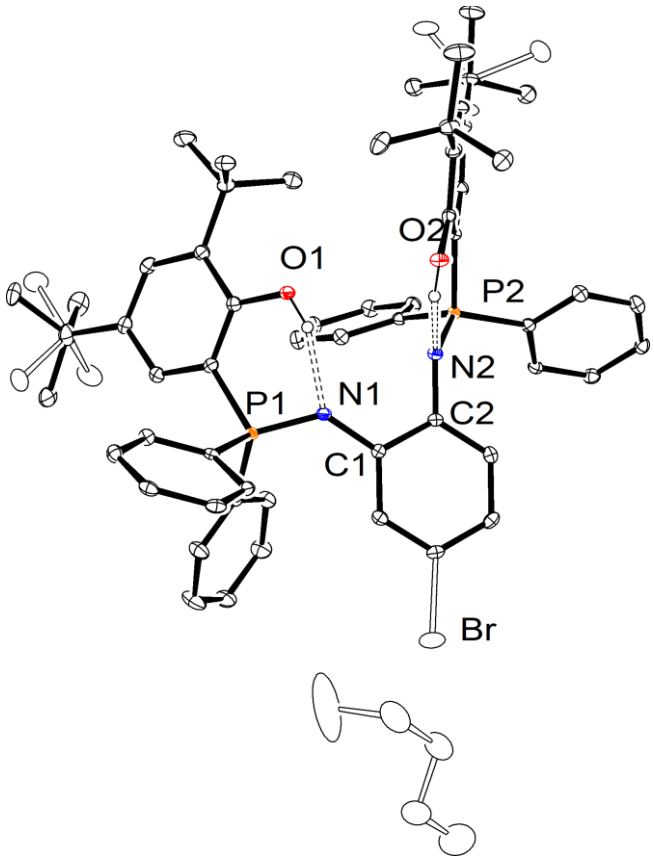

Figure S9: Crystal structure of $1bH_2$

Table S2: Crystal data and structure refinement of $1bH_2$

Identification code	1bH2
Internal reference	Cu_ral181016_0m
Empirical formula	$C_{62.79}H_{77.45}Br_{0.04}N_2O_2P_2$
Formula weight	957.33
Temperature/K	100
Crystal system	triclinic
Space group	P-1
a/Å	9.6276(3)
b/Å	15.3921(5)
c/Å	19.3866(6)
α/°	73.0290(15)
β/°	82.9270(15)
γ/°	88.8730(16)
Volume/Å^3	2726.46(15)
Z	2
ρ_{calc}g/cm^3	1.166
μ/mm^{-1}	1.092
F(000)	1031.0
Crystal size/mm^3	0.37 × 0.05 × 0.05
Radiation	CuKα (λ = 1.54178)
2Θ range for data collection/°	4.802 to 133.562
Index ranges	-11 ≤ h ≤ 11, -18 ≤ k ≤ 18, -22 ≤ l ≤ 22
Reflections collected	25461
Independent reflections	9579 [R_{int} = 0.0418, R_{sigma} = 0.0467]
Data/restraints/parameters	9579/28/710
Goodness-of-fit on F^2	1.041
Final R indexes [I>=2σ (I)]	R_1 = 0.0553, wR_2 = 0.1364
Final R indexes [all data]	R_1 = 0.0718, wR_2 = 0.1467
Largest diff. peak/hole / e Å^{-3}	1.97/-0.62
CCDC	1978292

Special refinement details for $1bH_2$

Two tert-butyl groups were found disordered. Each was anisotropically refined on two positions with occupation factors converging to 0.543/0.457 and 0.835/0.165. During the refinement a rather strong residual density was found close to the aromatic spacer. This density was successfully modeled by a bromine atom with an occupation factor of m = 0.042. This is consistent with the use of a brominated precursor for this ligand. A pentane solvent molecule is present in the asymmetric unit. Being too close to the bromine atom its multiplicity has been fixed to the 1-m value.

Synthesis of ligand $1cH_2$

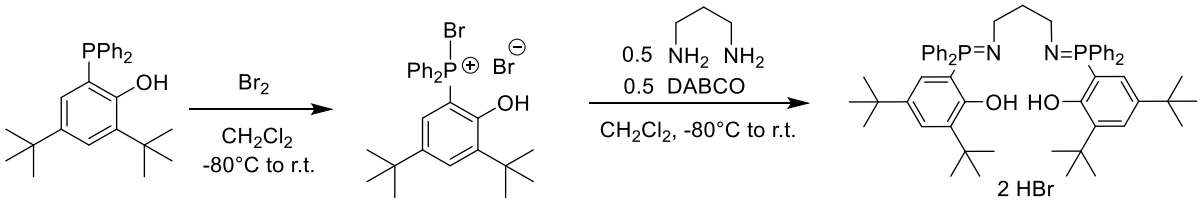

$1cH_2$.2HBr (3.8g, 59%)

2,4-Di-*tert*-butyl-6-(diphenylphosphino)phenol (5 g, 12.8 mmol) was dissolved in dichloromethane (200 mL) and cooled to -80°C under agitation. Bromine (0.66 mL, 12.8 mmol) was added to the solution and the mixture was stirred for 30 min at -80°C. Diazabicyclooctane (712 mg, 6.4 mmol) and 1,3-diaminopropane (0.53 mL, 6.4 mmol) in 20 mL dichloromethane were added at -80°C and the reaction mixture was allowed to reach r.t. and then stirred for 16 h. After removing the dichloromethane under vaccum, 100 mL of THF were added and the mixture filtered to remove the solid DABCO.2HBr. After removing the THF under vaccum, the residue was suspended in diethyl ether (100 mL) and a white solid was filtered. After washing with diethyl ether (50 mL), **$1cH_2$.2HBr** was obtained as a white powder (3.8 g, 59%). The ^{1}H and $^{31}P\{^{1}H\}$ NMR spectra were identical to those of previously reported material.[2]

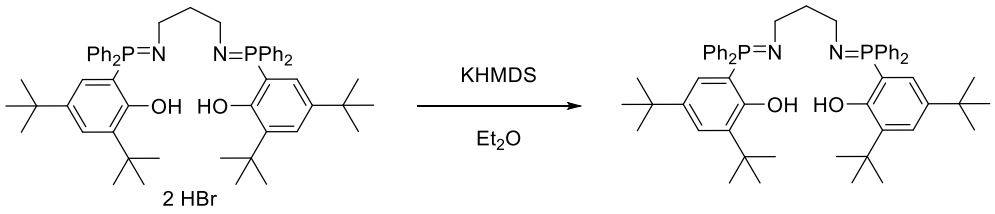

$1cH_2$.2HBr **$1cH_2$** *(2.68 g, 89%)*

$1cH_2$.2HBr (3.05 g, 3 mmol) was suspended in diethyl ether (150 mL) and KHMDS (1.2 g, 6 mmol) was dissolved separately in diethyl ether (40 mL). The KHMDS solution was added to **$1cH_2$.2HBr** and the mixture was stirred at room temperature for 2 h. The reaction mixture was filtered through diatomaceous earth, and the solid residue was washed with diethyl ether (15 mL). The volatiles were removed under vacuum, and the residue was suspended in pentane (100 mL) for 1 h. After filtration, **$1cH_2$** was obtained as a white powder (2.68 g, 89% yield).

^{1}H NMR (500 MHz, CD_2Cl_2, 300 K): δ= 9.13 (s, 2H, OH), 7.66-7.58 (m, 8H, *o*/*m* of PPh_2), 7.57-6.51 (m, 4H, *p* of PPh_2), 7.45-7.38 (m, 8H, *m*/*o* of PPh_2), 7.34 (d, $^{4}J_{HH}$= 2.55 Hz, 2H, *H3* of PAr), 6.39 (dd, $^{3}J_{HP}$= 15.57, $^{4}J_{HH}$= 2.55 Hz, 2H, *H5* of PAr), 3.02 (m, 4H, NCH_2), 1.69 (quint, $^{3}J_{HH}$= 6.47 Hz, 2H, NCH_2CH_2), 1.40 (s, 18H, ^{t}Bu), 1.09 (s, 18H, ^{t}Bu).

^{13}C NMR (125.7 MHz, CD_2Cl_2, 300 K): δ= 174.3 (d, $^{2}J_{CP}$= 4.3 Hz, *C*1 of PAr), 141.0 (d, $^{3}J_{CP}$= 9.3 Hz, *C*2 of PAr), 133.7 (d, J_{CP}= 10.5 Hz, *o*/*m* of PPh_2), 133.3 (s, *p* of PPh_2), 132.3 (d, $^{3}J_{CP}$= 15.4 Hz, *C*4 of PAr), 130.1 (s, *C*3 of PAr), 129.6 (d, J_{CP}= 12.1 Hz, *m*/*o* of PPh_2), 127.4 (d, $^{1}J_{CP}$= 97.1 Hz, *C*i of PPh_2), 126.8 (d, $^{2}J_{CP}$= 14.1 Hz, C5 of PAr), 100.4 (d, $^{1}J_{CP}$= 112.7 Hz, *C*6 of PAr), 41.6 (s, CH_2 of NCH_2), 35.9 (s, *C* of ^{t}Bu), 34.5 (s, *C* of ^{t}Bu), 33.8 (m, CH_2 of NCH_2-CH_2), 31.9 (s, CH_3 of ^{t}Bu), 29.7 (s, CH_3 of ^{t}Bu).

$^{31}P\{^{1}H\}$ NMR (202.4MHz, CD_2Cl_2, 300 K): δ= 39.4 ($\nu_{1/2}$= 4 Hz)

HR/MS : calculated 851.48288 $[M+H]^+$; measured (ESI) 851.48055 (Δ= 2.735 ppm)

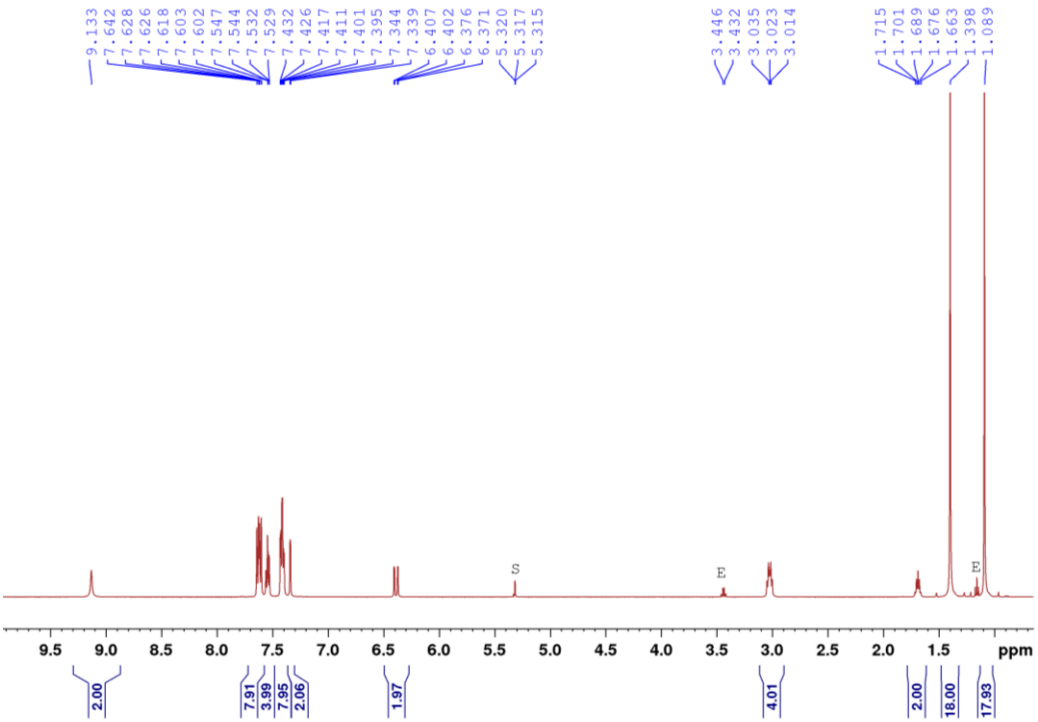

Figure S10: ^{1}H NMR (500 MHz, CD_2Cl_2, 300 K) (E: diethylether) of 1cH_2

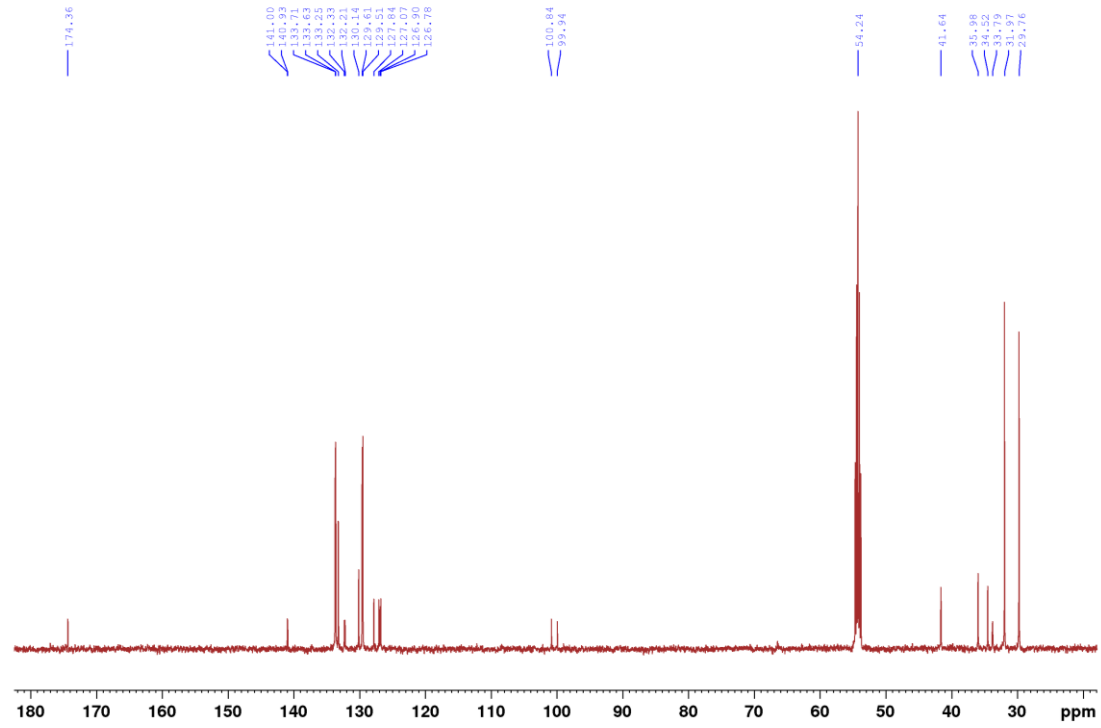

Figure S11: $^{13}C\{^{1}H\}$ NMR (125.7 MHz, CD_2Cl_2, 300 K) of 1cH_2

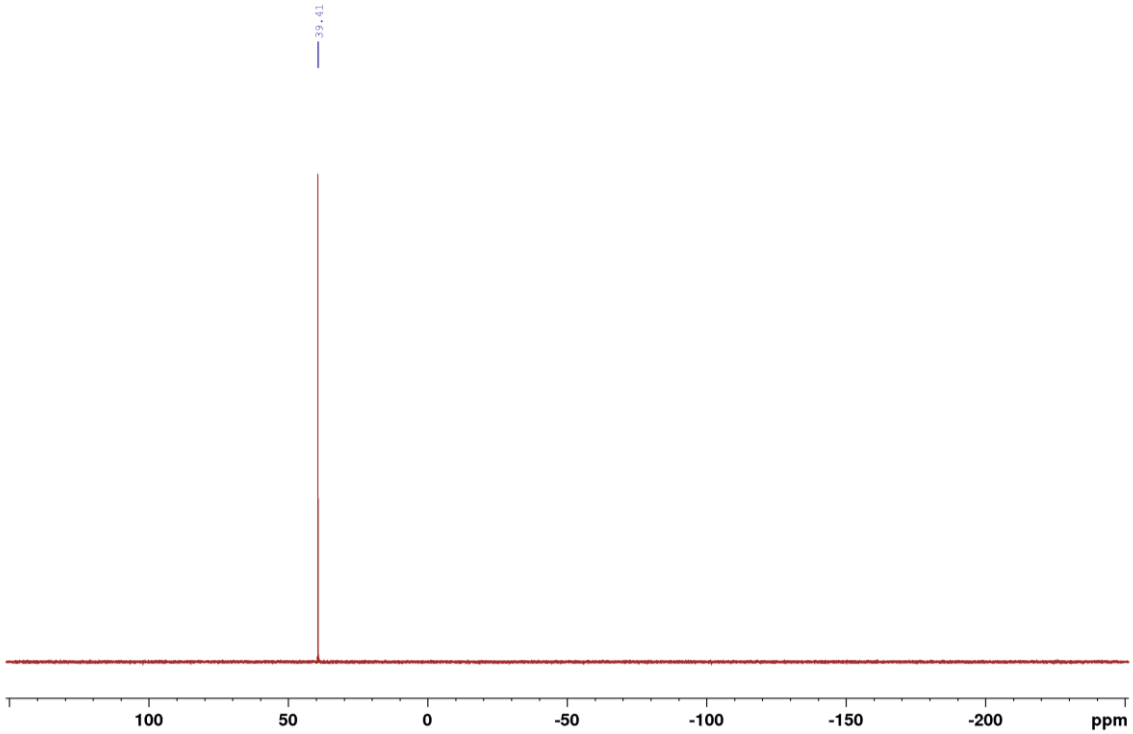

Figure S12: $^{31}P\{^{1}H\}$ NMR (202.4MHz, CD_2Cl_2, 300 K) of $1cH_2$

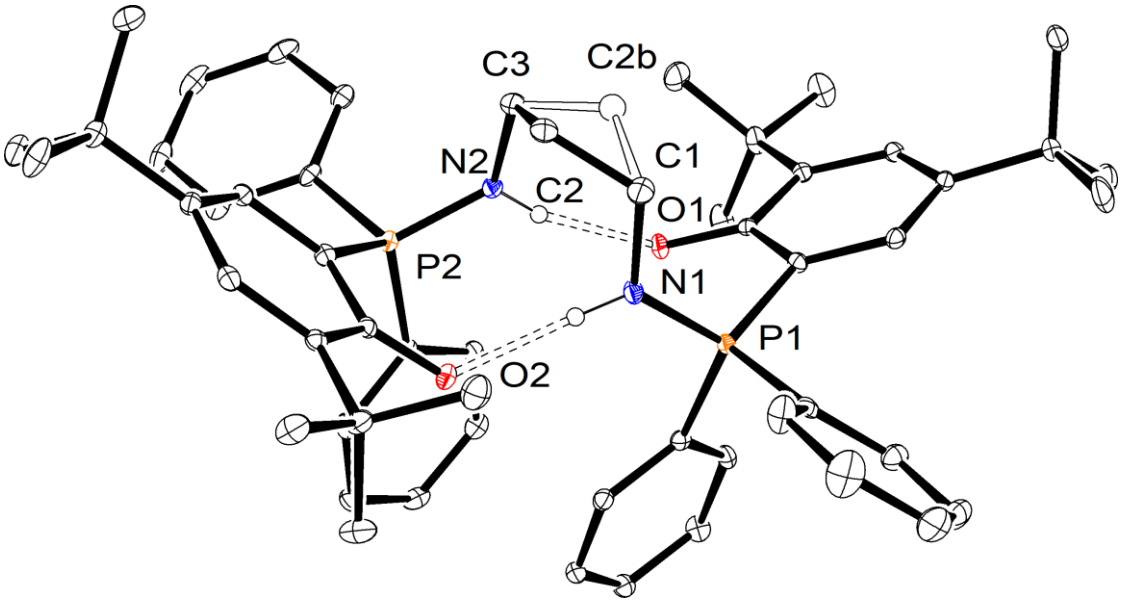

Figure S13: Crystal structure of $1cH_2$

Table S3: Crystal data and structure refinement of $1cH_2$

Identification code	1cH2
Internal reference	ral140917_0m
Empirical formula	$C_{55}H_{68}N_2O_2P_2$
Formula weight	851.05
Temperature/K	115
Crystal system	orthorhombic
Space group	$P2_12_12_1$
a/Å	9.7379(4)
b/Å	18.0542(8)
c/Å	28.0036(19)
α/°	90
β/°	90
γ/°	90
Volume/Å^3	4923.3(4)
Z	4
ρ_{calc}g/cm^3	1.148
μ/mm^{-1}	0.130
F(000)	1832.0
Crystal size/mm^3	0.27 × 0.22 × 0.08
Radiation	MoKα (λ = 0.71073)
2Θ range for data collection/°	4.428 to 55.134
Index ranges	-7 ≤ h ≤ 12, -13 ≤ k ≤ 23, -35 ≤ l ≤ 36
Reflections collected	22819
Independent reflections	11079 [R_{int} = 0.0319, R_{sigma} = 0.0562]
Data/restraints/parameters	11079/0/573
Goodness-of-fit on F^2	1.031
Final R indexes [I>=2σ (I)]	R_1 = 0.0395, wR_2 = 0.0807
Final R indexes [all data]	R_1 = 0.0499, wR_2 = 0.0851
Largest diff. peak/hole / e Å^{-3}	0.29/-0.26
Flack parameter	0.06(3)
CCDC	1978291

Special refinement details for $1cH_2$

The central carbon atom of the propylene spacer was found to be slightly disordered over two positions. The minor component was isotropically refined and the occupation factors converged to 0.75/0.25.

Complex 2a:

^{1}H-^{1}H COSY (500 MHz, C_6D_6, 300 K)[selected cross-peaks]: 7.30-7.22 / 7.12-7.07 (*o* of PPh_2 / *m* of PPh_2), 6.74 / 6.56 (*m* of ZrBn / *p* of ZrBn), 6.74 / 6.13 (*m* of ZrBn / *o* of ZrBn).

^{1}H-^{13}C HMBC (500 MHz / 126 MHz, C_6D_6, 300 K)[selected cross-peaks]: 7.82 / 166.5 (*H*3 of PAr / *C*1 of PAr), 7.82 / 127.7 (*H*3 of PAr / *C*5 of PAr), 7.82 / 36.2 (*H*3 of Par / *C* of $^{t}Bu^{2}$), 7.82 / 34.3 (*H*3 of PAr / *C* of $^{t}Bu^{4}$), 7.30-7.22 / 132.3 (*o* of PPh_2 / *p* of PPh_2), 7.30-7.22 / 129.1 (*o* of PPh_2 / *m* of PPh_2), 7.12-7.07 / 133.8 (*m* and/or *p* of PPh_2 / *o* of PPh_2), 7.12-7.07 / 129.1 (*m* and/or *p* of PPh_2 / *m* of PPh_2), 6.74 / 155.9 (*m* of ZrBn / *i* of ZrBn), 6.65 / 166.5 (*H*5 of PAr / *C*1 of PAr), 6.65 / 129.8 (*H*5 of PAr / *C*3 of PAr), 6.74 / 34.3 (*H*5 of PAr / *C* of $^{t}Bu^{4}$), 6.56 / 125.5 (*p* of ZrBn / *o* of ZrBn), 6.13 / 116.7 (*o* of ZrBn / *p* of ZrBn), 6.13 / 59.8 (*o* of ZrBn / CH_2 of ZrBn), 2.36 / 155.9 (CH_2 of ZrBn / *i* of ZrBn), 2.36 / 125.5 (CH_2 of ZrBn / *o* of ZrBn), 1.96 / 138.9 (CH_3 of $^{t}Bu^{2}$ / *C*2 of PAr), 1.96 / 36.2 (CH_3 of $^{t}Bu^{2}$ / *C* of $^{t}Bu^{2}$), 1.96 / 30.9 (CH_3 of $^{t}Bu^{2}$ / CH_3 of $^{t}Bu^{2}$), 1.13 / 138.4 (CH_3 of $^{t}Bu^{4}$ / *C*4 of PAr).

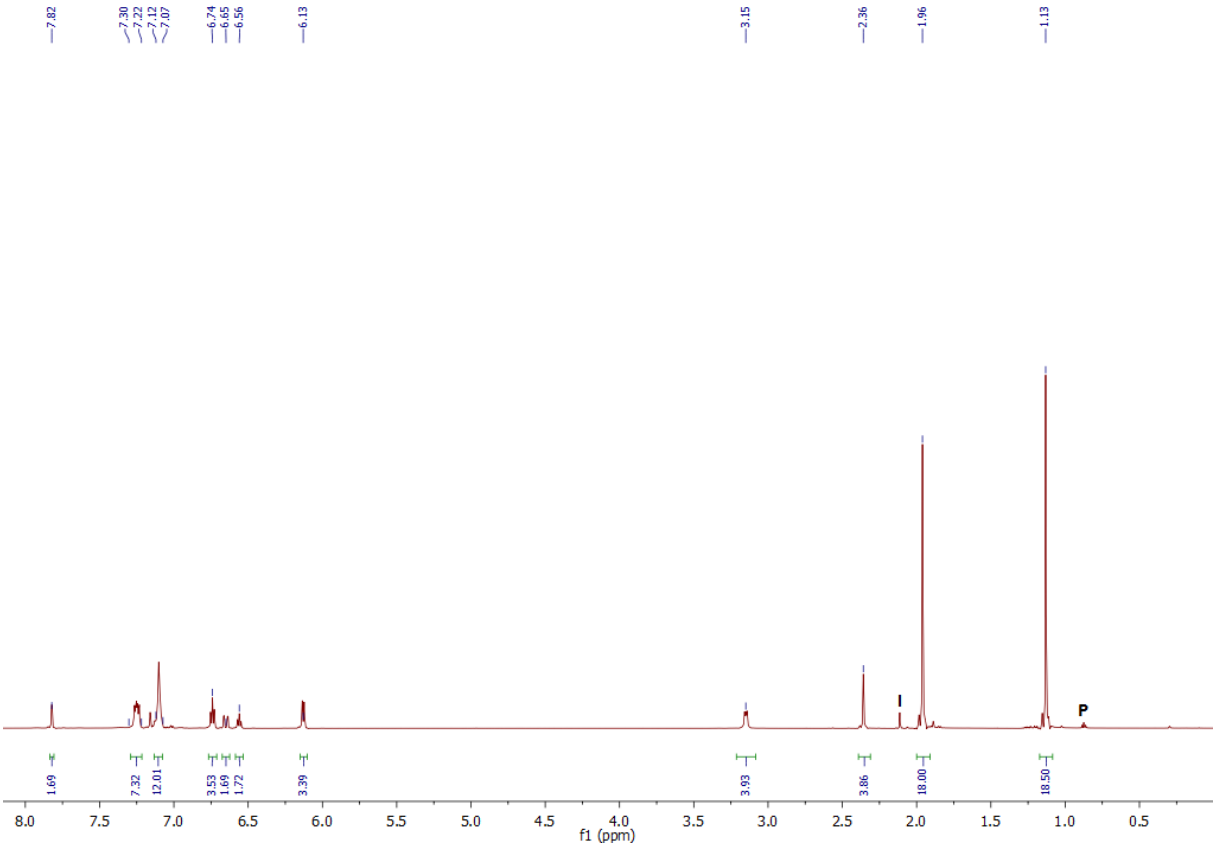

Figure S14: ^{1}H NMR (500 MHz, C_6D_6, 300 K)(i: impurity; p: pentane) of 2a

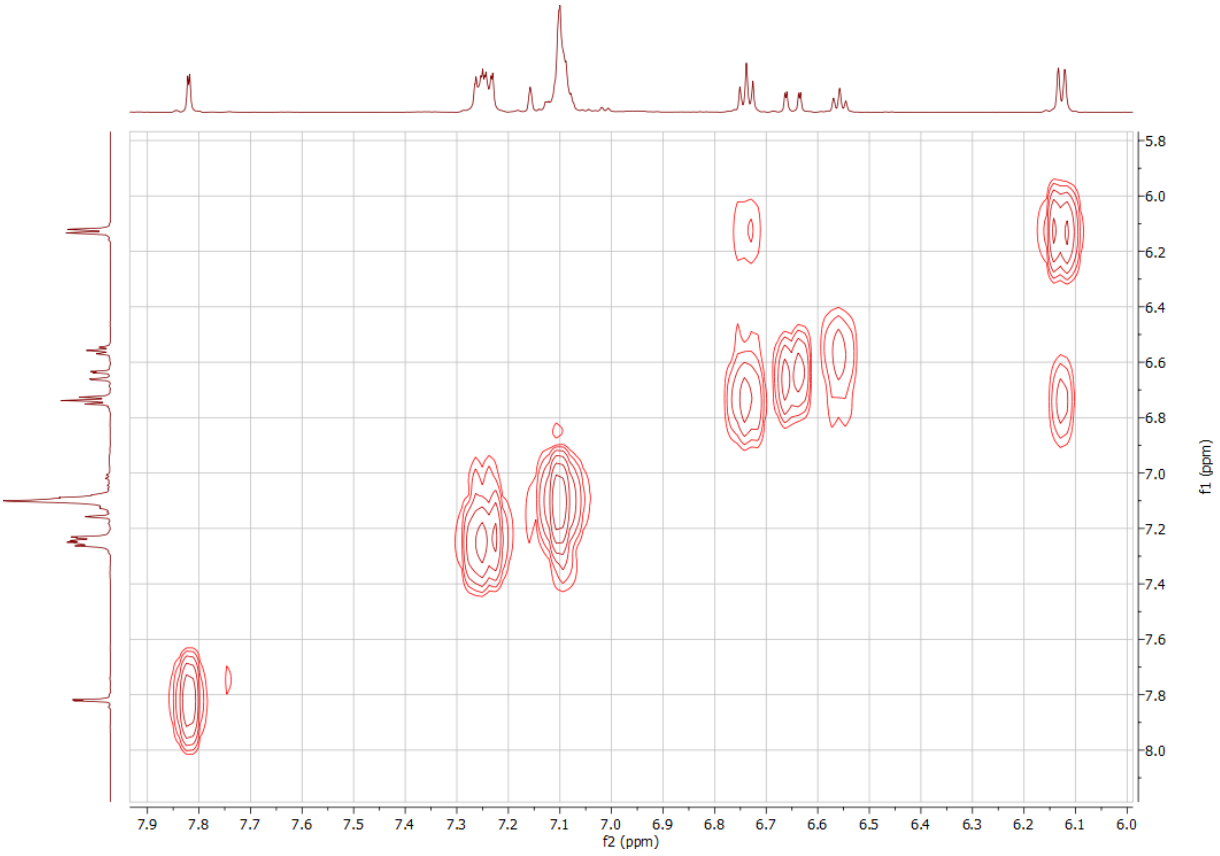

Figure S15: ^{1}H-^{1}H COSY (126 MHz, C_6D_6, 300 K)(aromatic region) of 2a

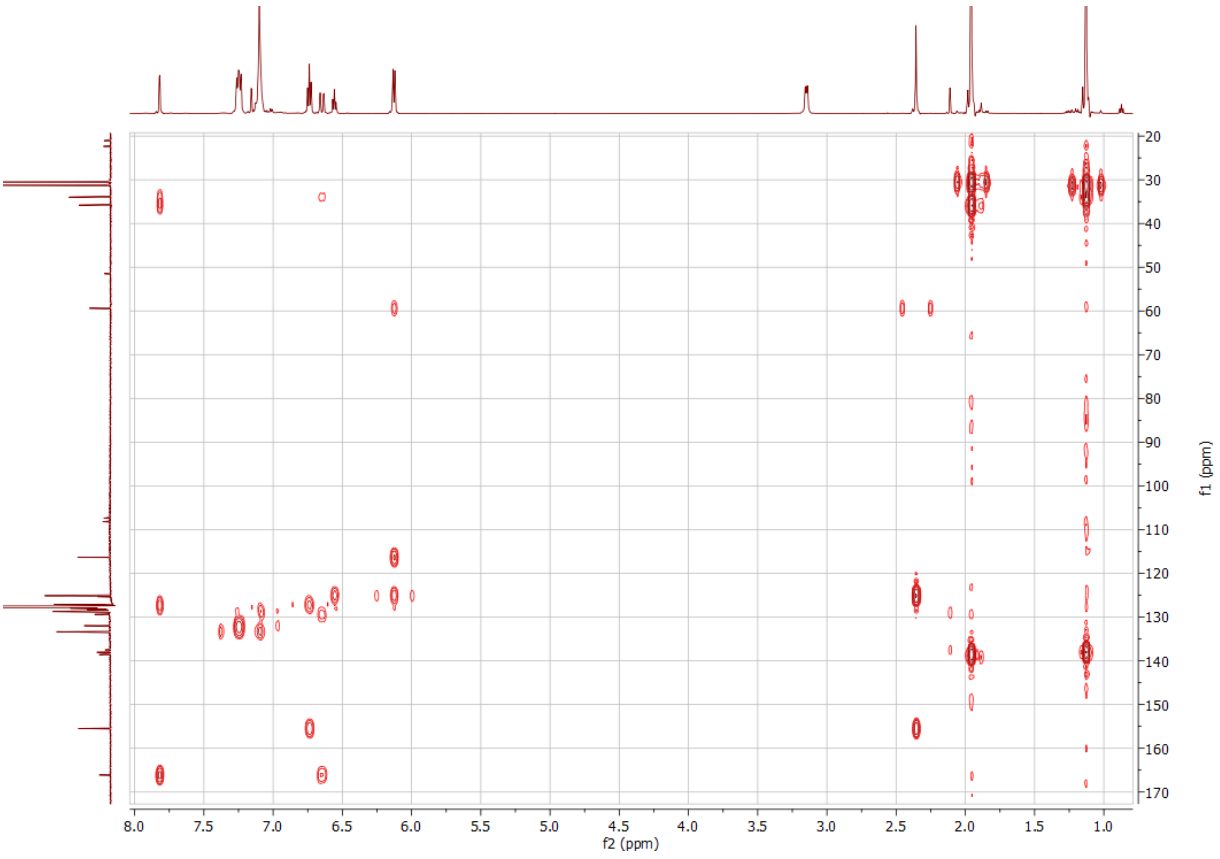

Figure S16: ^{1}H-^{13}C HMBC (500 MHz / 126 MHz, C_6D_6, 300 K)(whole spectrum) of 2a

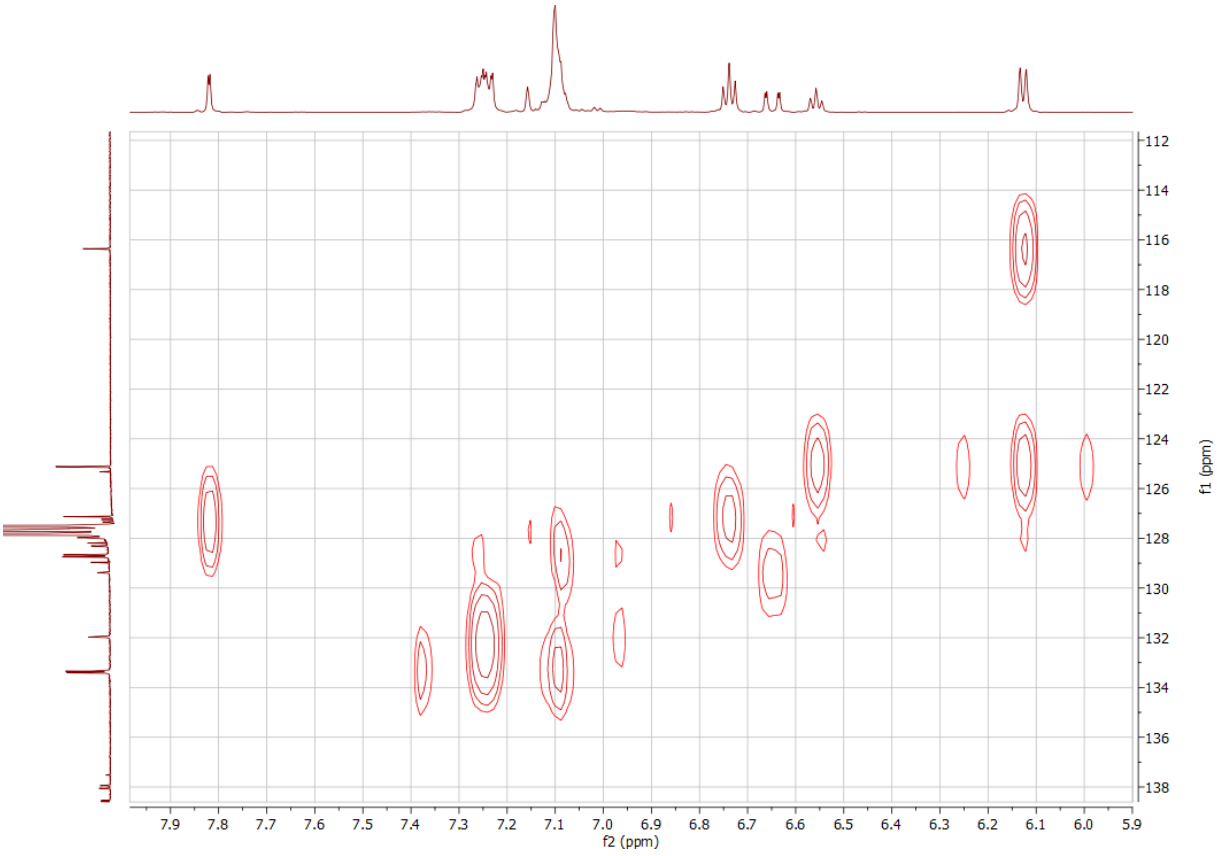

Figure S17: ^{1}H-^{13}C HMBC (500 MHz / 126 MHz, C_6D_6, 300 K)(zoom) of 2a

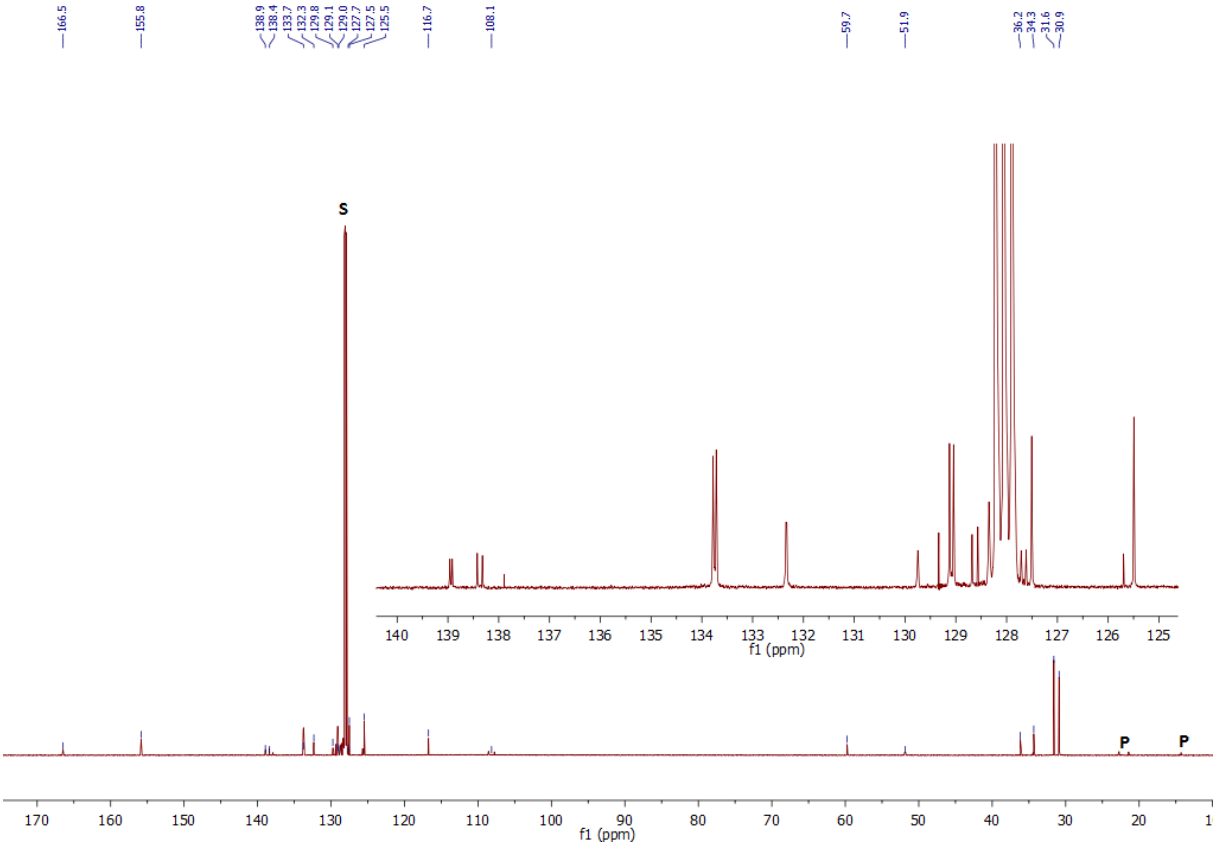

Figure S18: $^{13}C\{^{1}H\}$ NMR (126 MHz, C_6D_6, 300 K)(p: pentane; s: solvent) of 2a

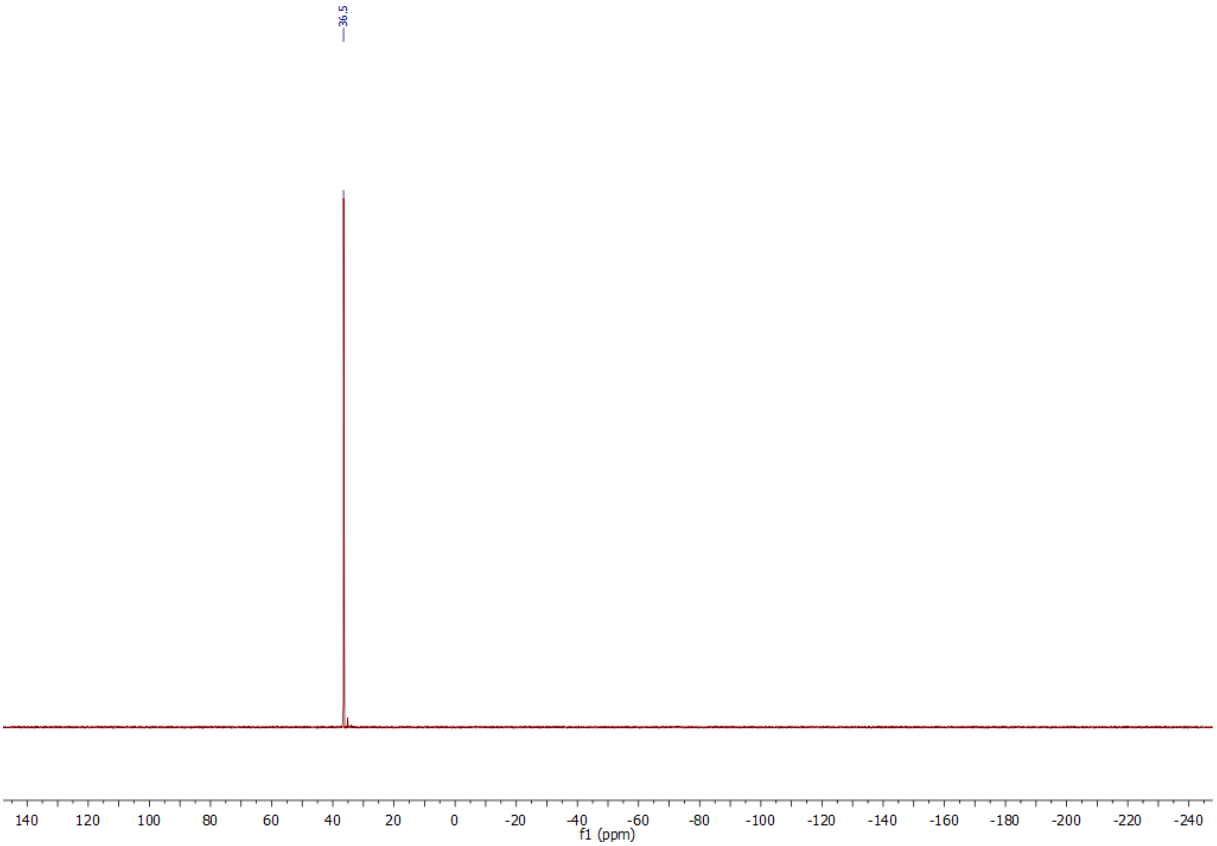

Figure S19: $^{31}P\{^{1}H\}$ NMR (202 MHz, C_6D_6, 300 K) of 2a

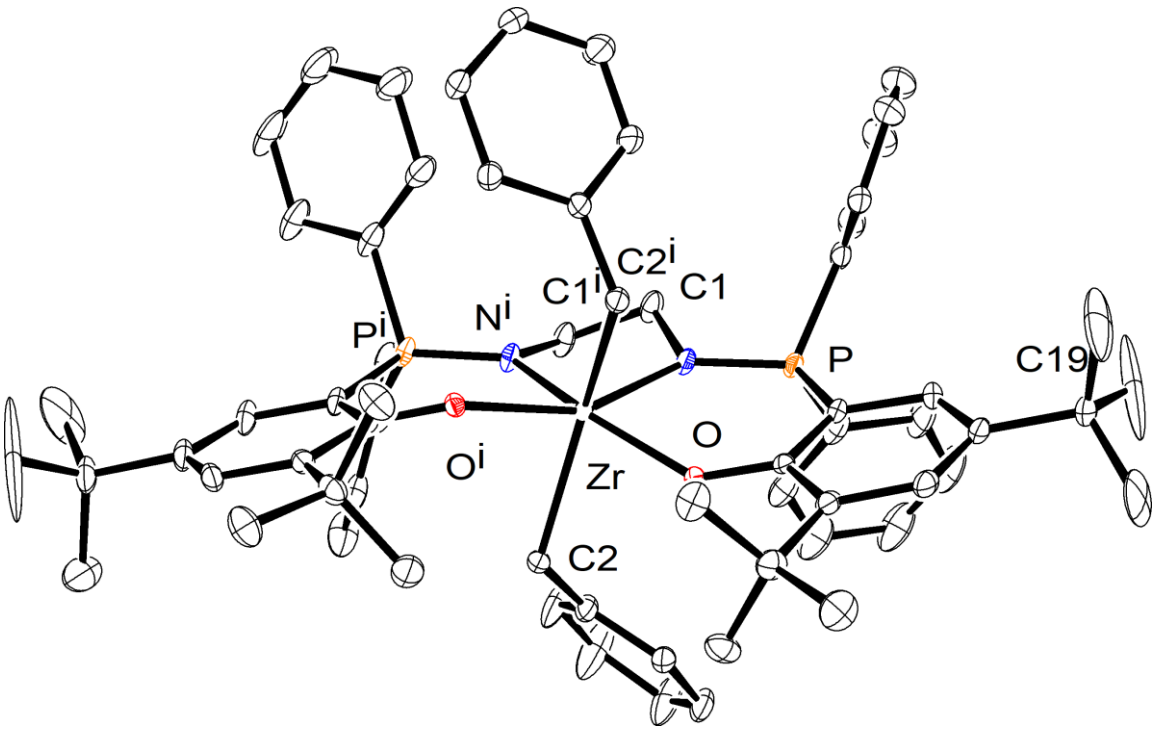

Figure S20: Crystal structure of 2a. [i]1-X, +Y, 3/2-Z.

Table S4: Crystal data and structure refinement of 2a

Identification code	**2a**
Internal reference	AD290318_0m
Empirical formula	$C_{68}H_{78}N_2O_2P_2Zr$
Formula weight	1108.48
Temperature/K	110
Crystal system	monoclinic
Space group	C2/c
a/Å	18.8787(11)
b/Å	15.7181(9)
c/Å	27.6141(15)
α/°	90
β/°	105.6510(10)
γ/°	90
Volume/Å^3	7890.3(8)
Z	4
ρ_{calc}g/cm^3	0.933
μ/mm^{-1}	0.214
F(000)	2344.0
Crystal size/mm^3	0.25 × 0.25 × 0.25
Radiation	MoKα (λ = 0.71073)
2Θ range for data collection/°	6.128 to 57.47
Index ranges	-15 ≤ h ≤ 25, -21 ≤ k ≤ 21, -37 ≤ l ≤ 37
Reflections collected	71040
Independent reflections	10194 [R_{int} = 0.0518, R_{sigma} = 0.0374]
Data/restraints/parameters	10194/0/339
Goodness-of-fit on F^2	1.042
Final R indexes [I>=2σ (I)]	R_1 = 0.0514, wR_2 = 0.1390
Final R indexes [all data]	R_1 = 0.0659, wR_2 = 0.1497
Largest diff. peak/hole / e Å^{-3}	1.74/-1.16
CCDC	1978287

Special refinement details for 2a

Only one half of the molecule is present in the asymmetric unit, the whole molecule is generated by action of a 2_1 symmetry operator. The methyl carbon atoms of one of the tert-butyl groups (C19) exhibits rather elongated anisotropic displacement parameters. This could be an indication that the position of this tert-butyl group fluctuates around an average position of a few degrees and, since this disorder seems rather continuous than discrete, we simply let the anisotropic displacement parameters taking account for that.

Three remaining electron density areas are located in the last Fourier difference maps of the asymmetric unit. If two of them clearly suggest the presence of a toluene solvent molecule the third one is too diffuse for clearly identify a molecule. Anyway, any attempts to refine these solvent molecules do not give satisfactory results and the contribution of molecules from the diffraction intensities were subtracted by the application of the Squeeze procedure. The procedure subtracted 152.4 electrons by asymmetric unit whereas 3 toluene molecules count for 150 electrons.

Complex 2b:

^{1}H-^{1}H COSY (500 MHz, d_8-THF 210 K)[selected cross-peaks]: δ = 6.52 / 6.01 (*m* of ZrBn(T) / *o* of ZrBn(T)).

^{1}H-^{13}C HMBC (500 MHz / 126 MHz, d_8-THF 210 K)[selected cross-peaks]: δ = 7.55 / 166.7 (*H*3 of PAr(T) / *C*1 of PAr(T)), 7.48 / 163.0 (*H*3 of PAr(β) / *C*1 of PAr(β)), 7.31 / 165.6 (*H*3 of PAr(β) / *C*1 of PAr(β)), 7.08 / 163.0 (*H*5 of PAr(β) / *C*1 of PAr(β)), 7.08 / 34.8 (*H*5 of PAr(β) / *C* of ^{t}Bu^{4}(β)), 6.75 / 153.2 (*m* of ZrBn(β) / *i* of ZrBn(β)), 6.75 / 127.0 (*m* of ZrBn(β) / *m* of ZrBn(β)), 6.65 / 165.6 (*H*5 of PAr(β) / *C*1 of PAr(β)), 6.65 / 34.7 (*H*5 of PAr(β) / *C* of ^{t}Bu^{4}(β)), 6.52 / 154.7 (*m* of ZrBn(T) / *i* of ZrBn(T)), 6.52 / 127.3 (*m* of ZrBn(T) / *m* of ZrBn(T)), 6.46 / 154.5 (*m* of ZrBn(β) / *i* of ZrBn(β)), 6.46 / 126.9 (*m* of ZrBn(β) / *m* of ZrBn(β)), 6.35 / 166.7 (*H*5 of PAr(T) / *C*1 of PAr(T)), 6.35 / 130.6 (*H*5 of PAr(T) / *C*3 of PAr(T)), 6.35 / 34.6 (*H*5 of PAr(T) / *C* of ^{t}Bu^{4}(β)), 6.31 / 125.8 (*p* of ZrBn(T) / *o* of ZrBn(T)), 6.22 / 145.1 (*H*3 of NAr(β) / *C*1 of NAr(β)), 6.22 / 122.2 (*H*3 of NAr(β) / *C*2 of NAr(β)), 6.01 / 125.8 (*o* of ZrBn(T) / *o* of ZrBn(T)), 6.01 / 127.3 (*o* of ZrBn(T) / *m* of ZrBn(T)), 6.01 / 117.5 (*o* of ZrBn(T) / *p* of ZrBn(T)), 6.01 / 64.0 (*o* of ZrBn(T) / *C*H$_2$ of ZrBn(T)), 5.77 / 145.1 (*H*2 of NAr(β) / *C*1 of NAr(β)), 5.77 / 120.6 (*H*2 of NAr(β) / *C*3 of NAr(β)), 2.37 / 154.5 (C*H*$_2$ of ZrBn(β) / *i* of ZrBn(β)), 2.37 / 125.8 (C*H*$_2$ of ZrBn(β) / *o* of ZrBn(β)), 2.09 / 153.2 (C*H*$_2$ of ZrBn(β) / *i* of ZrBn(β)), 2.09 / 126.5 (C*H*$_2$ of ZrBn(β) / *o* of ZrBn(β)), 1.79 / 154.5 (C*H*$_2$ of ZrBn(β) / *i* of ZrBn(β)), 1.79 / 125.8 (C*H*$_2$ of ZrBn(β) / *o* of ZrBn(β)), 1.74 / 154.7 (C*H*$_2$ of ZrBn(T) / *i* of ZrBn(T)), 1.74 / 125.8 (C*H*$_2$ of ZrBn(T) / *o* of ZrBn(T)), 1.67 / 153.2 (C*H*$_2$ of ZrBn(β) / *i* of ZrBn(β)), 1.67 / 126.5 (C*H*$_2$ of ZrBn(β) / *o* of ZrBn(β)), 1.42 / 138.7 (C*H*$_3$ of ^{t}Bu^{2}(β) / *C*2 of PAr(β)), 1.42 / 36.1 (C*H*$_3$ of ^{t}Bu^{2}(β) / *C* of ^{t}Bu^{2}(β)), 1.42 / 30.6 (C*H*$_3$ of ^{t}Bu^{2}(β) / *C*H$_3$ of ^{t}Bu^{2}(β)), 1.27 / 138.0 (C*H*$_3$ of ^{t}Bu^{2}(T) / *C*2 of PAr(T)), 1.27 / 35.9 (C*H*$_3$ of ^{t}Bu^{2}(T) / *C* of ^{t}Bu^{2}(T)), 1.27 / 30.6 (C*H*$_3$ of ^{t}Bu^{2}(T) / *C*H$_3$ of ^{t}Bu^{2}(T)), 1.18 / 139.9 (C*H*$_3$ of ^{t}Bu^{4}(β) / *C*4 of PAr(β)), 1.18 / 138.7 (C*H*$_3$ of ^{t}Bu^{4}(β) / *C*4 of PAr(β)), 1.18 / 34.8 (C*H*$_3$ of ^{t}Bu^{4}(β) / *C* of ^{t}Bu^{4}(β)), 1.18 / 34.7 (C*H*$_3$ of ^{t}Bu^{4}(β) / *C* of ^{t}Bu^{4}(β)), 1.18 / 31.4 (C*H*$_3$ of ^{t}Bu^{4}(β) / *C*H$_3$ of ^{t}Bu^{4}(β)), 1.13 / 138.2 (C*H*$_3$ of ^{t}Bu^{4}(T) / *C*4 of PAr(T)), 1.13 / 34.6 (C*H*$_3$ of ^{t}Bu^{4}(T) / *C* of ^{t}Bu^{4}(T)), 1.13 / 31.4 (C*H*$_3$ of ^{t}Bu^{4}(T) / *C*H$_3$ of ^{t}Bu^{4}(T)), 0.52 / 139.8 (C*H*$_3$ of ^{t}Bu^{2}(β) / *C*2 of PAr(β)), 0.52 / 35.3 (C*H*$_3$ of ^{t}Bu^{2}(β) / *C* of ^{t}Bu^{2}(β)), 0.52 / 28.7 (C*H*$_3$ of ^{t}Bu^{2}(β) / *C*H$_3$ of ^{t}Bu^{2}(β)).

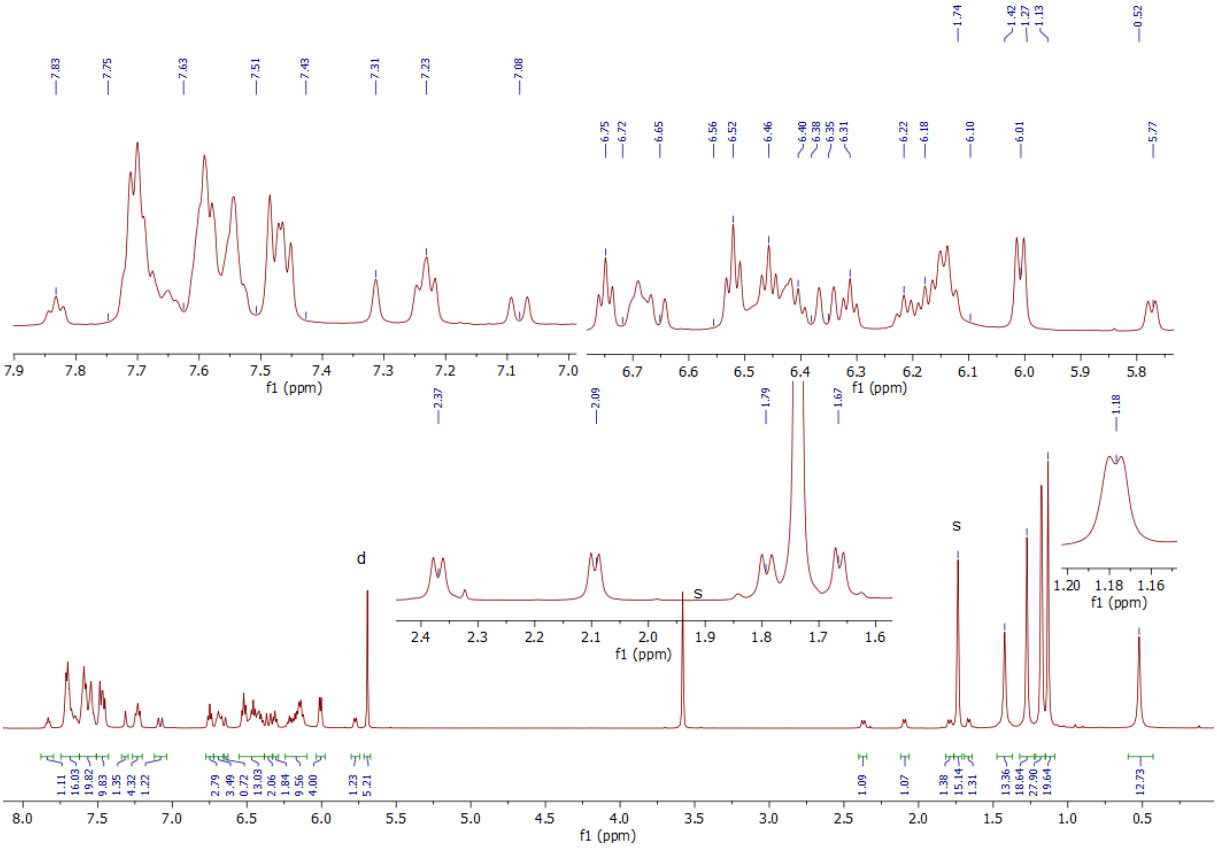

Figure S21: ^{1}H NMR (500 MHz, d_8-THF, 210 K)(s: solvent ; d: dichloromethane) of 2b

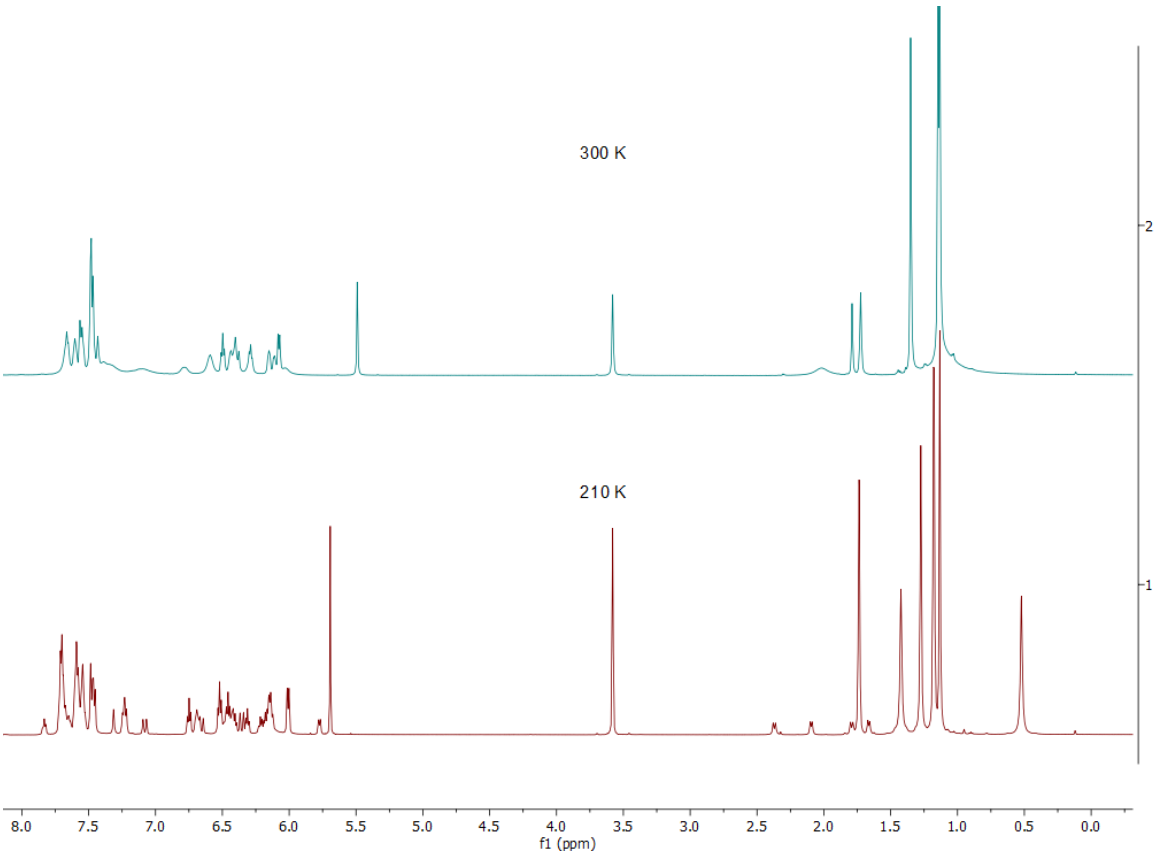

Figure S22: ^{1}H NMR (500 MHz, d_8-THF, 210 vs 300 K) of 2b

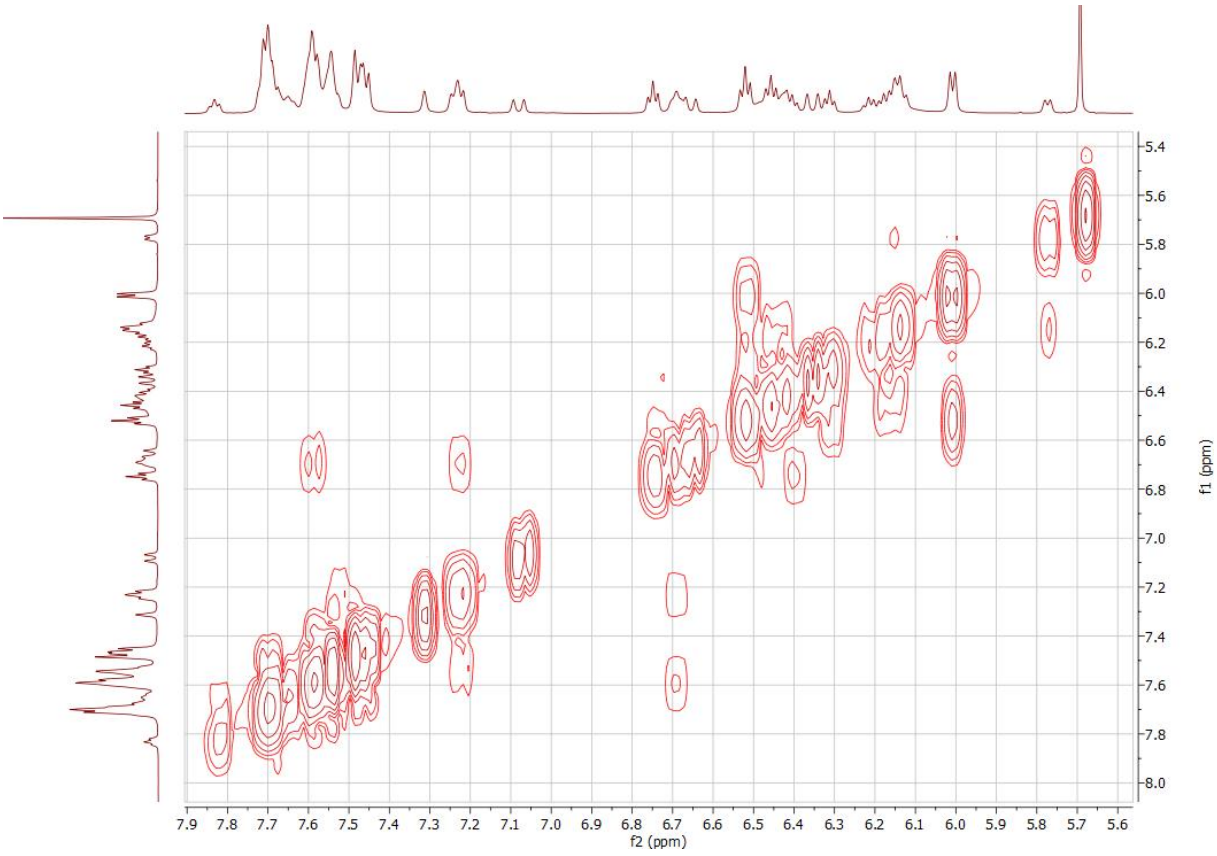

Figure S23: ^{1}H-^{1}H COSY (500 MHz, d_8-THF, 210 K)(Aromatic region) of 2b

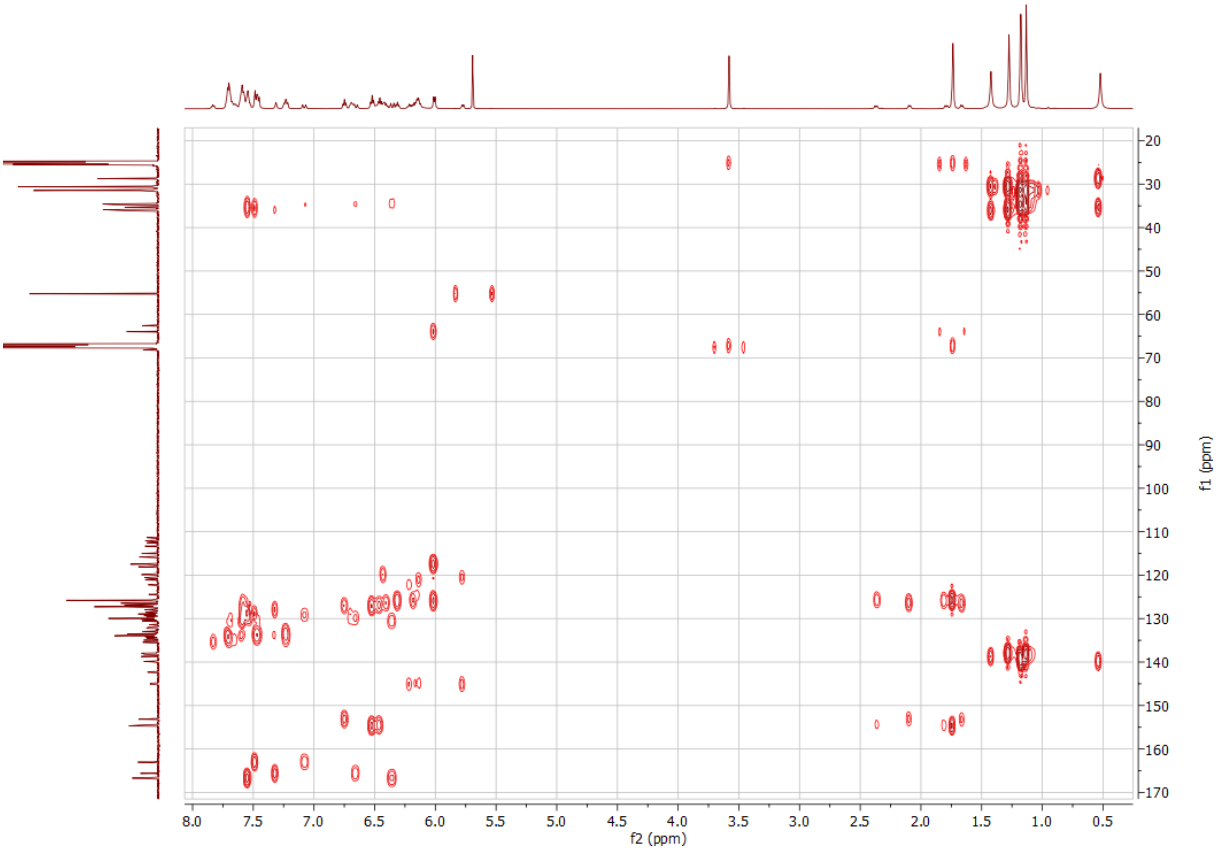

Figure S24: ^{1}H-^{13}C HMBC (500 MHz / 126MHz, d_8-THF, 210 K)(Full spectrum) of 2b

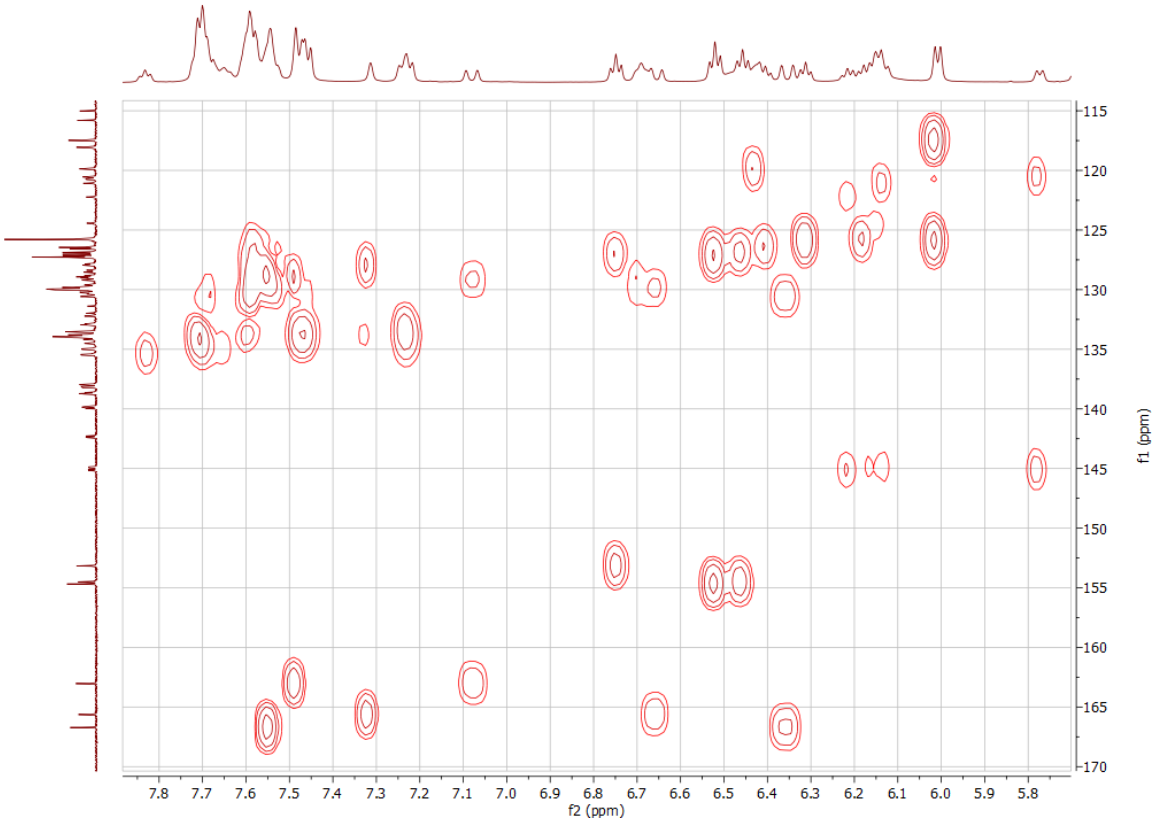

Figure S25: ^{1}H-^{13}C HMBC (500 MHz / 126MHz, d_8-THF, 210 K)(Zoom) of 2b

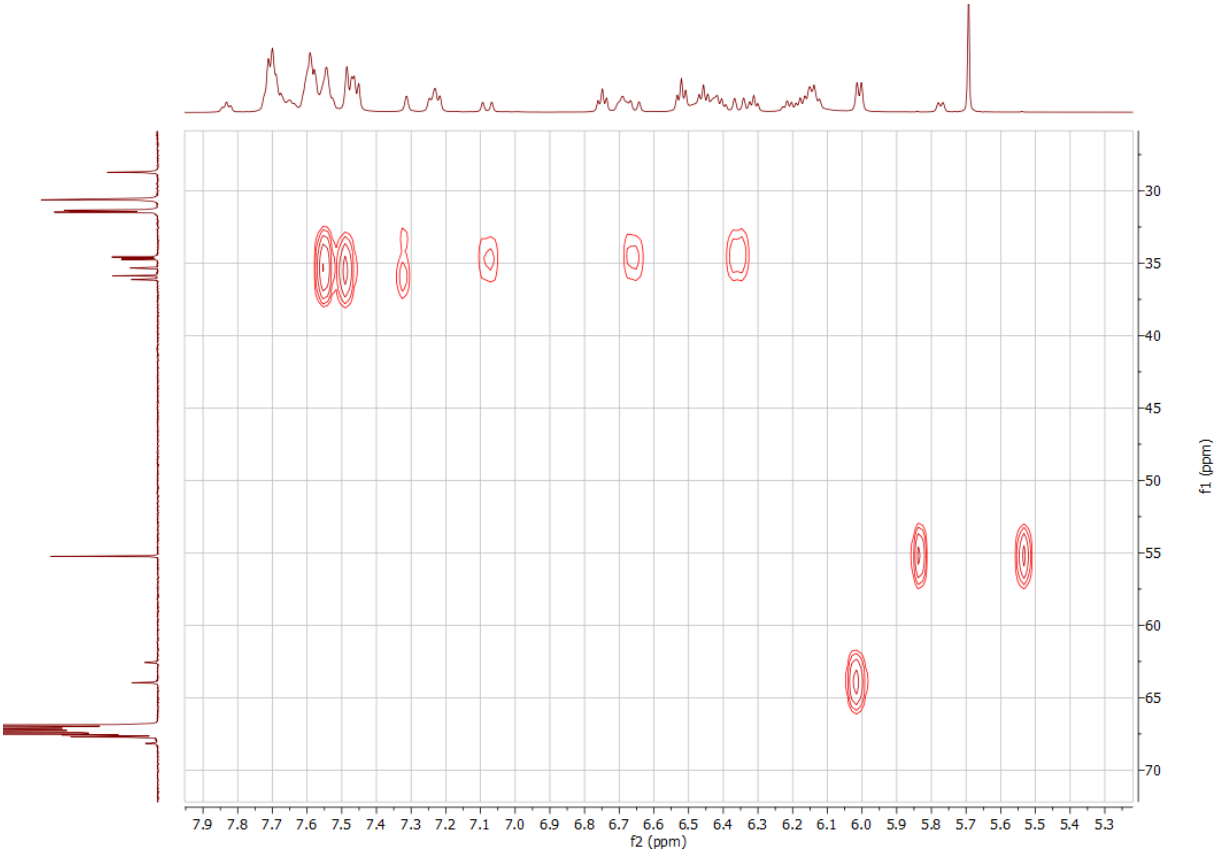

Figure S26: ^{1}H-^{13}C HMBC (500 MHz / 126MHz, d_8-THF, 210 K)(Zoom) of 2b

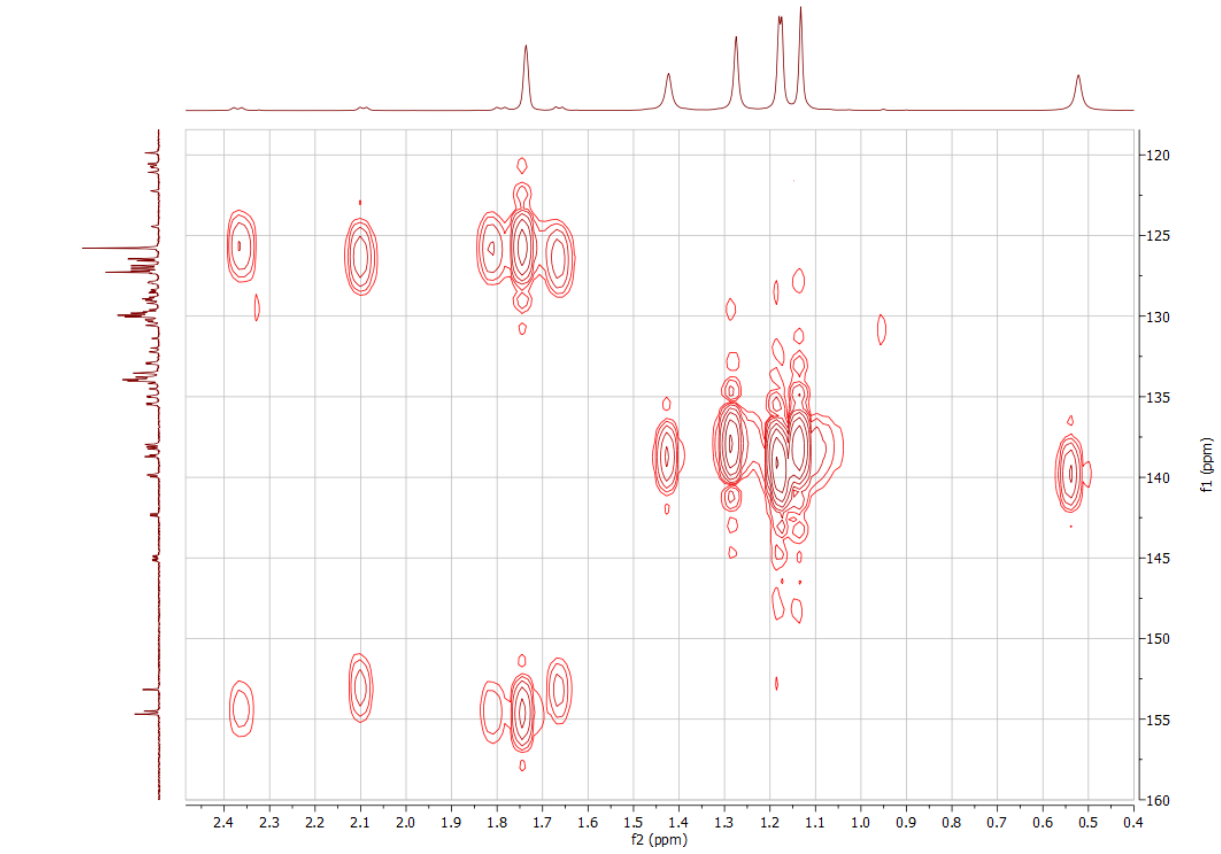

Figure S27: ^{1}H-^{13}C HMBC (500 MHz / 126MHz, d_8-THF, 210 K)(Zoom) of 2b

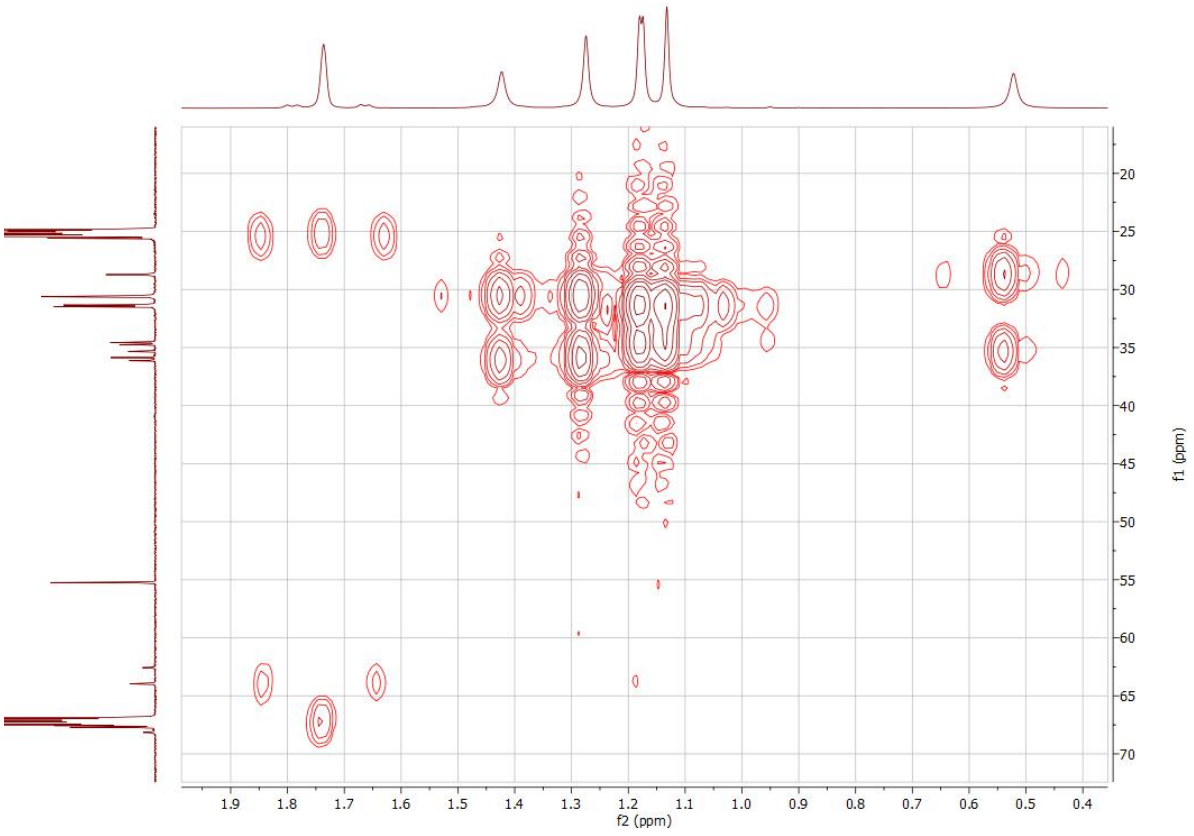

Figure S28: ^{1}H-^{13}C HMBC (500 MHz / 126MHz, d_8-THF, 210 K)(Zoom) of 2b

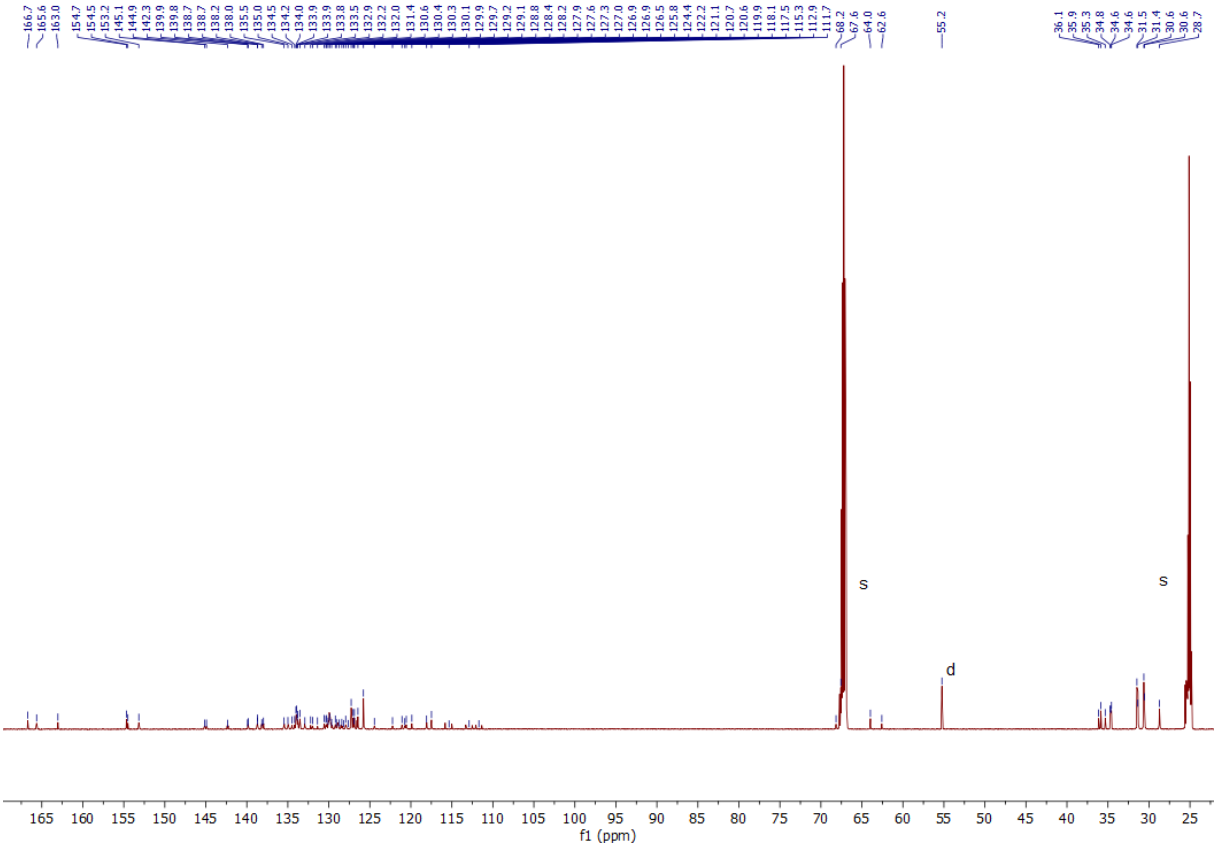

Figure S29: $^{13}C\{^{1}H\}$ NMR (126 MHz, d_8-THF, 210 K)(s: solvent ; d: dichloromethane) of 2b

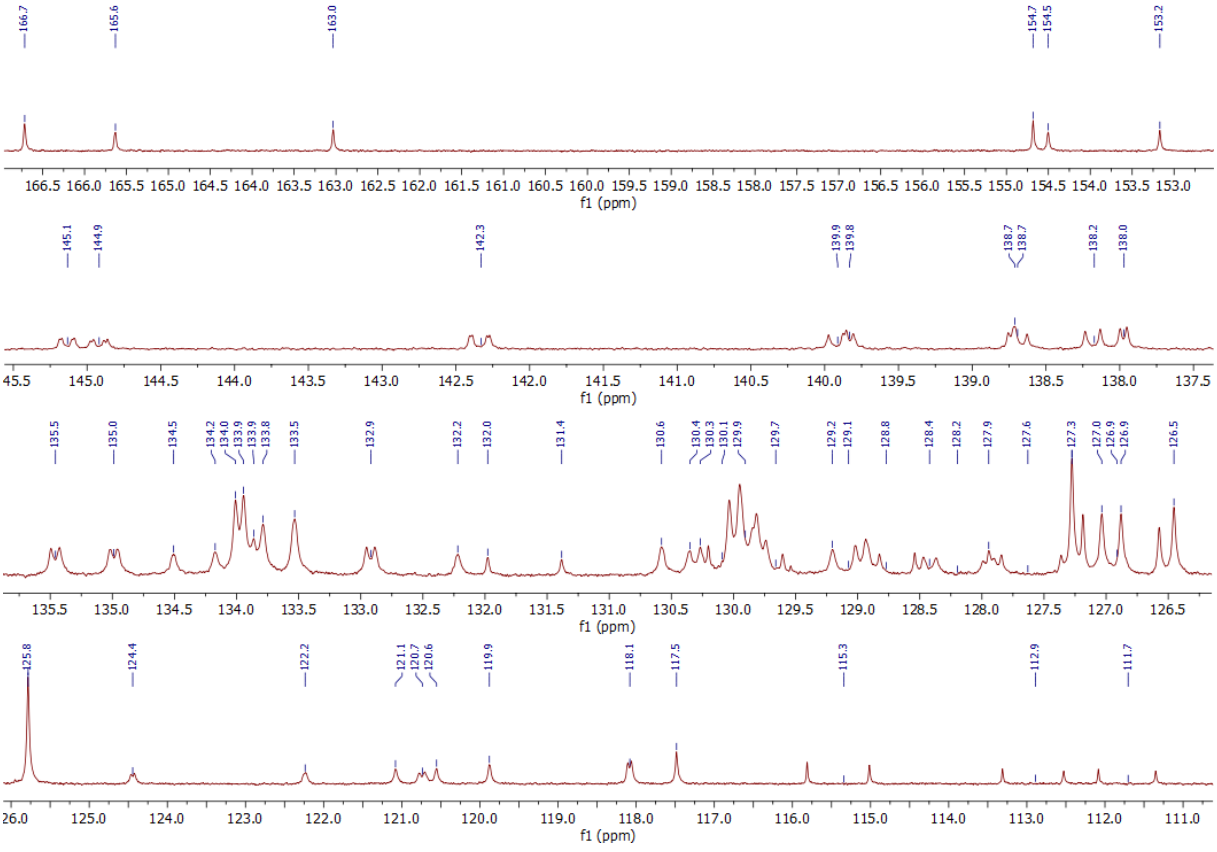

Figure S30: $^{13}C\{^{1}H\}$ NMR (126 MHz, d_8-THF, 210 K)(Aromatic region) of 2b

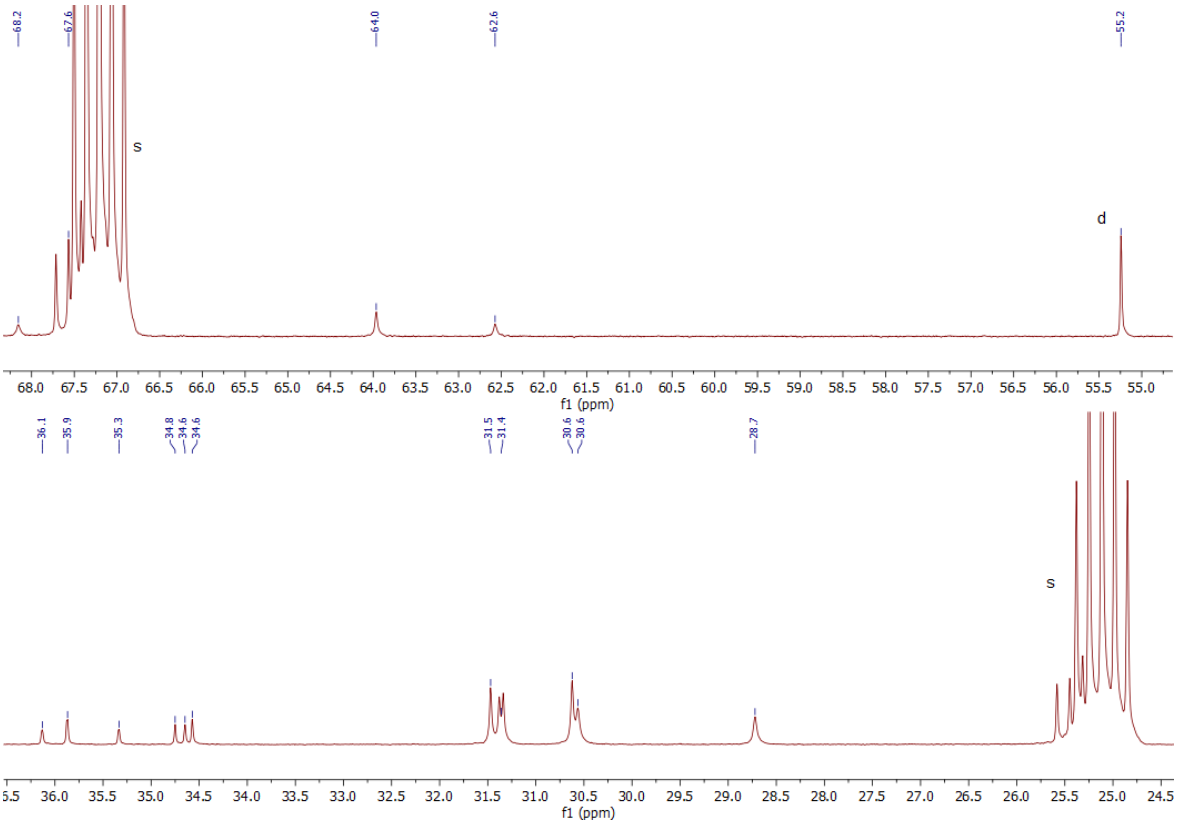

Figure S31: $^{13}C\{^{1}H\}$ NMR (126 MHz, d_8-THF, 210 K)(Aliphatic region)(s: solvent ; d: dichloromethane) of 2b

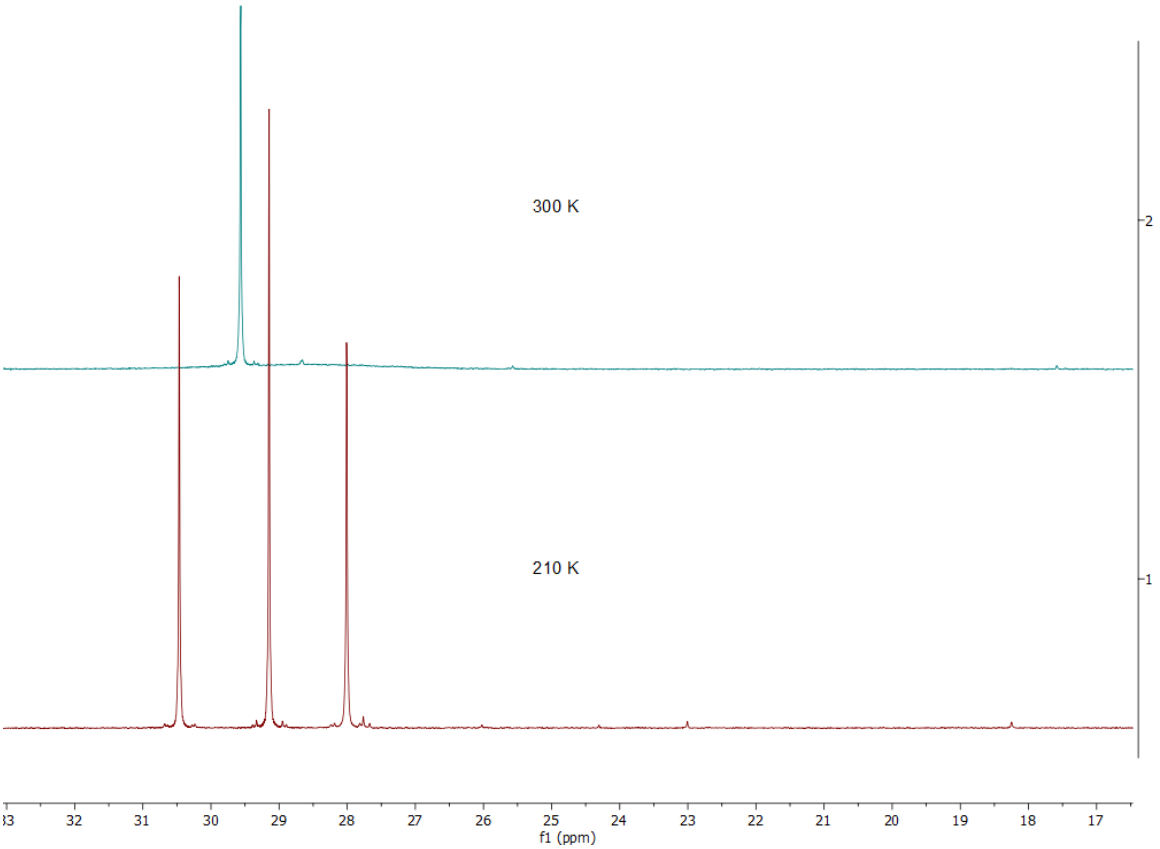

Figure S32: $^{31}P\{^{1}H\}$ NMR (202 MHz, d_8-THF, 210 vs 300 K) of 2b

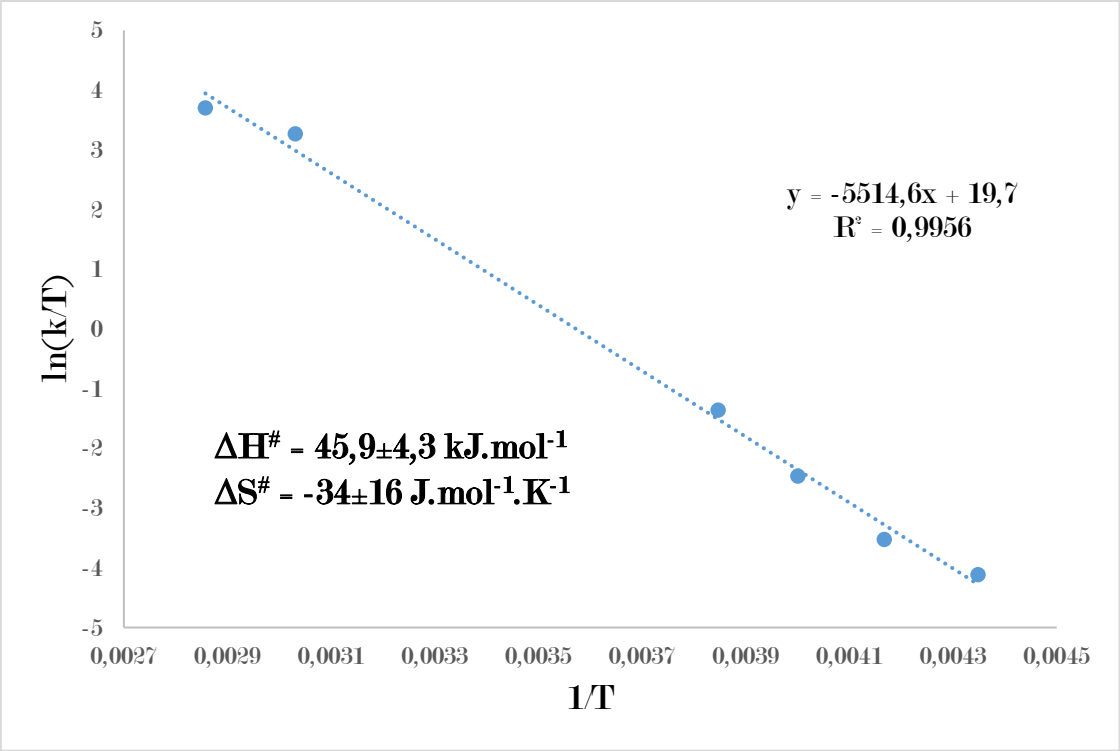

Figure S33: Eyring plot of ln(k/T) against 1/T for the isomerisation between the Δ and Λ enantiomers of the *cis*-β isomer of 2b. Expanded incertainties, given at the 95% confidence interval, are estimated from the residual variance of the fit.

Complex 2c

^{1}H-^{1}H COSY (600.2 MHz, $CDCl_3$, 300 K) [selected cross-peaks]: 7.71 / 6.72 (*H*3 of PAr / *H*5 of PAr), 6.95 / 6.76 (*m* of ZrBn / *o* of ZrBn), 6.95 / 6.58 (*m* of ZrBn / *p* of ZrBn), 6.76 / 1.81 (*o* of ZrBn /CH_2 of ZrBn), 2.25 / 1.35 (NCH_2 / NCH$_2$CH_2)

^{1}H-^{13}C HMBC (600.2 MHz / 150.9 MHz, $CDCl_3$, 300 K) [selected cross-peaks]: 7.71 / 165.4 (*H*3 of PAr / *C*1 of PAr), 7.71 / 35.4 (*H*3 of PAr / C of *t*Bu^2), 7.71 / 34.4 (*H*3 of PAr / C of *t*Bu^4), 6.72 / 165.4 (*H*5 of PAr / *C*1 of PAr), 6.72/ 34.4 (*H*5 of PAr / C of *t*Bu^4), 1.83 / 148.4 (CH_2 of ZrBn / Ci of ZrBn), 1.83 / 126.6 (CH_2 of ZrBn / *o* of ZrBn), 1.51 / 139.5 (H of ^{t}Bu^2 / *C*2 of PAr), 1.51 / 35.4 (H of ^{t}Bu^2 / C of *t*Bu^2), 1.22 / 140.3 (H of ^{t}Bu^4 / *C*4 of PAr), 1.22 / 34.4 (H of ^{t}Bu^4 / C of *t*Bu^4).

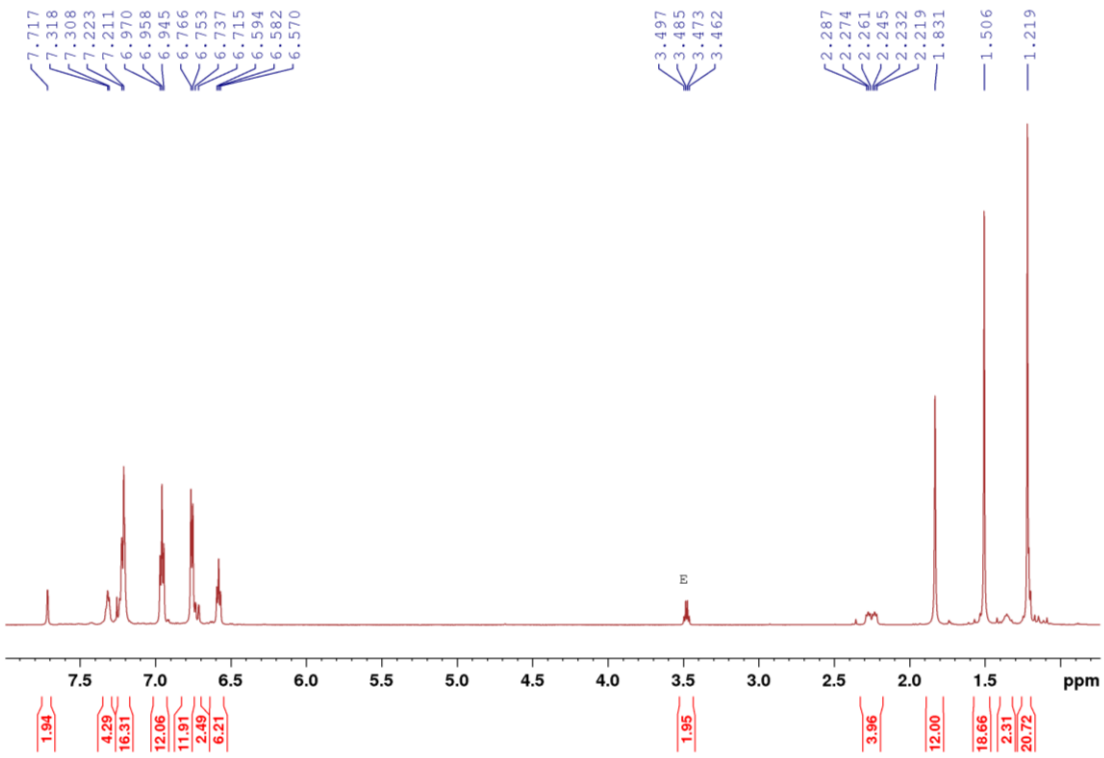

Figure S34 ^{1}H NMR (600 MHz, $CDCl_3$, 300 K) of 2c

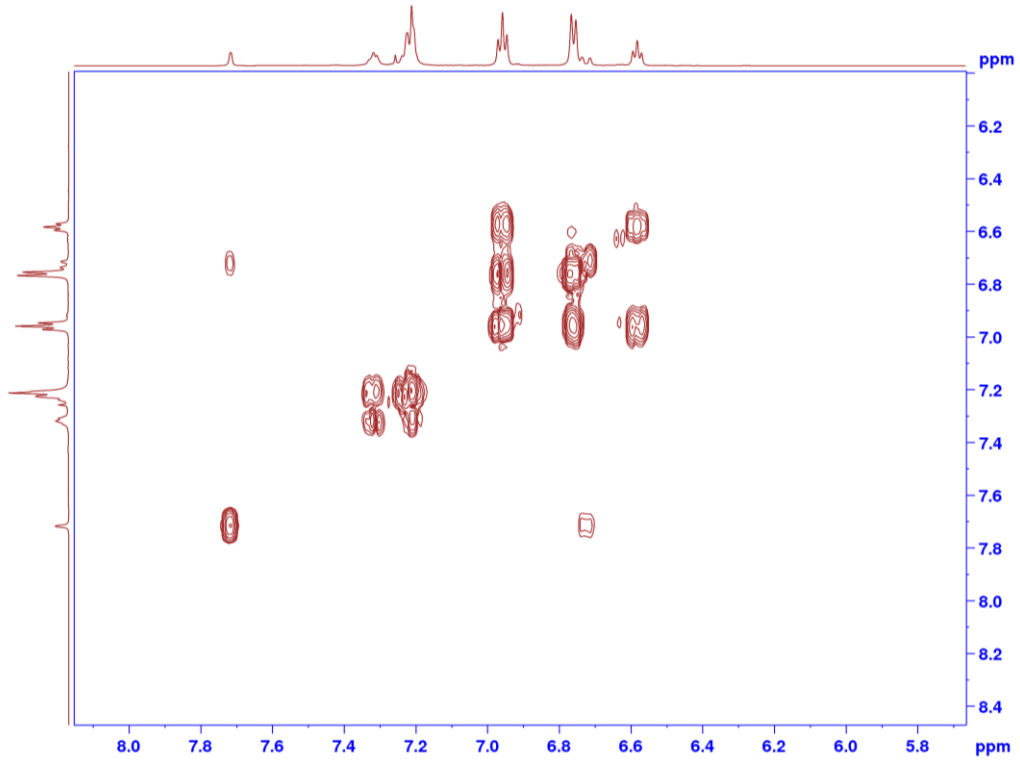

Figure S35 ^{1}H-^{1}H COSY NMR (600 MHz, $CDCl_3$, 300 K) (zoom) of 2c

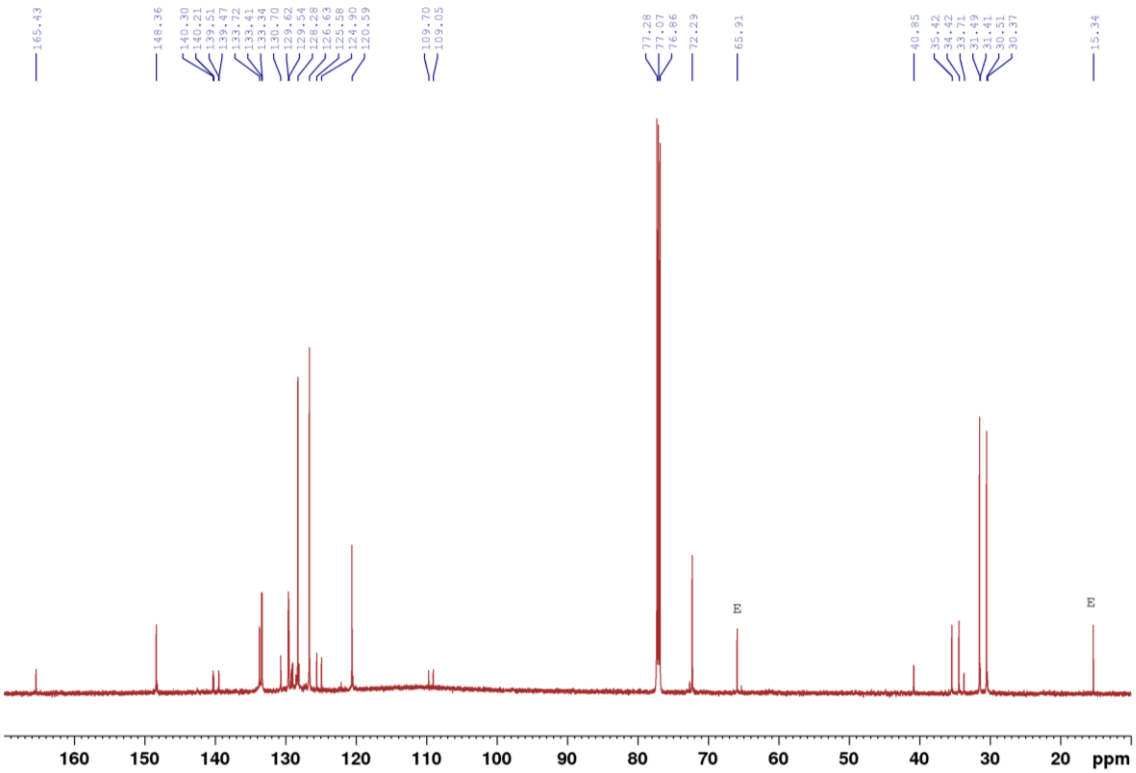

Figure S36: $^{13}C\{^{1}H\}$ NMR (150.9 MHz, $CDCl_3$, 300 K) of 2c

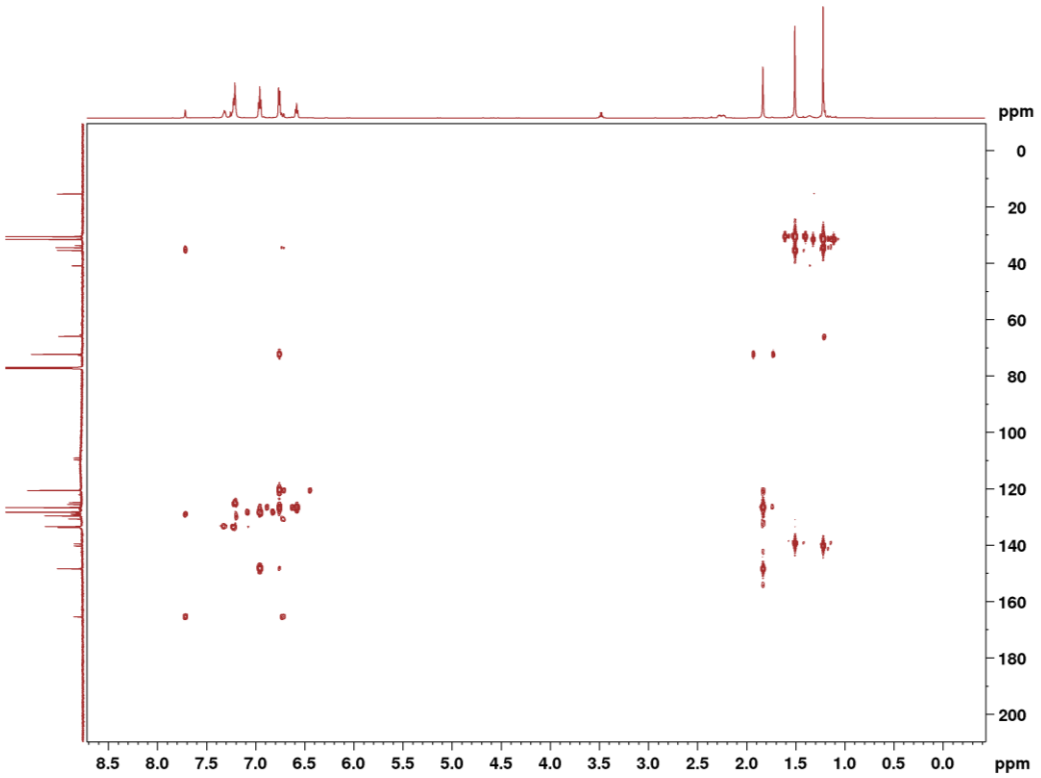

Figure S37: ^{1}H-^{13}C HMBC (600 MHz / 151 MHz, $CDCl_3$, 300 K) of 2c

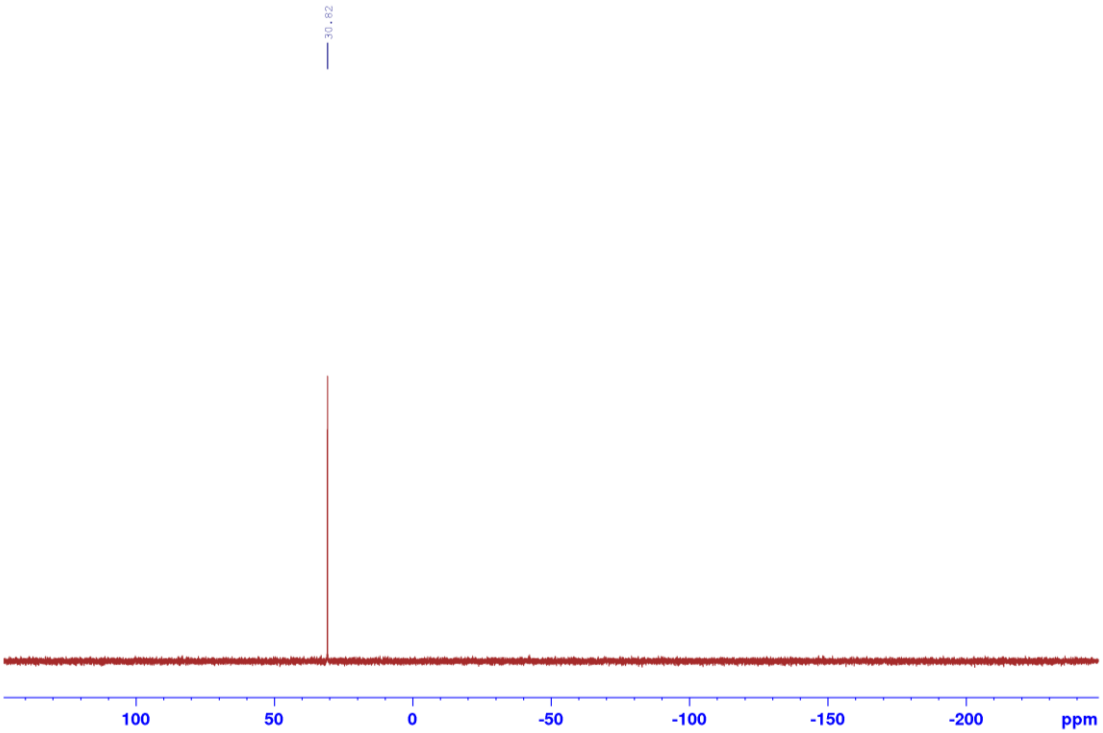

Figure S38: $^{31}P\{^{1}H\}$ NMR (243MHz, $CDCl_3$, 300 K) of 2c

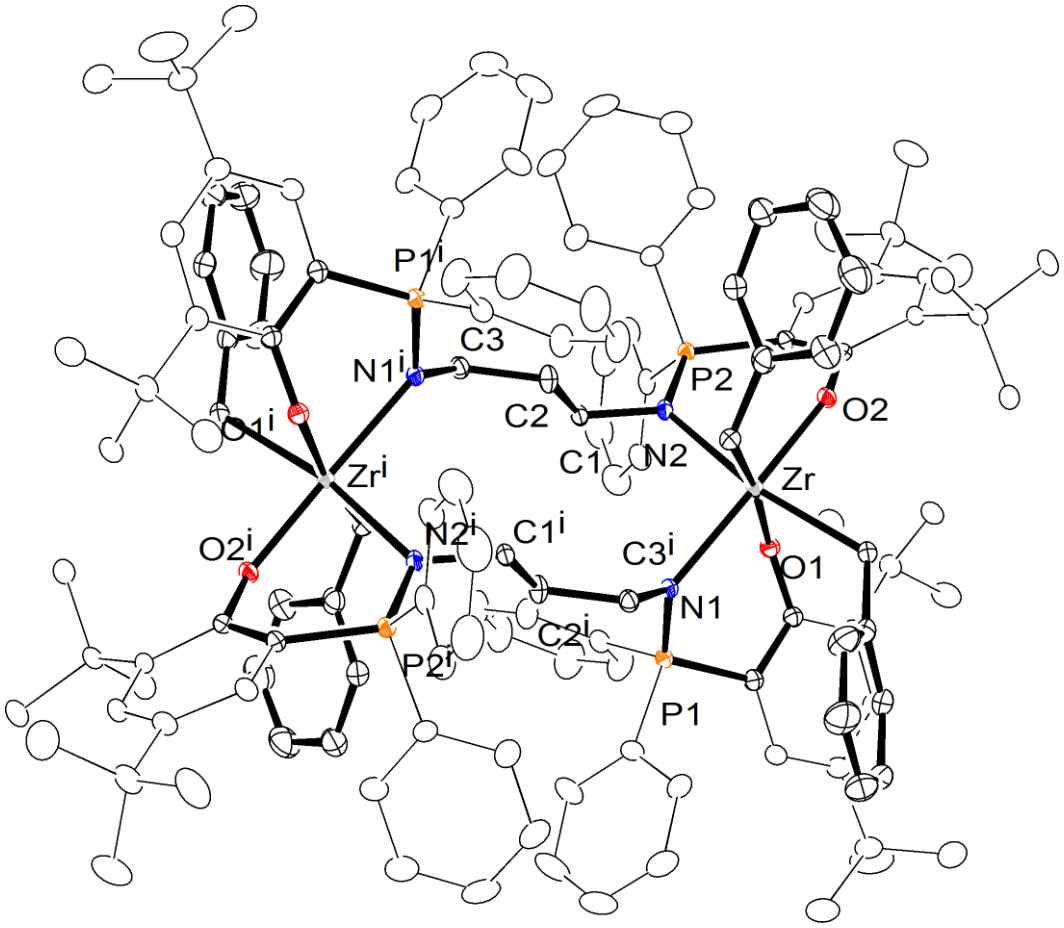

Figure S39: Crystal structure of 2c'. ^{i}1-X, 1-Y, 1-Z.

Table S5: Crystal data and structure refinement of 2c'

Identification code	2c'
Internal reference	mo_ral100317b_0m
Empirical formula	$C_{138}H_{160}N_4O_4P_4Zr_2$
Formula weight	2245.01
Temperature/K	100
Crystal system	monoclinic
Space group	$P2_1/c$
a/Å	16.9665(10)
b/Å	27.0540(17)
c/Å	18.9109(12)
α/°	90
β/°	116.2737(18)
γ/°	90
Volume/Å^3	7783.6(8)
Z	2
ρ_{calc}g/cm^3	0.958
μ/mm^{-1}	0.218
F(000)	2376.0
Crystal size/mm^3	0.32 × 0.3 × 0.3
Radiation	MoKα (λ = 0.71073)
2Θ range for data collection/°	5.384 to 55.162
Index ranges	-22 ≤ h ≤ 20, -35 ≤ k ≤ 35, -24 ≤ l ≤ 24
Reflections collected	199749
Independent reflections	17921 [R_{int} = 0.0476, R_{sigma} = 0.0294]
Data/restraints/parameters	17921/0/697
Goodness-of-fit on F^2	1.034
Final R indexes [I>=2σ (I)]	R_1 = 0.0567, wR_2 = 0.1528
Final R indexes [all data]	R_1 = 0.0783, wR_2 = 0.1749
Largest diff. peak/hole / e Å^{-3}	1.26/-0.60
CCDC	1978289

Special refinement details for 2c'

Only one half of the molecule is present in the asymmetric unit, the whole molecule is generated by action of an inversion center.

The compound crystallized with a deuterated THF molecule (from NMR tube) but the final difference electron density map was not clear enough to include and refine this molecule in the model. The contribution of this solvent from the diffraction intensities was then subtracted by the application of the Squeeze procedure. The procedure subtracted 39 electrons by asymmetric unit whereas a THF molecule count for 40 electrons.

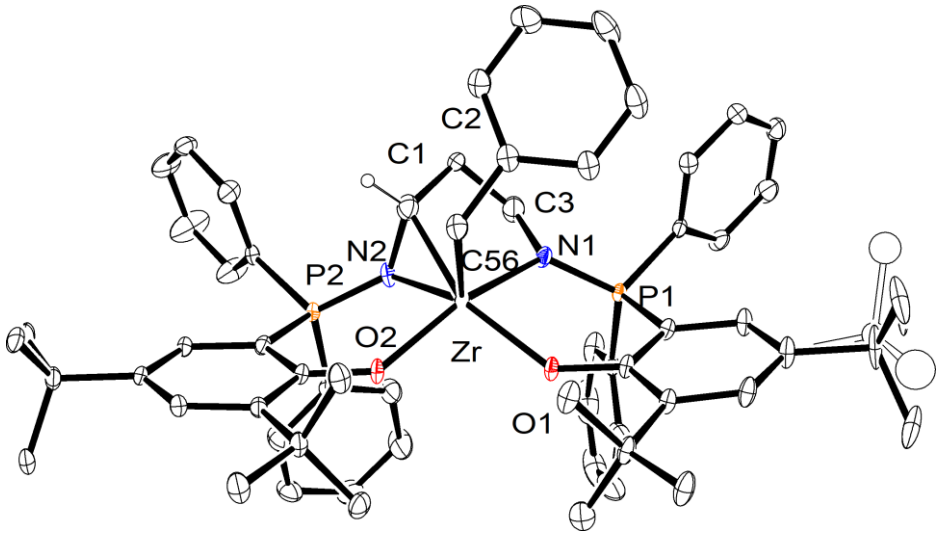

Figure S40: Crystal structure of 2c”

Table S6: Crystal data and structure refinement of 2c”

Identification code	2c''
Internal reference	platon_sq.ins with ral220317_0m.hkl
Empirical formula	$C_{80}H_{114}N_2O_2P_2Zr$
Formula weight	1288.89
Temperature/K	115.0
Crystal system	triclinic
Space group	P-1
a/Å	13.2872(7)
b/Å	16.4819(10)
c/Å	16.7752(9)
α/°	69.077(2)
β/°	75.579(3)
γ/°	80.202(3)
Volume/Å^3	3310.0(3)
Z	2
ρ_{calc}g/cm^3	1.293
μ/mm^{-1}	0.265
F(000)	1388.0
Crystal size/mm^3	0.25 × 0.2 × 0.12
Radiation	MoKα (λ = 0.71073)
2Θ range for data collection/°	4.54 to 55.23
Index ranges	-17 ≤ h ≤ 17, -21 ≤ k ≤ 21, -21 ≤ l ≤ 21
Reflections collected	86942
Independent reflections	15215 [R_{int} = 0.0866, R_{sigma} = 0.0781]
Data/restraints/parameters	15215/4/642
Goodness-of-fit on F^2	1.025
Final R indexes [I>=2σ (I)]	R_1 = 0.0531, wR_2 = 0.1366
Final R indexes [all data]	R_1 = 0.0913, wR_2 = 0.1546
Largest diff. peak/hole / e Å^{-3}	1.40/-0.75
CCDC	1978294

Special refinement details for 2c''

One of the tert-butyl groups was found disordered (elongated ADP ellipsoid). The model was improved by including a minor component refined as an isotropic rigid group.

A solvent mask was calculated and 295 electrons were found in a volume of 809 $Å^3$ in one void per unit cell. This is consistent with the presence of 3 C6H14 per Asymmetric Unit which account for 300 electrons per unit cell.

Complex 3a

^{1}H-^{1}H COSY (600 MHz, CD_2Cl_2, 250 K)[selected cross-peaks]: δ = 4.60 / 1.16 (C*H* of ^{i}Pr(β) / CH_3 of ^{i}Pr(β)), 3.90 / 2.68 (CH_2N(β) / CH_2N(β)), 3.90 / 2.55 (CH_2N(β) / CH_2N(β)), 3.70 / 0.51 (C*H* of ^{i}Pr(T) / CH_3 of ^{i}Pr(T)), 3.23 / 0.64 (C*H* of ^{i}Pr(β) / CH_3 of ^{i}Pr(β)), 3.23 / 0.54 (C*H* of ^{i}Pr(β) / CH_3 of ^{i}Pr(β)), 2.80 / 2.55 (CH_2N(β) / CH_2N(β)), 2.68 / 3.90 (CH_2N(β) / CH_2N(β)), 2.55 / 3.90 (CH_2N(β) / CH_2N(β)), 2.55 / 2.80 (CH_2N(β) / CH_2N(β)), 0.64 / 3.23 (CH_3 of ^{i}Pr(β) / C*H* of ^{i}Pr(β)), 0.54 / 3.23 (CH_3 of ^{i}Pr(β) / C*H* of ^{i}Pr(β)), 0.51 / 3.70 (CH_3 of ^{i}Pr(T) / C*H* of ^{i}Pr(T)).

^{1}H-^{13}C HMBC (600 MHz / 151 MHz, CD_2Cl_2, 250 K)[selected cross-peaks]: δ = 7.98 / 133.9 (*o* of PPh_2(β) / *o* of PPh_2(β)), 7.98 / 131.6 (*o* of PPh_2(β) / *i* of PAr(β)), 7.88 / 133.1 (*o* of PPh_2(β) / *o* of PPh_2(β)), 7.22 / 133.6 (*o* of PPh_2(β) / *o* of PPh_2(β)), 6.78 / 164.5 (*H*5 of PAr(β) / *C*1 of PAr(β)), 6.78 / 128.0 (*H*5 of PAr(β) / *C*3 of PAr(β)), 6.78 / 33.9 (*H*5 of PAr(β) / *C* of ^{t}Bu^4(β)), 6.69 / 168.3 (*H*5 of PAr(β) / *C*1 of PAr(β)), 6.69 / 34.0 (*H*5 of PAr(β) / *C* of ^{t}Bu^4(β)), 6.46 / 167.3 (*H*5 of PAr(T) / *C*1 of PAr(T)), 6.46 / 33.9 (*H*5 of PAr(T) / *C* of ^{t}Bu^4(T)), 2.55 / 50.1 (CH_2N(β) / *C*H_2N(β)), 1.47 / 139.0 (CH_3 of ^{t}Bu^2(β) / *C*2 of PAr(β)), 1.47 / 35.7 (CH_3 of ^{t}Bu^2(β) / *C* of ^{t}Bu^2(β)), 1.47 / 29.7 (CH_3 of ^{t}Bu^2(β) / *C*H_3 of ^{t}Bu^2(β)), 1.45 / 137.9 (CH_3 of ^{t}Bu^2(T) / *C*2 of PAr(T)), 1.47 / 35.5 (CH_3 of ^{t}Bu^2(T) / *C* of ^{t}Bu^2(T)), 1.47 / 29.7 (CH_3 of ^{t}Bu^2(T) / *C*H_3 of ^{t}Bu^2(T)), 1.22 / 69.4 (CH_3 of ^{i}Pr(β) / *C*H of ^{i}Pr(β)), 1.22 / 27.5 (CH_3 of ^{i}Pr(β) / *C*H_3 of ^{i}Pr(β)), 1.17 / 139.3 (CH_3 of ^{t}Bu^2(β) / *C*2 of PAr(β)), 1.17 / 35.3 (CH_3 of ^{t}Bu^2(β) / *C* of ^{t}Bu^2(β)), 1.17 / 29.4 (CH_3 of ^{t}Bu^2(β) / *C*H_3 of ^{t}Bu^2(β)), 1.16 / 69.4 (CH_3 of ^{i}Pr(β) / *C*H of ^{i}Pr(β)), 1.13 / 134.0 (CH_3 of ^{t}Bu^4(β) / *C*4 of PAr(β)), 0.64 / 69.2 (CH_3 of ^{i}Pr(β) / *C*H of ^{i}Pr(β)), 0.64 / 26.7 (CH_3 of ^{i}Pr(β) / *C*H_3 of ^{i}Pr(β)), 0.54 / 69.2 (CH_3 of ^{i}Pr(β) / *C*H of ^{i}Pr(β)), 0.54 / 26.7 (CH_3 of ^{i}Pr(β) / *C*H_3 of ^{i}Pr(β)), 0.51 / 67.6 (CH_3 of ^{i}Pr(T) / *C*H of ^{i}Pr(T)), 0.51 / 26.9 (CH_3 of ^{i}Pr(T) / *C*H_3 of ^{i}Pr(T)).

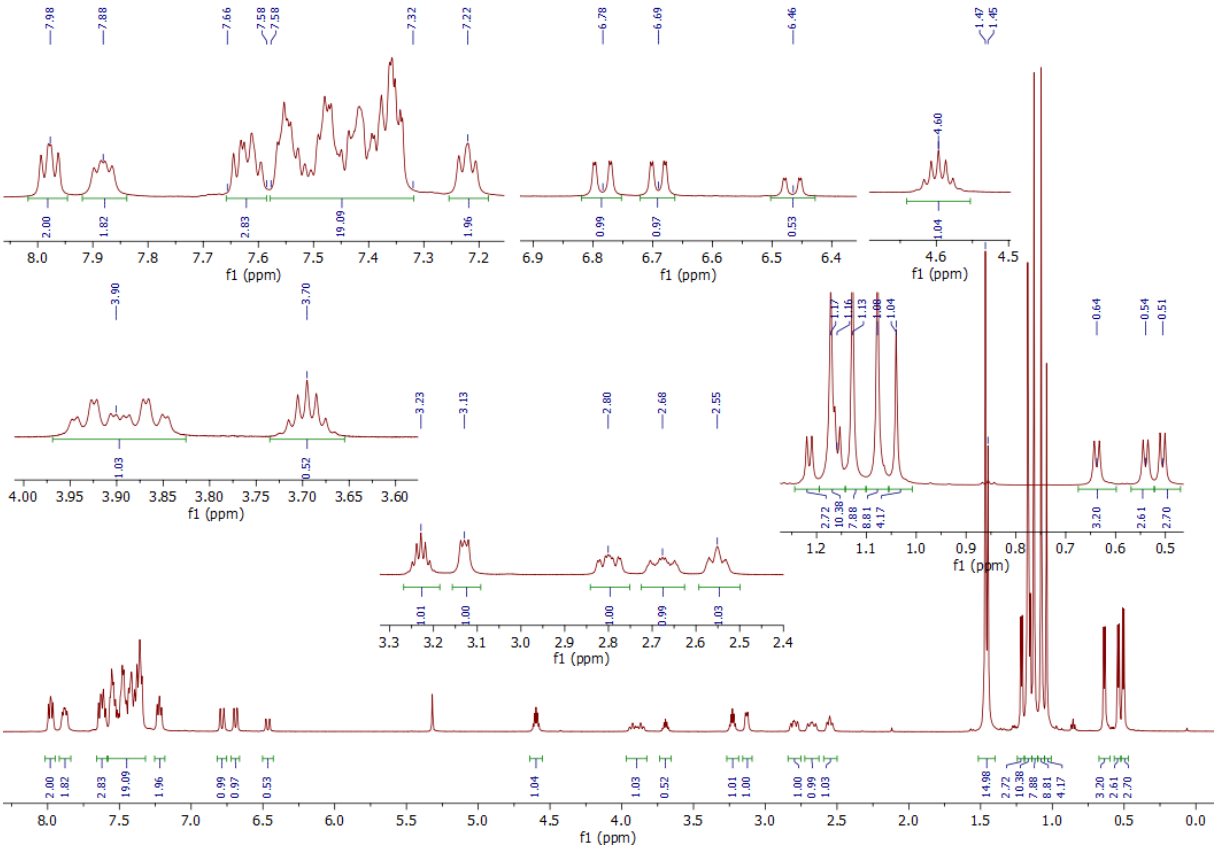

Figure S41: ^{1}H NMR (600 MHz, CD_2Cl_2, 250 K) of 3a

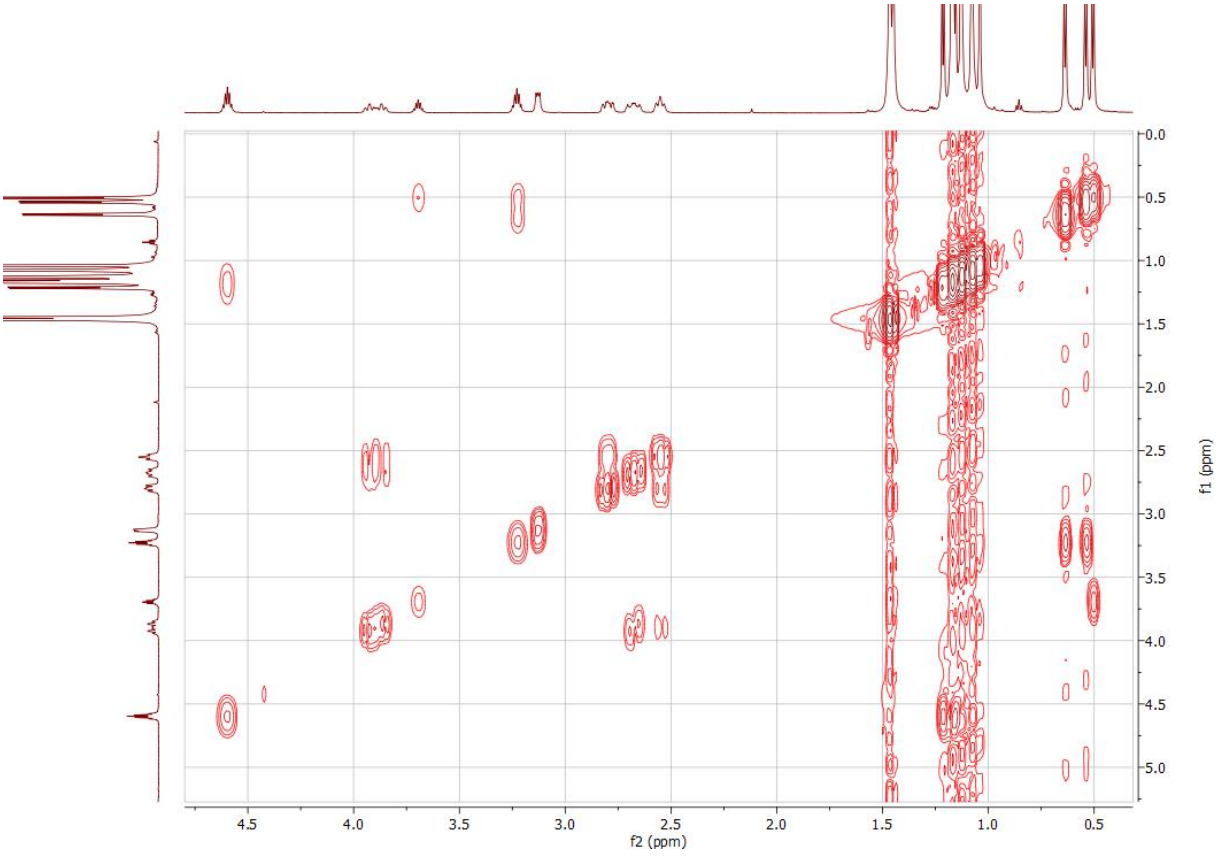

Figure S42: ^{1}H-^{1}H COSY (600 MHz, CD_2Cl_2, 250 K)(Aliphatic region) of 3a

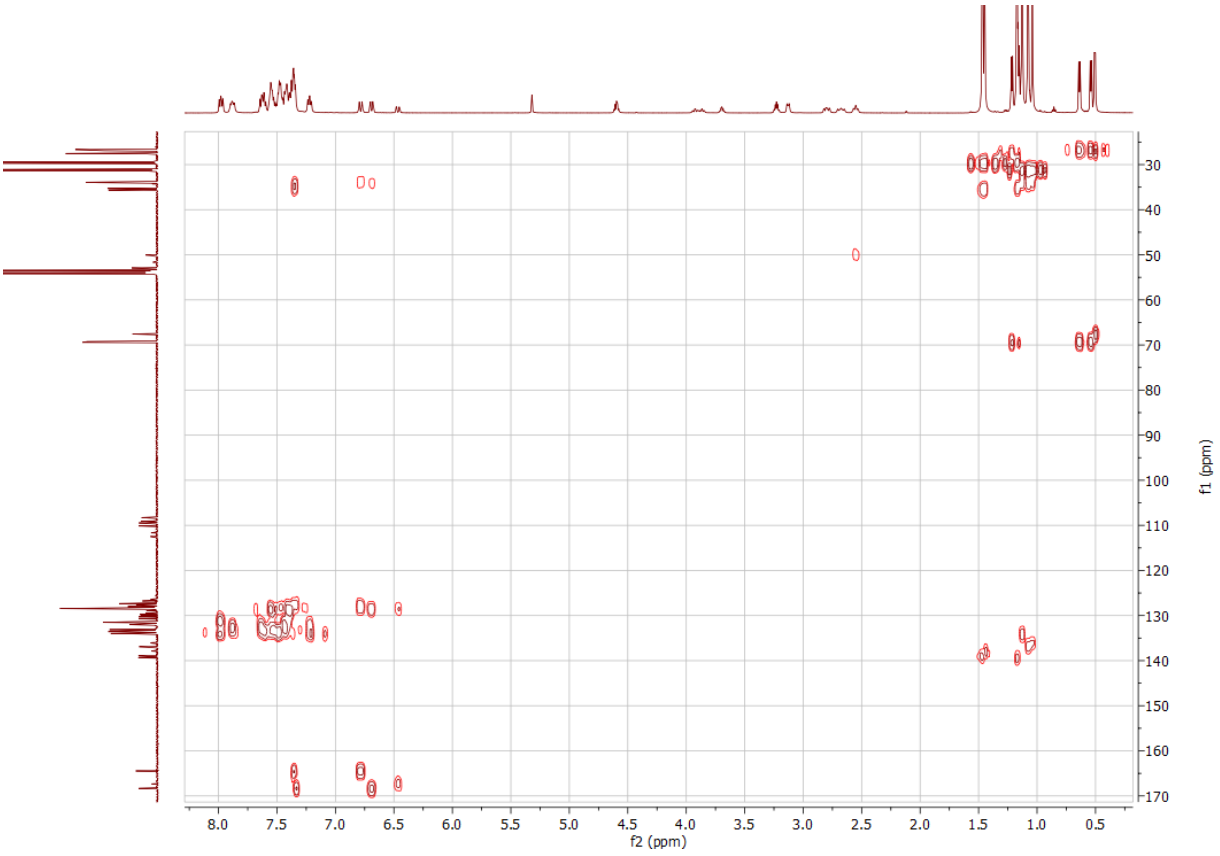

Figure S43: ^{1}H-^{13}C HMBC (600 MHz / 151 MHz, CD_2Cl_2, 250 K)(whole spectrum) of 3a

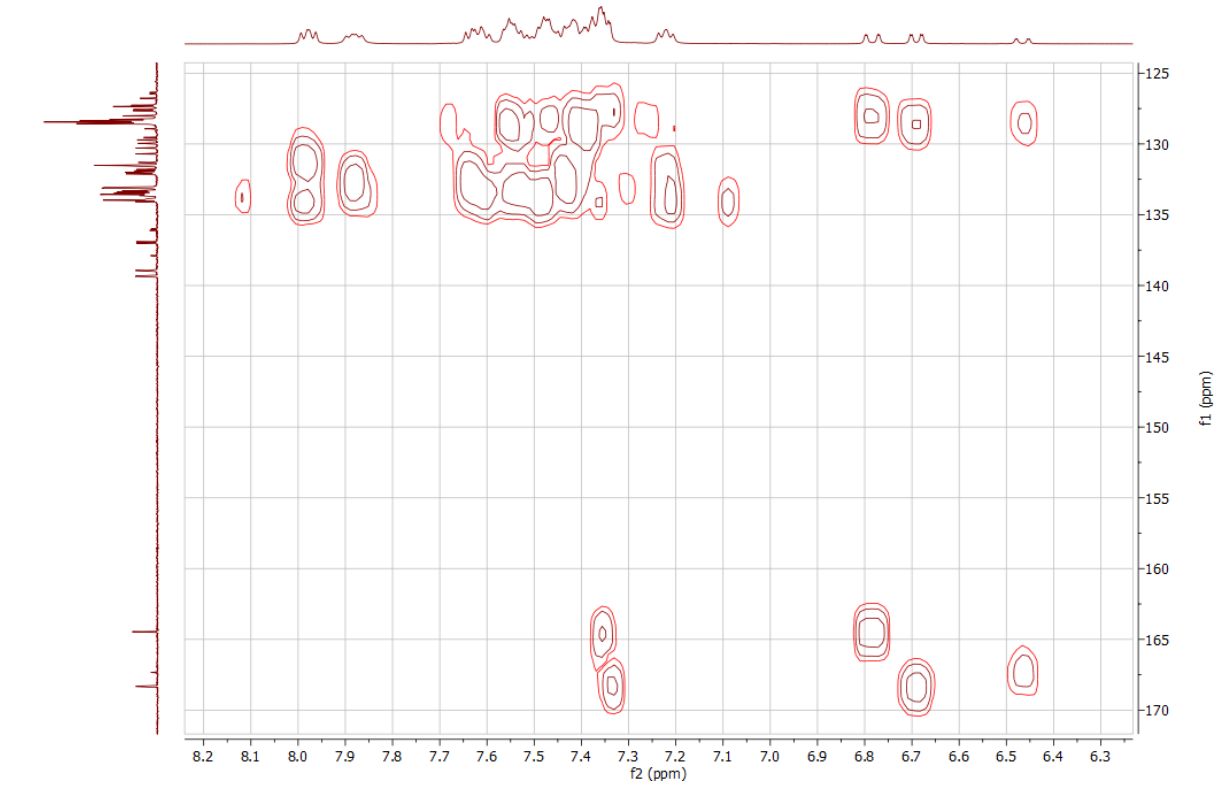

Figure S44: ^{1}H-^{13}C HMBC (600 MHz / 151 MHz, CD_2Cl_2, 250 K)(zoom) of 3a

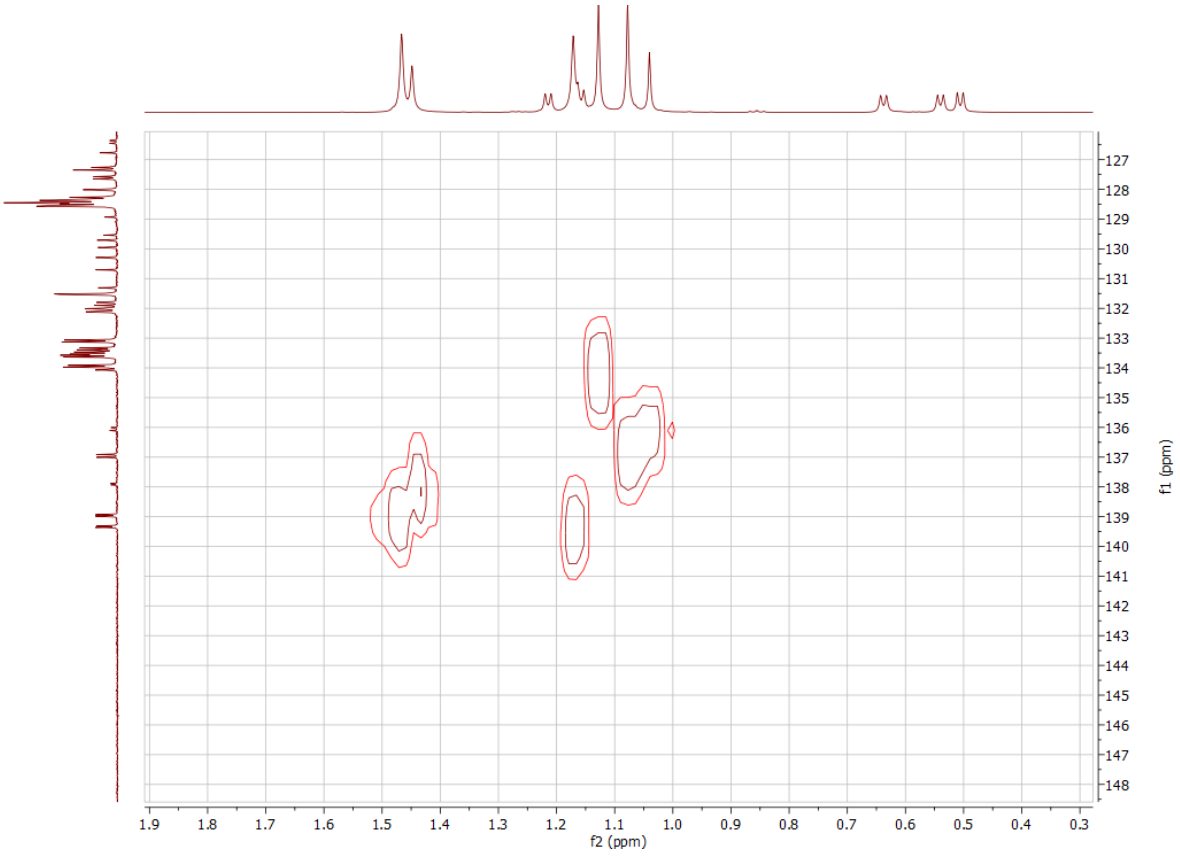

Figure S45: ^{1}H-^{13}C HMBC (600 MHz / 151 MHz, CD_2Cl_2, 250 K)(zoom) of 3a

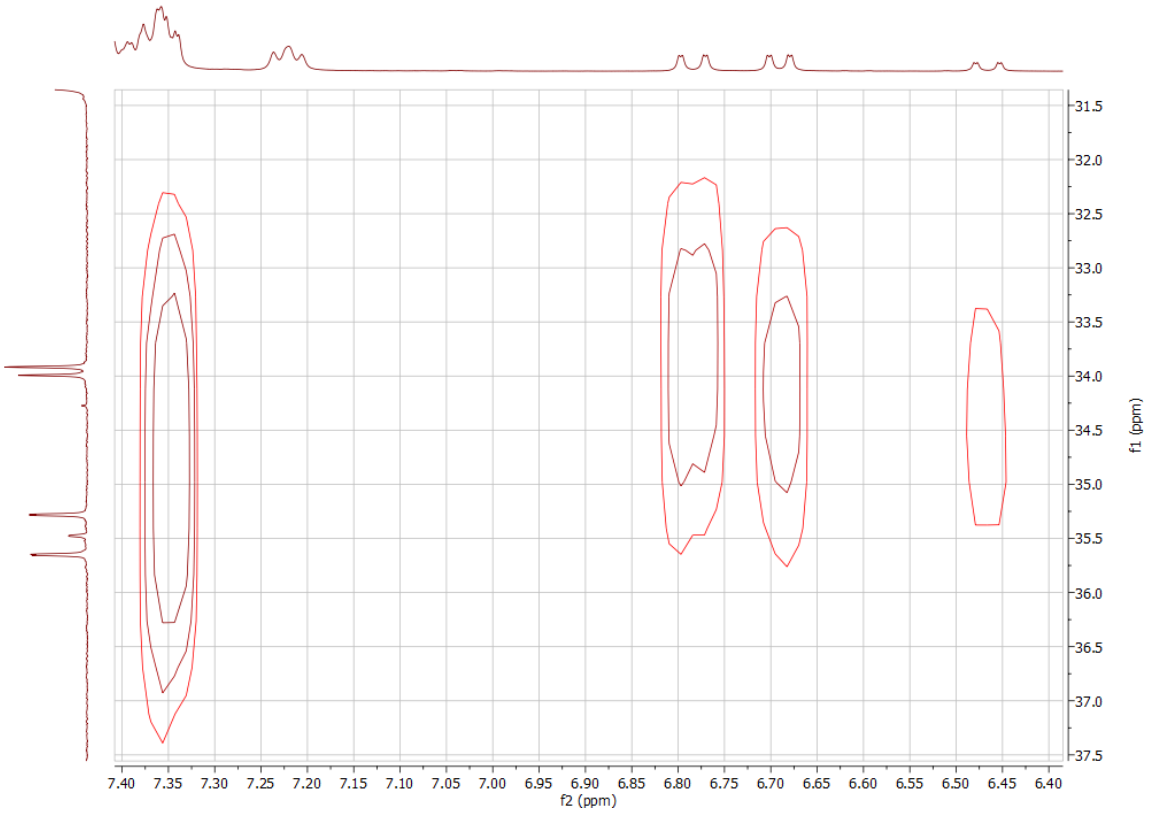

Figure S46: ^{1}H-^{13}C HMBC (600 MHz / 151 MHz, CD_2Cl_2, 250 K)(zoom) of 3a

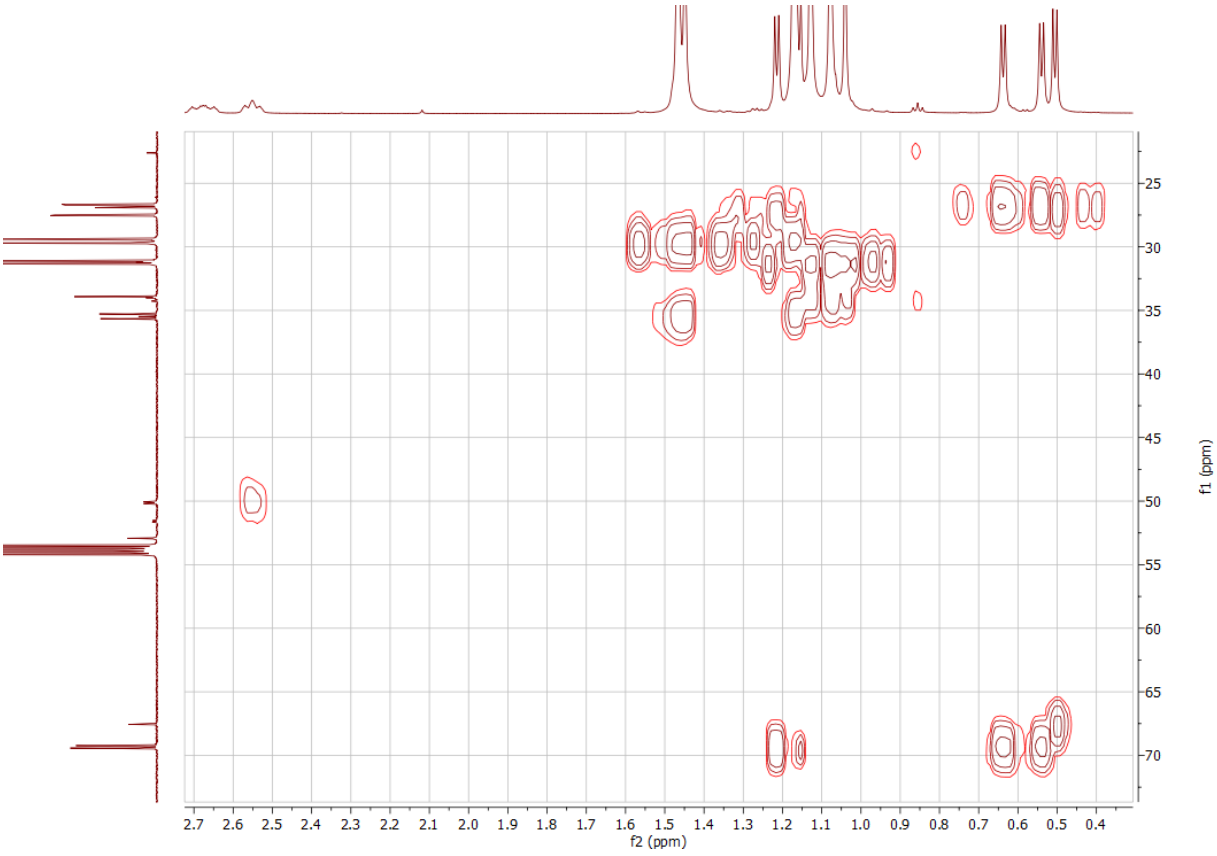

Figure S47: ^{1}H-^{13}C HMBC (600 MHz / 151 MHz, CD_2Cl_2, 250 K)(zoom) of 3a

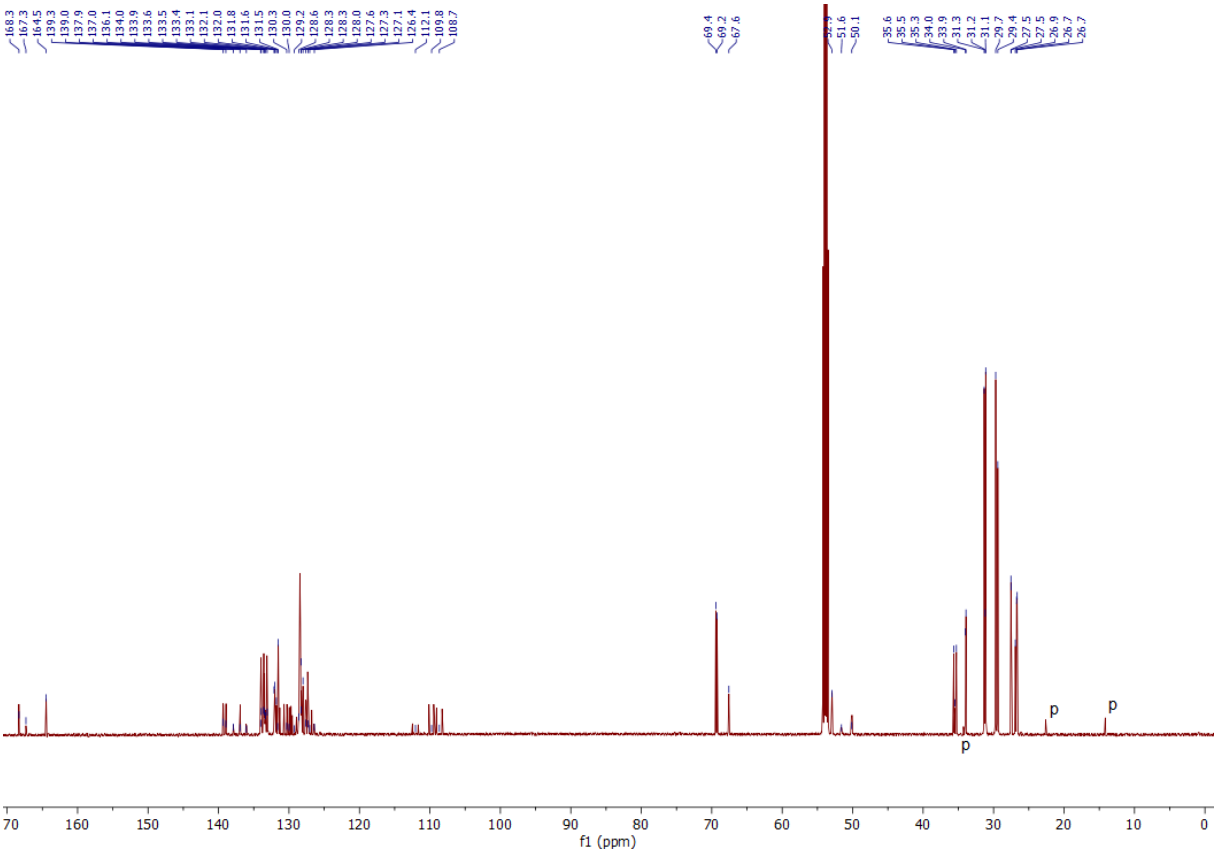

Figure S48: $^{13}C\{^{1}H\}$ NMR (151 MHz, CD_2Cl_2, 250 K)(whole spectrum) of 3a

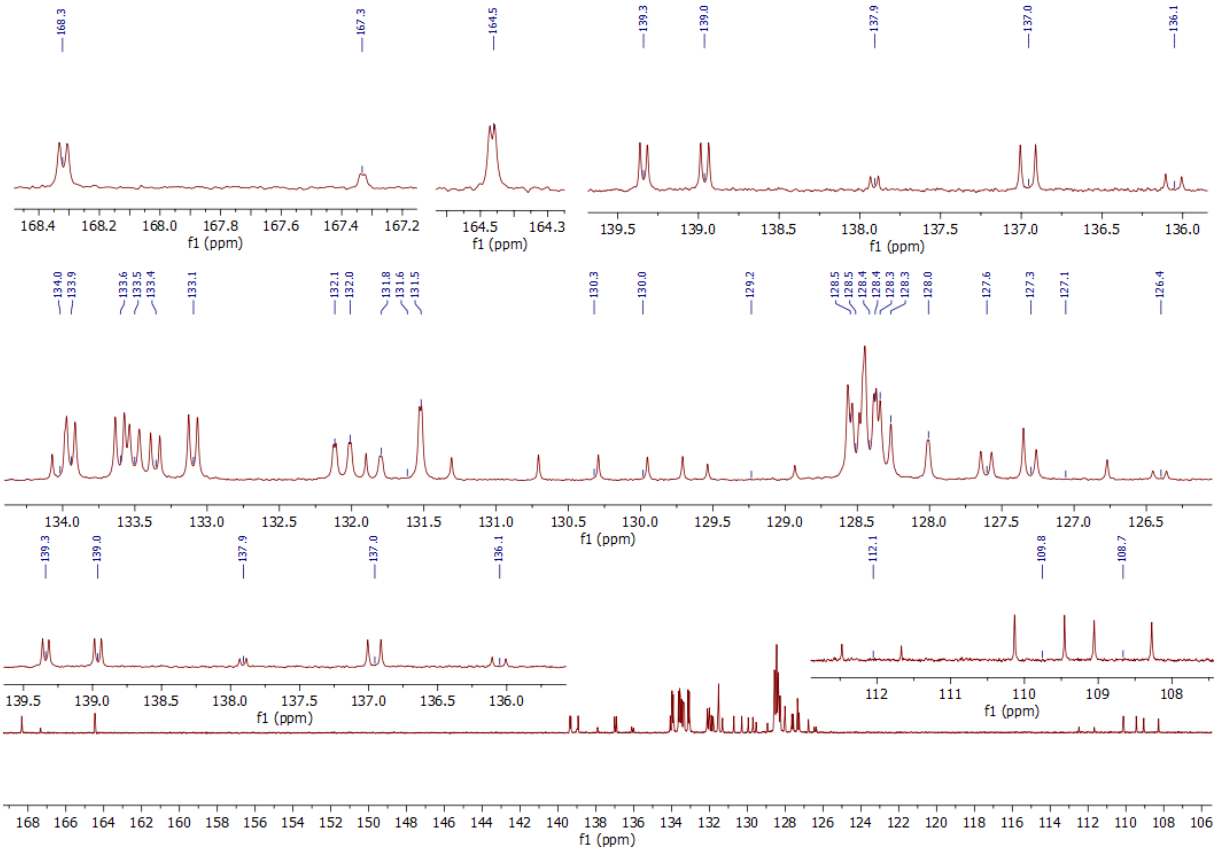

Figure S49: $^{13}C\{^{1}H\}$ NMR (151 MHz, CD_2Cl_2, 250 K)(aromatic region) of 3a

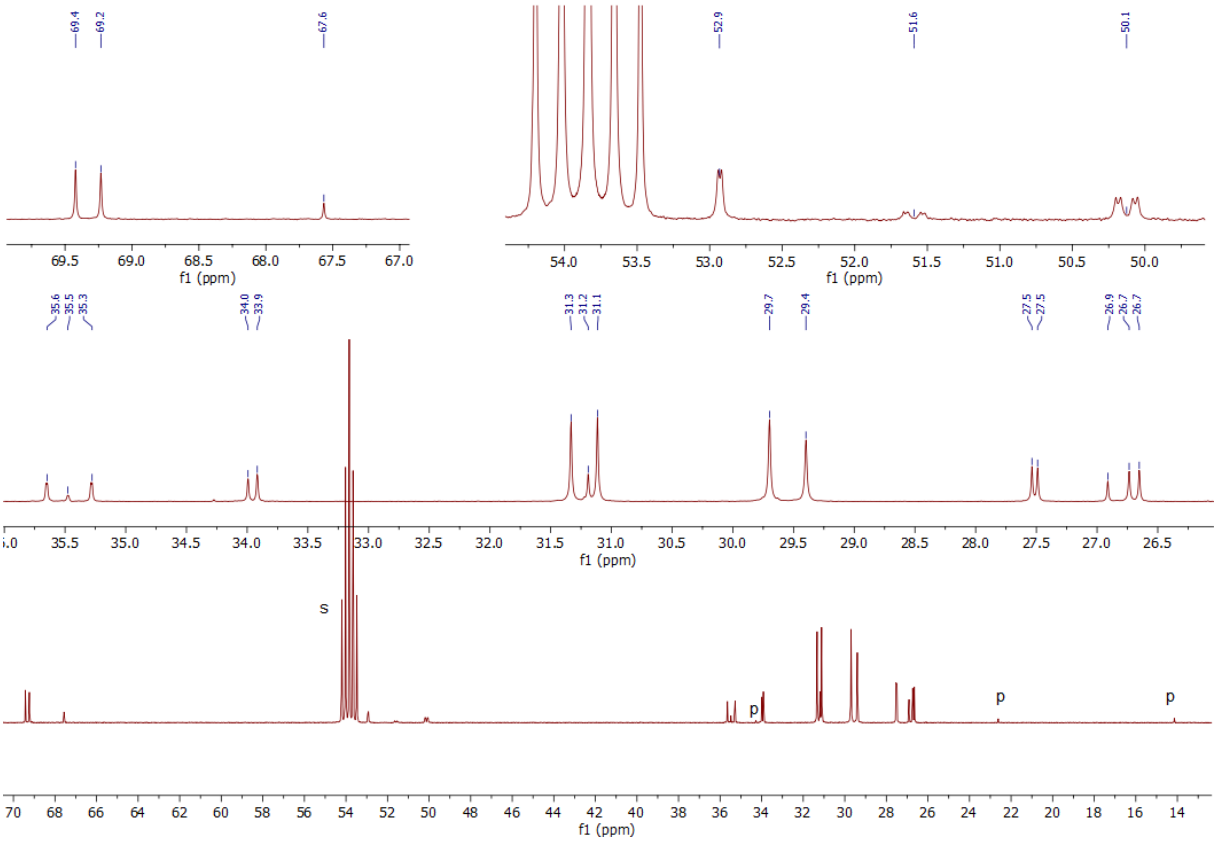

Figure S50: $^{13}C\{^{1}H\}$ NMR (151 MHz, CD_2Cl_2, 250 K)(aliphatic region) of 3a

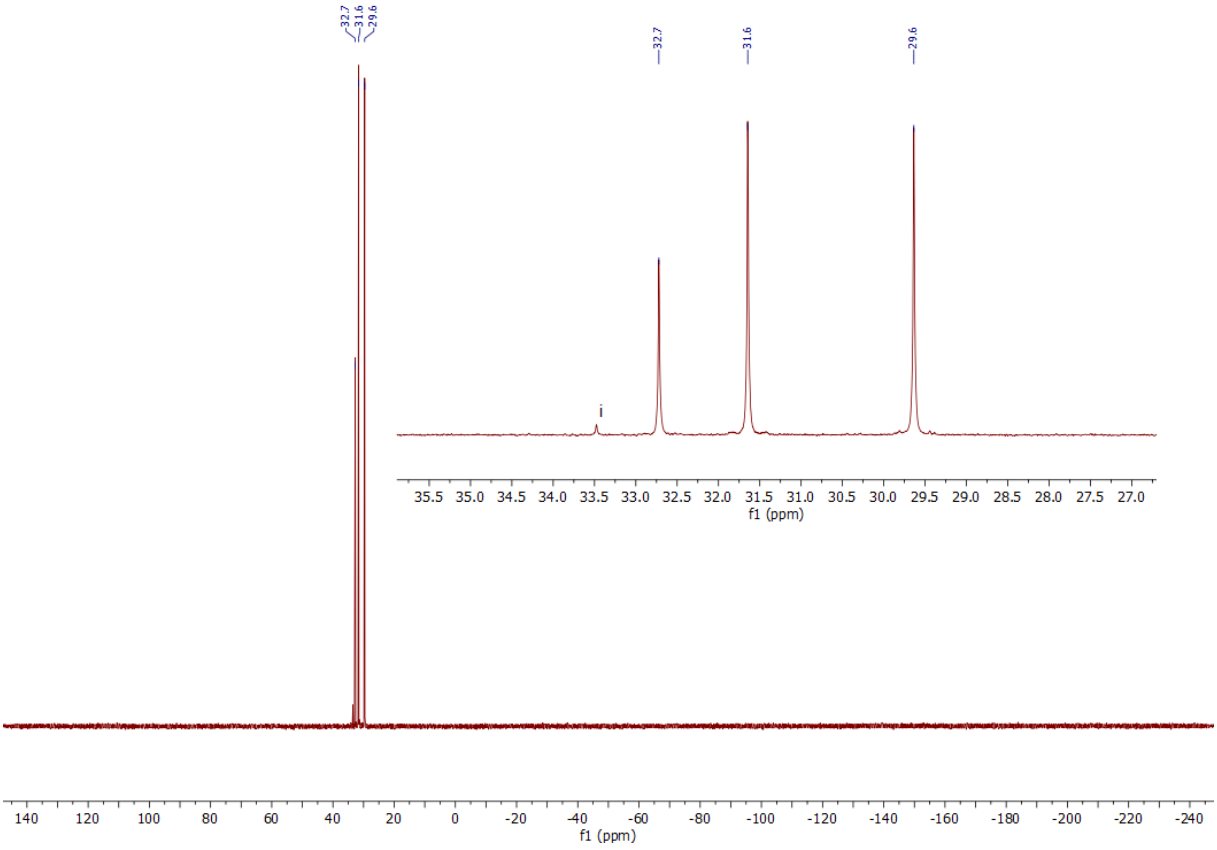

Figure S51: $^{31}P\{^{1}H\}$ NMR (243 MHz, CD_2Cl_2, 250 K) of 3a

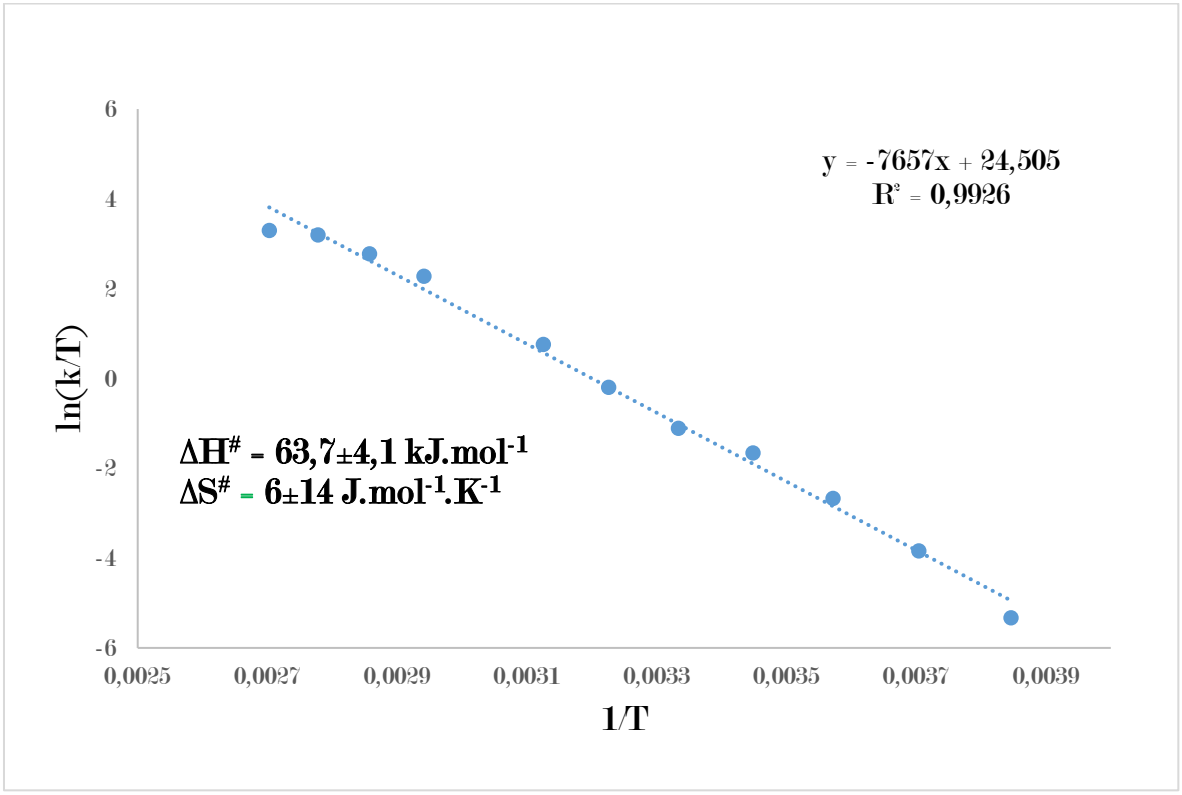

Figure S52: Eyring plot of ln(k/T) against 1/T for the isomerisation between the Δ and Λ enantiomers of the *cis*-β isomer of 3a. Expanded incertainties, given at the 95% confidence interval, are estimated from the residual variance of the fit.

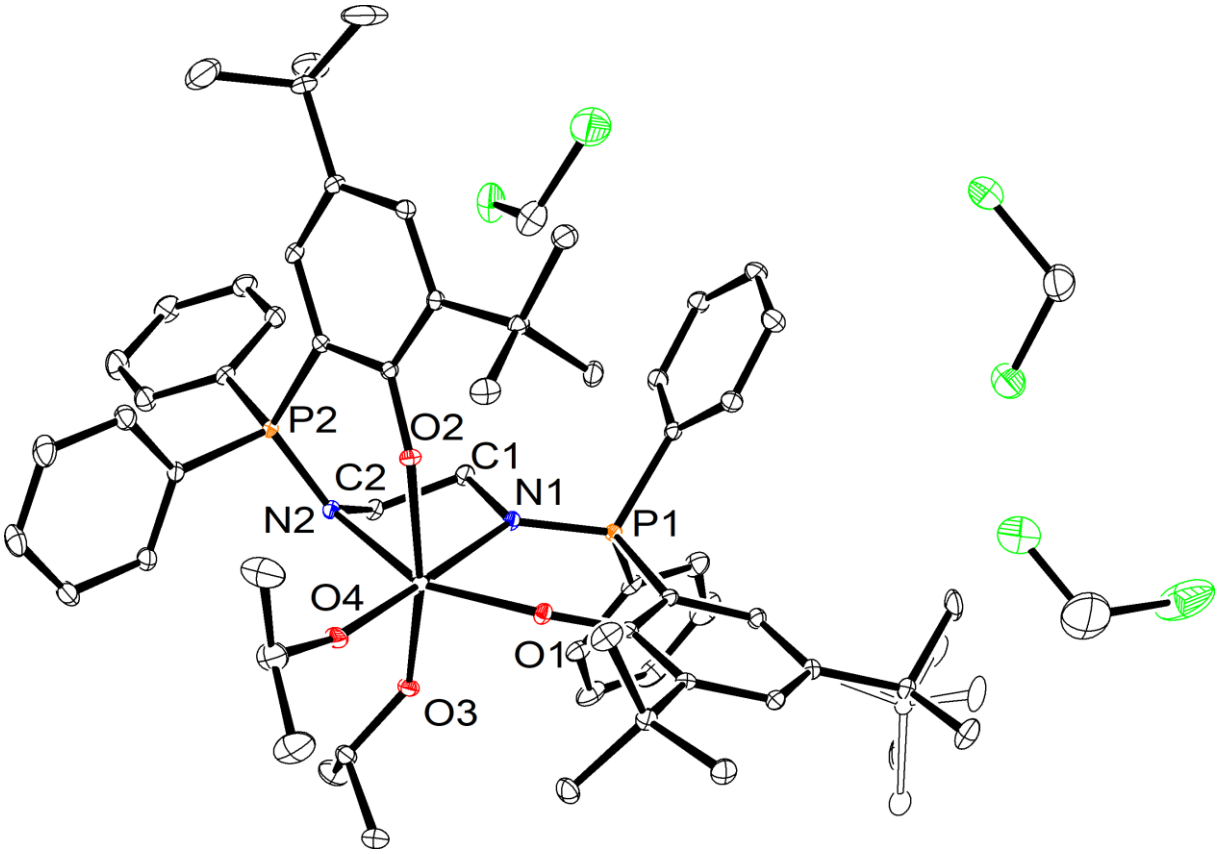

Figure S53: Crystal structure of 3a

Table S7: Crystal data and structure refinement of 3a

Identification code	3a
Internal reference	ral131016_0m
Empirical formula	$C_{63}H_{84}Cl_6N_2O_4P1Zr$
Formula weight	1299.18
Temperature/K	115
Crystal system	triclinic
Space group	P-1
a/Å	13.3263(4)
b/Å	15.6278(5)
c/Å	16.7838(6)
α/°	97.5780(16)
β/°	94.7670(15)
γ/°	106.9900(15)
Volume/Å^3	3286.27(19)
Z	2
ρ_{calc}g/cm^3	1.313
μ/mm^{-1}	0.505
F(000)	1360.0
Crystal size/mm^3	0.47 × 0.35 × 0.30
Radiation	MoKα (λ = 0.71073)
2Θ range for data collection/°	5.248 to 55.202
Index ranges	-17 ≤ h ≤ 17, -20 ≤ k ≤ 20, -21 ≤ l ≤ 21

Reflections collected	93582
Independent reflections	15091 [R_{int} = 0.0393, R_{sigma} = 0.0310]
Data/restraints/parameters	15091/54/741
Goodness-of-fit on F^2	1.045
Final R indexes [I>=2σ (I)]	R_1 = 0.0452, wR_2 = 0.1075
Final R indexes [all data]	R_1 = 0.0637, wR_2 = 0.1208
Largest diff. peak/hole / e $Å^{-3}$	1.85/-1.27
CCDC	1978290

Special refinement details for 3a

One of the tert-butyl groups was found disordered and anisotropically refined over two positions with occupation factors converging to 0.54/0.46.

Complex 3b:

^{1}H-^{1}H COSY (600 MHz, d_8-THF, 250 K)[selected cross-peaks]: δ = 4.19 / 1.02 (C*H* of ^{i}Pr(β) / CH_3 of ^{i}Pr(β)), 4.19 / 0.86 (C*H* of ^{i}Pr(β) / CH_3 of ^{i}Pr(β)), 3.78 / 0.65 (C*H* of ^{i}Pr(T) / CH_3 of ^{i}Pr(T)), 3.40 / 0.79 (C*H* of ^{i}Pr(β) / CH_3 of ^{i}Pr(β)), 3.40 / 0.49 (C*H* of ^{i}Pr(β) / CH_3 of ^{i}Pr(β)), 1.02 / 4.19 (CH_3 of ^{i}Pr(β) / C*H* of ^{i}Pr(β)), 0.86 / 4.19 (CH_3 of ^{i}Pr(β) / C*H* of ^{i}Pr(β)), 0.79 / 3.40 (CH_3 of ^{i}Pr(β) / C*H* of ^{i}Pr(β)), 0.65 / 3.78 (CH_3 of ^{i}Pr(T) / C*H* of ^{i}Pr(T)), 0.49 / 3.40 (CH_3 of ^{i}Pr(β) / C*H* of ^{i}Pr(β)).

^{1}H-^{13}C HMBC (600 MHz / 151 MHz, d_8-THF, 250 K)[selected cross-peaks]: δ = 8.01 / 133.9 (*o* of PPh_2(β) / *o* of PPh_2(β)), 7.82 / 134.2 (*o* of PPh_2(T) / *o* of PPh_2(T)), 7.82 / 132.7 (*o* of PPh_2(T) / *p* of PPh_2(T)), 7.61 / 134.2 (*p* of PPh_2(T) / *o* of PPh_2(T)), 7.35 / 165.1 (*H*3 of PAr(β) / *C*1 of PAr(β)), 7.32 / 168.8 (*H*3 of PAr(T) / *C*1 of PAr(T)), 7.30 / 169.1 (*H*3 of PAr(β) / *C*1 of PAr(β)), 7.03 / 134.7 (*o* of PPh_2(β) / *o* of PPh_2(β)), 7.03 / 132.1 (*o* of PPh_2(β) / *p* of PPh_2(β)), 6.61 / 165.1 (*H*5 of PAr(β) / *C*1 of PAr(β)), 6.61 / 34.5 (*H*5 of PAr(β) / *C* of ^{t}Bu^4(β)), 6.53 / 169.1 (*H*5 of PAr(β) / *C*1 of PAr(β)), 6.53 / 34.3 (*H*5 of PAr(β) / *C* of ^{t}Bu^4(β)), 6.42 / 168.8 (*H*5 of PAr(T) / *C*1 of PAr(T)), 6.42 / 34.4 (*H*5 of PAr(T) / *C* of ^{t}Bu^4(T)), 1.36 / 138.6 (CH_3 of ^{t}Bu^2(β) / *C*2 of PAr(β)), 1.36 / 36.0 (CH_3 of ^{t}Bu^2(β) / *C* of ^{t}Bu^2(β)), 1.36 / 30.2 (CH_3 of ^{t}Bu^2(β) / *C*H_3 of ^{t}Bu^2(β)), 1.30 / 137.9 (CH_3 of ^{t}Bu^2(T) / *C*2 of PAr(T)), 1.30 / 35.7 (CH_3 of ^{t}Bu^2(T) / *C* of ^{t}Bu^2(T)), 1.36 / 30.4 (CH_3 of ^{t}Bu^2(T) / *C*H_3 of ^{t}Bu^2(T)), 1.12 / 137.7 (CH_3 of ^{t}Bu^4(β) / *C*4 of PAr(β)), 1.12 /34.5 (CH_3 of ^{t}Bu^4(β) / *C* of ^{t}Bu^4(β)), 1.12 / 31.6 (CH_3 of ^{t}Bu^4(β) / *C*H_3 of ^{t}Bu^4(β)), 1.02 / 69.9 (CH_3 of ^{i}Pr(β) / *C*H of ^{i}Pr(β)), 1.02 / 27.1 (CH_3 of ^{i}Pr(β) / *C*H_3 of ^{i}Pr(β)), 1.00 / 139.9 (CH_3 of ^{t}Bu^2(β) / *C*2 of PAr(β)), 1.00 / 35.5 (CH_3 of ^{t}Bu^2(β) / *C* of ^{t}Bu^2(β)), 1.00 / 30.0 (CH_3 of ^{t}Bu^2(β) / *C*H_3 of ^{t}Bu^2(β)), 0.86 / 69.9 (CH_3 of ^{i}Pr(β) / *C*H of ^{i}Pr(β)), 0.86 / 27.4 (CH_3 of ^{i}Pr(β) / *C*H_3 of ^{i}Pr(β)), 0.79 / 70.2 (CH_3 of ^{i}Pr(β) / *C*H of ^{i}Pr(β)), 0.79 / 27.3 (CH_3 of ^{i}Pr(β) / *C*H_3 of ^{i}Pr(β)), 0.65 / 68.9 (CH_3 of ^{i}Pr(T) / *C*H of ^{i}Pr(T)), 0.65 / 27.5 (CH_3 of ^{i}Pr(T) / *C*H_3 of ^{i}Pr(T)), 0.49 / 70.2 (CH_3 of ^{i}Pr(β) / *C*H of ^{i}Pr(β)), 0.49 / 27.5 (CH_3 of ^{i}Pr(β) / *C*H_3 of ^{i}Pr(β)).

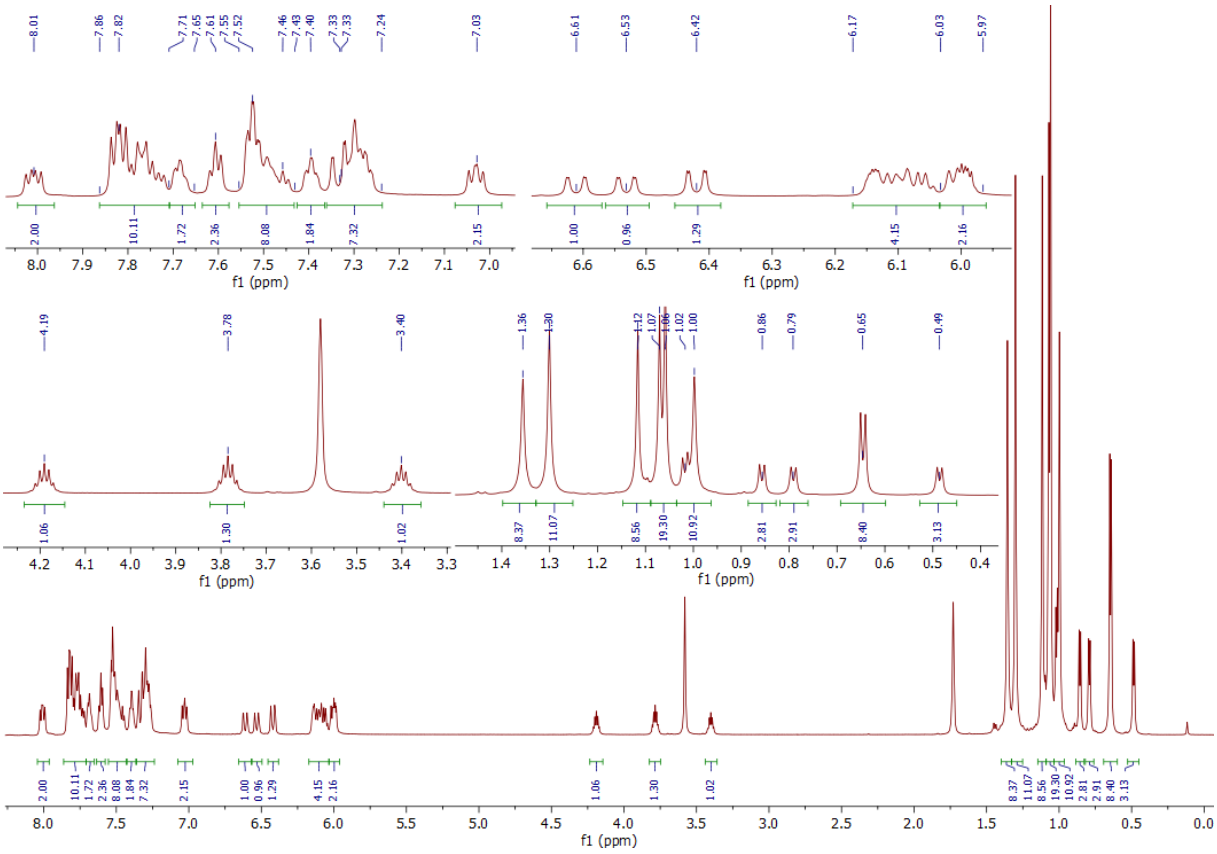

Figure S54: ^{1}H NMR (600 MHz, d_8-THF, 250 K) of 3b

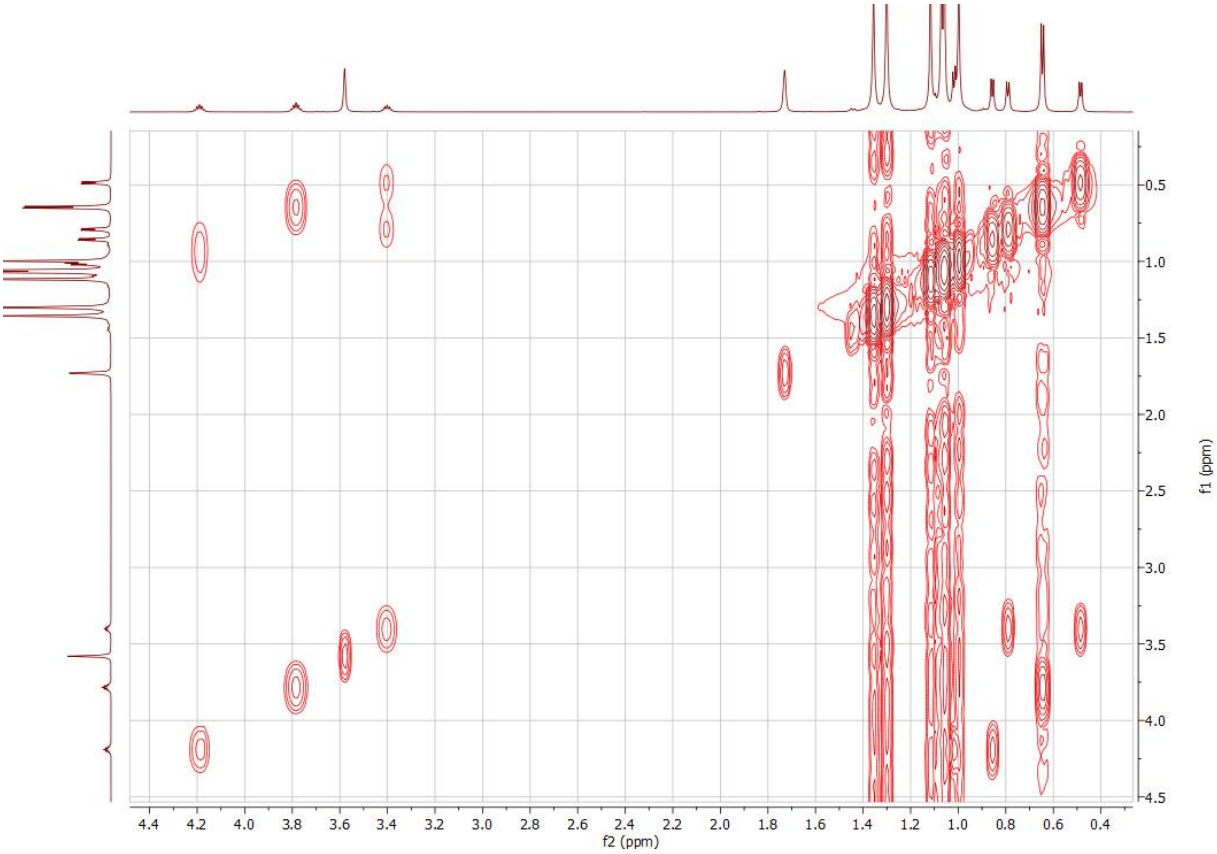

Figure S55: ^{1}H-^{1}H COSY (600 MHz, d_8-THF, 250 K) of 3b

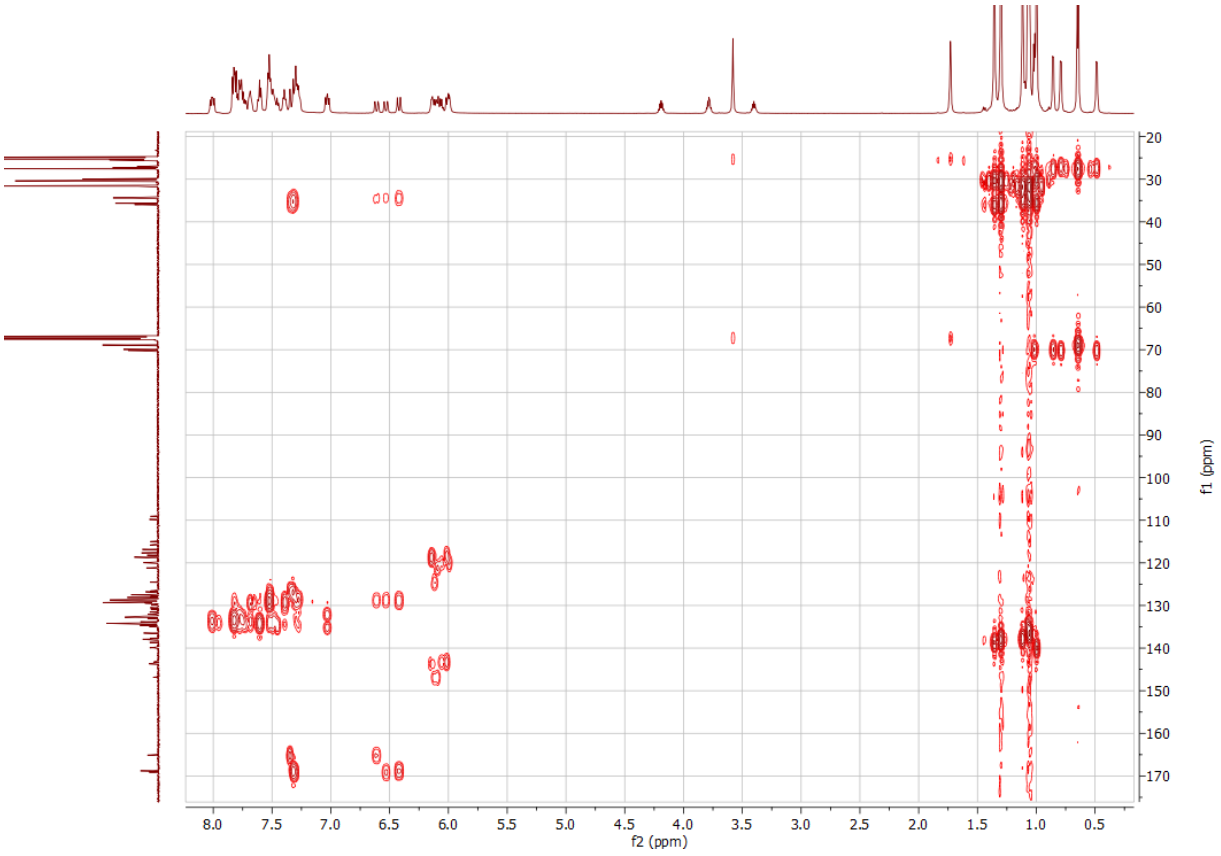

Figure S56: ^{1}H-^{13}C HMBC (600 MHz / 151 MHz, d_8-THF, 250 K)(whole spectrum) of 3b

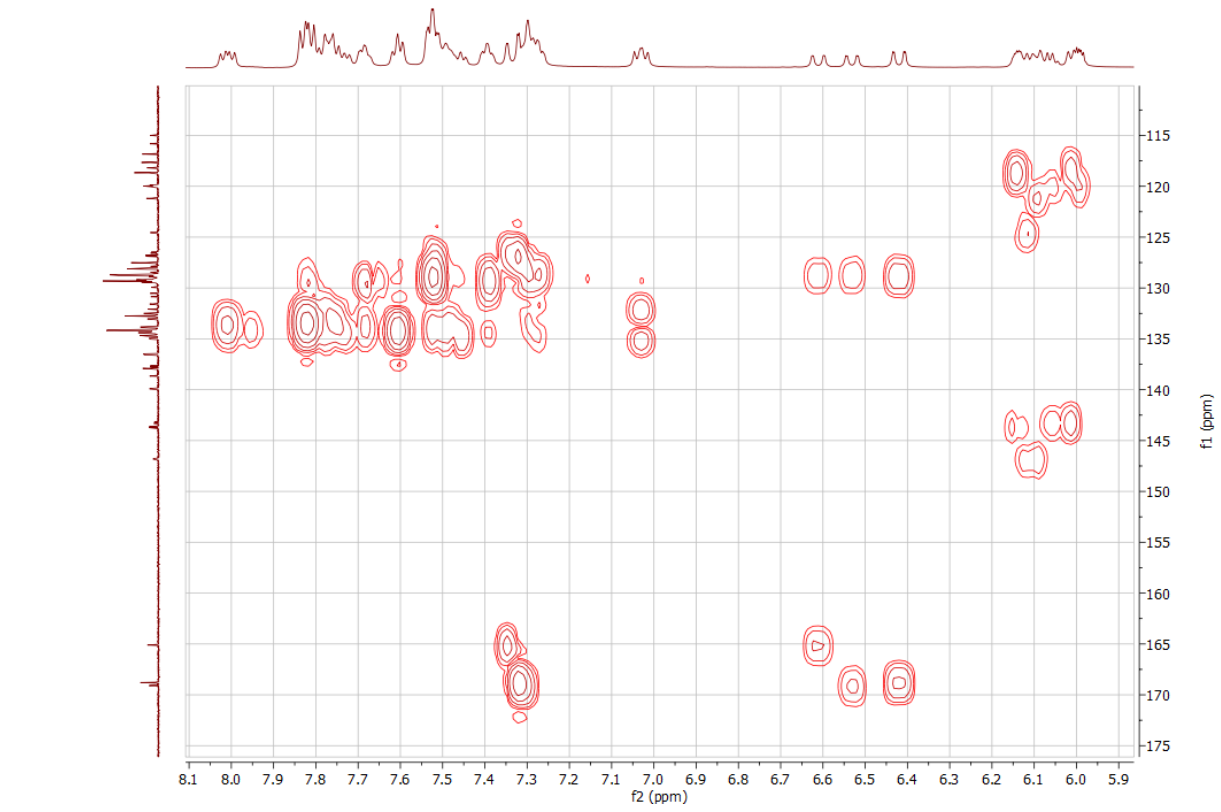

Figure S57: ^{1}H-^{13}C HMBC (600 MHz / 151 MHz, d_8-THF, 250 K)(zoom) of 3b

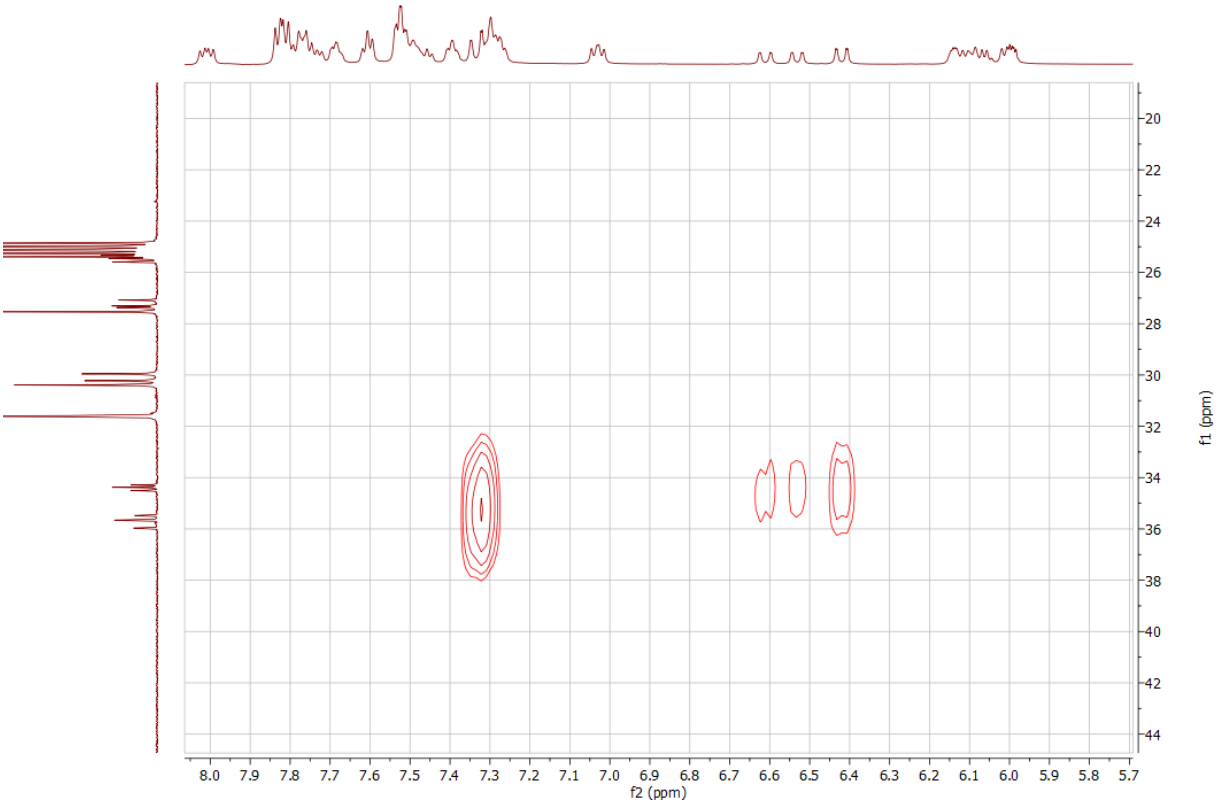

Figure S58: ^{1}H-^{13}C HMBC (600 MHz / 151 MHz, d_8-THF, 250 K)(zoom) of 3b

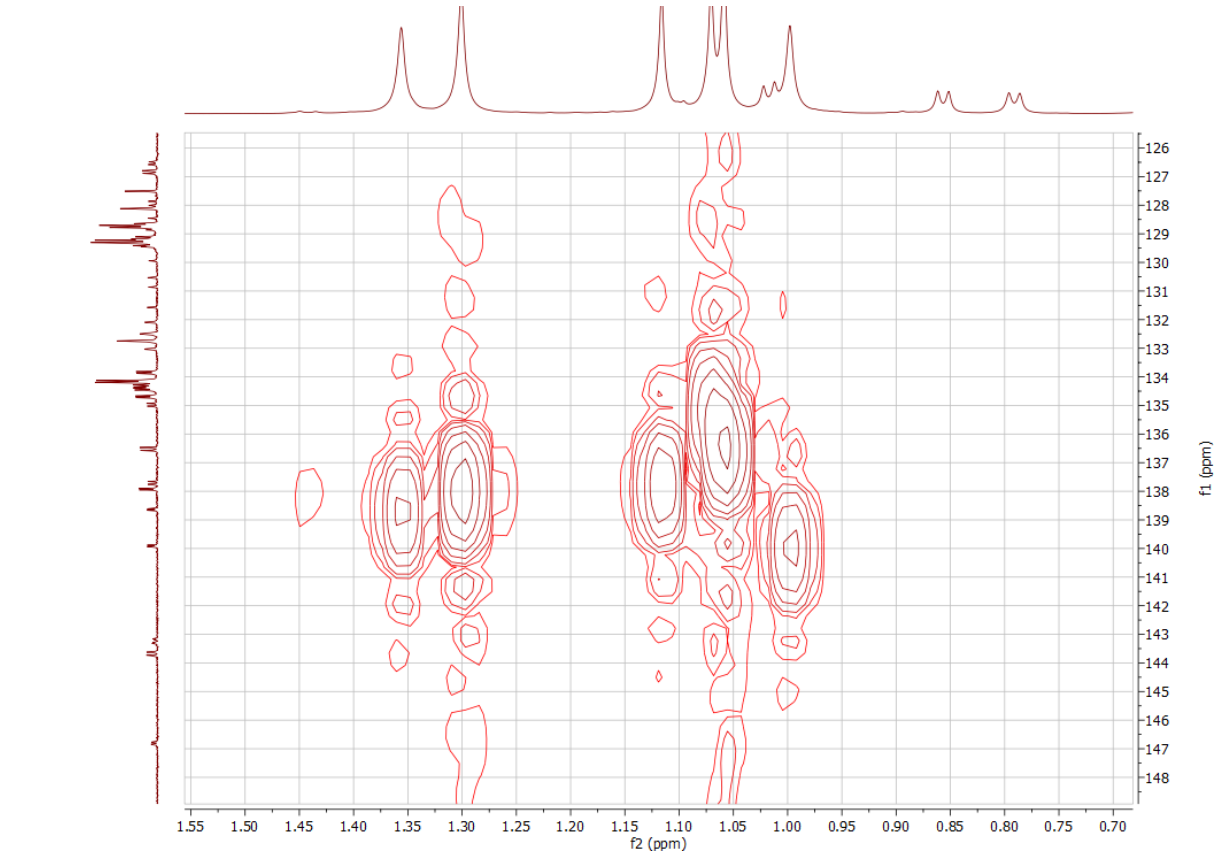

Figure S59: ^{1}H-^{13}C HMBC (600 MHz / 151 MHz, d_8-THF, 250 K)(zoom) of 3b

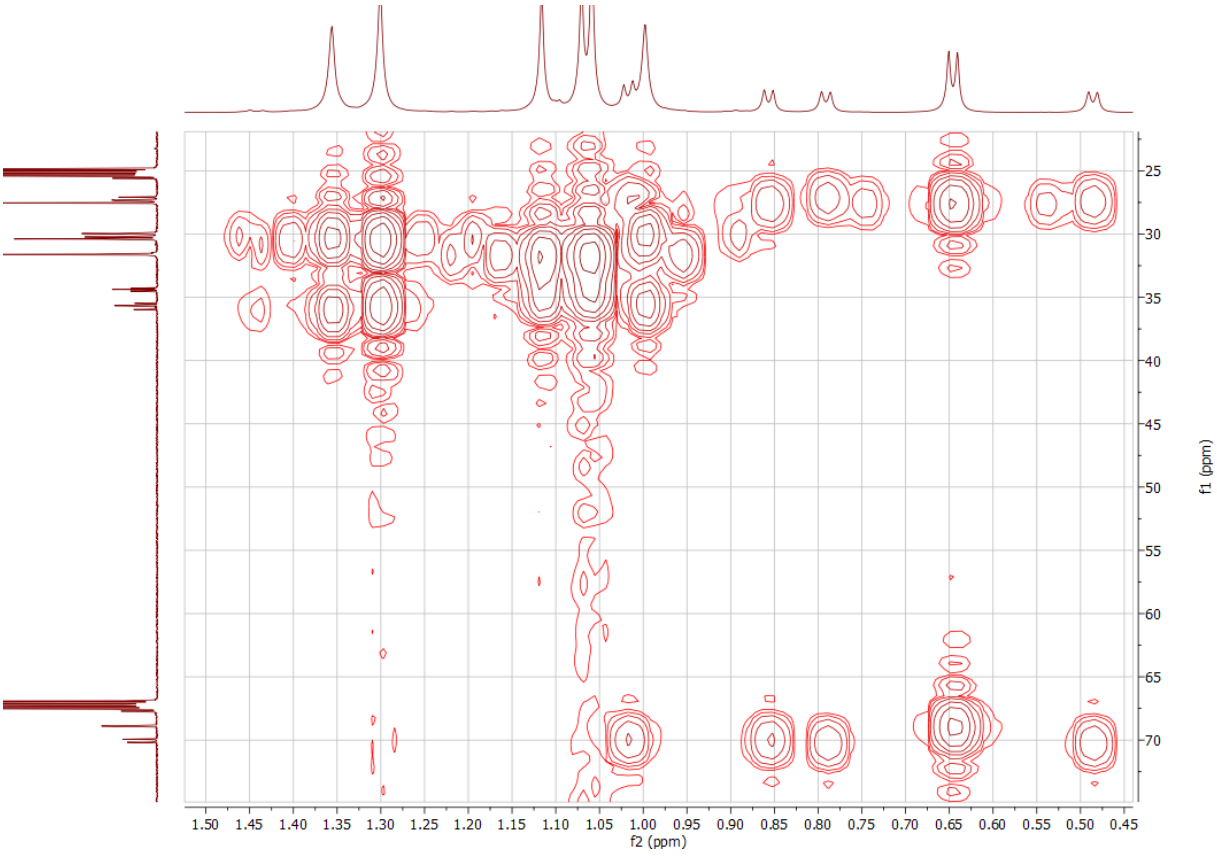

Figure S60: ^{1}H-^{13}C HMBC (600 MHz / 151 MHz, d_8-THF, 250 K)(zoom) of 3b

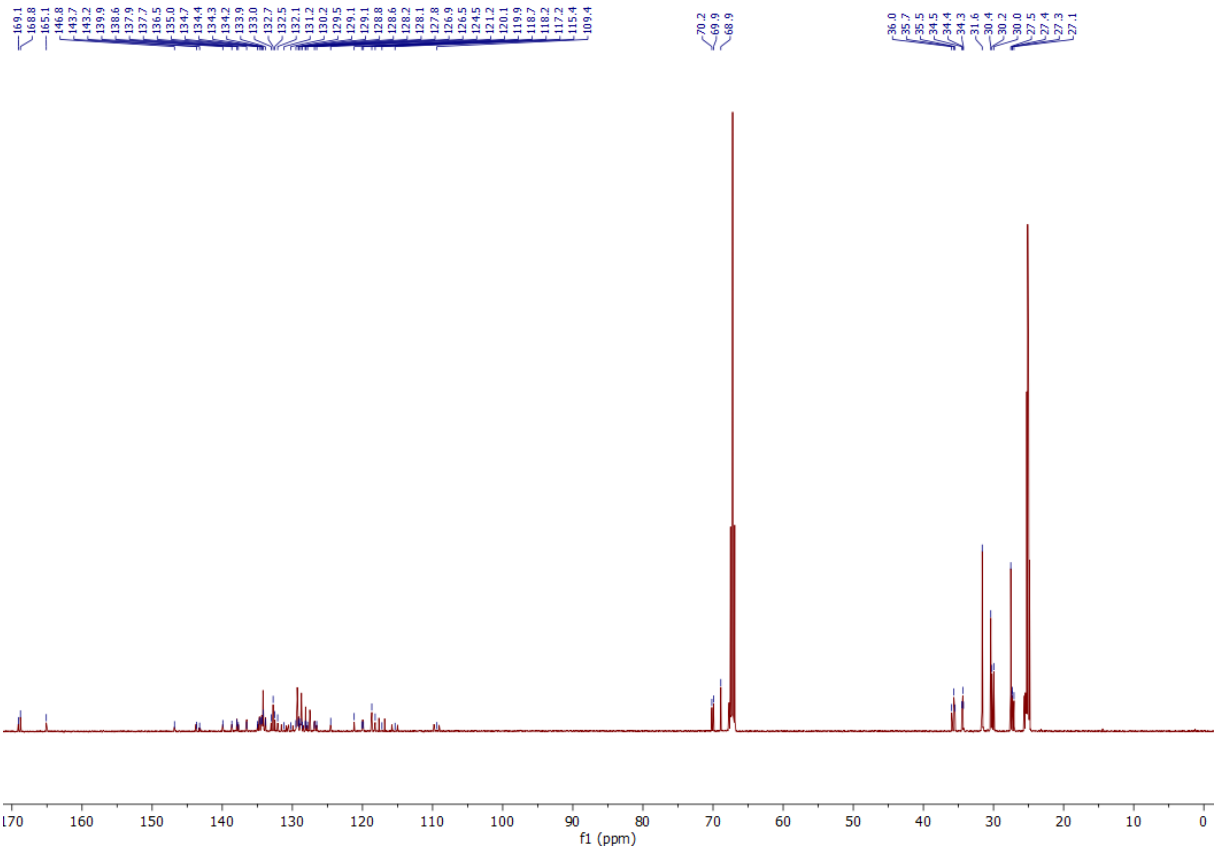

Figure S61: ^{13}C{^{1}H} NMR (151 MHz, d_8-THF, 250 K)(whole spectrum) of 3b

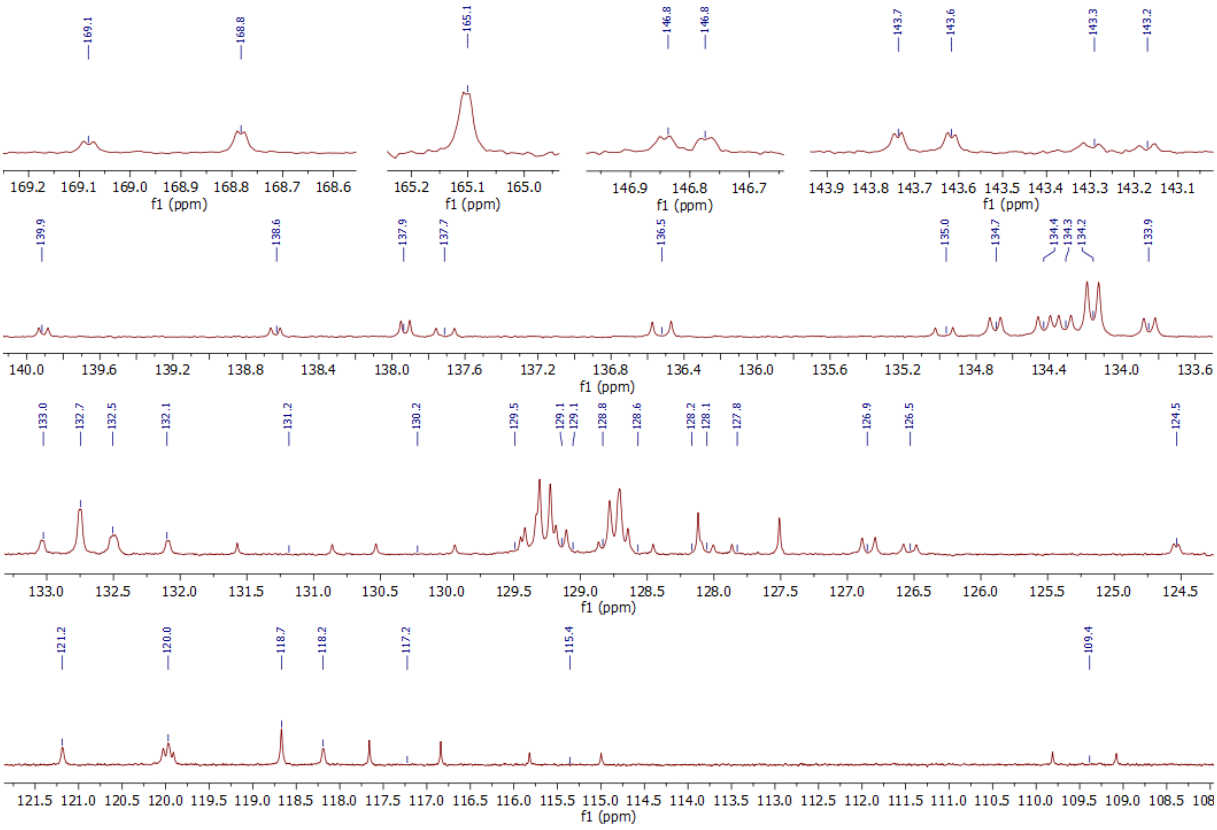

Figure S62: $^{13}C\{^{1}H\}$ NMR (151 MHz, d_8-THF, 250 K)(aromatic region) of 3b

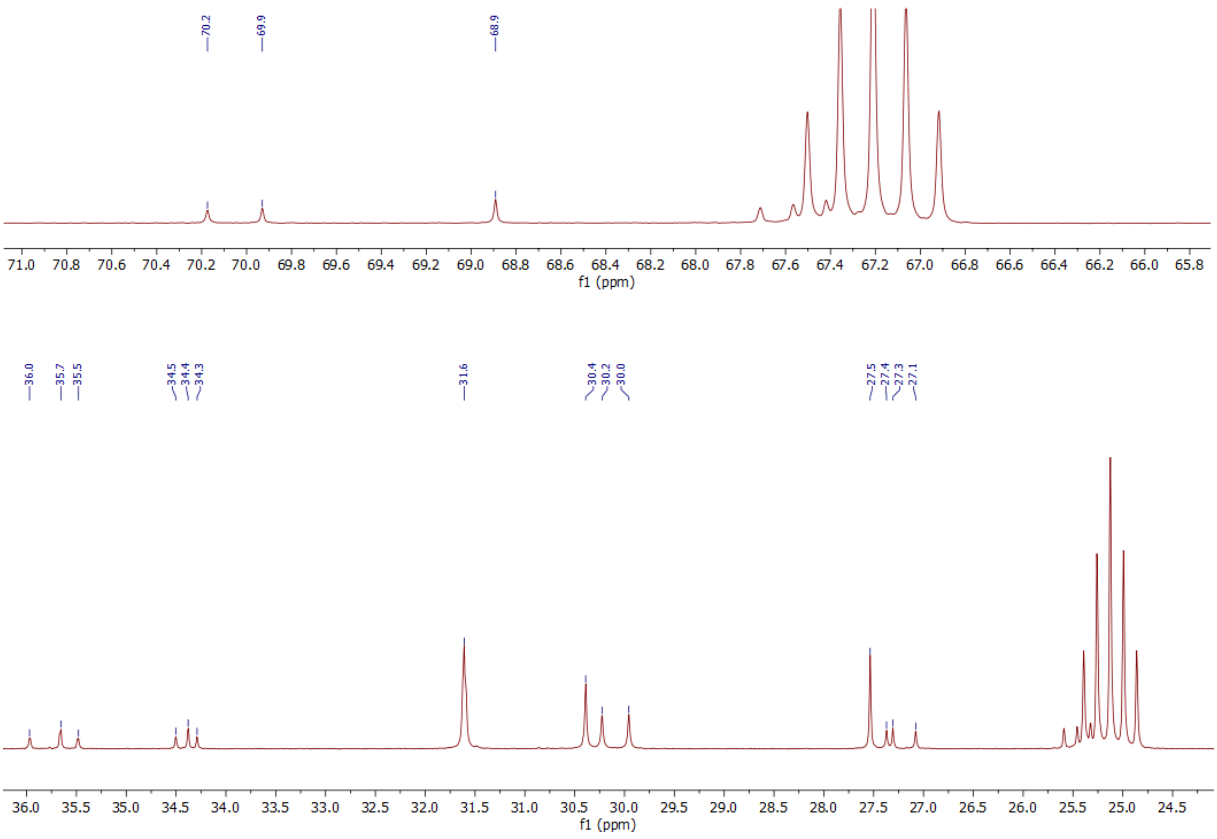

Figure S63: $^{13}C\{^{1}H\}$ NMR (151 MHz, d_8-THF, 250 K)(aliphatic region) of 3b

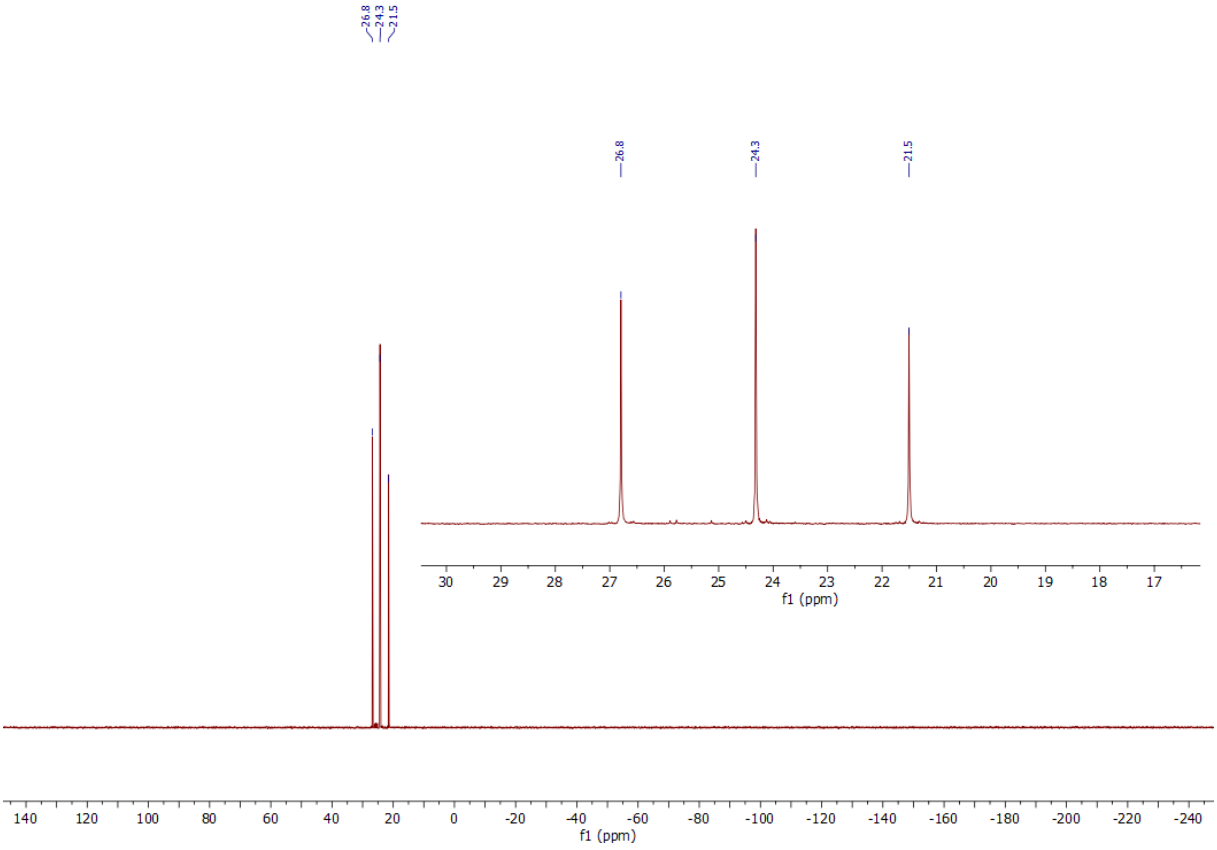

Figure S64: $^{31}P\{^{1}H\}$ NMR (243 MHz, d_8-THF, 250 K) of 3b

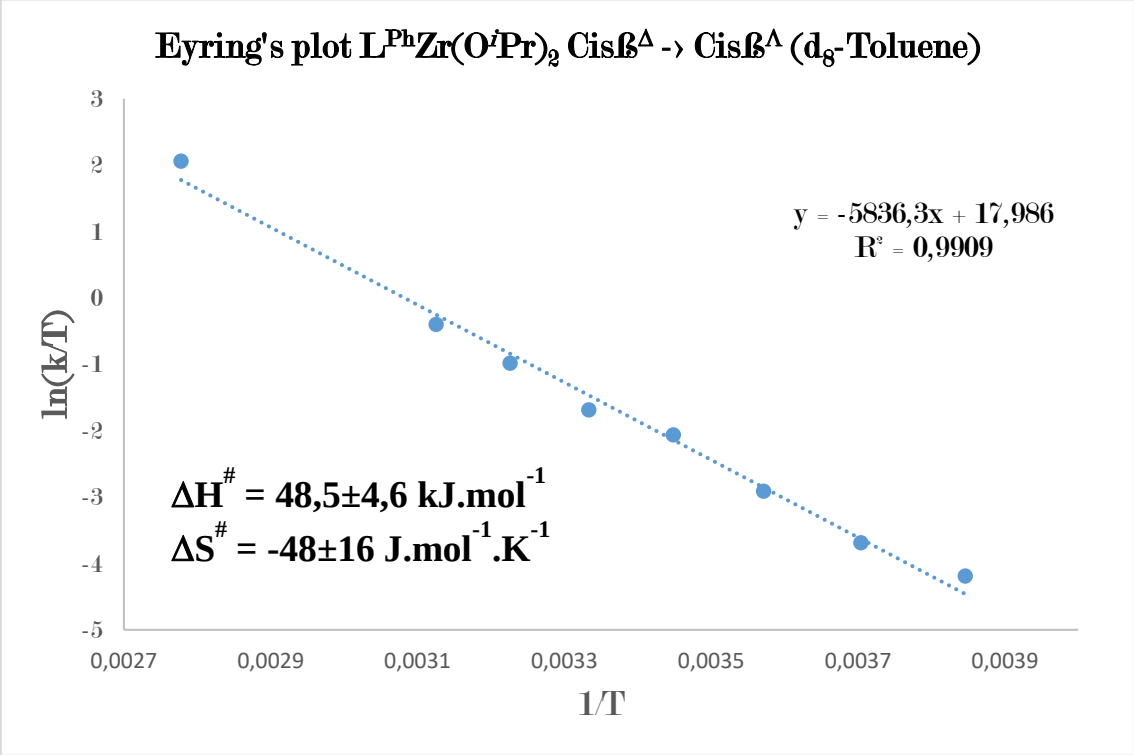

Figure S65: Eyring plot of ln(k/T) against 1/T for the isomerisation between the Δ and Λ enantiomers of the *cis*-β isomer of 3b. Expanded uncertainties, given at the 95% confidence interval, are estimated from the residual variance of the fit.

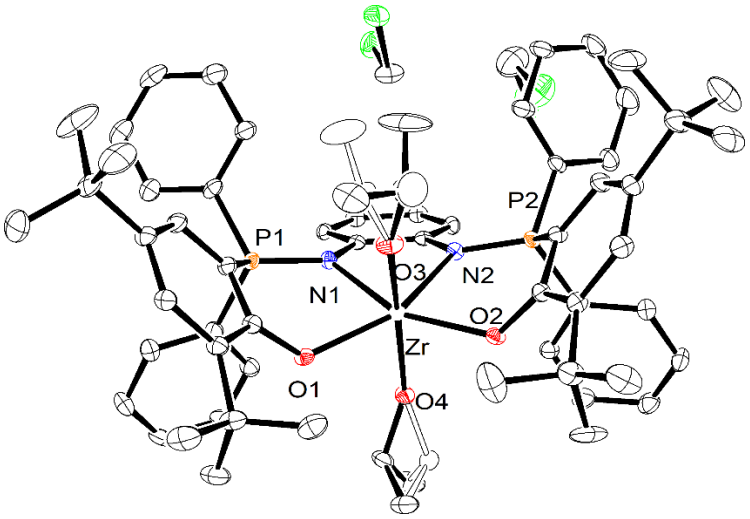

Figure S66: Crystal structure of 3b

Table S8: Crystal data and structure refinement of 3b

Identification code	3b
Internal reference	New2
Empirical formula	$C_{66}H_{82}Cl_4N_2O_4P_2Zr$
Formula weight	1262.29
Temperature/K	115
Crystal system	triclinic
Space group	P-1
a/Å	13.3206(9)
b/Å	13.3221(8)
c/Å	22.2555(13)
α/°	75.529(3)
β/°	77.372(3)
γ/°	101.728(3)
Volume/Å^3	3589.9(4)
Z	2
ρ_{calc}g/cm^3	1.168
μ/mm^{-1}	0.389
F(000)	1324.0
Crystal size/mm^3	0.25 × 0.25 × 0.25
Radiation	MoKα (λ = 0.71073)
2Θ range for data collection/°	4.26 to 55.154
Index ranges	-17 ≤ h ≤ 17, -17 ≤ k ≤ 17, -28 ≤ l ≤ 28
Reflections collected	94486
Independent reflections	16532 [R_{int} = 0.0821, R_{sigma} = 0.0648]
Data/restraints/parameters	16532/18/764
Goodness-of-fit on F^2	1.180
Final R indexes [I>=2σ (I)]	R_1 = 0.0888, wR_2 = 0.2535
Final R indexes [all data]	R_1 = 0.1181, wR_2 = 0.2687
Largest diff. peak/hole / e Å^{-3}	1.87/-1.05
CCDC	1978288

Special refinement details for 3b

Both isopropoxy groups attached to the Zr atom are disordered over 2 positions, for one of them the three carbon atoms occupy two positions while for the other one only the central carbon atom is splitted over two positions, the two methyl groups sharing the same positions.
Large solvent accessible void is found in the structure. The residual electron density is very diffuse and does not allow to locate additional solvent molecules. The crystal could have lost some solvent while retaining its structure and applying a squeeze procedure dis not significantly improve the resolution indices.

Complex 4a

^{1}H-^{1}H COSY (600 MHz, CD_2Cl_2, 300 K)[selected cross-peaks]: 7.59 / 7.26 (*m* of PPh_2 / *o* of PPh_2), 7.26 / 7.59 (*o* of PPh_2 / *m* of PPh_2), 6.83 / 6.23 (*m* of ZrBn / *o* of ZrBn), 6.23 / 6.83 (*o* of ZrBn / *m* of ZrBn).

^{1}H-^{13}C HMBC (600 MHz / 151 MHz, CD_2Cl_2, 300 K)[selected cross-peaks]: 7.71 / 161.4 (*H*3 of PAr / *C*1 of PAr), 7.71 / 128.2 (*H*3 of PAr / *C*5 of PAr), 7.71 / 36.2 (*H*3 of PAr / *C* of ^{t}Bu^{2}) 7.71 / 34.8 (*H*3 of PAr / *C* of ^{t}Bu^{4}), 6.85 / 149.2 (*m* of BBn / *i* of BBn), 6.85 / 127.1 (*m* of BBn / *m* of BBn), 6.83 / 145.0 (*m* of ZrBn / *i* of ZrBn), 6.83 / 129.1 (*m* of ZrBn / *m* of ZrBn), 6.72 / 128.9 (*o* of BBn / *o* of BBn), 6.72 / 122.6 (*o* of BBn / *p* of BBn), 6.58 / 161.4 (*H*5 of PAr / *C*1 of PAr), 6.58 / 131.4 (*H*5 of PAr / *C*3 of PAr), 6.23 / 126.2 (*o* of ZrBn / *o* of ZrBn), 6.23 / 122.4 (*o* of ZrBn / *p* of ZrBn), 6.23 / 67.6 (*o* of ZrBn / CH_2 of ZrBn), 2.79 / 149.2 (CH_2 of BBn / *i* of BBn), 2.79 / 128.9 (CH_2 of BBn / *o* of BBn), 2.03 / 145.0 (CH_2 of ZrBn / *i* of ZrBn), 1.58 / 139.1 (CH_3 of ^{t}Bu^{2} / *C*2 of PAr), 1.58 / 36.2 (CH_3 of ^{t}Bu^{2} / *C* of ^{t}Bu^{2}), 1.58 / 30.3 (CH_3 of ^{t}Bu^{2} / CH_3 of ^{t}Bu^{2}), 1.11 / 144.0 (CH_3 of ^{t}Bu^{4} / *C*4 of PAr), 1.11 / 34.8 (CH_3 of ^{t}Bu^{4} / *C* of ^{t}Bu^{4}), 1.11 / 31.3 (CH_3 of ^{t}Bu^{4} / CH_3 of ^{t}Bu^{4}).

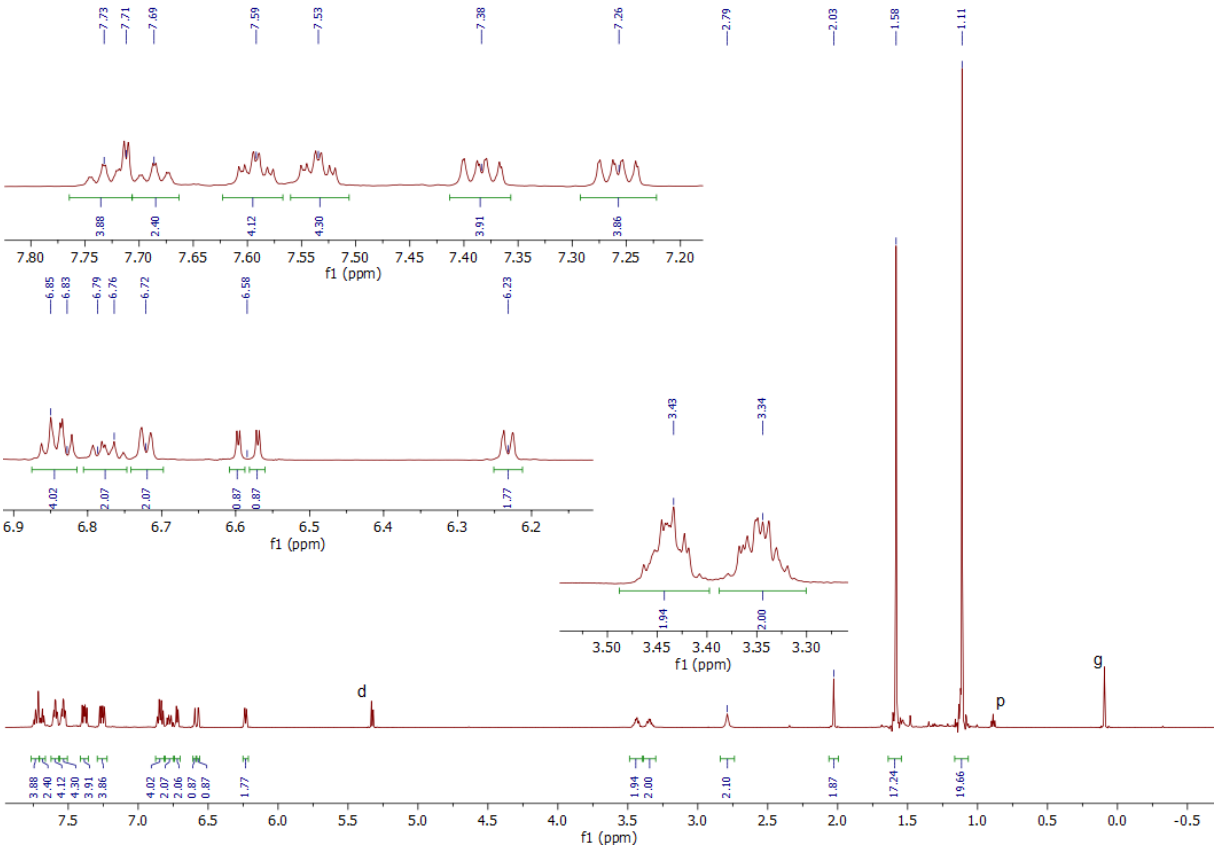

Figure S67: ^{1}H NMR (600 MHz, CD_2Cl_2, 300 K)(d: dichloromethane; g: Si grease; p: pentane) of 4a

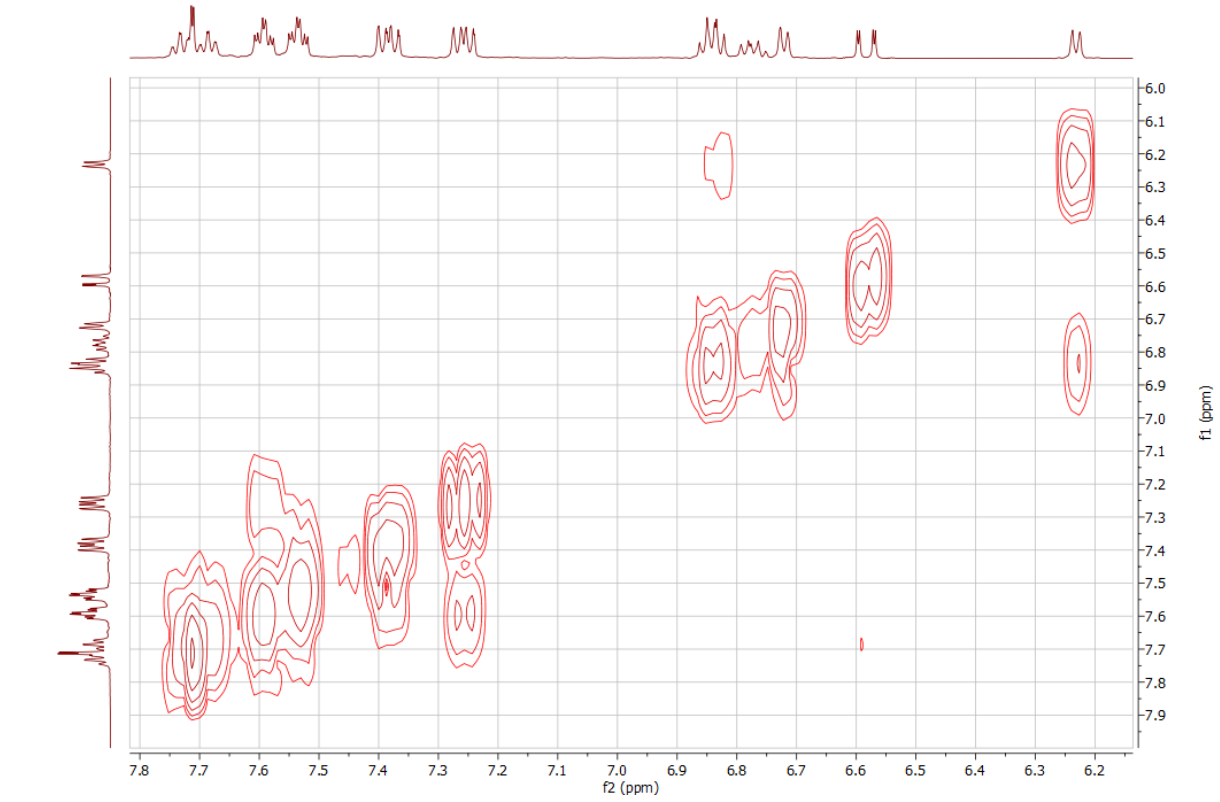

Figure S68: ^{1}H-^{1}H COSY (600 MHz, CD_2Cl_2, 300 K)(aromatic region) of 4a

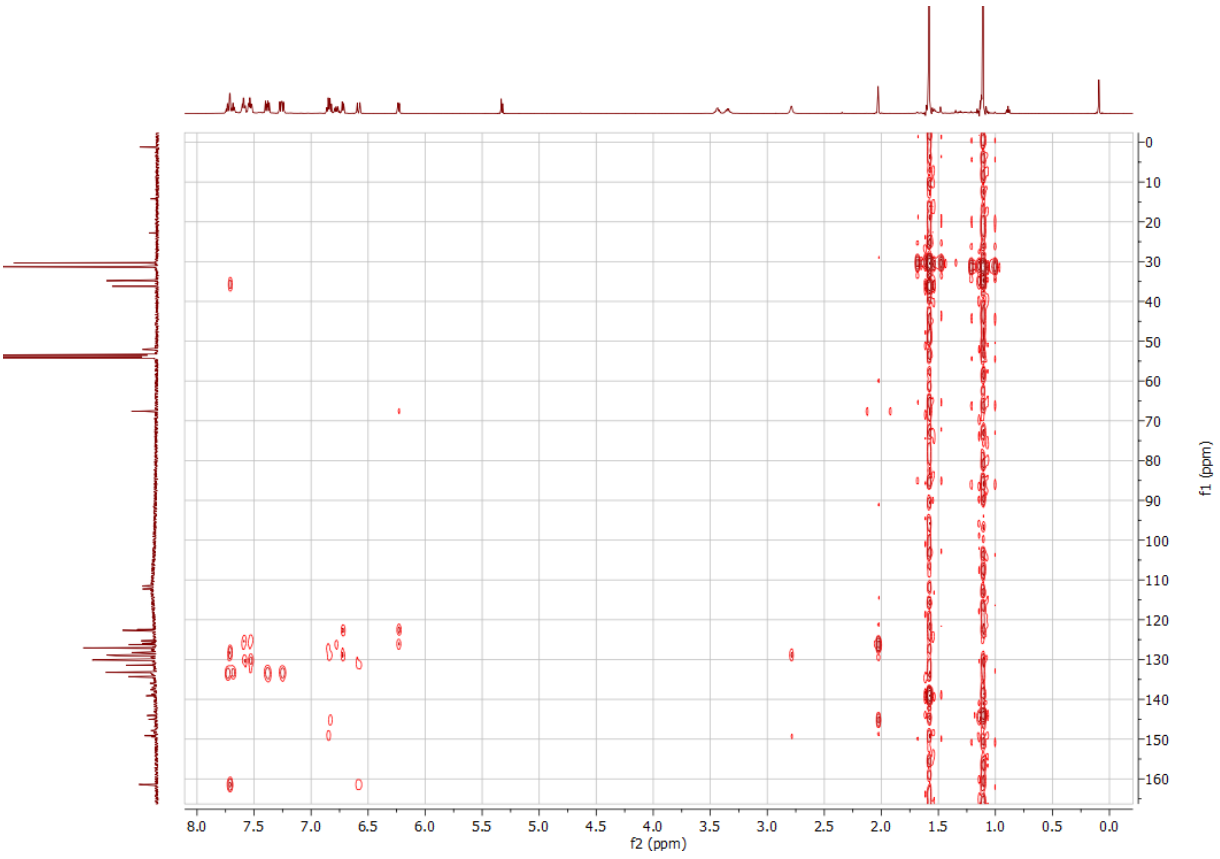

Figure S69: ^{1}H-^{13}C HMBC (600 MHz / 151 MHz, CD_2Cl_2, 300 K)(whole spectrum) of 4a

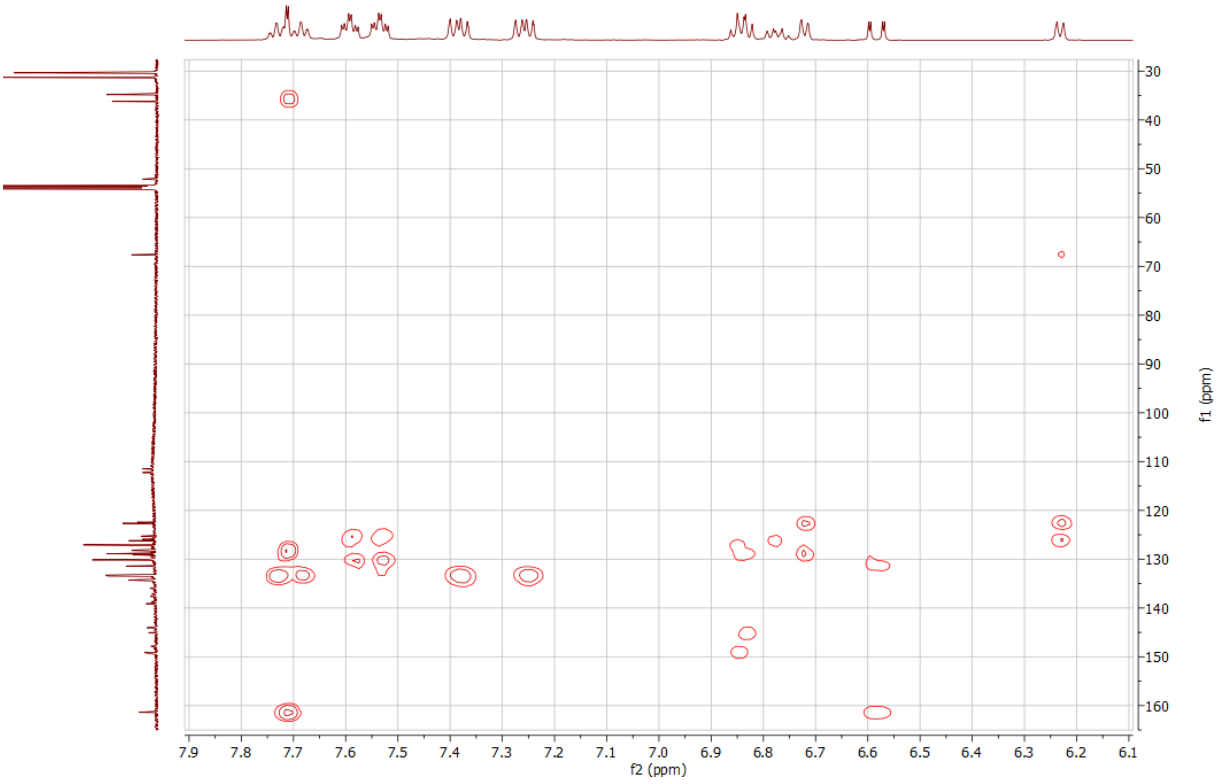

Figure S70: ^{1}H-^{13}C HMBC (600 MHz / 151 MHz, CD_2Cl_2, 300 K)(zoom) of 4a

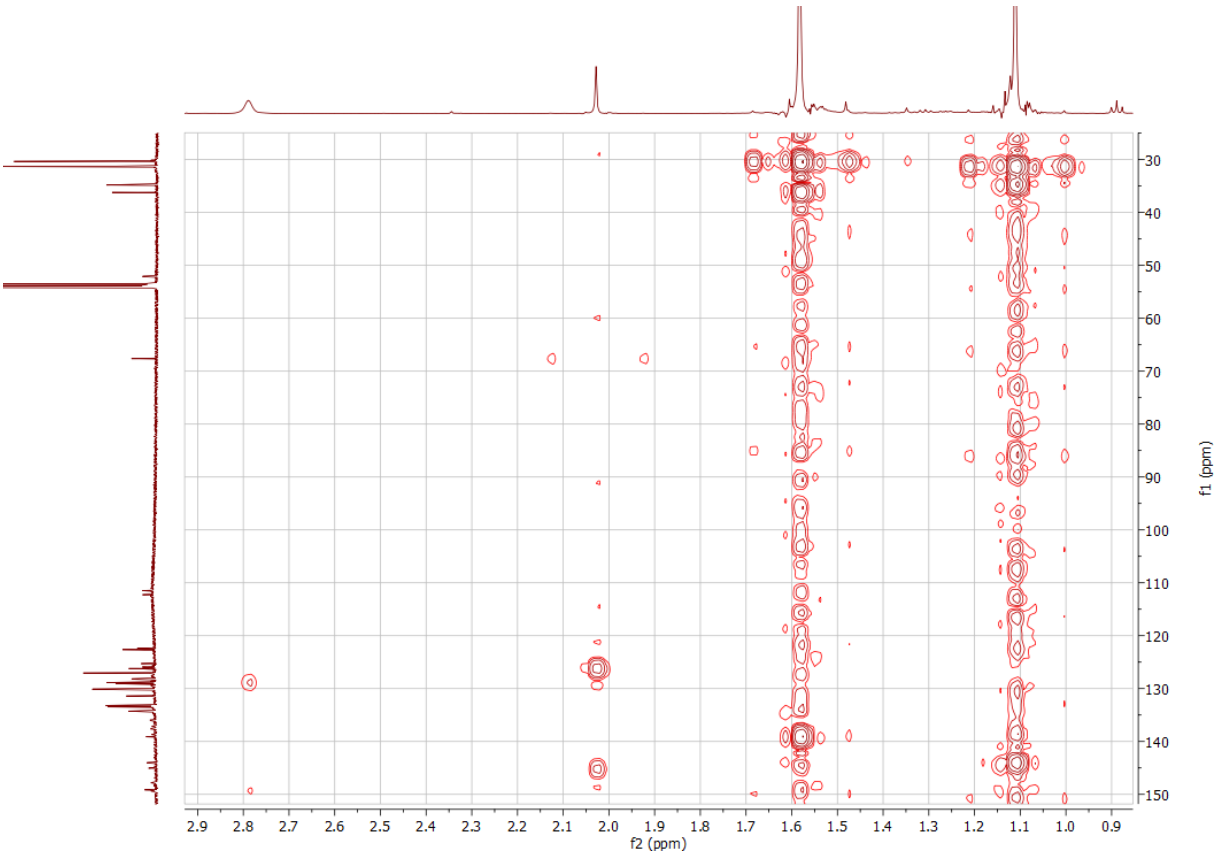

Figure S71: ^{1}H-^{13}C HMBC (600 MHz / 151 MHz, CD_2Cl_2, 300 K)(zoom) of 4a

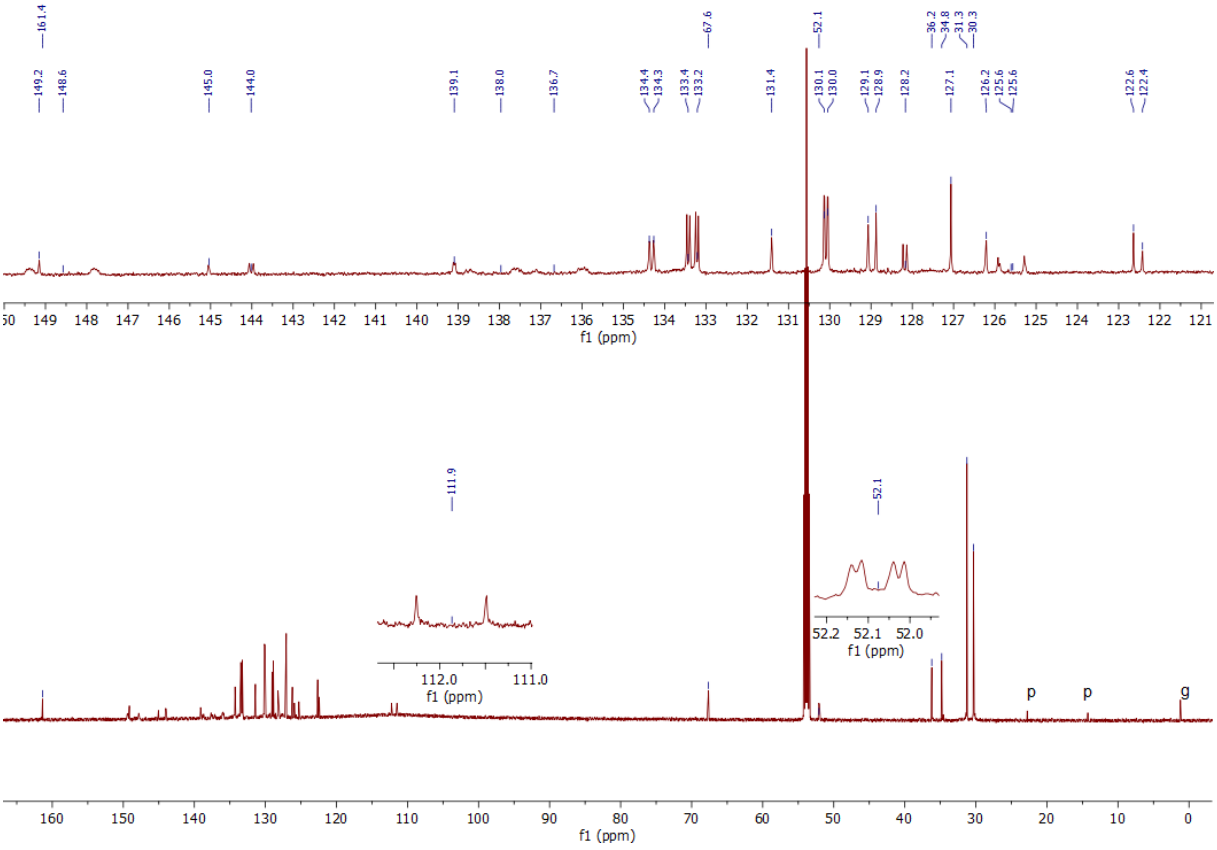

Figure S72: $^{13}C\{^1H\}$ NMR (151 MHz, CD_2Cl_2, 300 K)(g: Si grease; p: pentane) of 4a

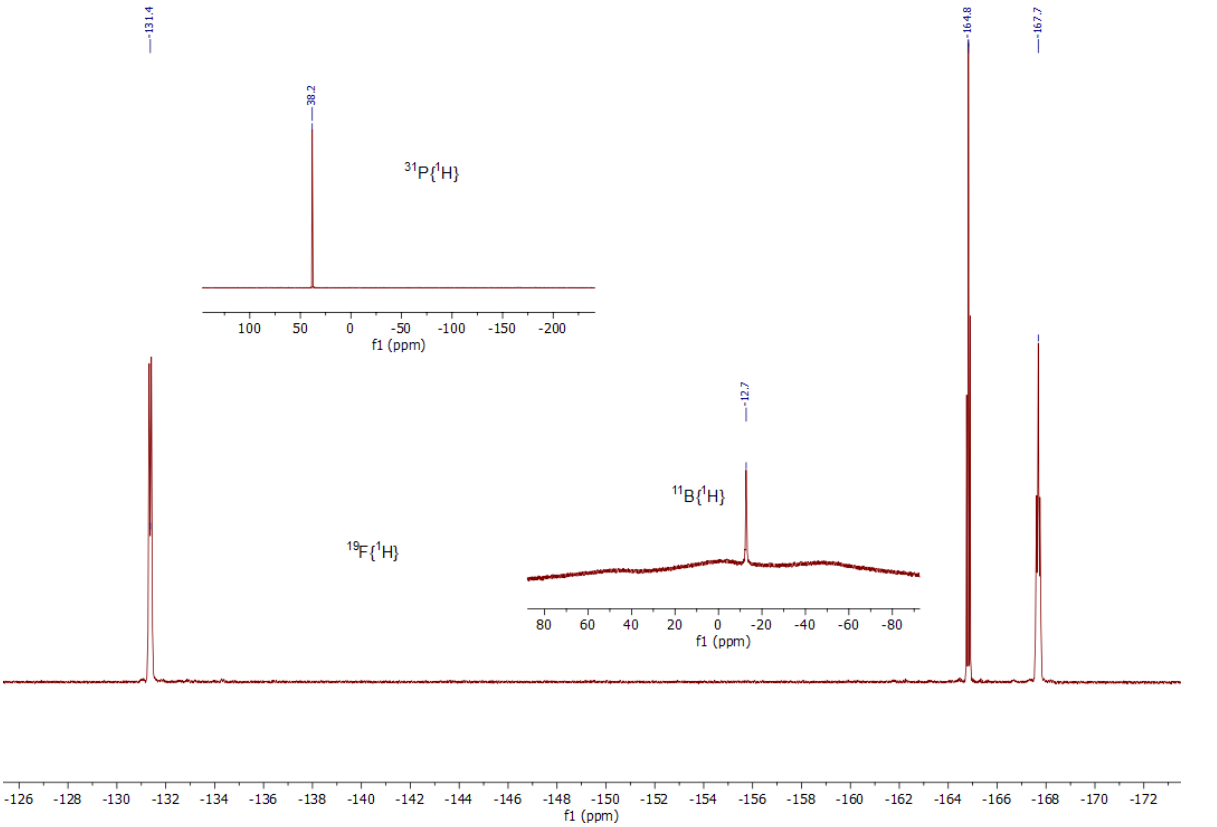

Figure S73: $^{31}P\{^1H\}$ NMR (122 MHz, CD_2Cl_2, 300 K); $^{19}F\{^1H\}$ NMR (286 MHz, CD_2Cl_2, 300 K); $^{11}B\{^1H\}$ NMR (96 MHz, CD_2Cl_2, 300 K) of 4a

Complex 4b:

^{1}H-^{1}H COSY (500 MHz, CD_2Cl_2, 300 K)[selected cross-peaks]: 7.70 / 6.81-6.66 (*H*3 of PAr / *H*5 of PAr), 7.56 / 7.27 (*p* of PPh_2 / *m* of PPh_2), 7.27 / 7.56 (*m* of PPh_2 / *p* of PPh_2), 6.81-6.66 / 7.70 (*H*5 of PAr / *H*3 of PAr), 6.37 / 6.07 (*H*3 of NAr / *H*2 of NAr), 6.07 / 6.37 (*H*2 of NAr / *H*3 of NAr).

^{1}H-^{13}C HMBC (500 MHz / 126 MHz, CD_2Cl_2, 300 K)[selected cross-peaks]: 7.83 / 134.1 (*p* of PPh_2 / *o* of PPh_2), 7.70 / 161.4 (*H*3 of PAr / *C*2 of PAr), 7.71/ 128.5 (*H*3 of PAr / *C*5 of PAr), 7.71 / 35.9 (*H*3 of PAr / C of $^{t}Bu^{2}$), 7.71 / 34.9 (*H*3 of PAr / C of $^{t}Bu^{4}$), 7.56 / 133.1 (*p* of PPh_2 / *o* of PPh_2), 7.37-7.30 / 134.1 (*o* of PPh_2 / *o* of PPh_2), 6.87 / 149.1 (*m* of BBn / *i* of BBn), 6.87 / 127.1 (*m* of BBn / *m* of BBn), 6.81-6.66 / 161.4 (*H*5 of PAr / *C*2 of PAr), 6.81-6.66 / 34.9 (*H*5 of PAr / C of $^{t}Bu^{4}$), 6.60 / 125.0 (*o* of ZrBn / *p* of ZrBn), 6.60 / 67.3 (*o* of ZrBn / CH_2 of ZrBn), 6.37 / 122.5 (*H*3 of NAr / *C*2 of NAr), 6.07 / 140.0 (*H*2 of NAr / *C*1 of NAr), 6.07 / 122.4 (*H*2 of NAr / *C*3 of NAr), 2.84 / 149.1 (CH_2 of BBn / *i* of BBn), 2.84 / 128.8 (CH_2 of BBn / *i* of C_6F_5), 2.15 / 137.0 (CH_2 of ZrBn / *i* of ZrBn), 2.15 / 128.4 (CH_2 of ZrBn / *o* of ZrBn), 1.36 / 139.2 (CH_3 of $^{t}Bu^{2}$ / *C*2 of PAr), 1.36 / 35.9 (CH_3 of $^{t}Bu^{2}$ / C of $^{t}Bu^{2}$), 1.36 / 30.4 (CH_3 of $^{t}Bu^{2}$ / CH_3 of $^{t}Bu^{2}$), 1.19 / 144.1 (CH_3 of $^{t}Bu^{4}$ / *C*4 of PAr), 1.19 / 34.9 (CH_3 of $^{t}Bu^{4}$ / C of $^{t}Bu^{4}$), 1.19 / 31.3 (CH_3 of $^{t}Bu^{4}$ / CH_3 of $^{t}Bu^{4}$).

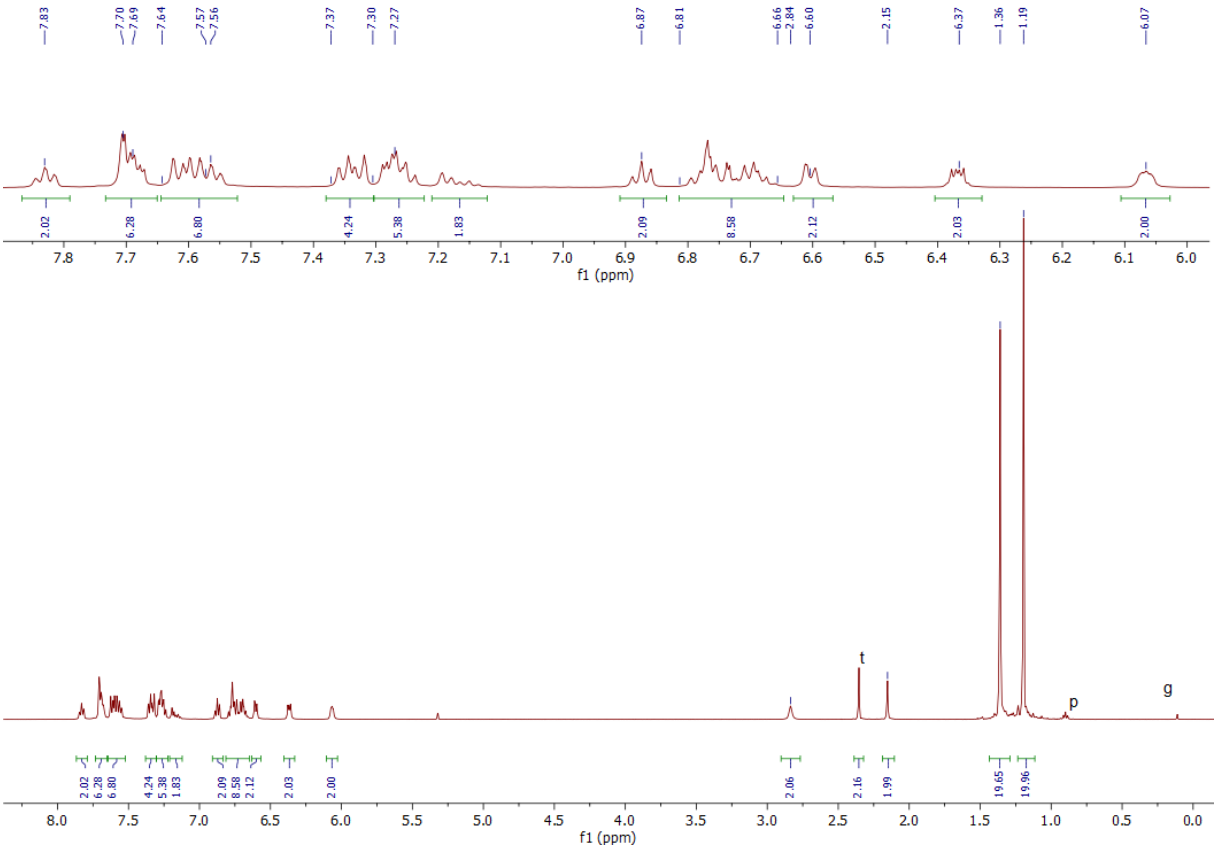

Figure S74: ^{1}H NMR (500 MHz, CD_2Cl_2, 300 K)(t: toluene; g: Si grease; p: pentane) of 4b

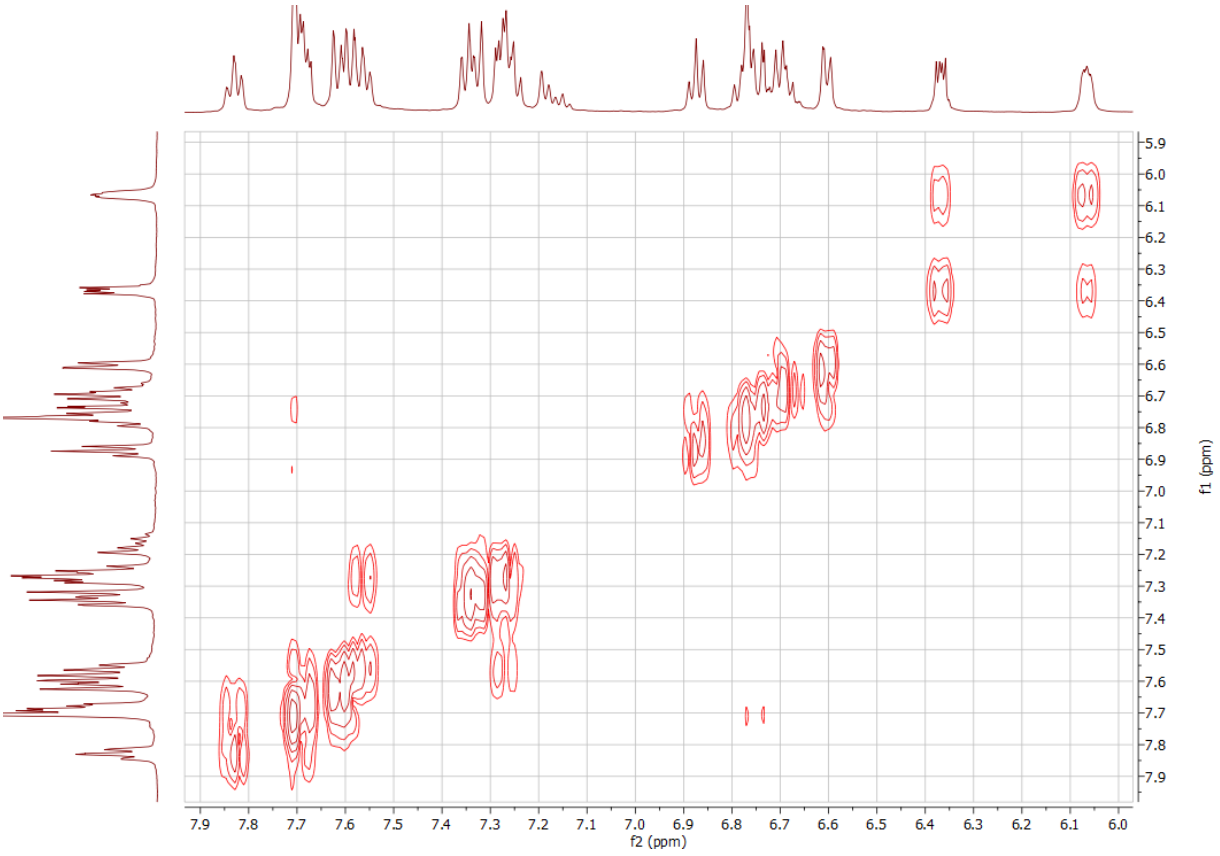

Figure S75: ^{1}H-^{1}H COSY (500 MHz, CD_2Cl_2, 300 K)(aromatic region) of 4b

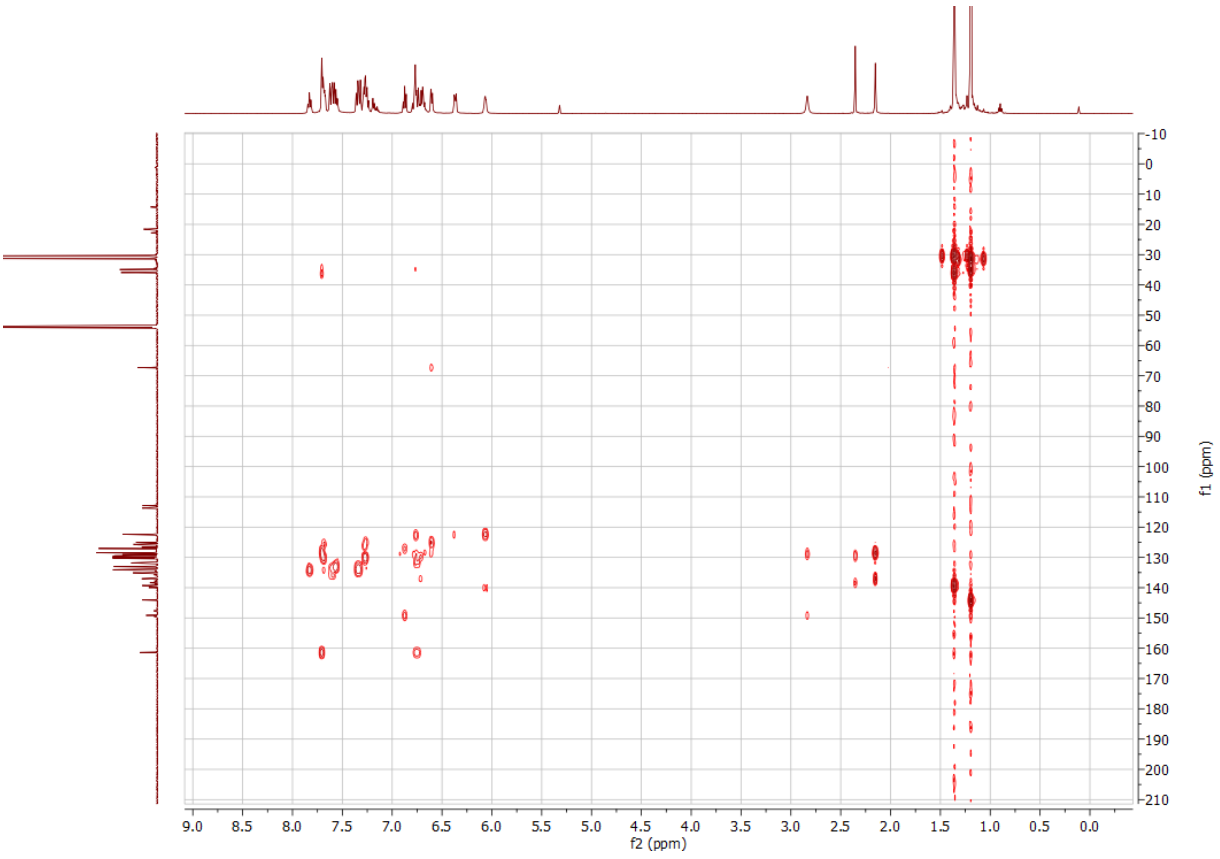

Figure S76: ^{1}H-^{13}C HMBC (500 MHz / 126 MHz, CD_2Cl_2, 300 K)(whole spectrum) of 4b

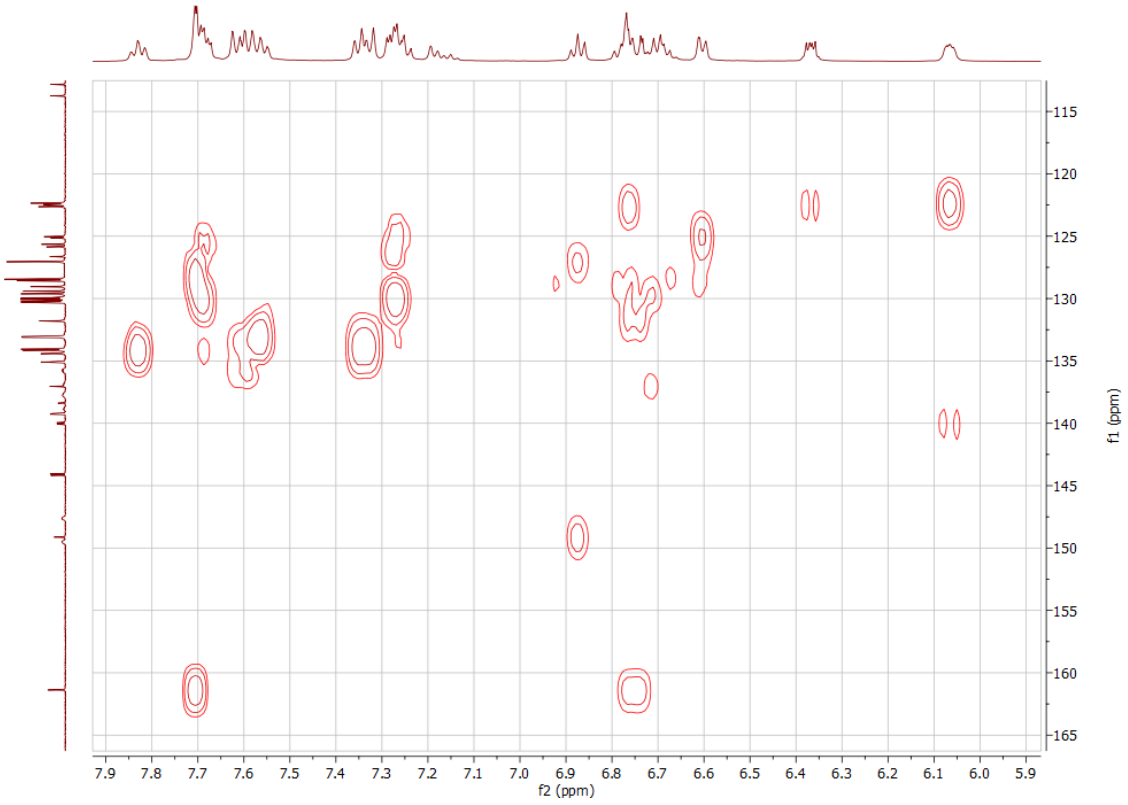

Figure S77: ^{1}H-^{13}C HMBC (500 MHz / 126 MHz, CD_2Cl_2, 300 K)(zoom) of 4b

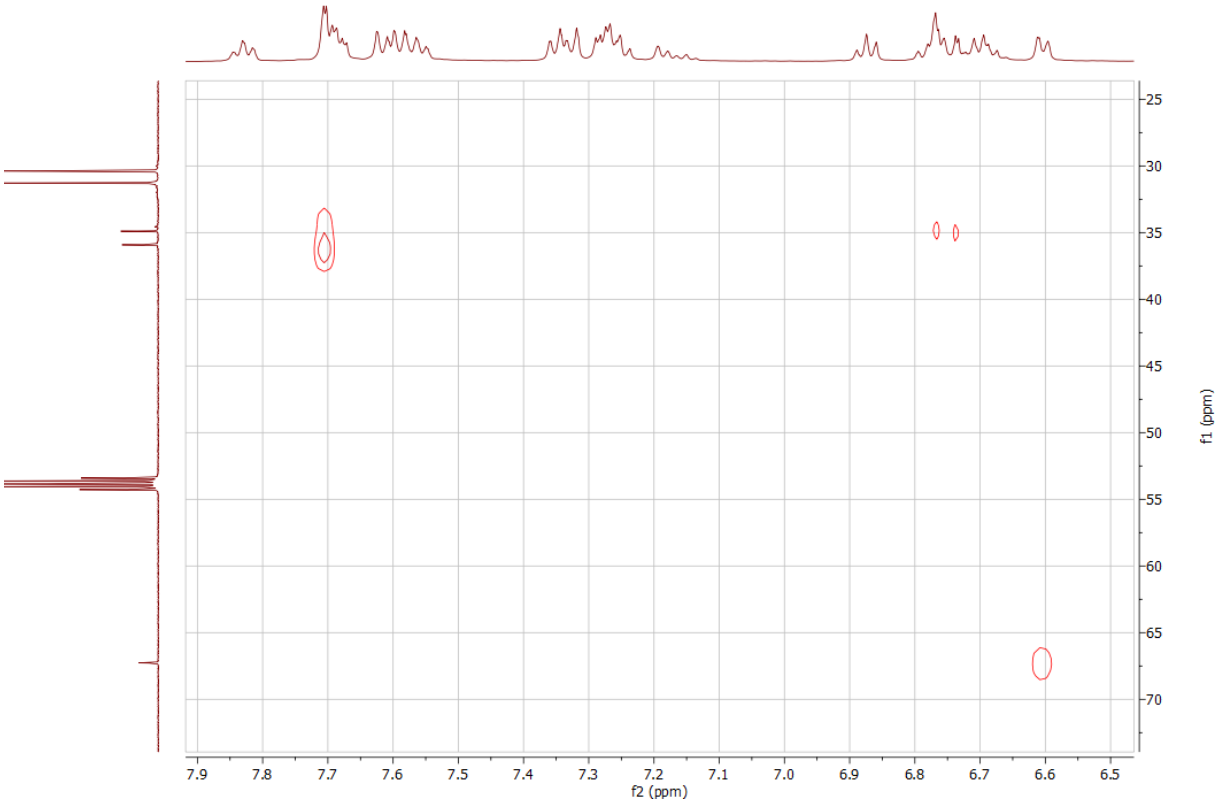

Figure S78: ^{1}H-^{13}C HMBC (500 MHz / 126 MHz, CD_2Cl_2, 300 K)(zoom) of 4b

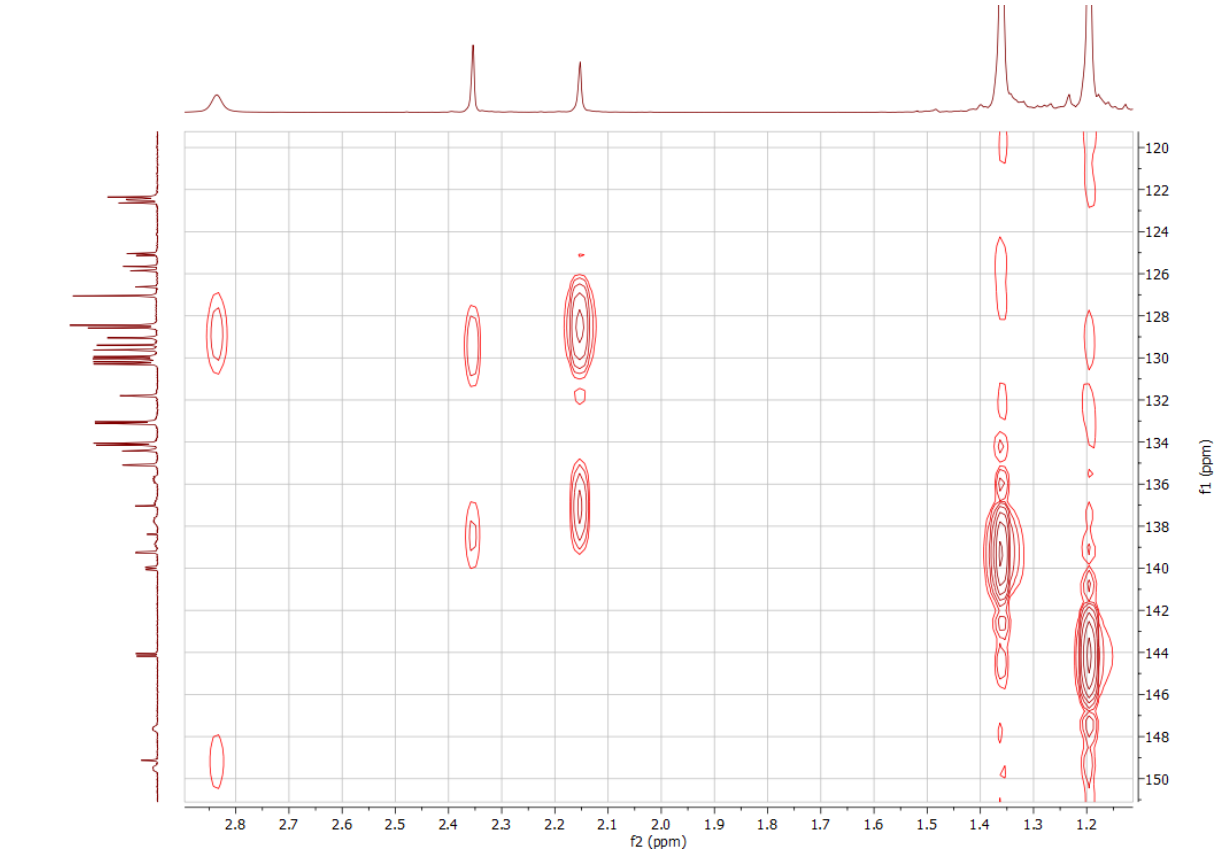

Figure S79: ^{1}H-^{13}C HMBC (500 MHz / 126 MHz, CD_2Cl_2, 300 K)(zoom) of 4b

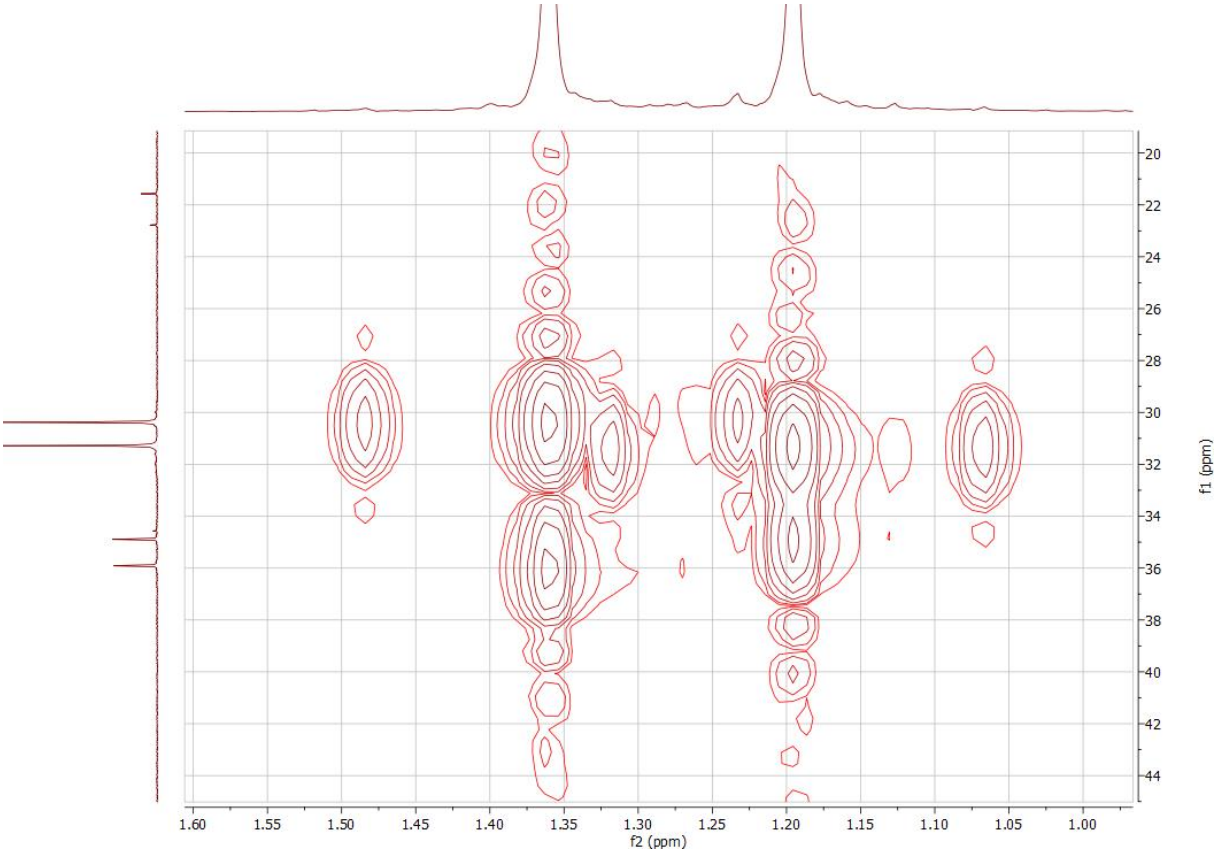

Figure S80: ^{1}H-^{13}C HMBC (500 MHz / 126 MHz, CD_2Cl_2, 300 K)(zoom) of 4b

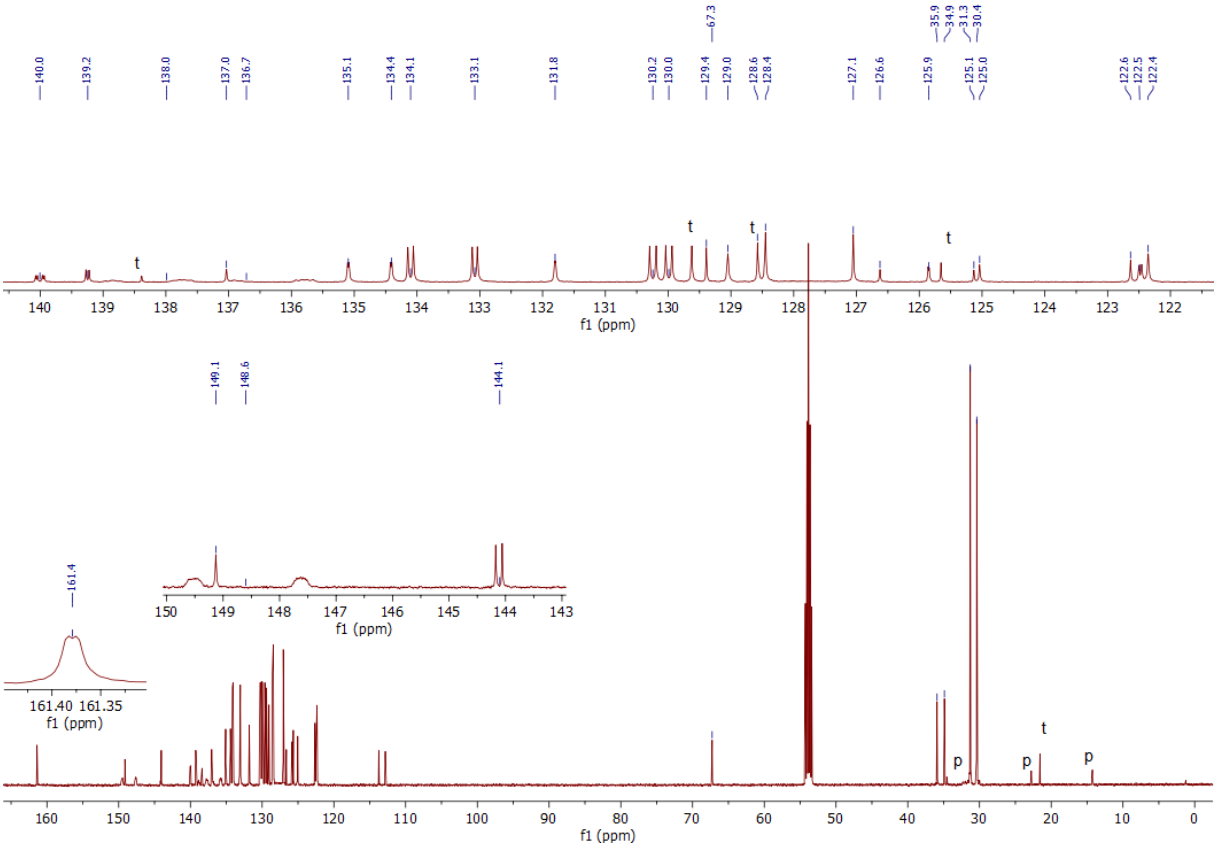

Figure S81: $^{13}C\{^{1}H\}$ NMR (126 MHz, CD_2Cl_2, 300 K)(t: toluene; p: pentane) of 4b

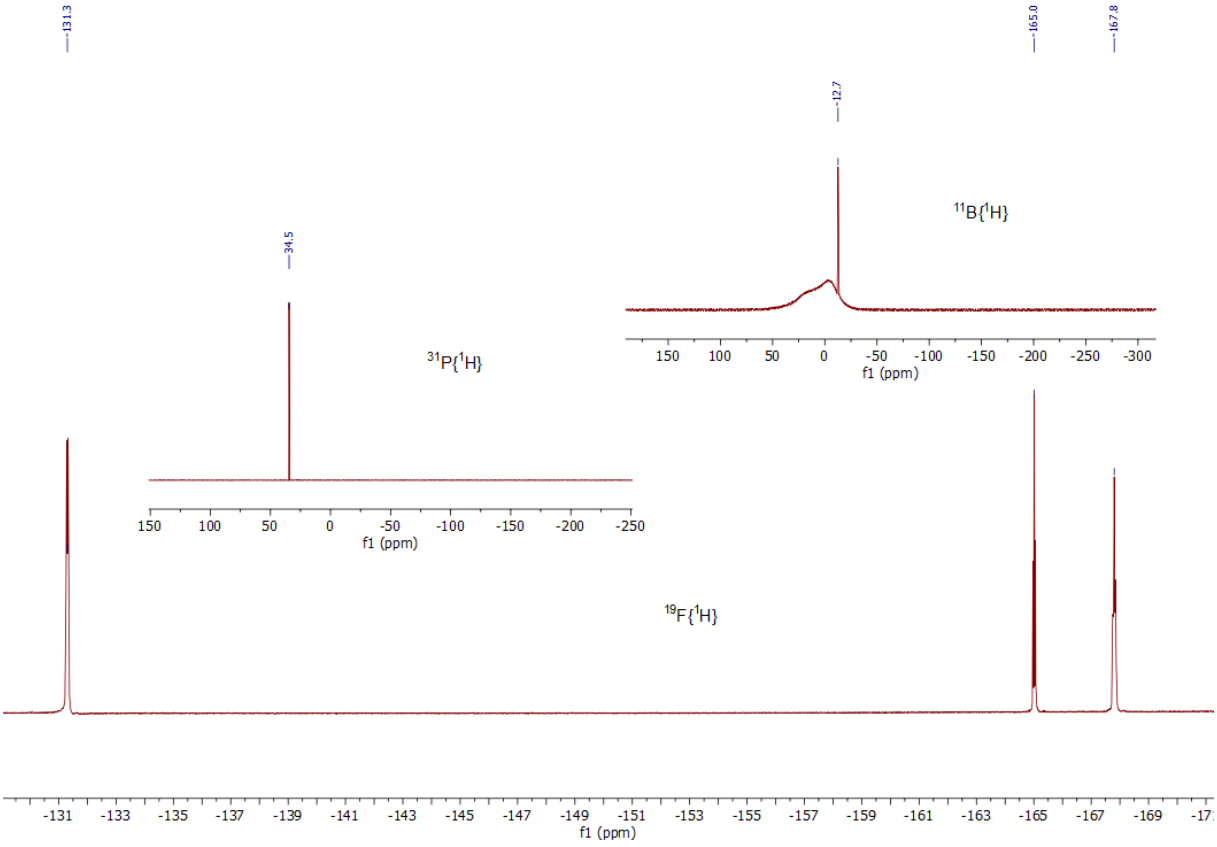

Figure S82: $^{31}P\{^{1}H\}$ NMR (202 MHz, CD_2Cl_2, 300 K); $^{19}F\{^{1}H\}$ NMR (470 MHz, CD_2Cl_2, 300 K); $^{11}B\{^{1}H\}$ NMR (160 MHz, CD_2Cl_2, 300 K) of 4b

Complex 5a

^{1}H-^{1}H COSY (600 MHz, CD_2Cl_2, 300 K)[selected cross-peaks]: 7.64-7.51 / 6.63 (*H*3 of PPh_2 / *H*5 of PPh_2), 6.86 / 6.73 (*m* of BBn / *o* of BBn), 6.73 / 6.86 (*o* of BBn / *m* of BBn), 6.63 / 7.64-7.51 (*H*5 of PPh_2 / *H*3 of PPh_2), 3.95 / 0.73 (C*H* of ^{i}Pr / CH_3 of ^{i}Pr), 3.50 / 3.33 (CH_2N / CH_2N), 3.33 / 3.50 (CH_2N / CH_2N), 0.73 / 3.95 (CH_3 of ^{i}Pr / C*H* of ^{i}Pr).

^{1}H-^{13}C HMBC (600 MHz / 151 MHz, CD_2Cl_2, 300 K)[selected cross-peaks]: 7.64-7.51 / 36.1 (*H*3 of PAr / *C* of ^{t}Bu^{2}), 7.64-7.51 / 34.7 (*H*3 of PAr / *C* of ^{t}Bu^{4}), 6.86 / 149.1 (*m* of BBn / *i* of BBn), 6.86 / 127.1 (*m* of BBn / *m* of BBn), 6.73 / 129.0 (*o* of BBn / *o* of BBn), 6.73 / 122.6 (*o* of BBn / *p* of BBn), 6.63 / 162.0 (*H*5 of PAr / *C*1 of PAr), 6.63 / 131.0 (*H*5 of PAr / *C*3 of PAr), 6.63 / 34.7 (*H*5 of PAr / *C* of ^{t}Bu^{4}), 2.80 / 149.1 (CH_2 of BBn / *i* of BBn), 2.80 / 128.8 (CH_2 of BBn / *i* of C_6F_5), 1.51 / 139.1 (CH_3 of ^{t}Bu^{2} / *C*2 of PAr), 1.51 / 36.1 (CH_3 of ^{t}Bu^{2} / *C* of ^{t}Bu^{2}), 1.51 / 30.2 (CH_3 of ^{t}Bu^{2} / CH_3 of ^{t}Bu^{2}), 1.09 / 142.8 (CH_3 of ^{t}Bu^{4} / *C*4 of PAr), 1.09 / 34.7 (CH_3 of ^{t}Bu^{4} / *C* of ^{t}Bu^{4}), 1.09 / 31.2 (CH_3 of ^{t}Bu^{4} / CH_3 of ^{t}Bu^{4}), 0.73 / 76.1 (CH_3 of ^{i}Pr / *C*H of ^{i}Pr), 0.73 / 26.2 (CH_3 of ^{i}Pr / CH_3 of ^{i}Pr).

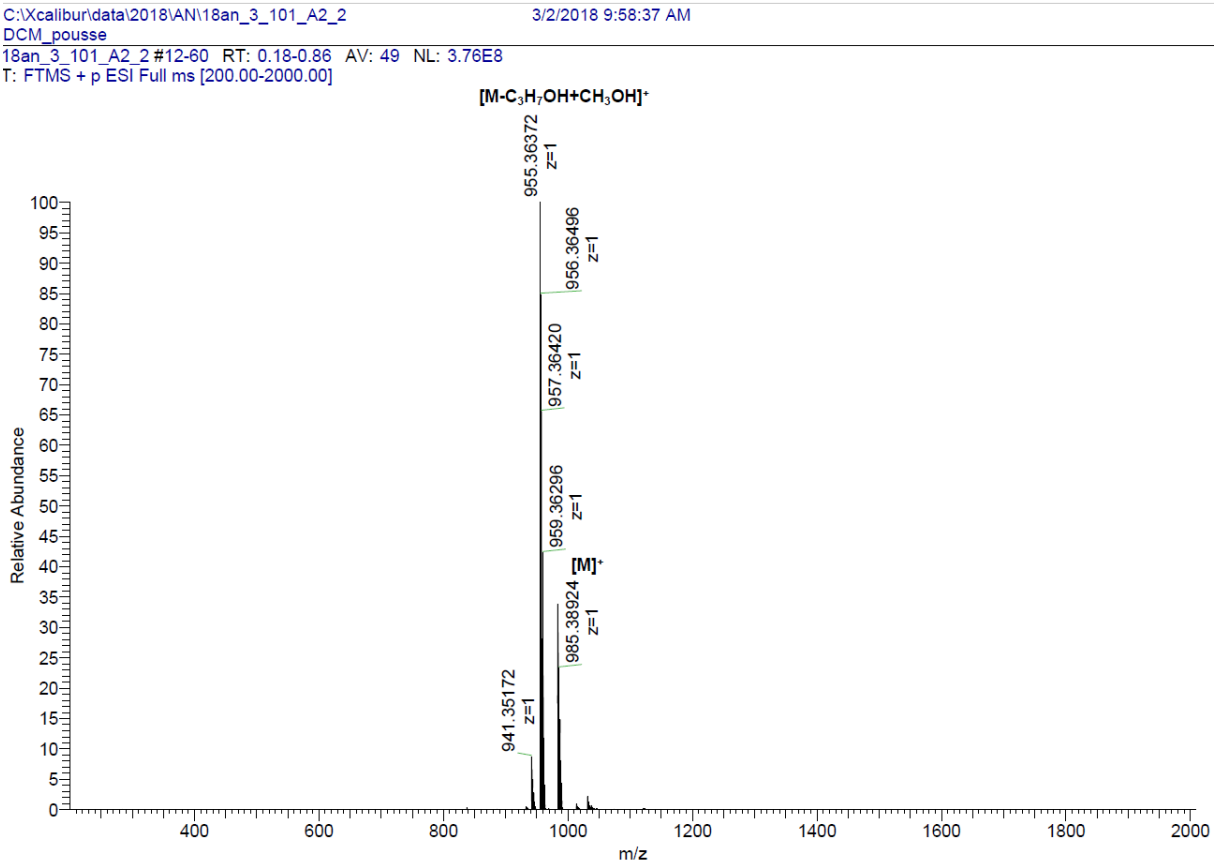

Figure S83: HRMS (ESI-pos)(whole spectrum) of 5a

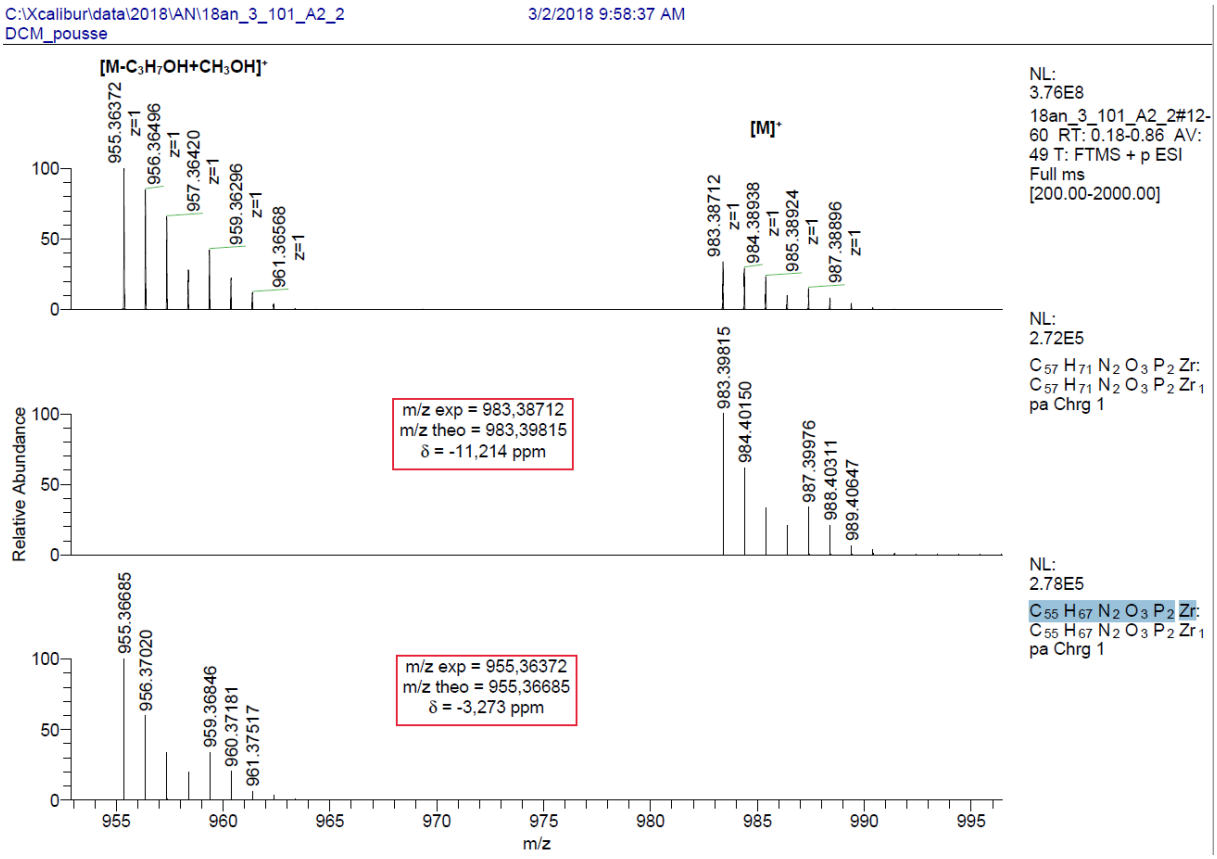

Figure S84: HRMS (ESI-pos)(detail) of 5a

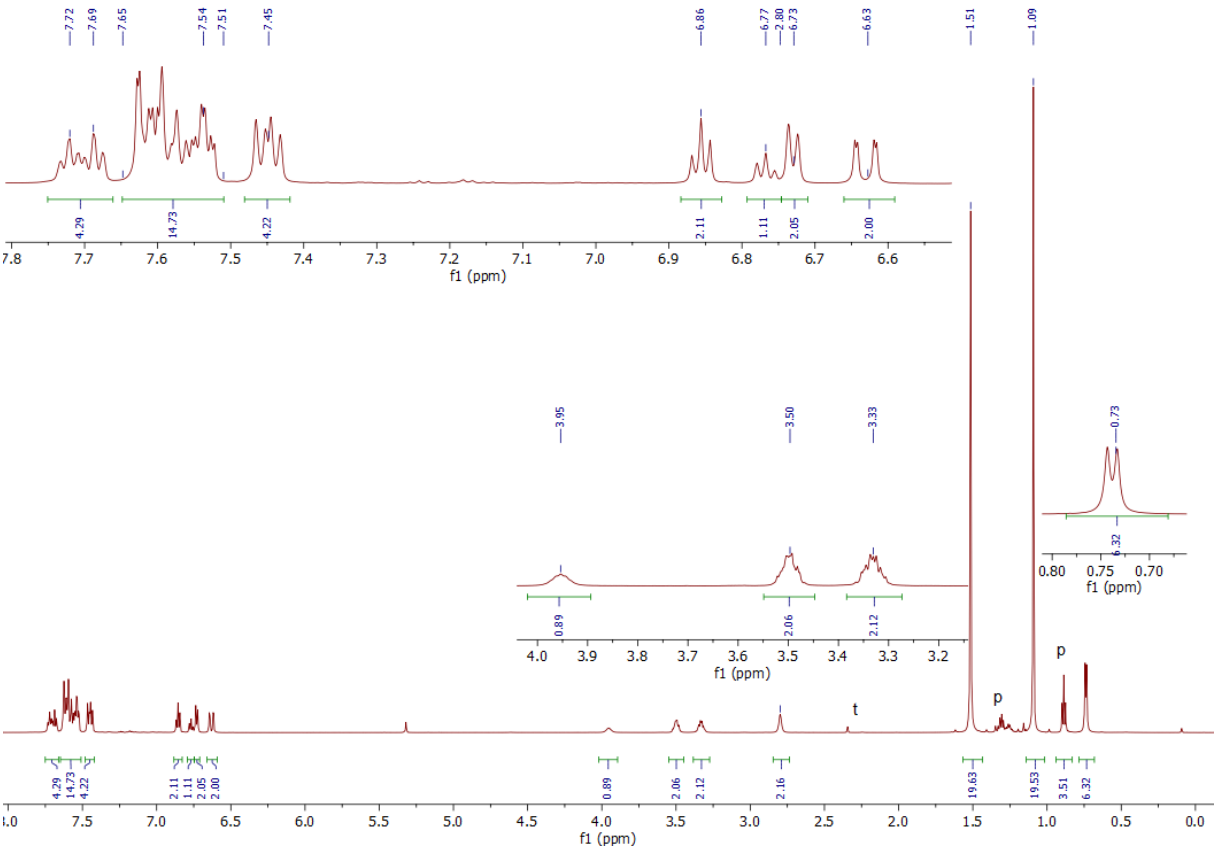

Figure S85: ^{1}H NMR (500 MHz, CD_2Cl_2, 300 K)(p: pentane; t: toluene) of 5a

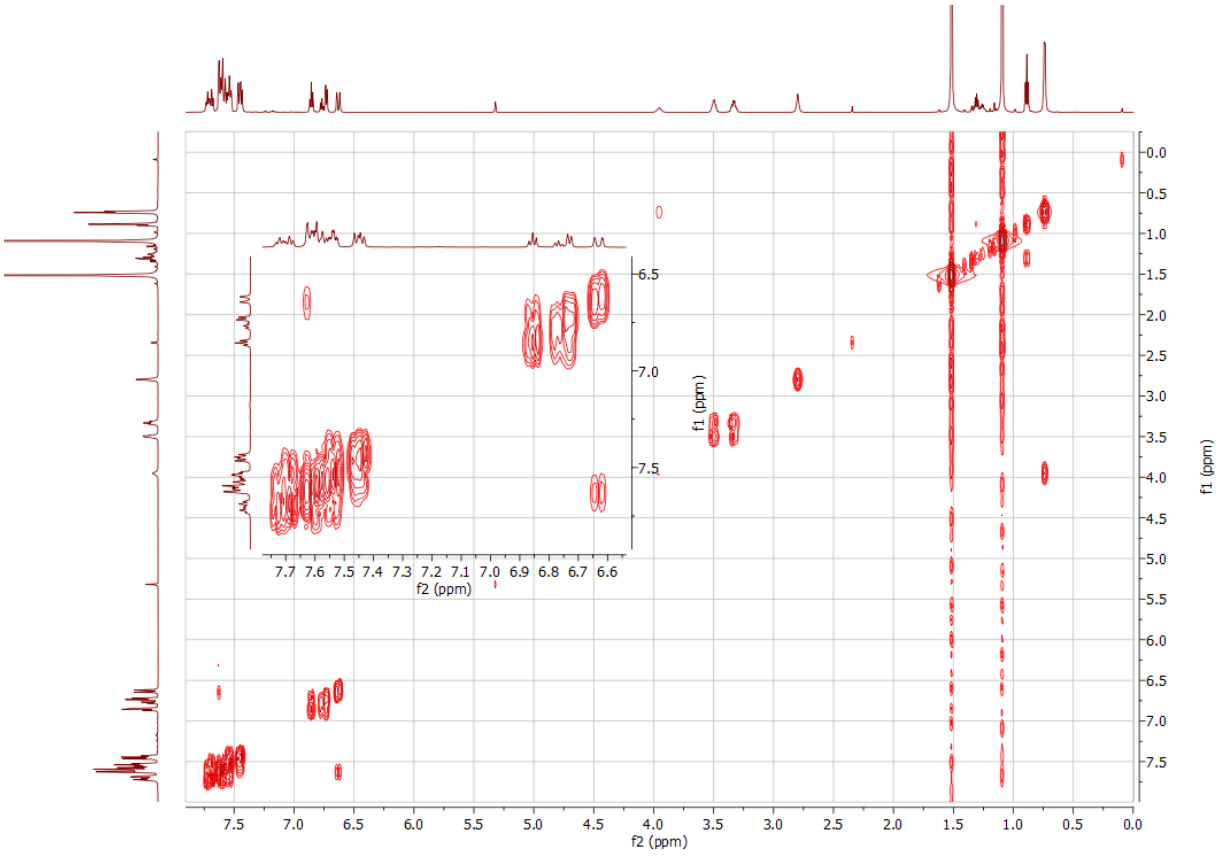

Figure S86: ^{1}H-^{1}H COSY (600 MHz, CD_2Cl_2, 300 K) of 5a

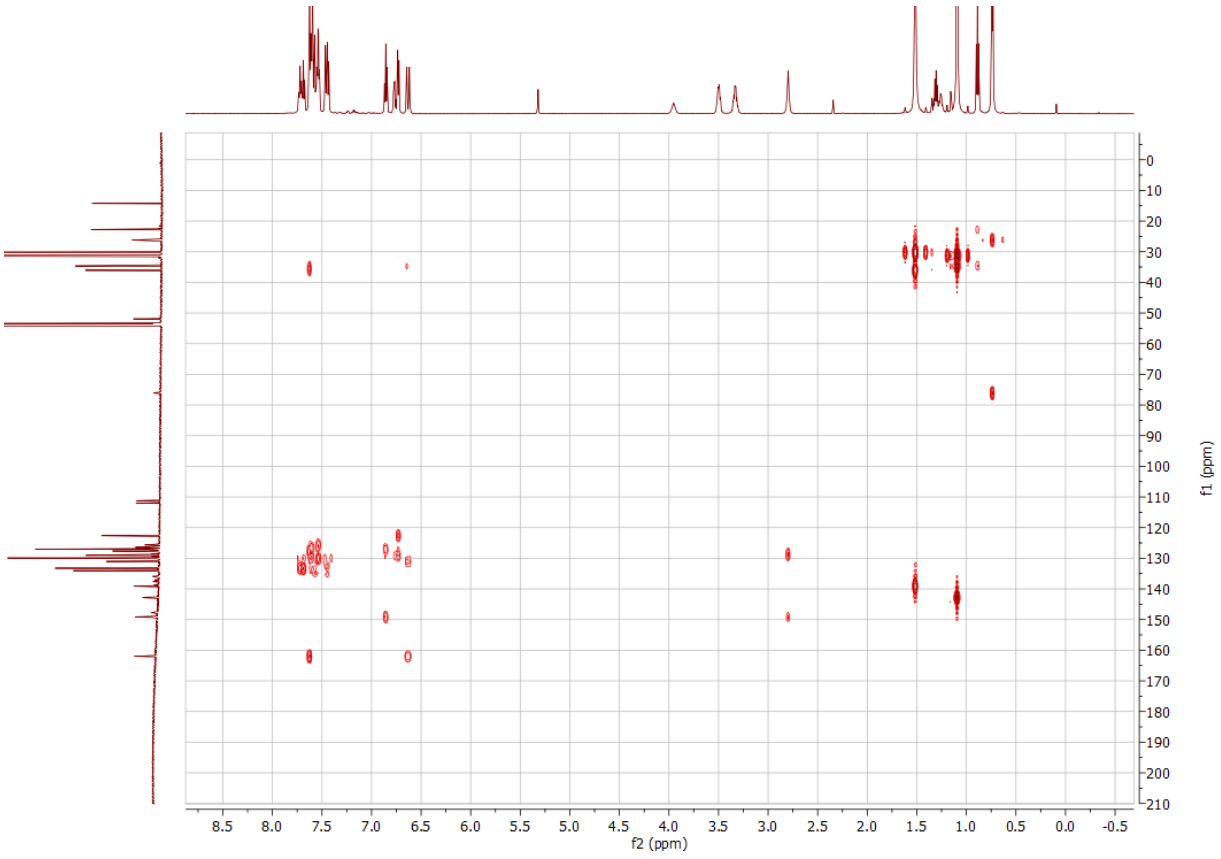

Figure S87: ^{1}H-^{13}C HMBC (600 MHz / 151 MHz, CD_2Cl_2, 300 K)(whole spectrum) of 5a

Figure S88: ^{1}H-^{13}C HMBC (600 MHz / 151 MHz, CD_2Cl_2, 300 K)(zoom) of 5a

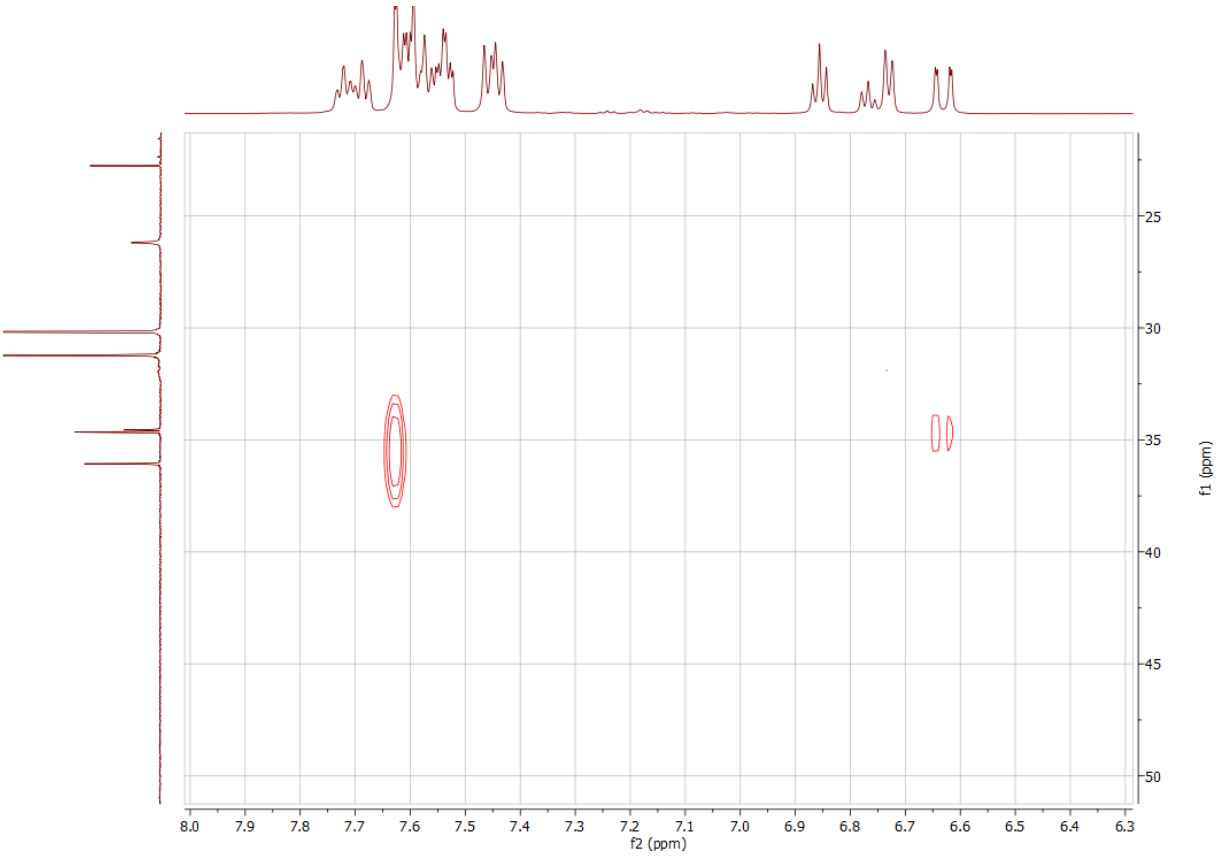

Figure S89: ^{1}H-^{13}C HMBC (600 MHz / 151 MHz, CD_2Cl_2, 300 K)(zoom) of 5a

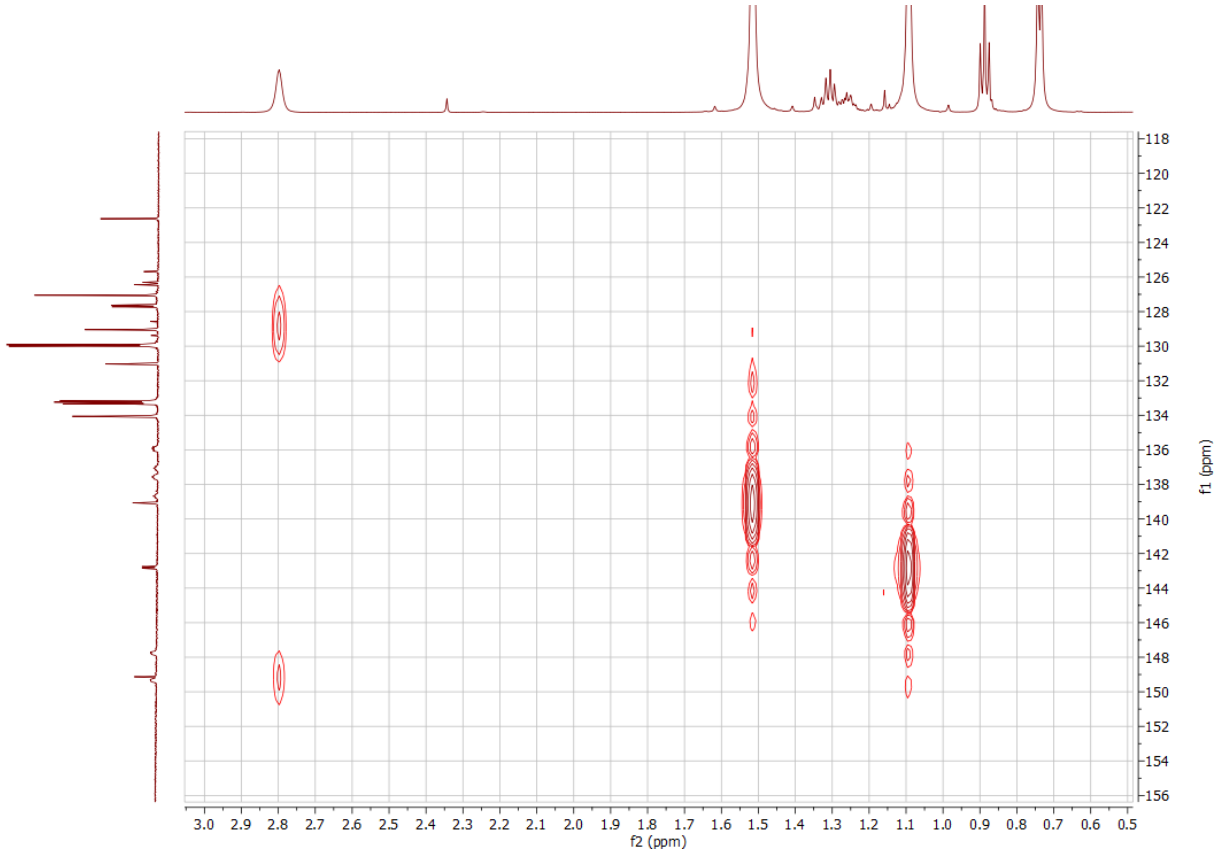

Figure S90: ^{1}H-^{13}C HMBC (600 MHz / 151 MHz, CD_2Cl_2, 300 K)(zoom) of 5a

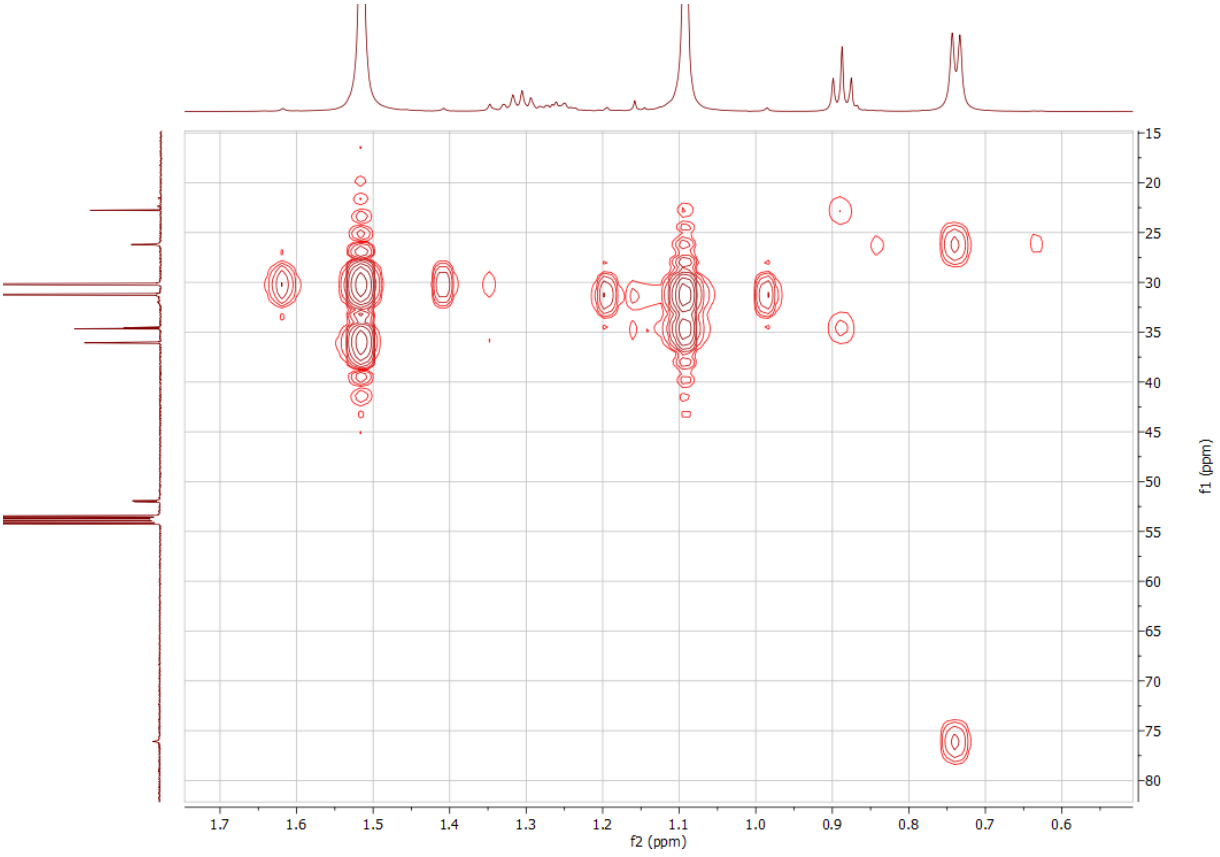

Figure S91: ^{1}H-^{13}C HMBC (600 MHz / 151 MHz, CD_2Cl_2, 300 K)(zoom) of 5a

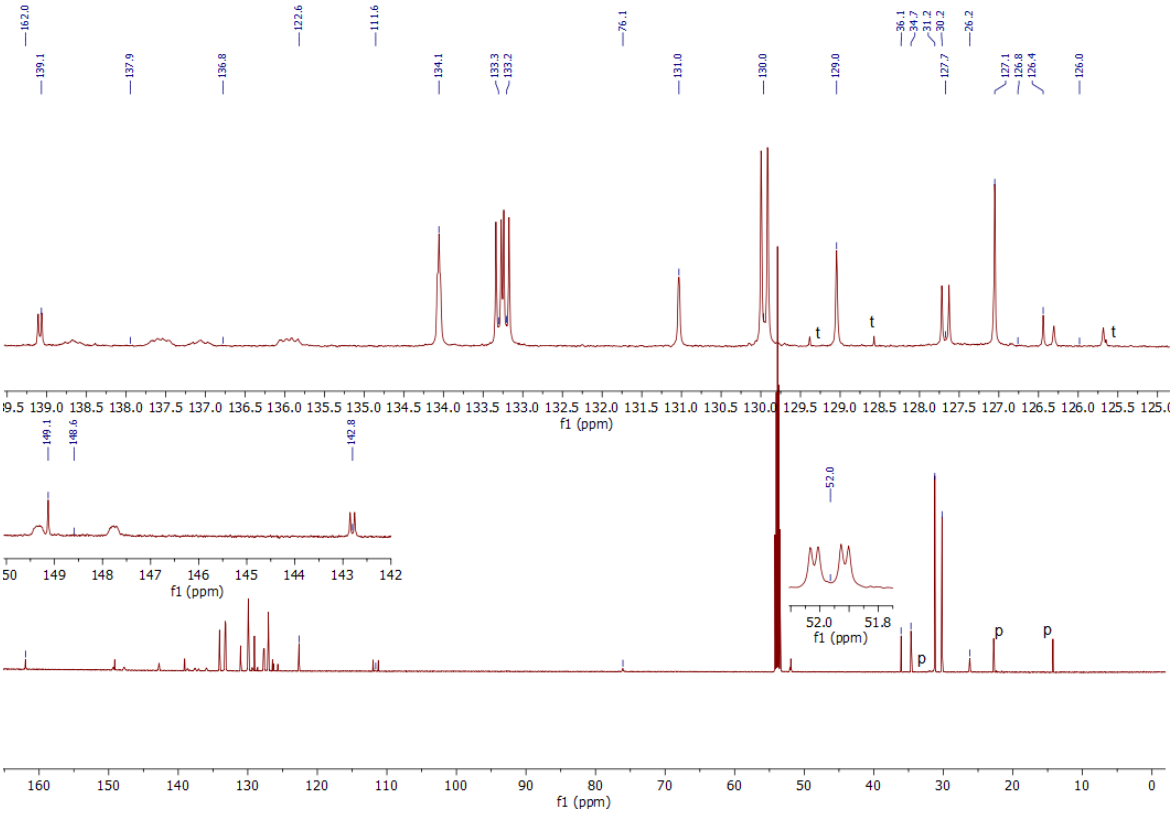

Figure S92: $^{13}C\{^{1}H\}$ NMR (151 MHz, CD_2Cl_2, 300 K)(t: toluene; p: pentane) of 5a

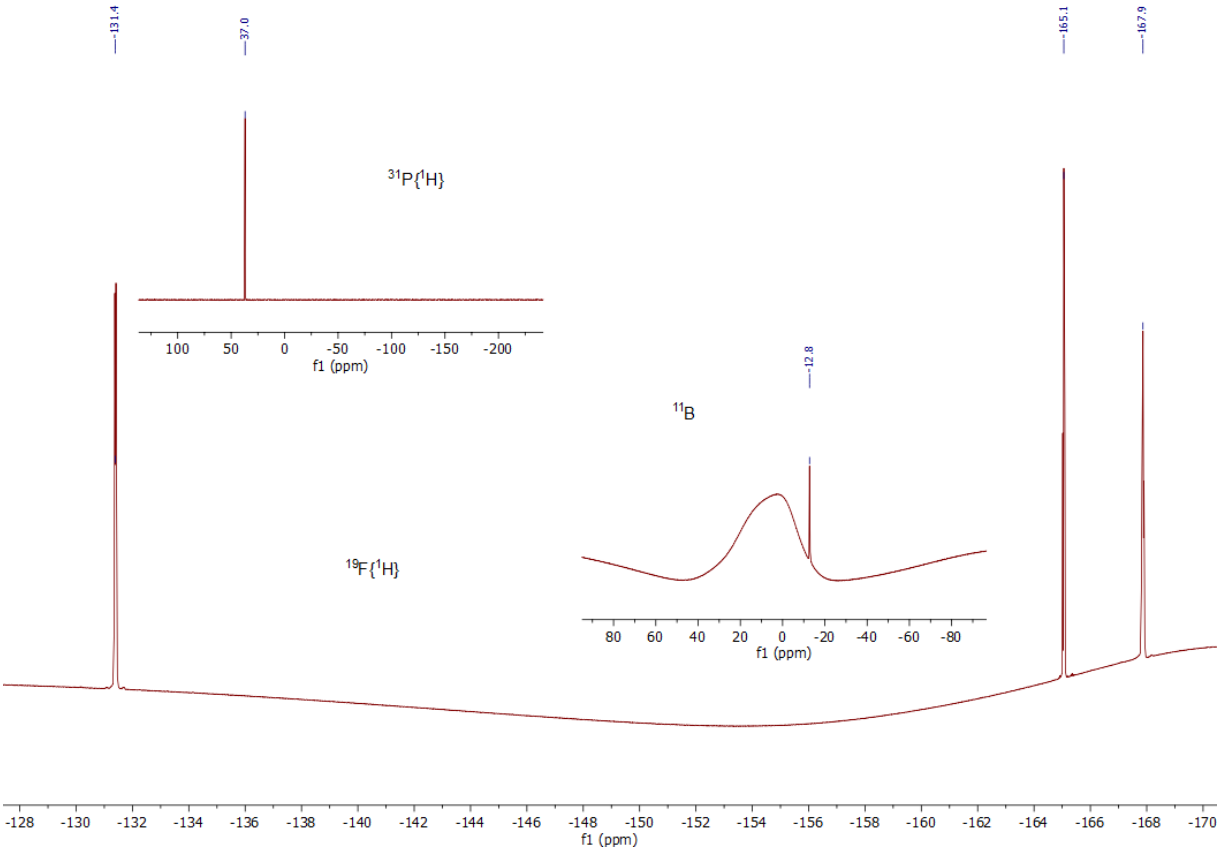

Figure S93 : $^{31}P\{^{1}H\}$ NMR (202 MHz, CD_2Cl_2, 300 K); $^{19}F\{^{1}H\}$ NMR (470 MHz, CD_2Cl_2, 300 K); $^{11}B\{^{1}H\}$ NMR (160 MHz, CD_2Cl_2, 300 K) of 5a

Attempted synthesis of complex 5b

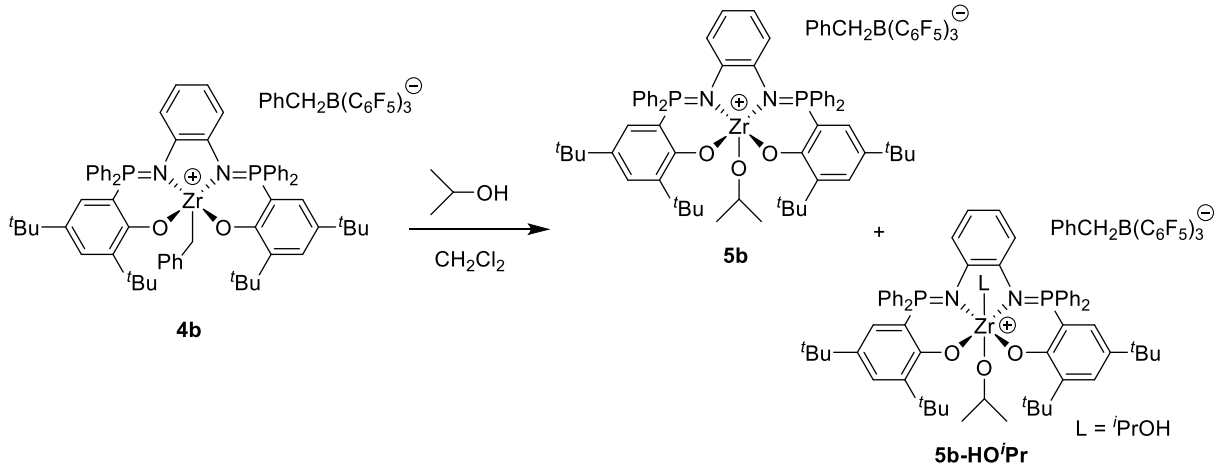

Complex **4b** (0.435 g, 0.25 mmol) was dissolved in dichloromethane (4 mL) and a 0.1 M solution of isopropanol in dichloromethane (2.5 mL, 0.25 mmol) was added. The reaction mixture was stirred for 2 hrs. The volatiles were removed under vacuum to give an oily meringue, which was triturated in pentane (5 mL) to give a light-brown oil. The supernatant solution was removed and the oil was washed with pentane (5x3 mL), then dried under vacuum to give a mixture of **5b** and (presumably) its ^{i}PrOH adduct. The ratio of 5**b** to **5b-^{i}PrOH** was determined to be 85:15 at 240 K by integration of the $^{31}P\{^{1}H\}$ NMR spectrum. Repeating the synthesis using identical conditions to those used for the synthesis of **5a** did not afford pure **5b**.

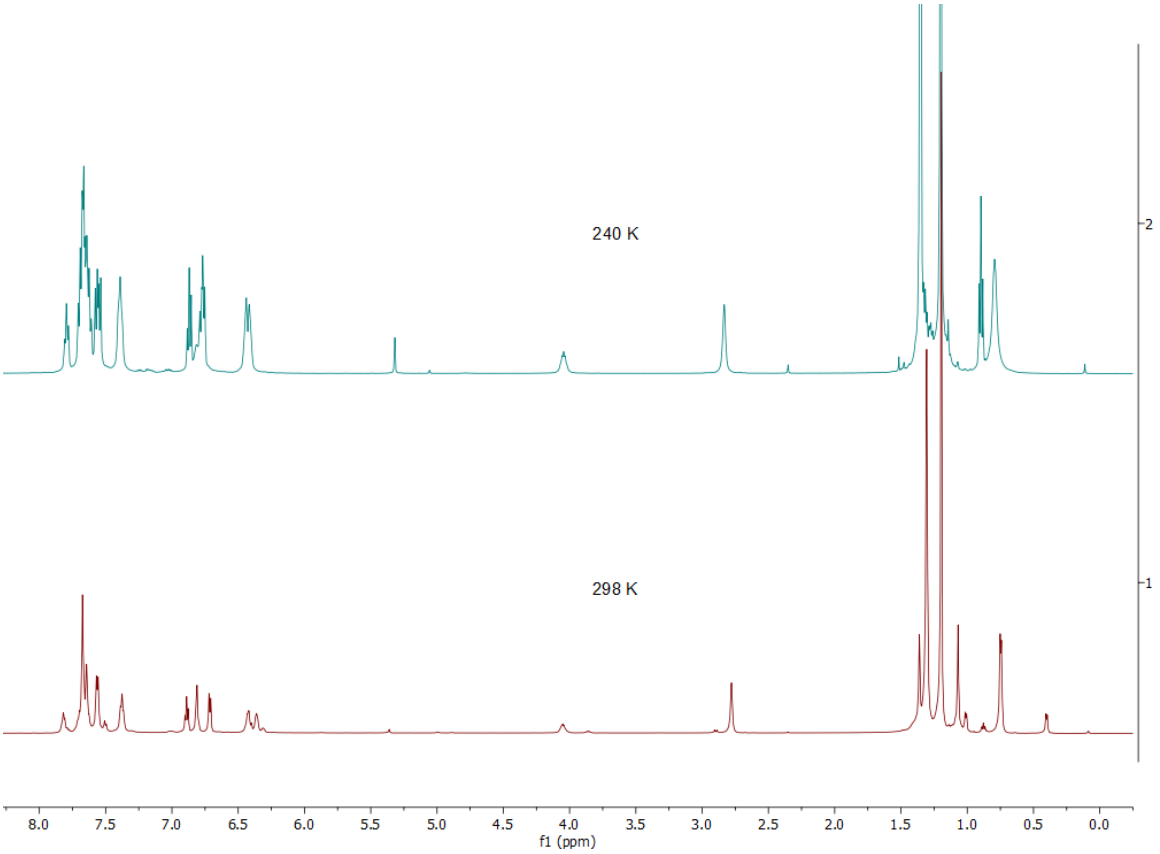

Figure S94: ^{1}H NMR (500 / 600 MHz, CD_2Cl_2, 298 / 240 K) of 5b / 5b-^{i}PrOH

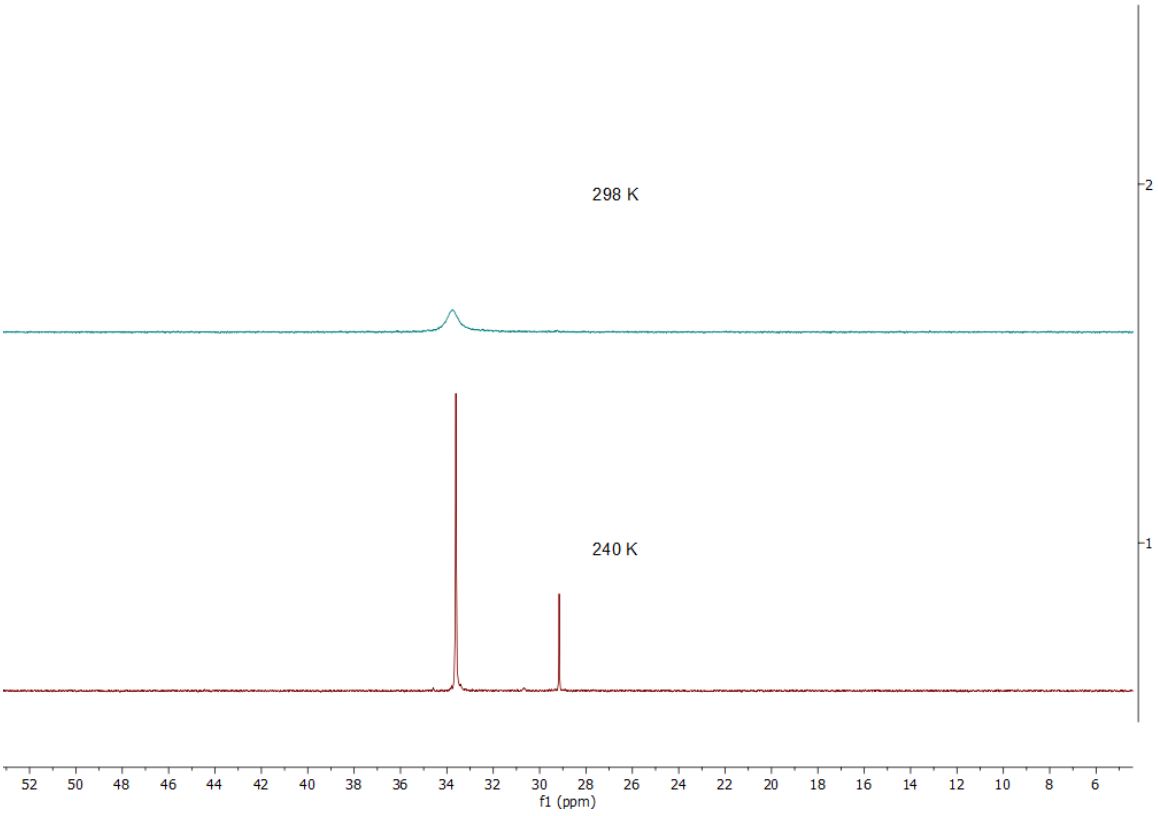

Figure S95: $^{31}P\{^{1}H\}$ NMR (202 / 243 MHz, CD_2Cl_2, 298 / 240 K) of 5b / 5b-^{i}PrOH

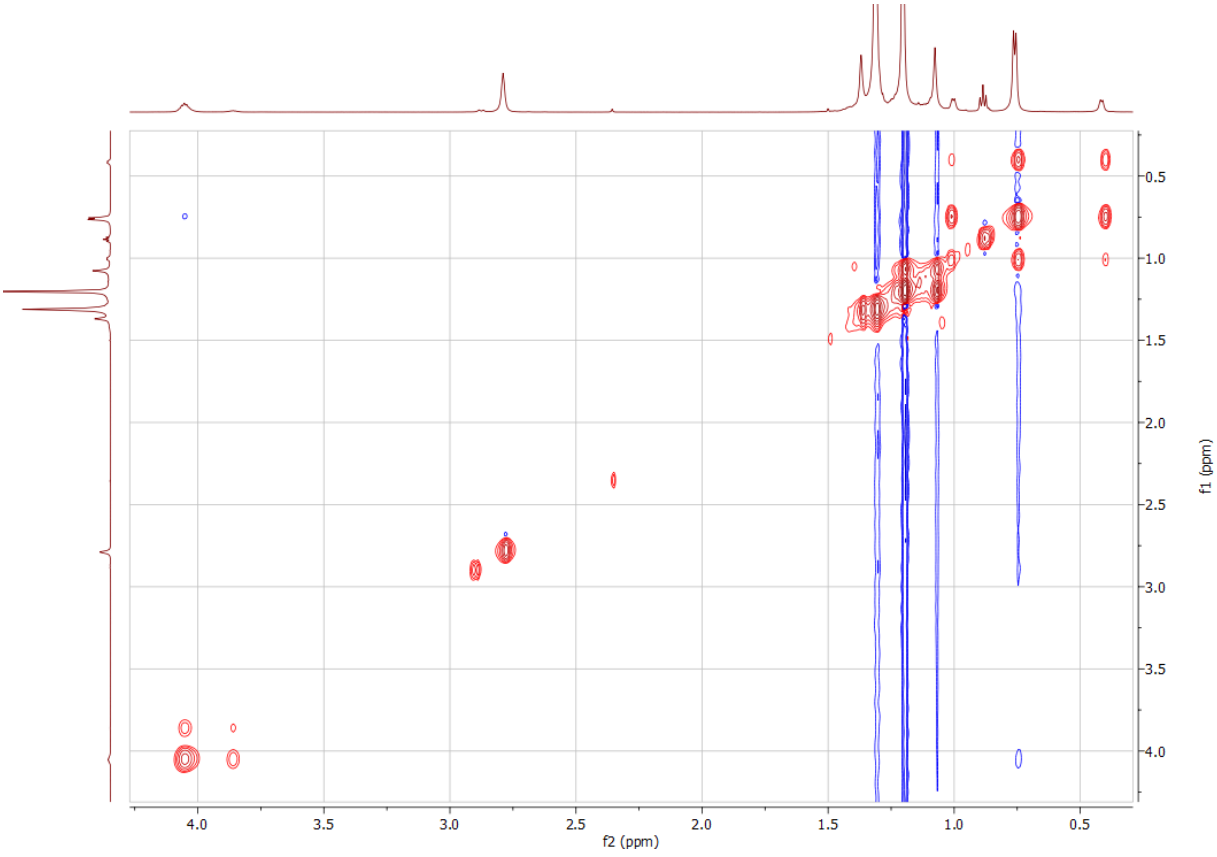

Figure S96: ^{1}H-^{1}H NOESY (600 MHz, CD_2Cl_2, 240 K)(aliphatic region) of 5b / 5b-^{i}PrOH

Complex 6a

^{1}H-^{1}H COSY (600 MHz, CD_2Cl_2, 298 K)[selected cross-peak]: 4.84 / 1.30 (C*H* of lactate / CH_3 of lactate).

^{1}H-^{13}C HMBC (600 MHz / 151 MHz, CD_2Cl_2, 298 K)[selected cross-peaks]: 7.65-7.55 / 162.6 (two *H*3 of PAr / *C*1 of PAr), 7.65-7.55 / 127.2 (*H*3 of PAr / *C*5 of PAr), 7.65-7.55 / 127.1 (*H*3 of PAr / *C*5 of PAr), 7.65-7.55 / 35.7 (*H*3 of PAr / two *C* of ^{t}Bu^{2}), 7.65-7.55 / 34.7 (*H*3 of PAr / *C* of ^{t}Bu^{4}), 6.86 / 149.1 (*m* of BBn / *i* of BBn), 6.86 / 127.1 (*m* of BBn / *m* of BBn), 6.81-6.71 / 162.6 (two *H*5 of PAr / *C*1 of PAr), 6.81-6.71 / 130.6 (two *H*5 of PAr / two *C*3 of PAr), 4.84 / 21.4 (C*H* of lactate / CH_3 of lactate), 3.68 / 192.9 (OCH_3 of lactate / *C*=O of lactate), 2.81 / 149.1 (CH_2 of BBn / *i* of BBn), 2.81 / 129.1 (CH_2 of BBn / *o* of BBn), 1.36 / 139.1 (CH_3 of ^{t}Bu^{2} / *C*2 of PAr), 1.36 / 35.7 (CH_3 of ^{t}Bu^{2} / *C* of ^{t}Bu^{2}), 1.36 / 29.9 (CH_3 of ^{t}Bu^{2} / *C*H$_3$ of ^{t}Bu^{2}), 1.34 / 139.1 (CH_3 of ^{t}Bu^{2} / *C*2 of PAr), 1.34 / 35.7 (CH_3 of ^{t}Bu^{2} / *C* of ^{t}Bu^{2}), 1.34 / 29.8 (CH_3 of ^{t}Bu^{2} / *C*H$_3$ of ^{t}Bu^{2}), 1.30 / 192.9 (CH_3 of lactate / *C*=O of lactate), 1.30 / 77.2 (CH_3 of lactate / *C*H of lactate), 1.15 / 142.1 (CH_3 of ^{t}Bu^{4} / two *C*4 of PAr), 1.15 / 34.7 (CH_3 of ^{t}Bu^{4} / *C* of ^{t}Bu^{4}), 1.15 / 31.4 (CH_3 of ^{t}Bu^{4} / *C*H$_3$ of ^{t}Bu^{4}).

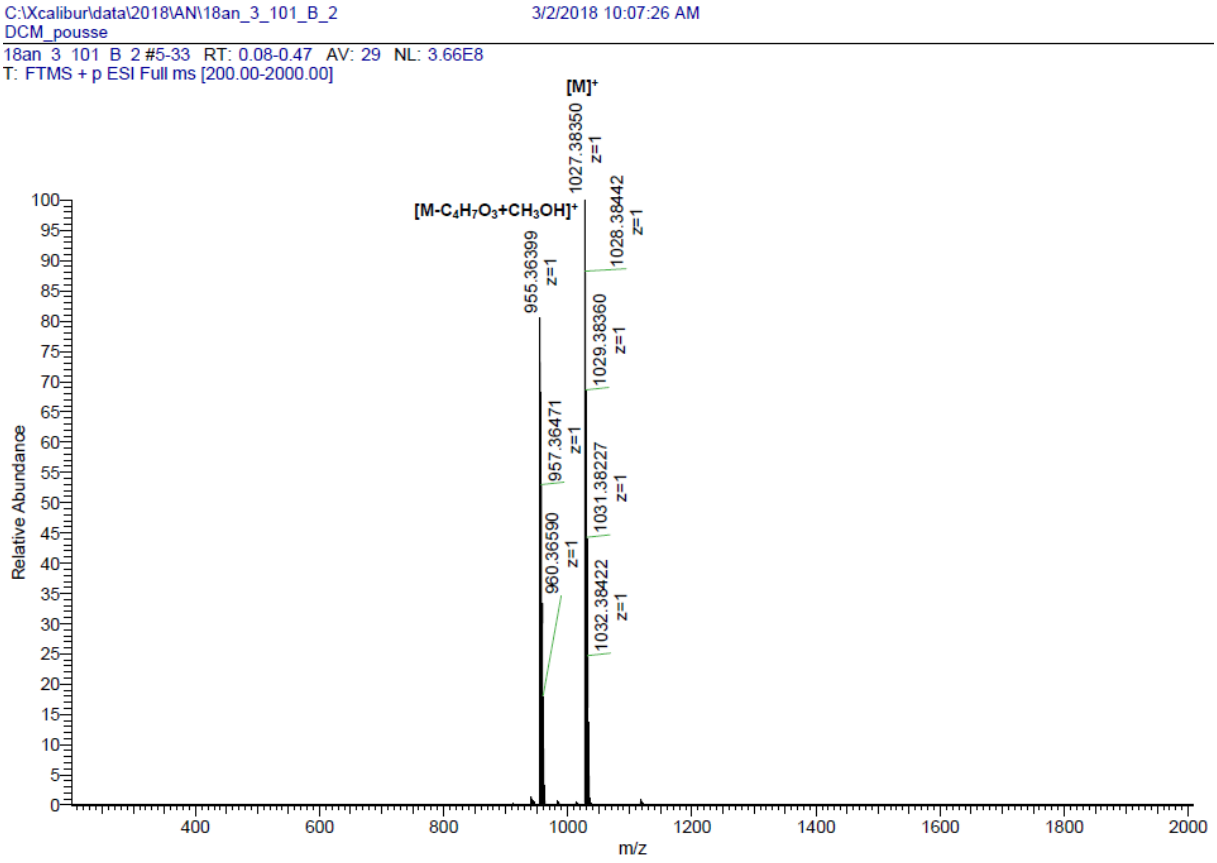

Figure S97: HRMS (ESI-pos)(whole spectrum) of 6a

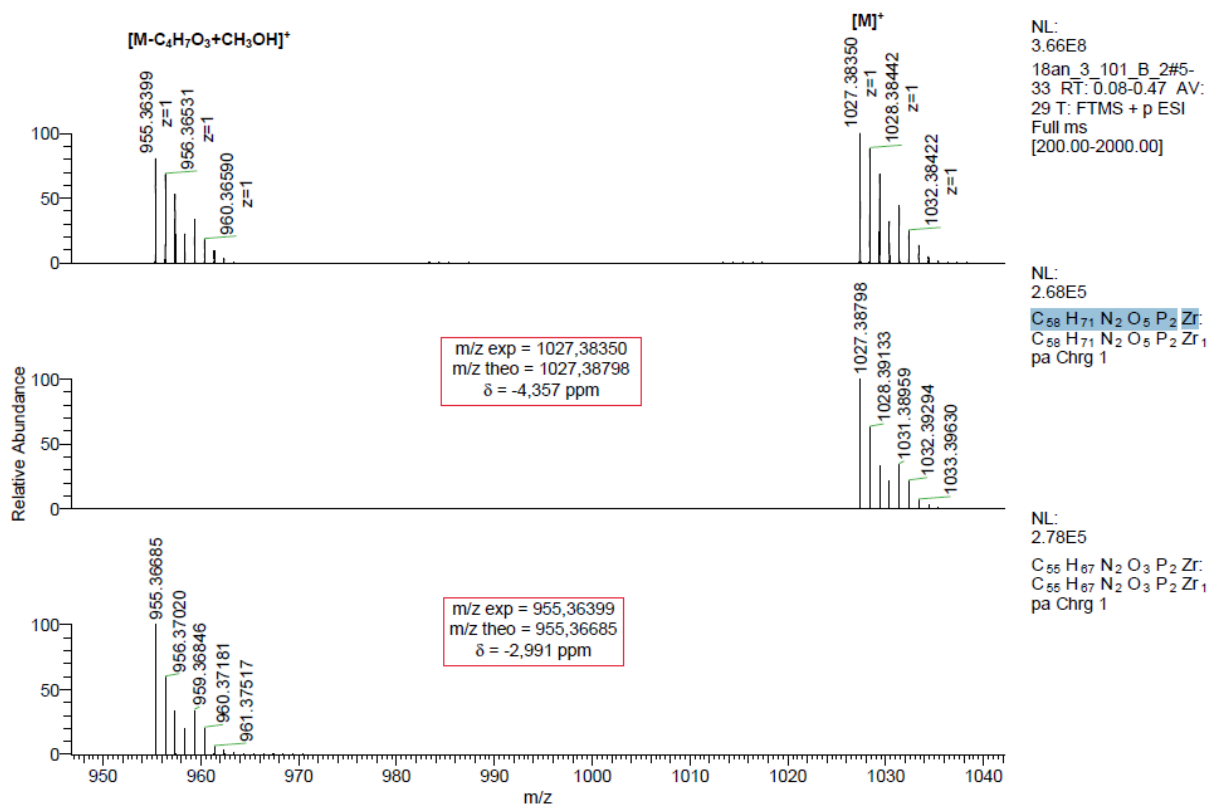

Figure S98: HRMS (ESI-pos)(detail) of 6a

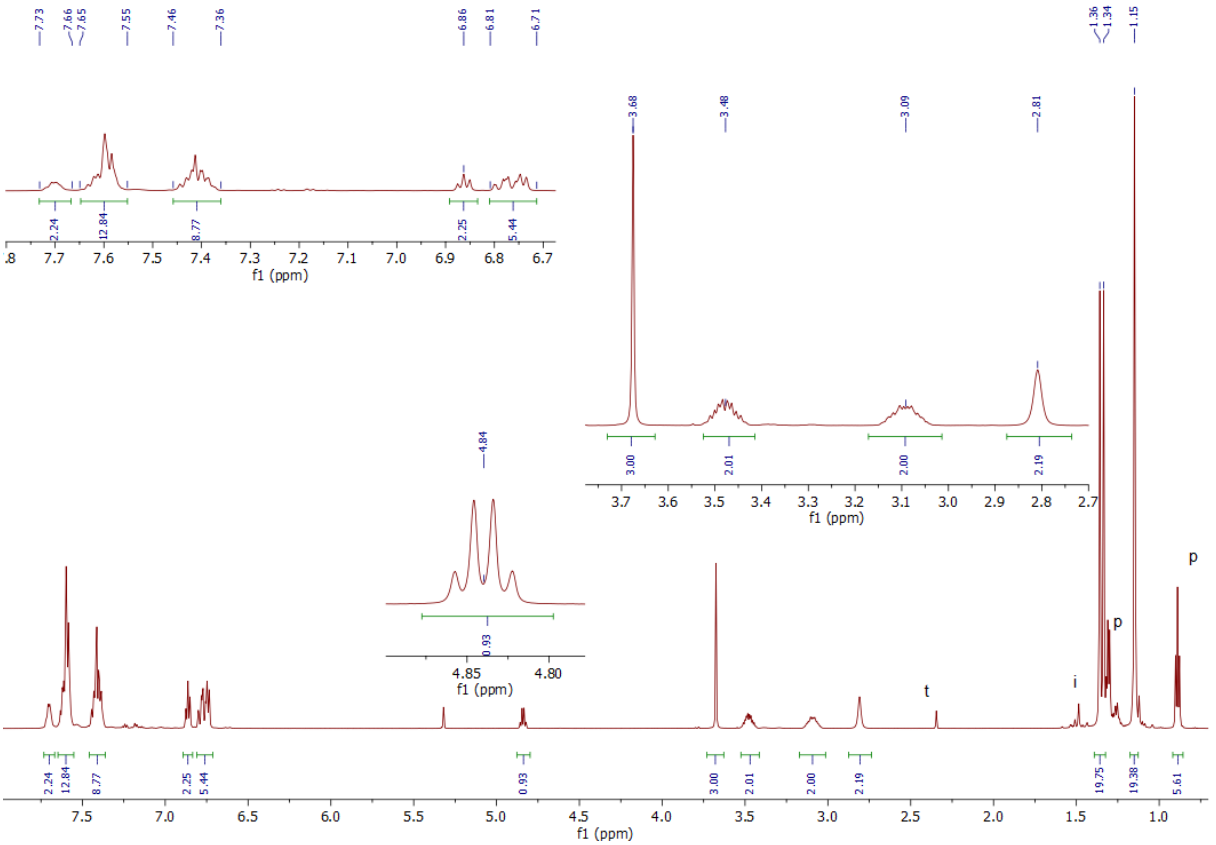

Figure S99: ^{1}H NMR (600 MHz, CD_2Cl_2, 298 K)(i: impurity, p: pentane; t: toluene) of 6a

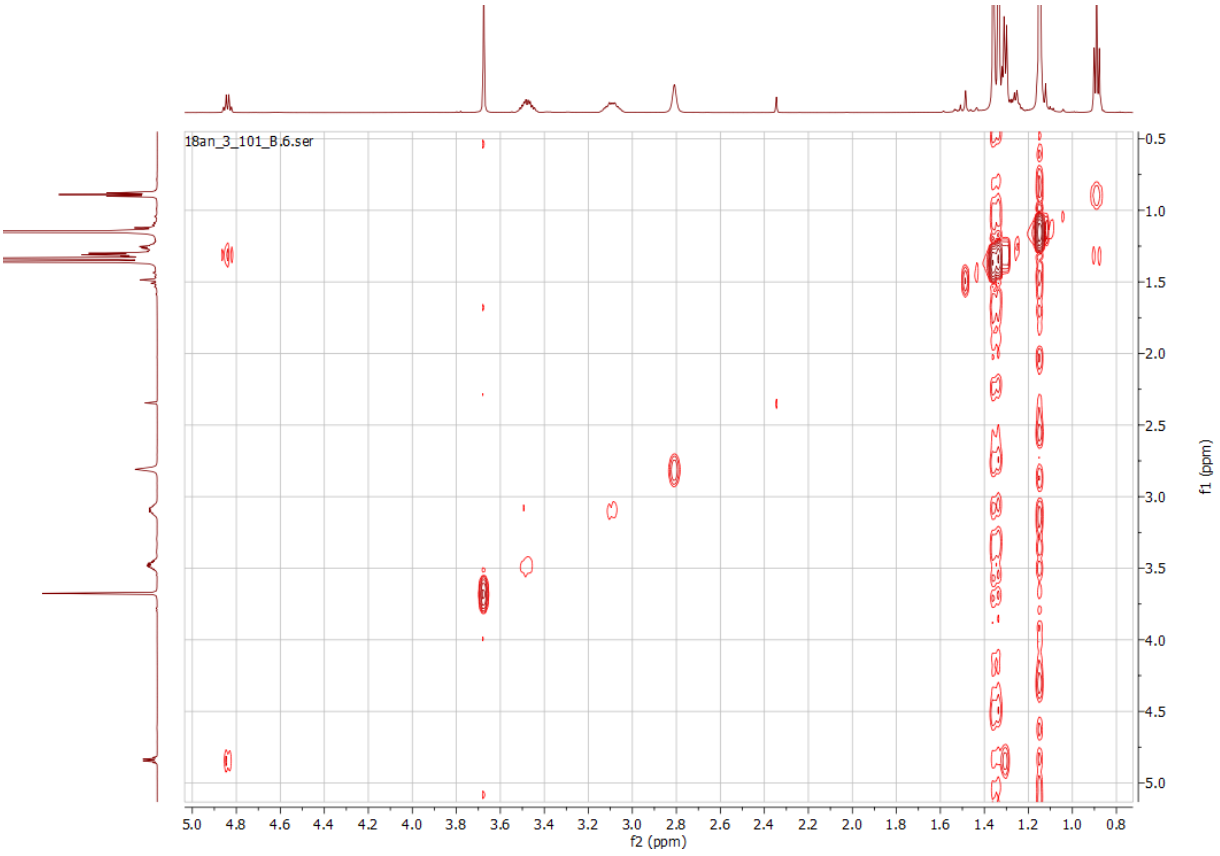

Figure S100: ^{1}H-^{1}H COSY (600 MHz, CD_2Cl_2, 298 K) of 6a

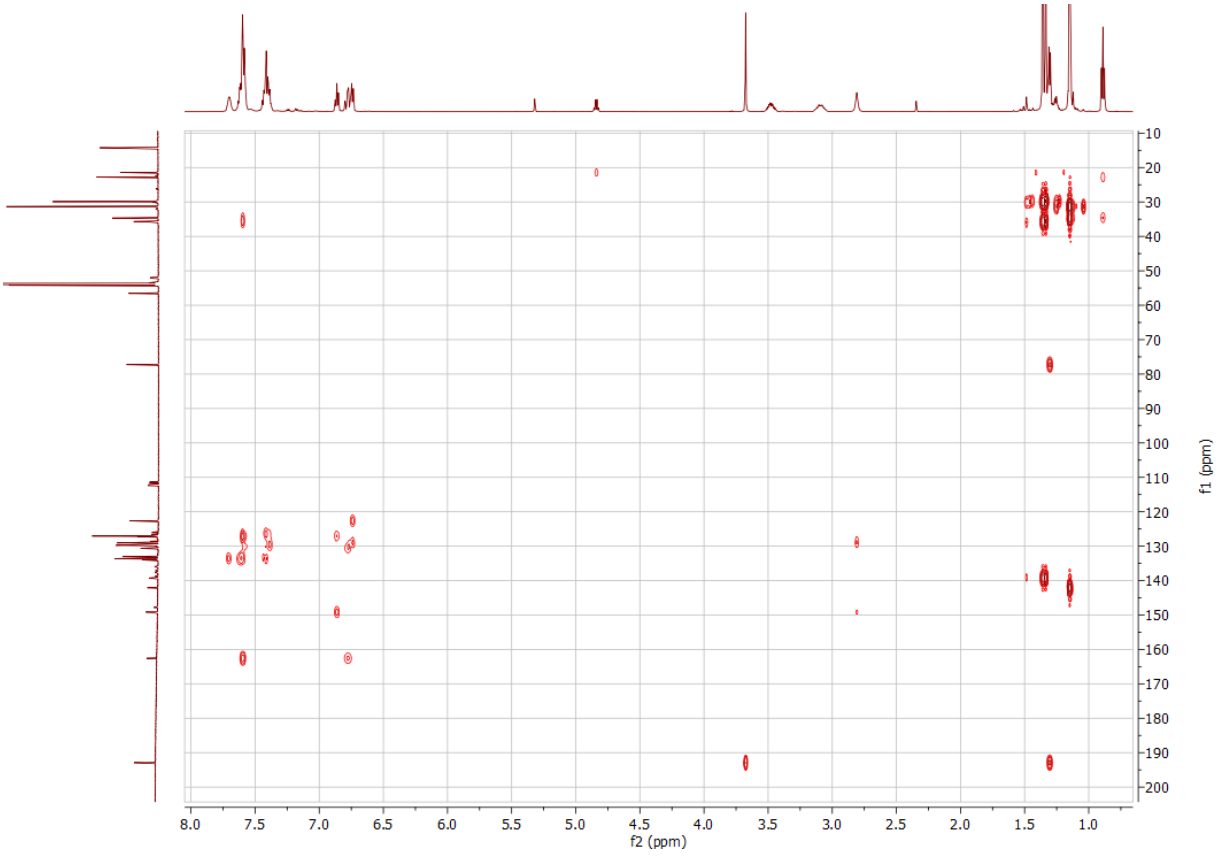

Figure S101: ^{1}H-^{13}C HMBC (600 MHz / 151 MHz, CD_2Cl_2, 298 K)(whole spectrum) of 6a

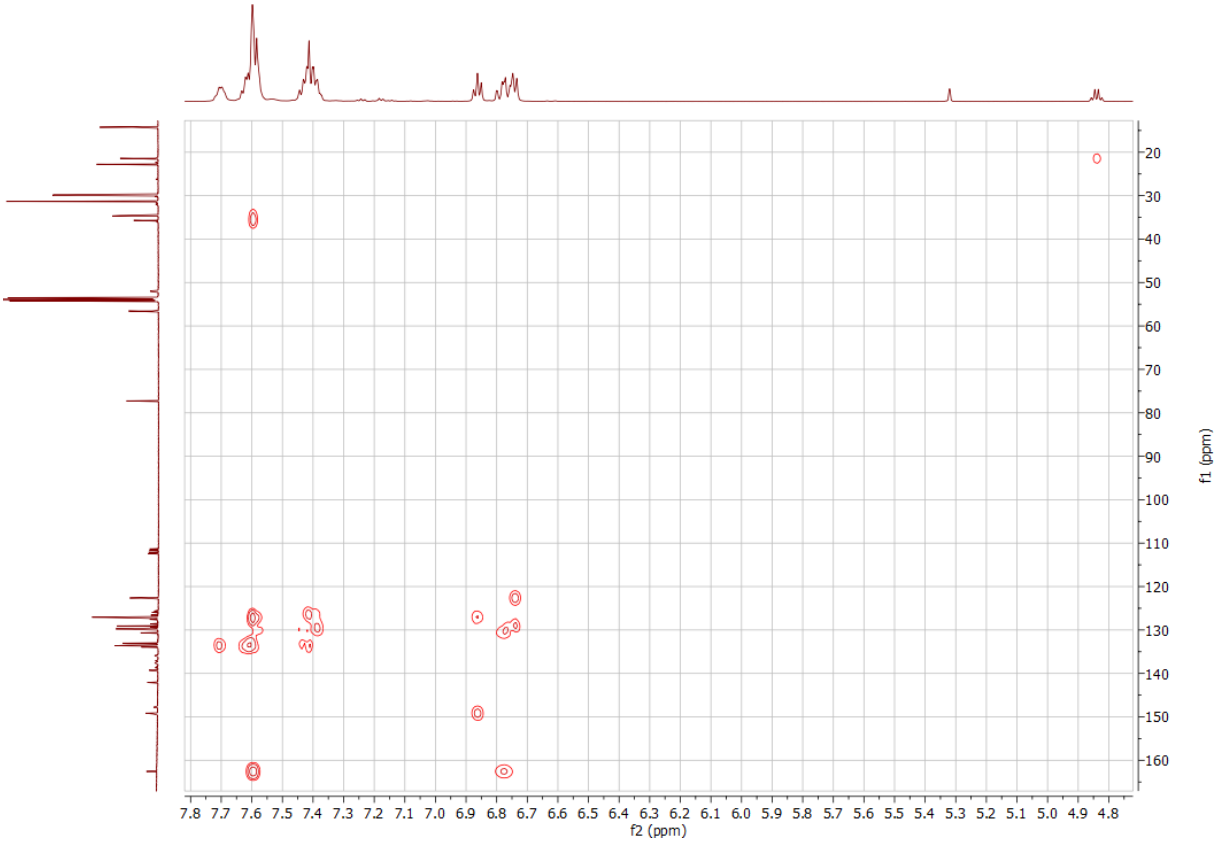

Figure S102: ^{1}H-^{13}C HMBC (600 MHz / 151 MHz, CD_2Cl_2, 298 K)(zoom) of 6a

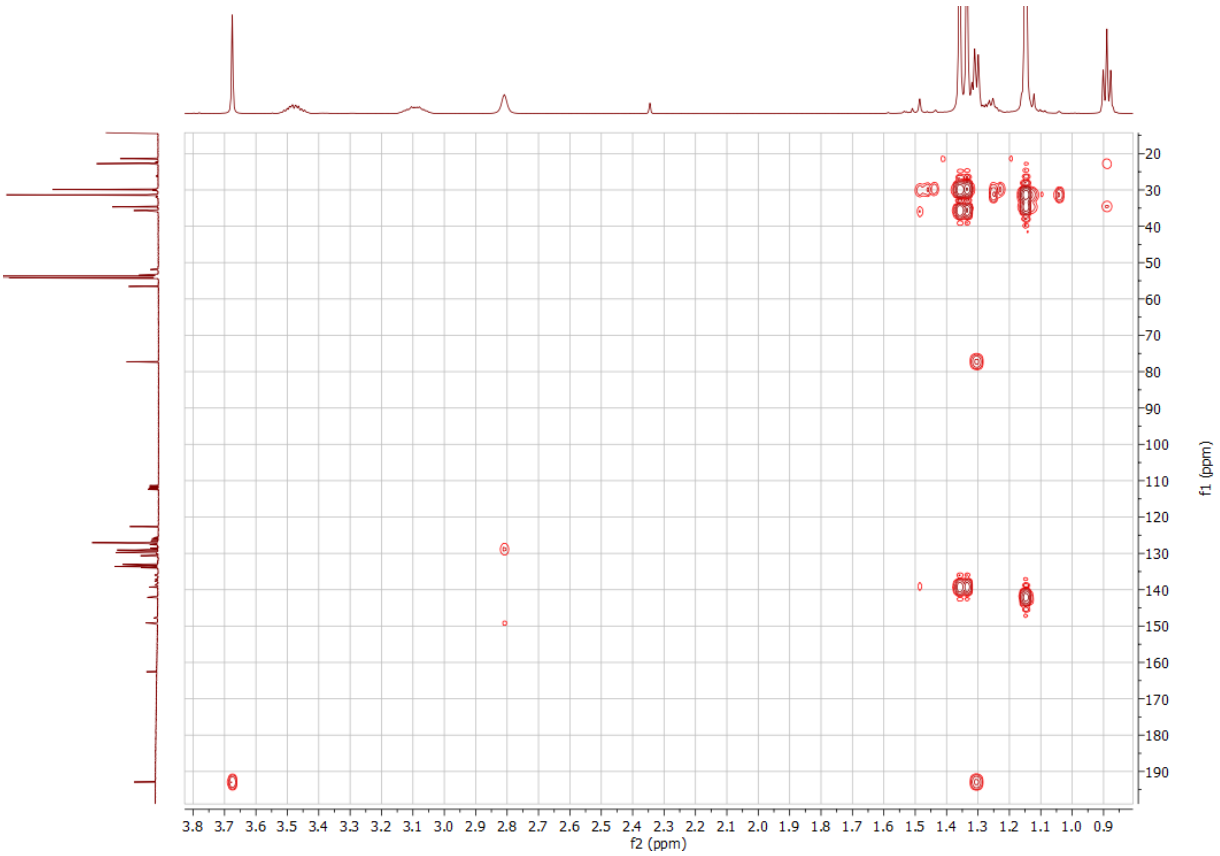

Figure S103: ^{1}H-^{13}C HMBC (600 MHz / 151 MHz, CD_2Cl_2, 298 K)(zoom) of 6a

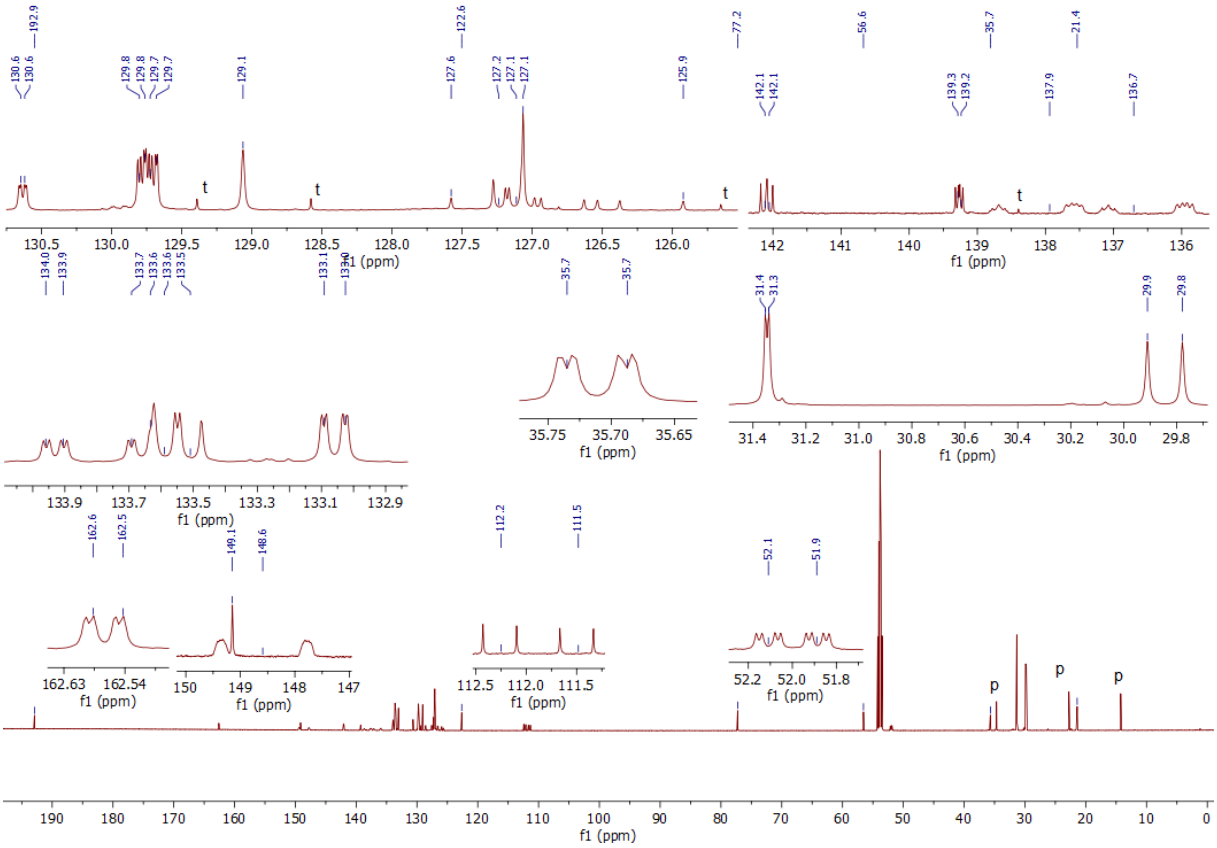

Figure S104: $^{13}C\{^1H\}$ NMR (151 MHz, CD_2Cl_2, 298 K)(t: toluene; p: pentane) of 6a

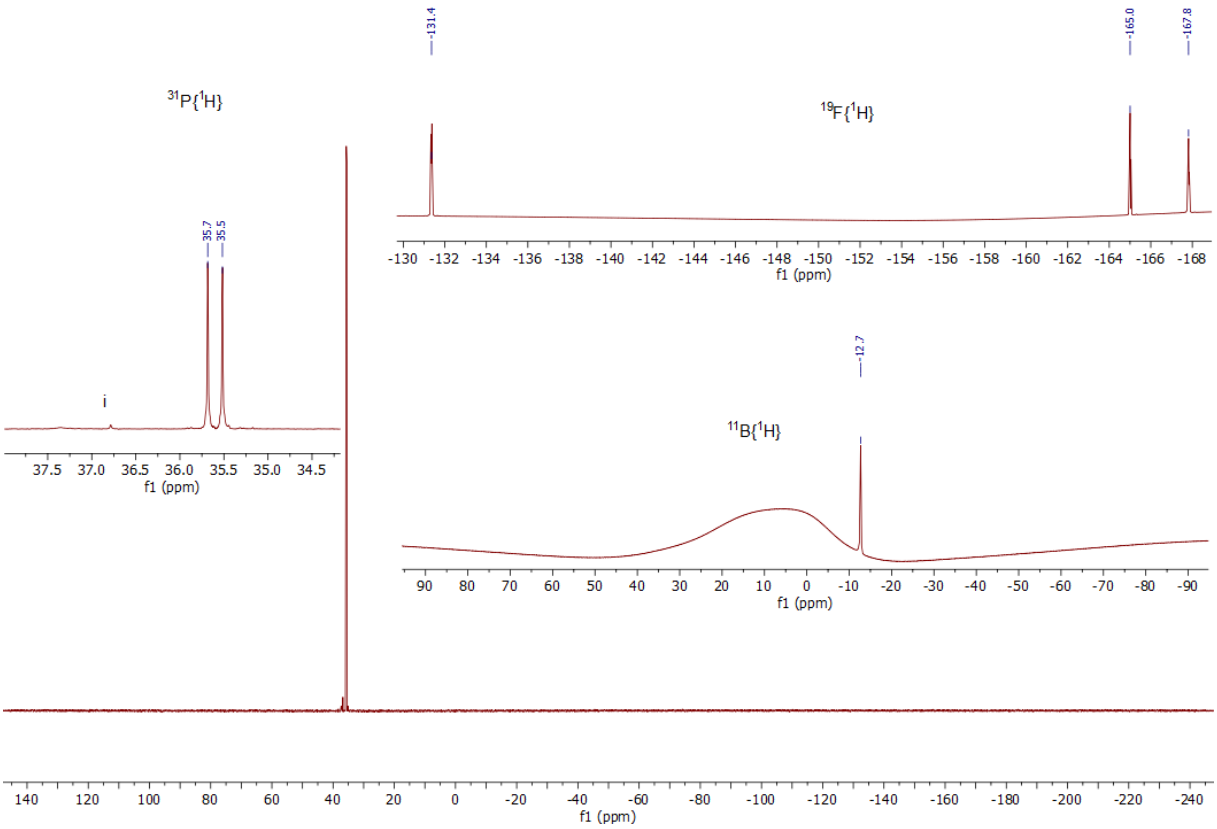

Figure S105: $^{31}P\{^1H\}$ NMR (243 MHz, CD_2Cl_2, 298 K); $^{19}F\{^1H\}$ NMR (570 MHz, CD_2Cl_2, 298 K); $^{11}B\{^1H\}$ NMR (192 MHz, CD_2Cl_2, 298 K) of 6a

Complex 6b

The cosy spectrum was uninformative due to multiple overlapping signals in the aromatic and aliphatic regions.

^{1}H-^{13}C HMBC (500 MHz / 126 MHz, CD_2Cl_2, 298 K)[selected cross-peaks]: 7.67-7.54 / 162.6 (*H*3 of PAr / *C*1 of PAr), 7.67-7.54 / 162.4 (*H*3 of PAr / *C*1 of PAr), 7.67-7.54 / 35.6 (*H*3 of PAr / *C* of ^{t}Bu^{2}), 6.89 / 162.4 (*H*5 of PAr / *C*1 of PAr), 6.89 / 34.8 (*H*5 of PAr / *C* of ^{t}Bu^{4}), 6.87 / 149.1 (*m* of BBn / *i* of BBn), 6.87 / 127.1 (*m* of BBn / *m* of BBn), 6.81 / 162.6 (*H*5 of PAr / *C*1 of PAr), 6.81 / 34.8 (*H*5 of PAr / *C* of ^{t}Bu^{4}), 6.78 / 122.7 (*o* of BBn / *p* of BBn), 6.76 / 129.1 (*p* of BBn / *o* of BBn), 6.42 / 141.6 (*H*3 of NAr / *C*1 of NAr), 6.39 / 141.1 (*H*3 of NAr / *C*1 of NAr), 6.20 / 141.1 (*H*2 of NAr / *C*1 of NAr), 6.16 / 141.6 (*H*2 of NAr / *C*1 of NAr), 4.61 / 192.8 (C*H* of lactate / *C*=O of lactate), 4.61 / 21.4 (C*H* of lactate / *C*H_3 of lactate), 3.58 / 192.8 (OCH_3 of lactate / *C*=O of lactate), 2.82 / 149.2 (CH_2 of BBn / *i* of BBn), 2.82 / 129.1 (CH_2 of BBn / *o* of BBn).

.

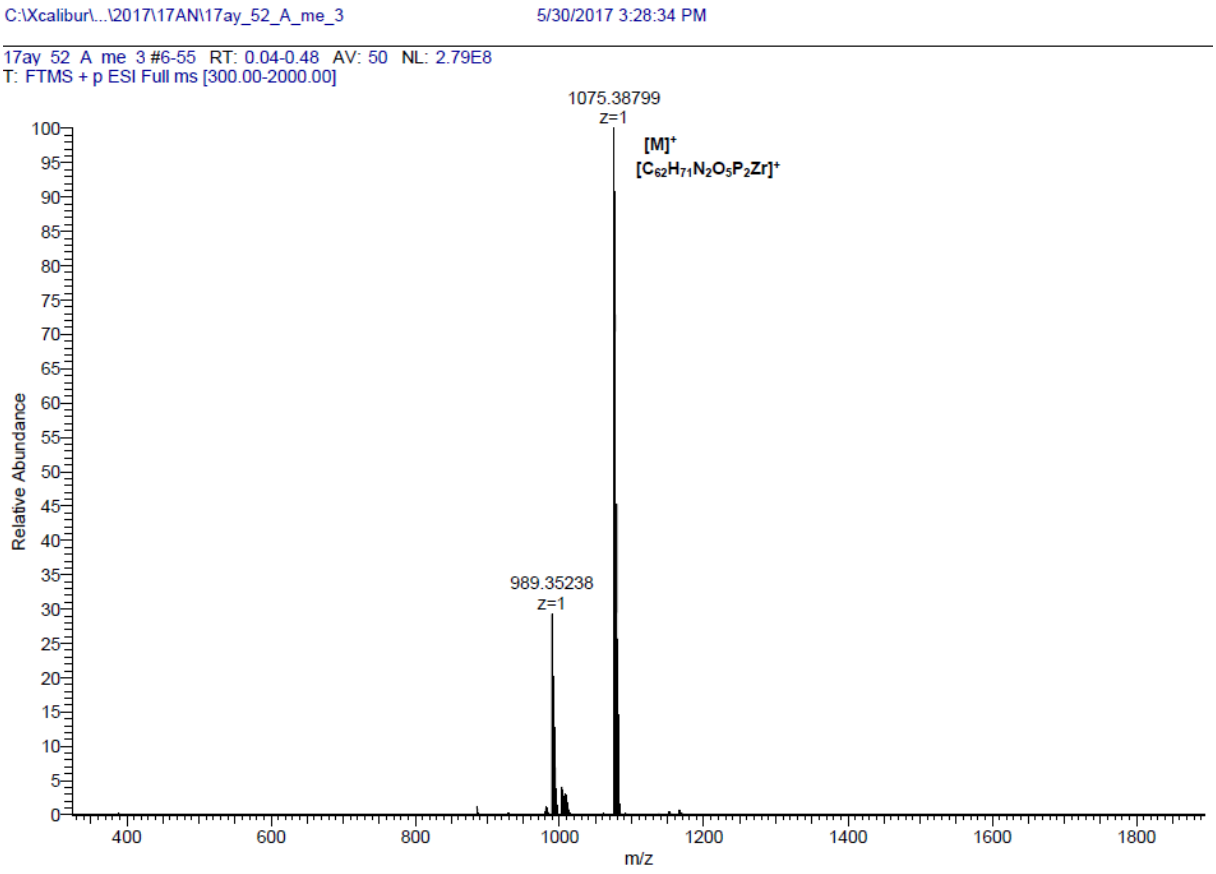

Figure S106: HRMS (ESI-pos)(whole spectrum) of 6b

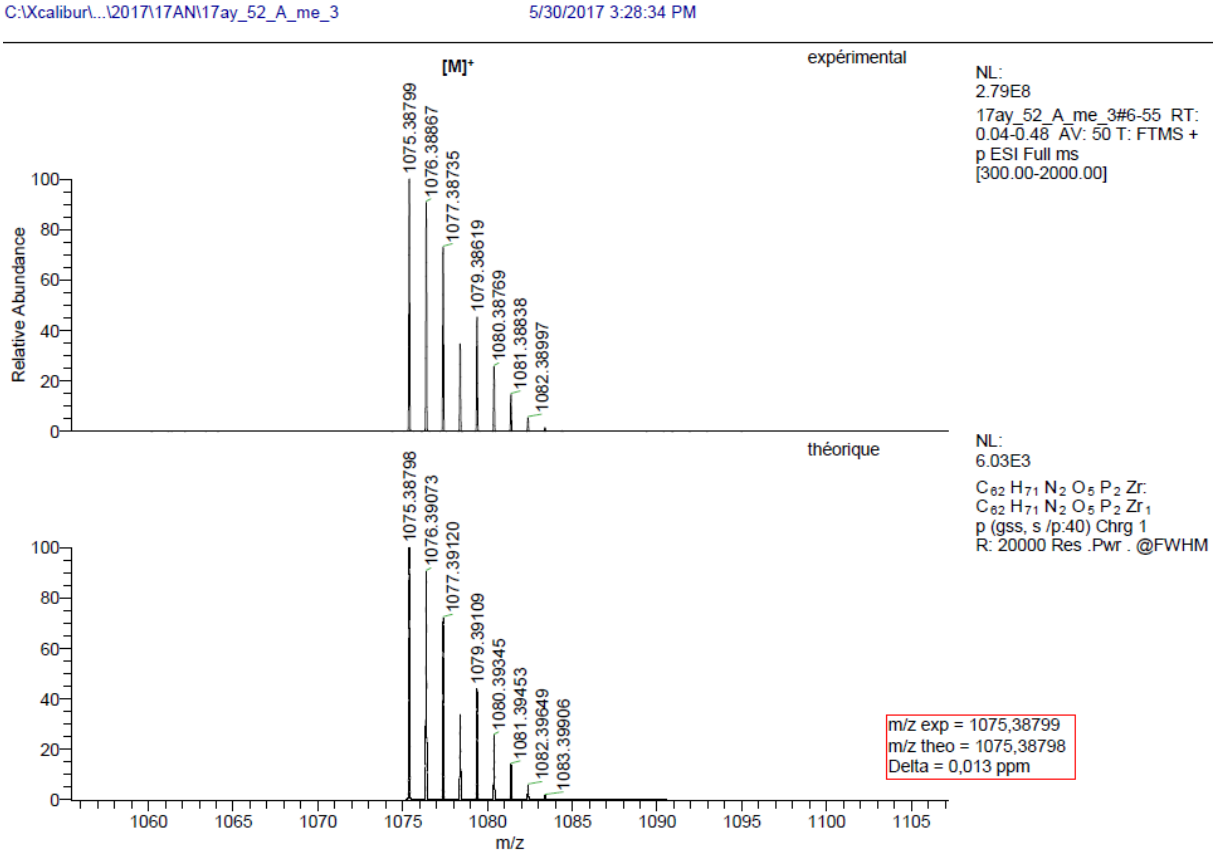

Figure S107: HRMS (ESI-pos)(detail) of 6b

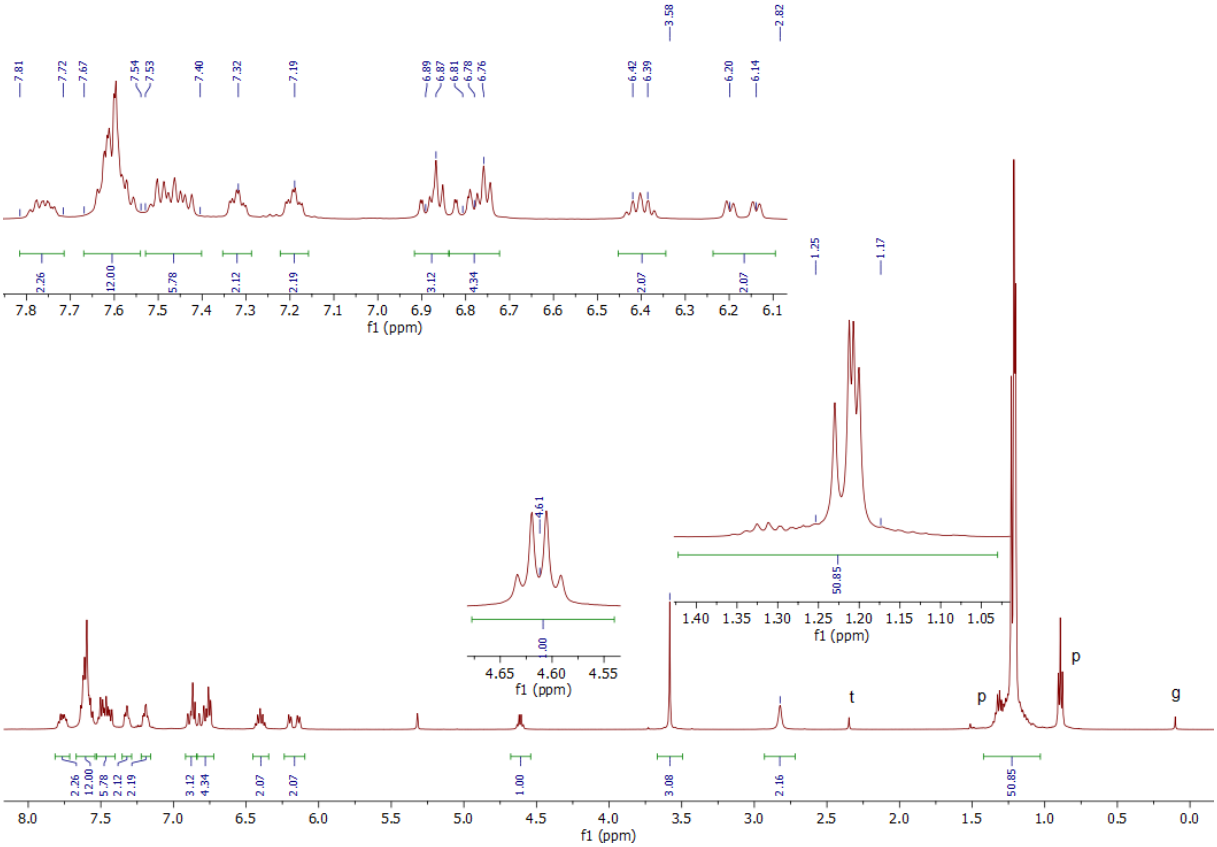

Figure S108: ^{1}H NMR (500 MHz, CD_2Cl_2, 298 K)(g: Si grease, p: pentane; t: toluene) of 6b

Figure S109: ^{1}H-^{13}C HMBC (500 MHz / 126 MHz, CD_2Cl_2, 298 K)(whole spectrum) of 6b

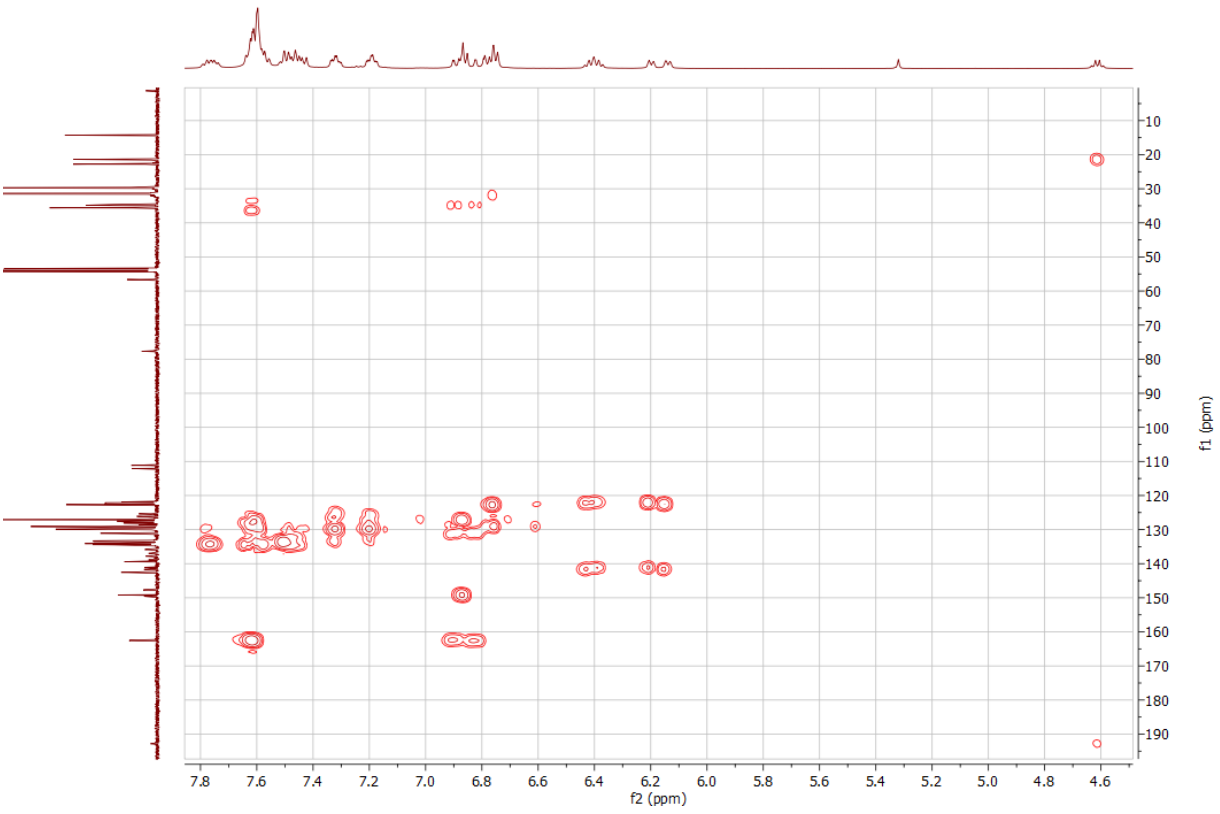

Figure S110: ^{1}H-^{13}C HMBC (500 MHz / 126 MHz, CD_2Cl_2, 298 K)(zoom) of 6b

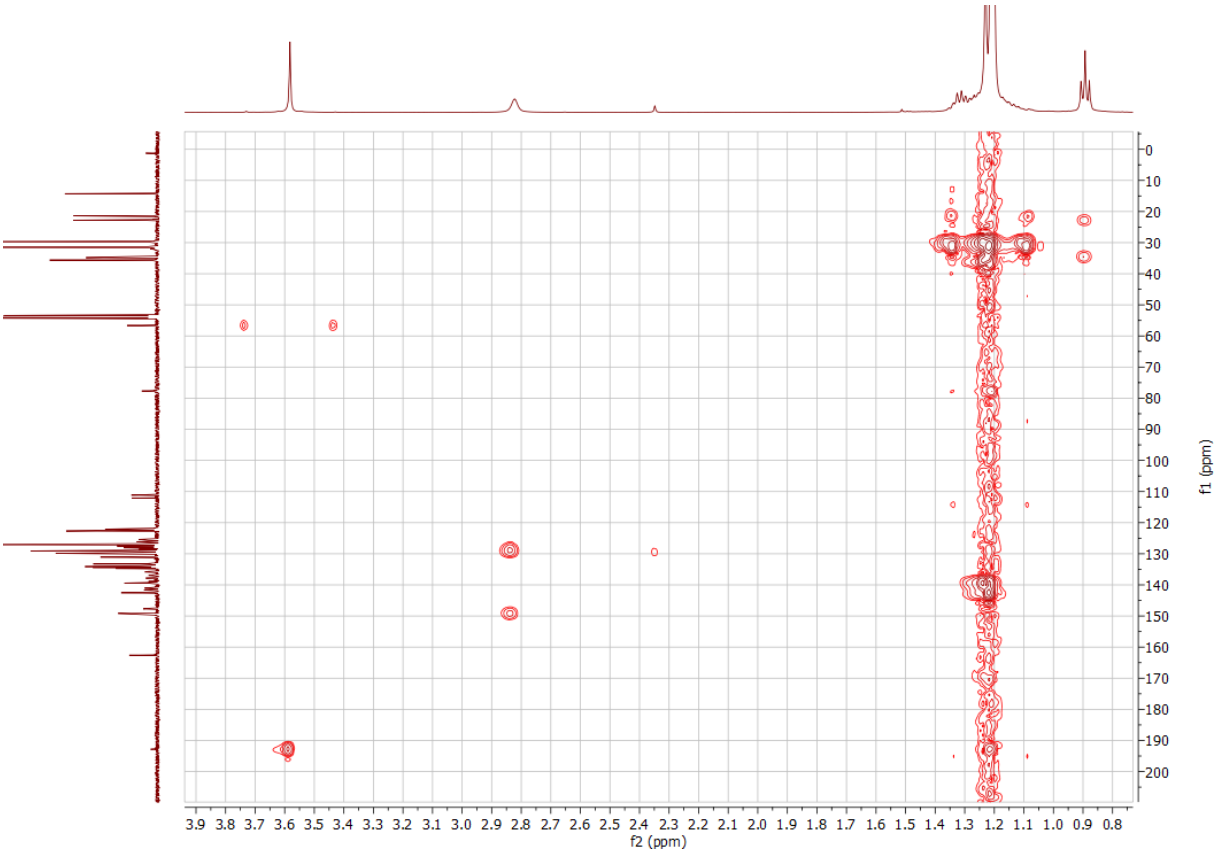

Figure S111: ^{1}H-^{13}C HMBC (500 MHz / 126 MHz, CD_2Cl_2, 298 K)(zoom) of 6b

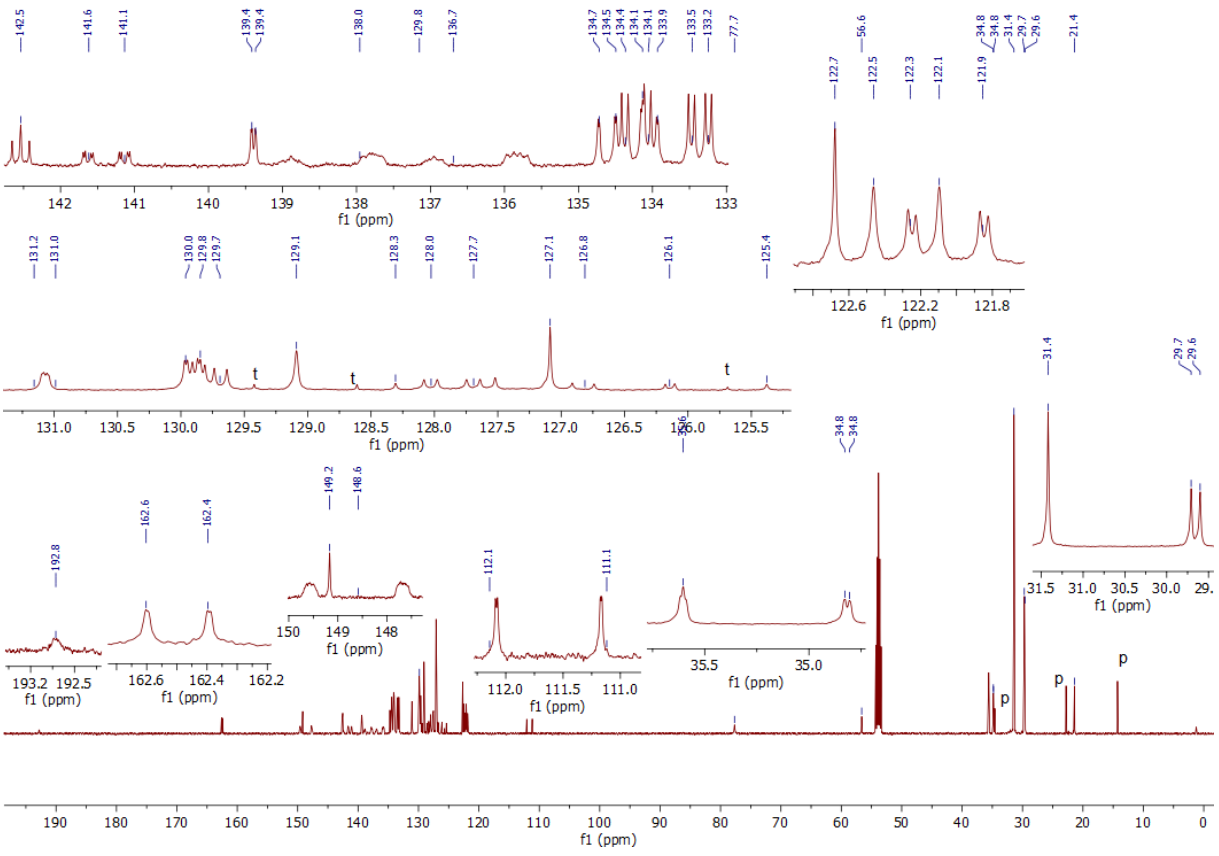

Figure S112: $^{13}C\{^{1}H\}$ NMR (126 MHz, CD_2Cl_2, 298 K)(t: toluene; p: pentane) of 6b

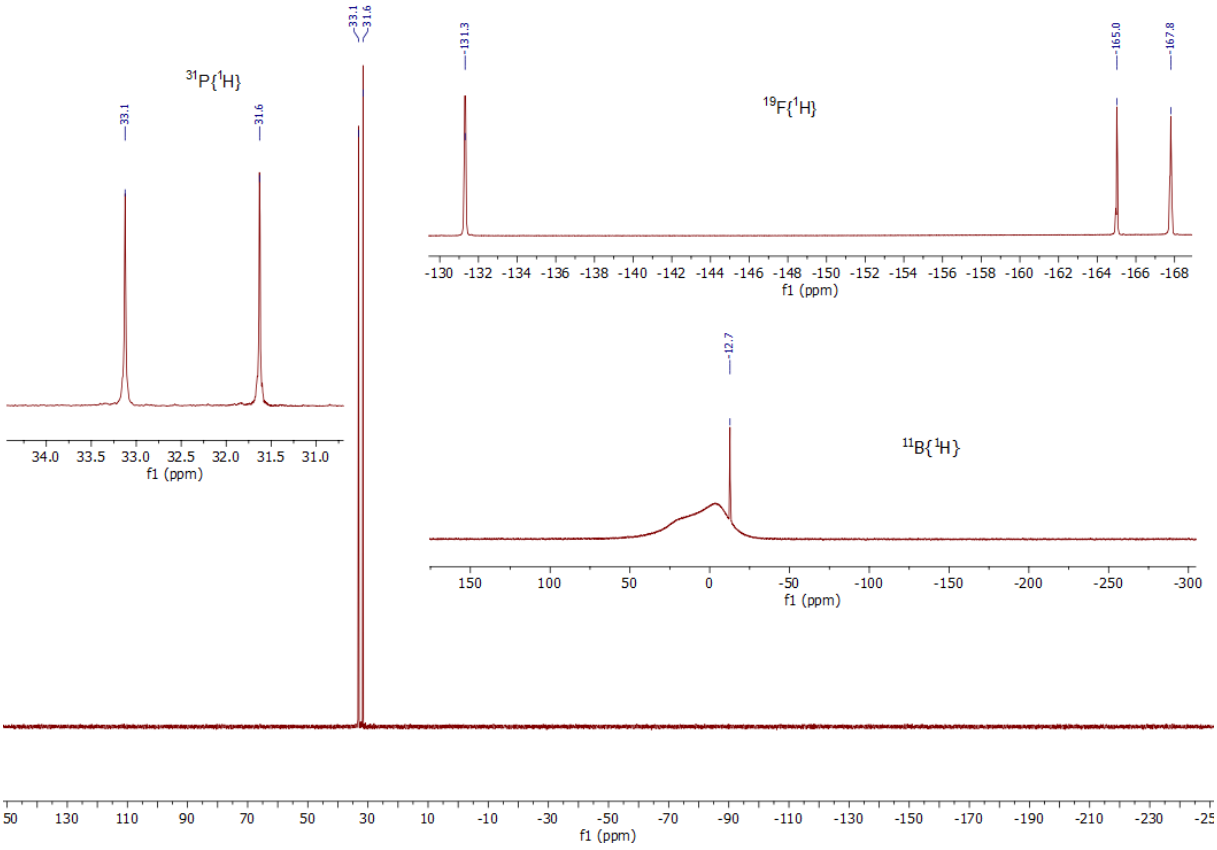

Figure S113: $^{31}P\{^{1}H\}$ NMR (202 MHz, CD_2Cl_2, 298 K); $^{19}F\{^{1}H\}$ NMR (470 MHz, CD_2Cl_2, 298 K); $^{11}B\{^{1}H\}$ NMR (160 MHz, CD_2Cl_2, 298 K) of 6b

Complex 7a

^{1}H-^{13}C HMBC (500 MHz / 126 MHz, d_8-THF, 300 K)[selected cross-peaks]: 8.01 / 132.3 (*o* of PPh_2 / *p* of PPh_2), 6.86 / 170.2 (*H*5 of PAr / *C*1 of PAr), 6.86 / 34.5 (*H*5 of PAr / *C* of $^{t}Bu^4$), 6.81 / 169.9 (*H*3 of PAr / *C*1 of PAr), 6.81 / 127.9 (*H*3 of PAr / *C*3 of PAr), 6.81 / 34.5 (*H*5 of PAr / *C* of $^{t}Bu^4$), 1.49 / 140.0 (CH_3 of $^{t}Bu^2$ / *C*2 of PAr), 1.49 / 36.2 (CH_3 of $^{t}Bu^2$ / *C* of $^{t}Bu^2$), 1.49 / 30.5 (CH_3 of $^{t}Bu^2$ / CH_3 of $^{t}Bu^2$), 1.23 / 134.1 (CH_3 of $^{t}Bu^4$ / *C*4 of PAr), 1.23 / 34.5 (CH_3 of $^{t}Bu^4$ / *C* of $^{t}Bu^4$), 1.23 / 31.8 (CH_3 of $^{t}Bu^4$ / CH_3 of $^{t}Bu^4$), 1.10 / 137.1 (CH_3 of $^{t}Bu^4$ / *C*4 of PAr), 1.10 / 34.5 (CH_3 of $^{t}Bu^4$ / *C* of $^{t}Bu^4$), 1.23 / 31.6 (CH_3 of $^{t}Bu^4$ / CH_3 of $^{t}Bu^4$), 1.02 / 140.6 (CH_3 of $^{t}Bu^2$ / *C*2 of PAr), 1.02 / 35.9 (CH_3 of $^{t}Bu^2$ / *C* of $^{t}Bu^2$), 1.02 / 30.3 (CH_3 of $^{t}Bu^2$ / CH_3 of $^{t}Bu^2$).

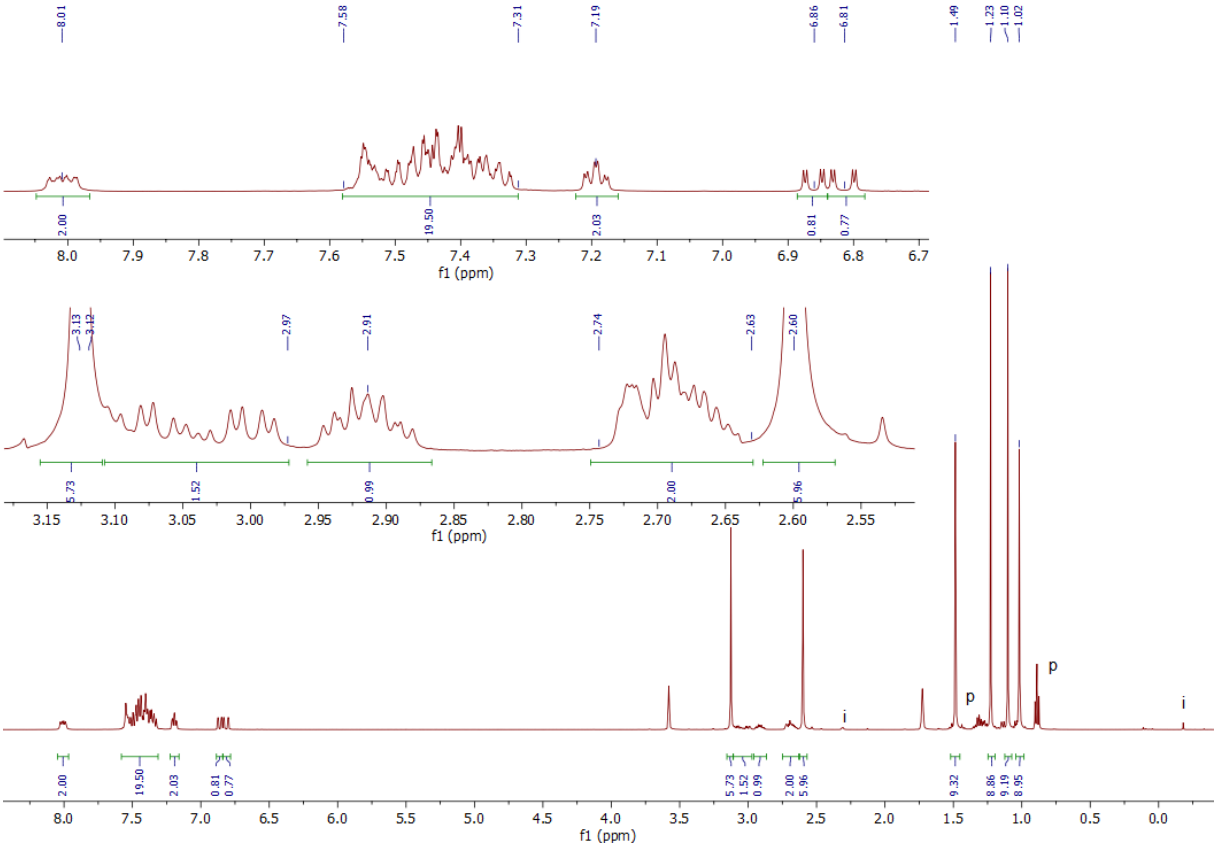

Figure S114: ^{1}H NMR (500 MHz, d_8-THF, 300 K)(p: pentane; i: impurity) of 7a

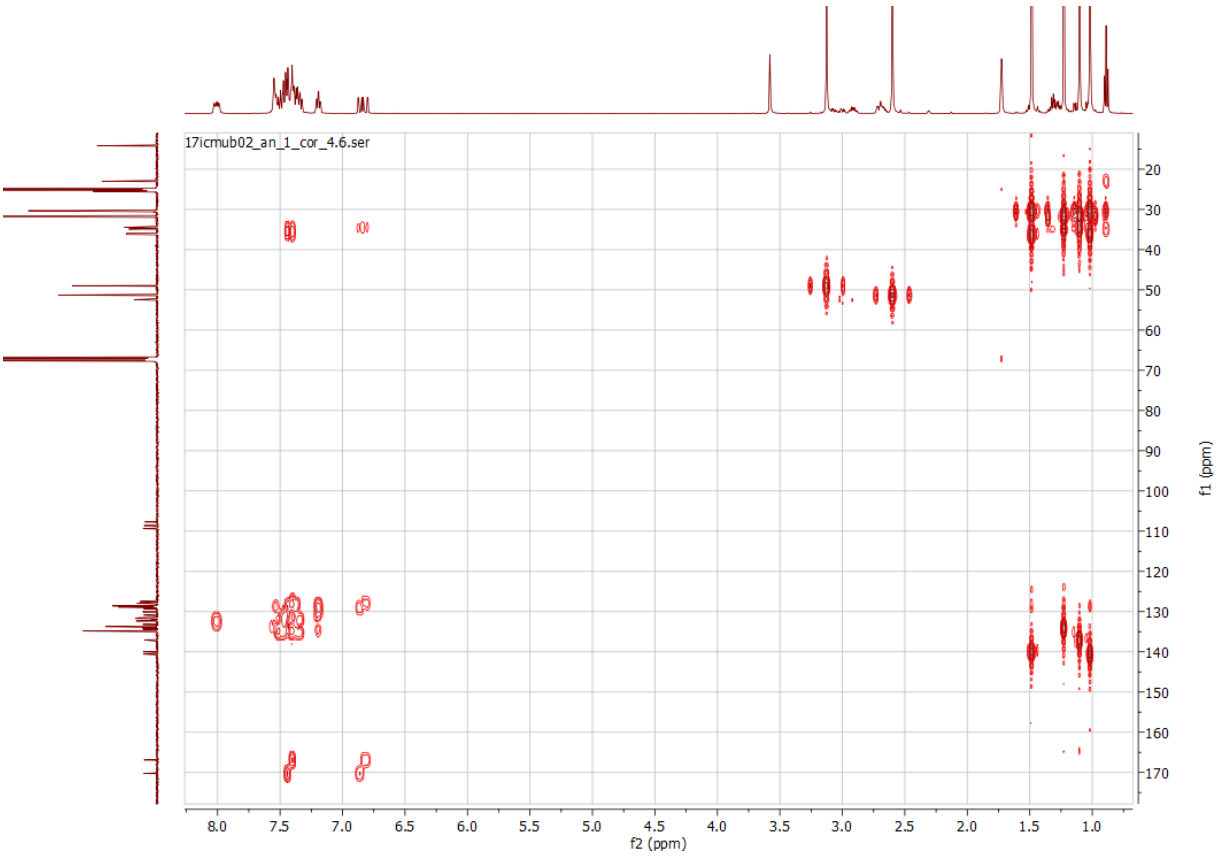

Figure S115: ^{1}H-^{13}C HMBC (500 MHz / 126 MHz, d_8-THF, 300 K)(whole spectrum) of 7a

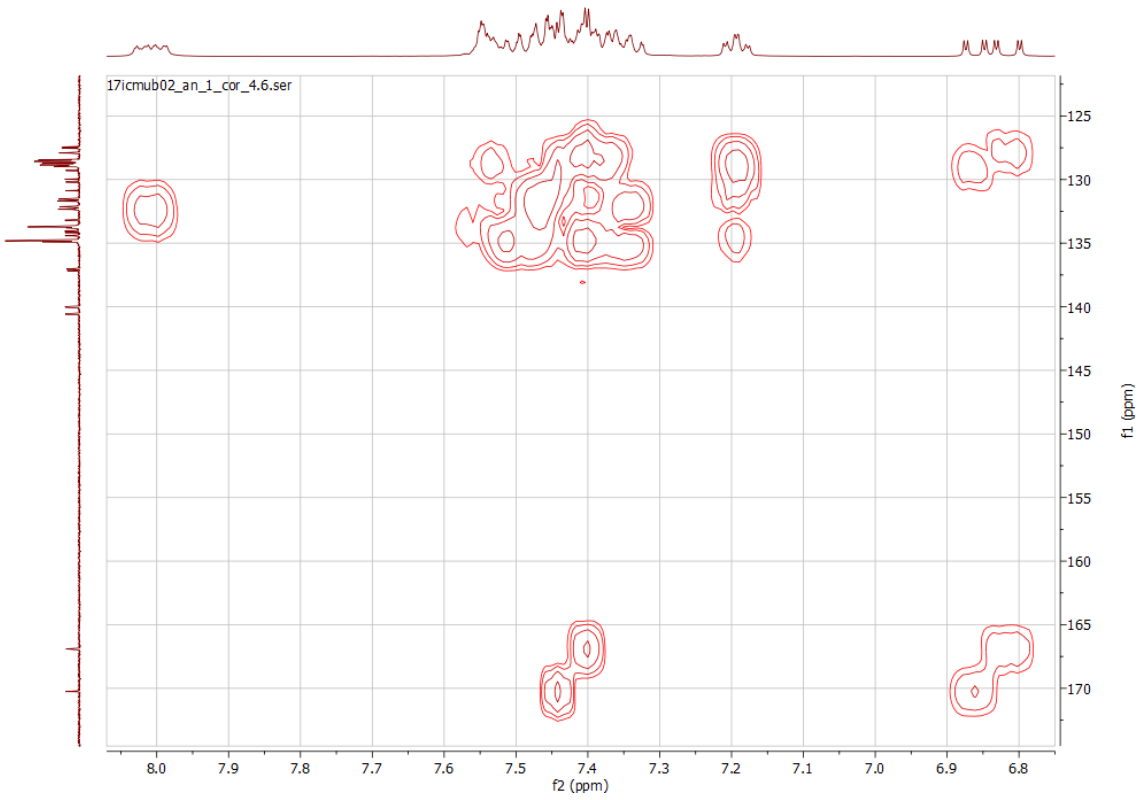

Figure S116: ^{1}H-^{13}C HMBC (500 MHz / 126 MHz, d_8-THF, 300 K)(zoom) of 7a

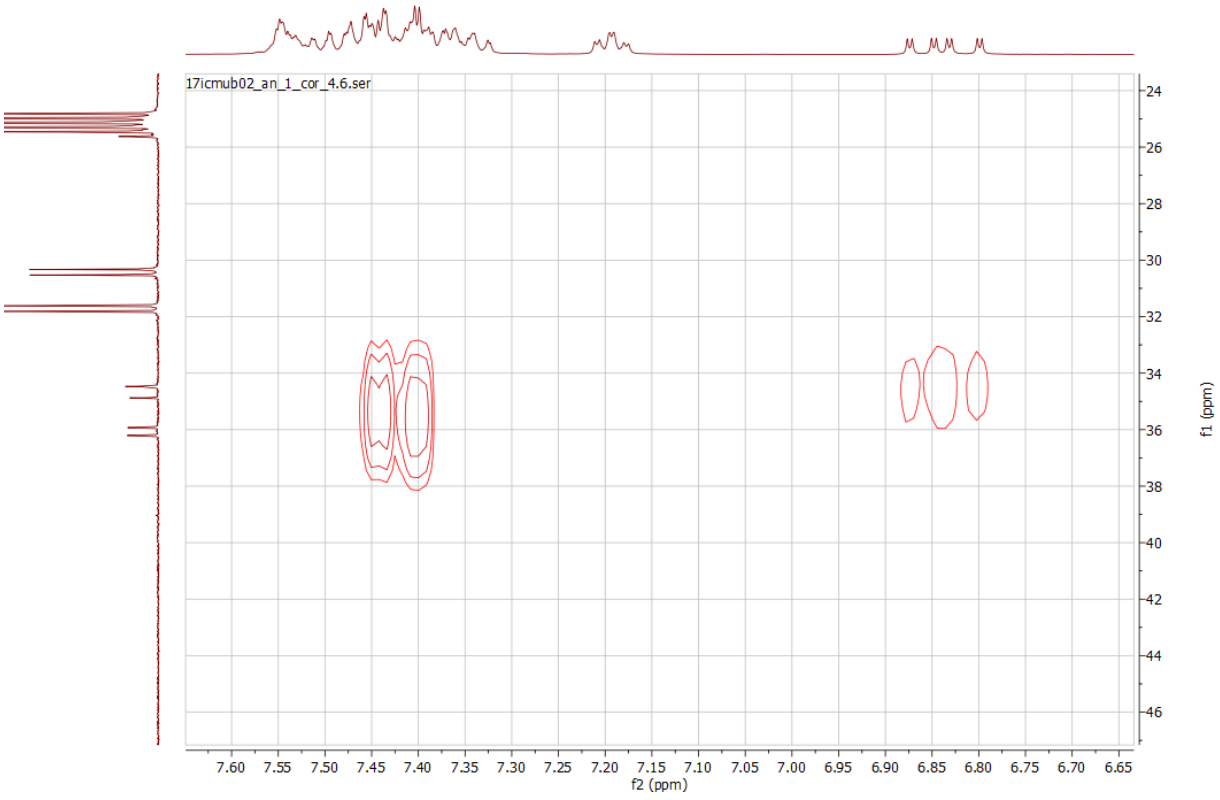

Figure S117: ^{1}H-^{13}C HMBC (500 MHz / 126 MHz, d_8-THF, 300 K)(zoom) of 7a

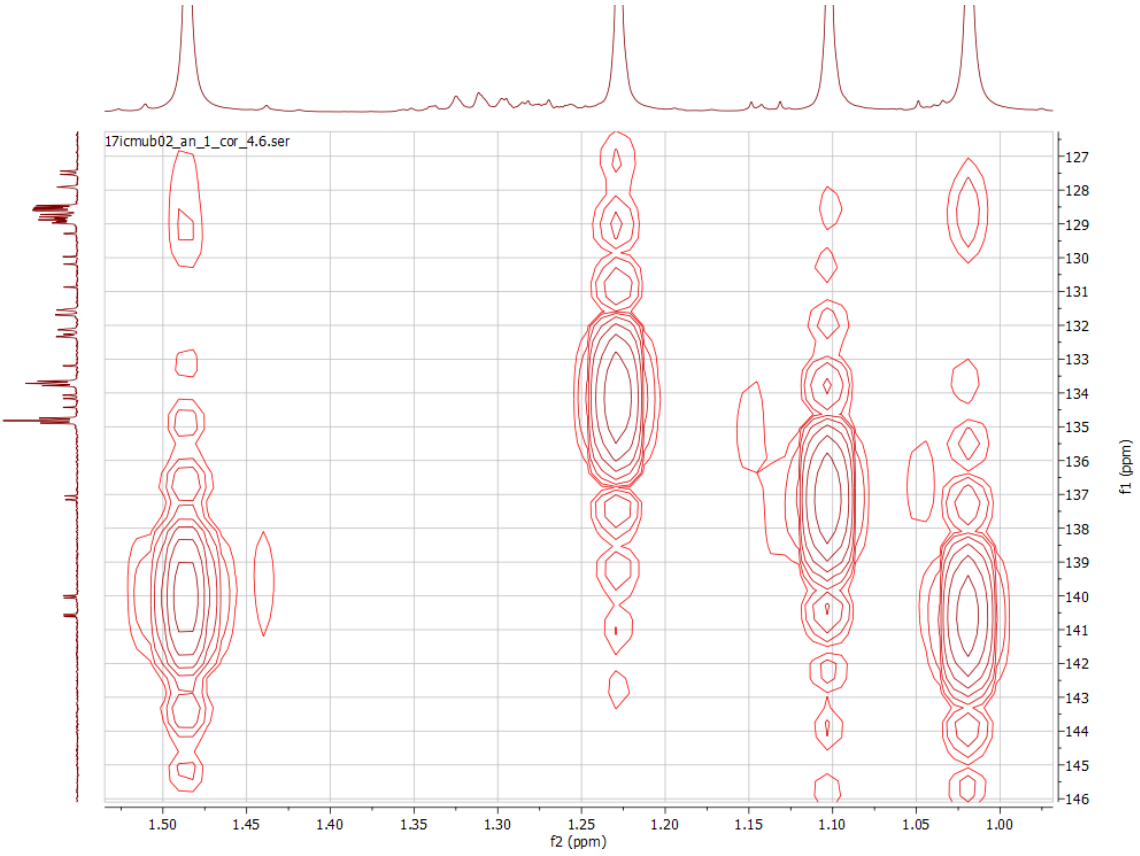

Figure S118: ^{1}H-^{13}C HMBC (500 MHz / 126 MHz, d_8-THF, 300 K)(zoom) of 7a

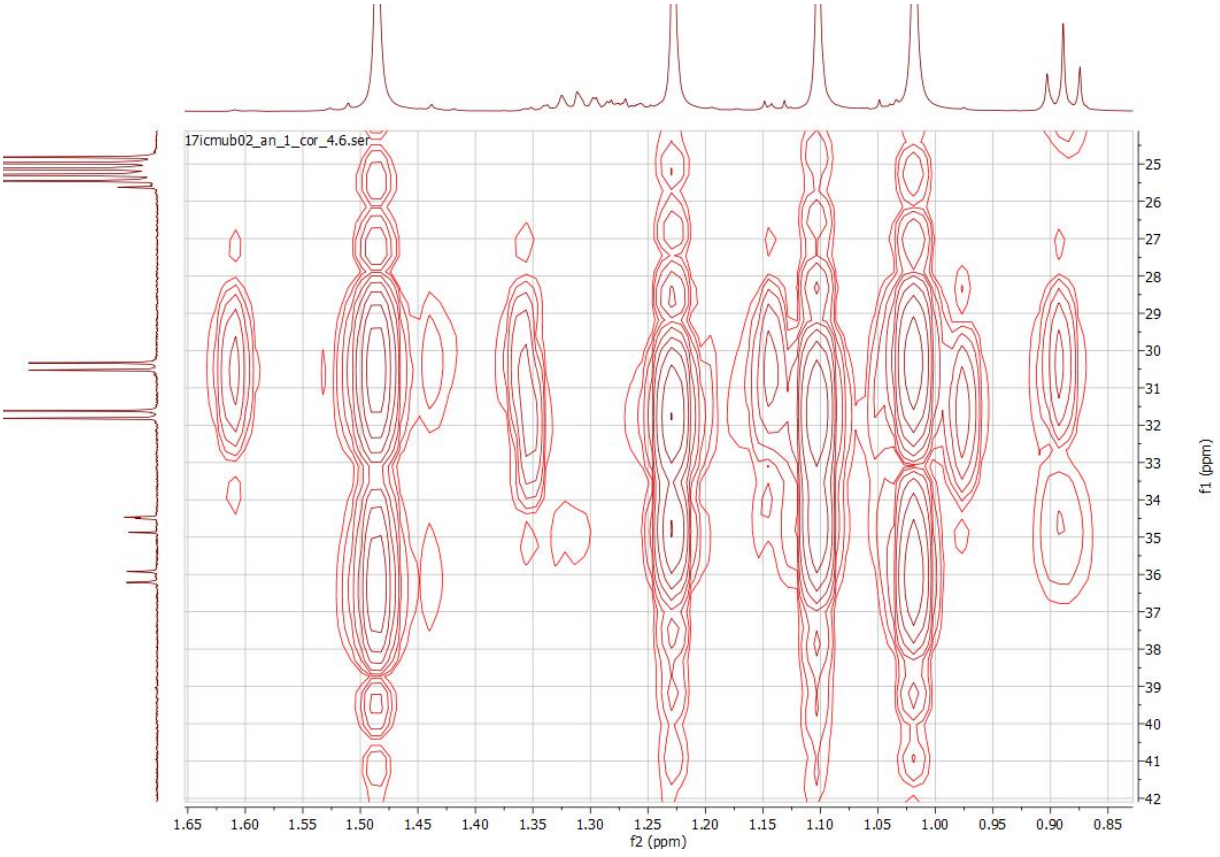

Figure S119: ^{1}H-^{13}C HMBC (500 MHz / 126 MHz, d_8-THF, 300 K)(zoom) of 7a

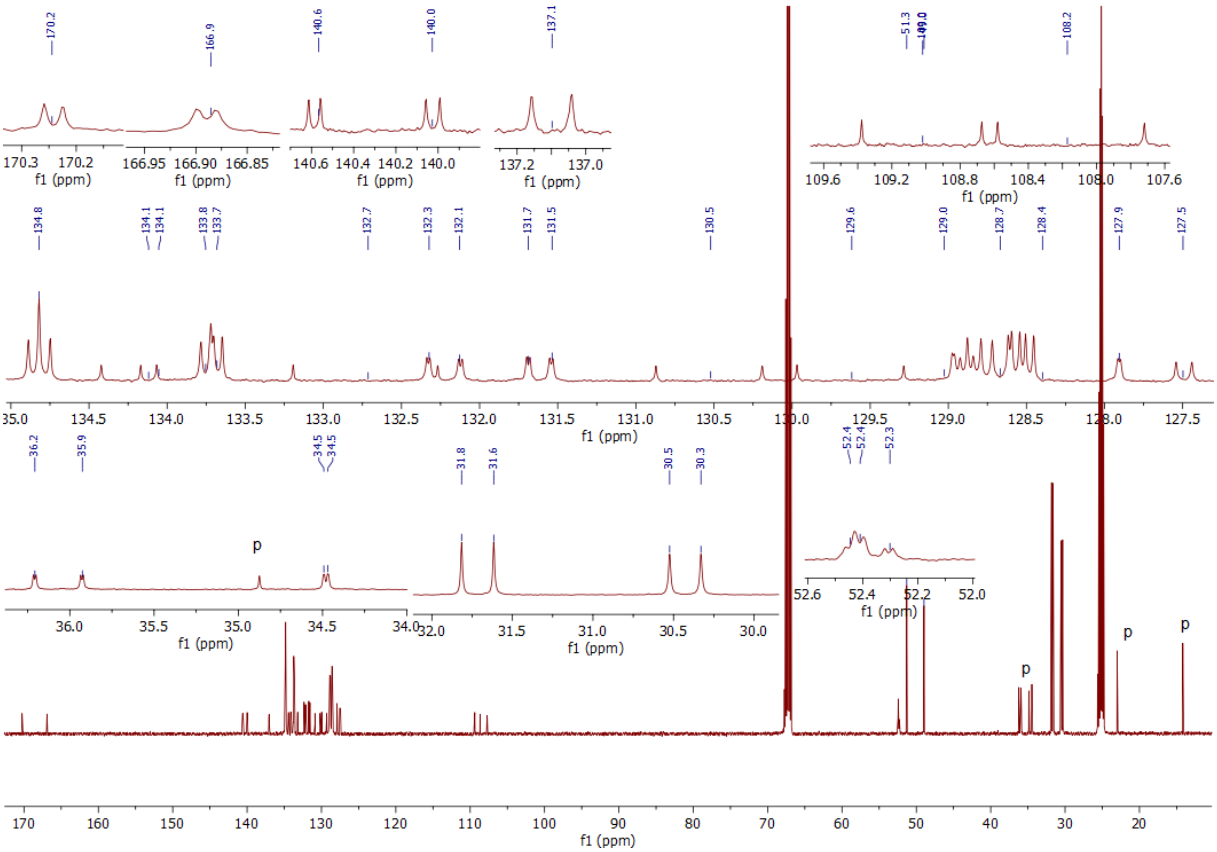

Figure S120: $^{13}C\{^{1}H\}$ NMR (126 MHz, d_8-THF, 300 K) of 7a

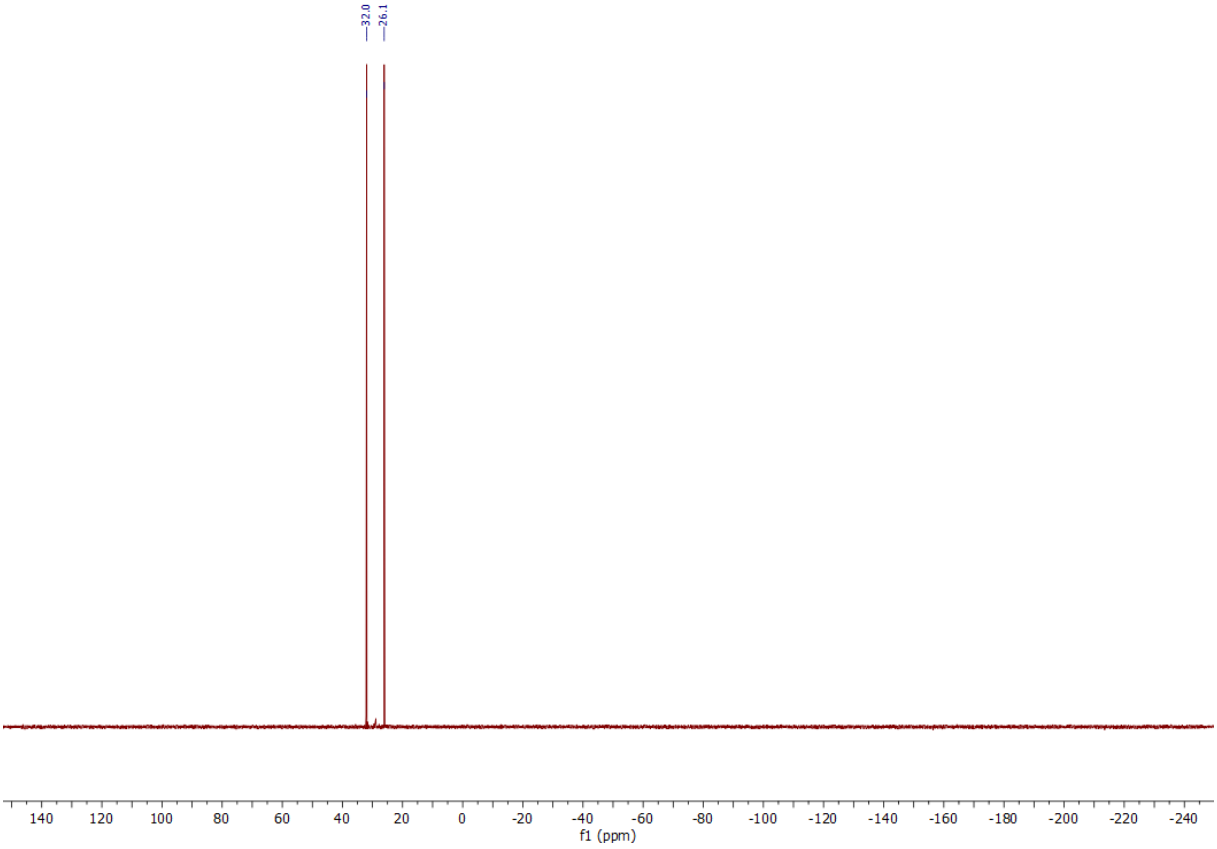

Figure S121: $^{31}P\{^{1}H\}$ NMR (202 MHz, d_8-THF, 300 K) of 7a

Complex 7b

^{1}H-^{1}H COSY (500 MHz, C_6D_6, 300 K)[selected cross-peaks]: 8.28 / 7.28 (*o* of PPh_2 / *m* of PPh_2), 7.95 / 6.97-6.90 (*o* of PPh_2 / *m* of PPh_2), 7.72 / 6.82 (*H*3 of PAr / *H*5 of PAr), 7.68 / 6.97-6.90 (*o* of PPh_2 / *m* of PPh_2), 7.62 / 6.75 (*H*3 of PAr / *H*5 of PAr), 7.28 / 8.28 (*m* of PPh_2 / *o* of PPh_2), 7.13 / 6.71 (*o* of PPh_2 / *m* of PPh_2), 7.06 / 6.97-6.90 (*p* of PPh_2 / *m* of PPh_2), 6.97-6.90 / 7.95 (*m* of PPh_2 / *o* of PPh_2), 6.97-6.90 / 7.68 (*m* of PPh_2 / *o* of PPh_2), 6.97-6.90 / 7.06 (*m* of PPh_2 / *p* of PPh_2), 6.89 / 6.71 (*p* of PPh_2 / *m* of PPh_2), 6.82 / 7.72 (*H*5 of PAr / *H*3 of PAr), 6.75 / 7.62 (*H*5 of PAr / *H*3 of PAr), 6.71 / 7.13 (*m* of PPh_2 / *o* of PPh_2), 6.71 / 6.89 (*m* of PPh_2 / *p* of PPh_2).

^{1}H-^{13}C HMBC (500 MHz / 126 MHz, C_6D_6, 300 K)[selected cross-peaks]: 7.72 / 167.1 (*H*3 of PAr / *C*1 of PAr), 7.72 / 127.7 (*H*3 of PAr / *C*5 of PAr), 7.72 / 36.1 (*H*3 of PAr / *C* of $^{t}Bu^{2}$), 7.72 / 34.3 (*H*3 of PAr / *C* of $^{t}Bu^{4}$), 7.62 / 169.3 (*H*3 of PAr / *C*1 of PAr), 7.62 / 129.4 (*H*3 of PAr / *C*5 of PAr), 7.62 / 35.6 (*H*3 of PAr / *C* of $^{t}Bu^{2}$), 7.62 / 34.0 (*H*3 of PAr / *C* of $^{t}Bu^{4}$), 6.82 / 167.1 (*H*5 of PAr / *C*1 of PAr), 6.82 / 128.7 (*H*5 of PAr / *C*3 of PAr), 6.82 / 34.3 (*H*5 of PAr / *C* of $^{t}Bu^{4}$), 6.75 / 169.3 (*H*5 of PAr / *C*1 of PAr), 6.75 / 128.6 (*H*5 of PAr / *C*3 of PAr), 6.75 / 34.0 (*H*5 of PAr / *C* of $^{t}Bu^{4}$), 6.46 /144.1 (*H*2 of NAr / *C*1 of NAr), 6.46 / 117.5 (*H*2 of NAr / *C*3 of NAr), 6.41 / 147.4 (*H*3 of NAr / *C*1 of NAr), 6.41 / 124.6 (*H*3 of NAr / *C*2 of NAr), 6.26 / 144.1 (*H*3 of NAr / *C*1 of NAr), 6.26 / 118.9 (*H*3 of NAr / *C*2 of NAr), 6.19 / 147.4 (*H*2 of NAr / *C*1 of NAr), 6.19 / 120.8 (*H*2 of NAr / *C*3 of NAr), 3.44 / 49.1 (NMe_2 / NMe_2), 2.91 / 51.5 (NMe_2 / NMe_2), 1.76 / 139.6 (CH_3 of $^{t}Bu^{2}$ / *C*2 of PAr), 1.76 / 36.1 (CH_3 of $^{t}Bu^{2}$ / *C* of $^{t}Bu^{2}$), 1.76 / 30.8 (CH_3 of $^{t}Bu^{2}$ / CH_3 of $^{t}Bu^{2}$), 1.34 / 140.7 (CH_3 of $^{t}Bu^{2}$ / *C*2 of PAr), 1.34 / 35.6 (CH_3 of $^{t}Bu^{2}$ / *C* of $^{t}Bu^{2}$), 1.34 / 30.5 (CH_3 of $^{t}Bu^{2}$ / CH_3 of $^{t}Bu^{2}$), 1.24 / 137.1 (CH_3 of $^{t}Bu^{4}$ / *C*4 of PAr), 1.24 / 34.3 (CH_3 of $^{t}Bu^{4}$ / *C* of $^{t}Bu^{4}$), 1.24 / 31.8 (CH_3 of $^{t}Bu^{4}$ / CH_3 of $^{t}Bu^{4}$), 1.17 / 134.3 (CH_3 of $^{t}Bu^{4}$ / *C*4 of PAr), 1.17 / 34.0 (CH_3 of $^{t}Bu^{4}$ / *C* of $^{t}Bu^{4}$), 1.17 / 31.7 (CH_3 of $^{t}Bu^{4}$ / CH_3 of $^{t}Bu^{4}$).

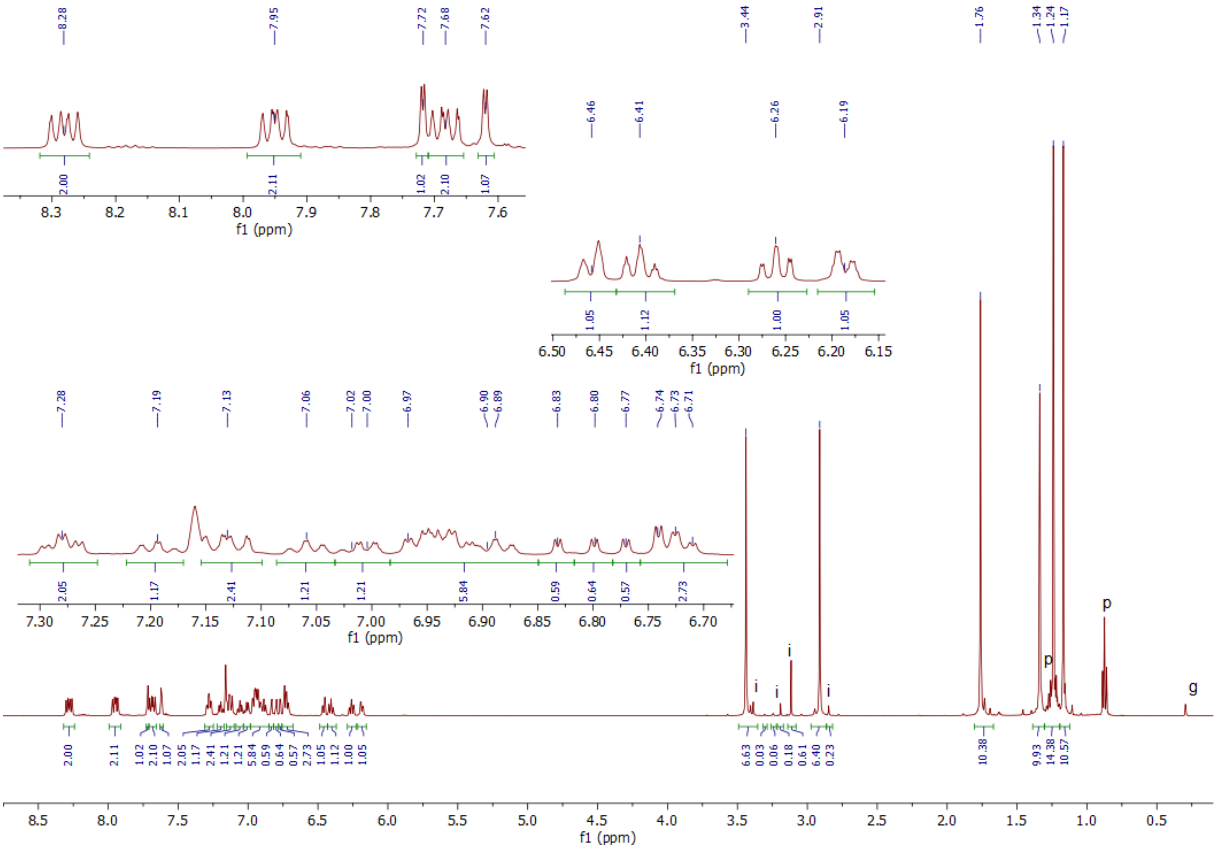

Figure S122: ^{1}H NMR (500 MHz, C_6D_6, 300 K)(p: pentane; i: impurity) of 7b

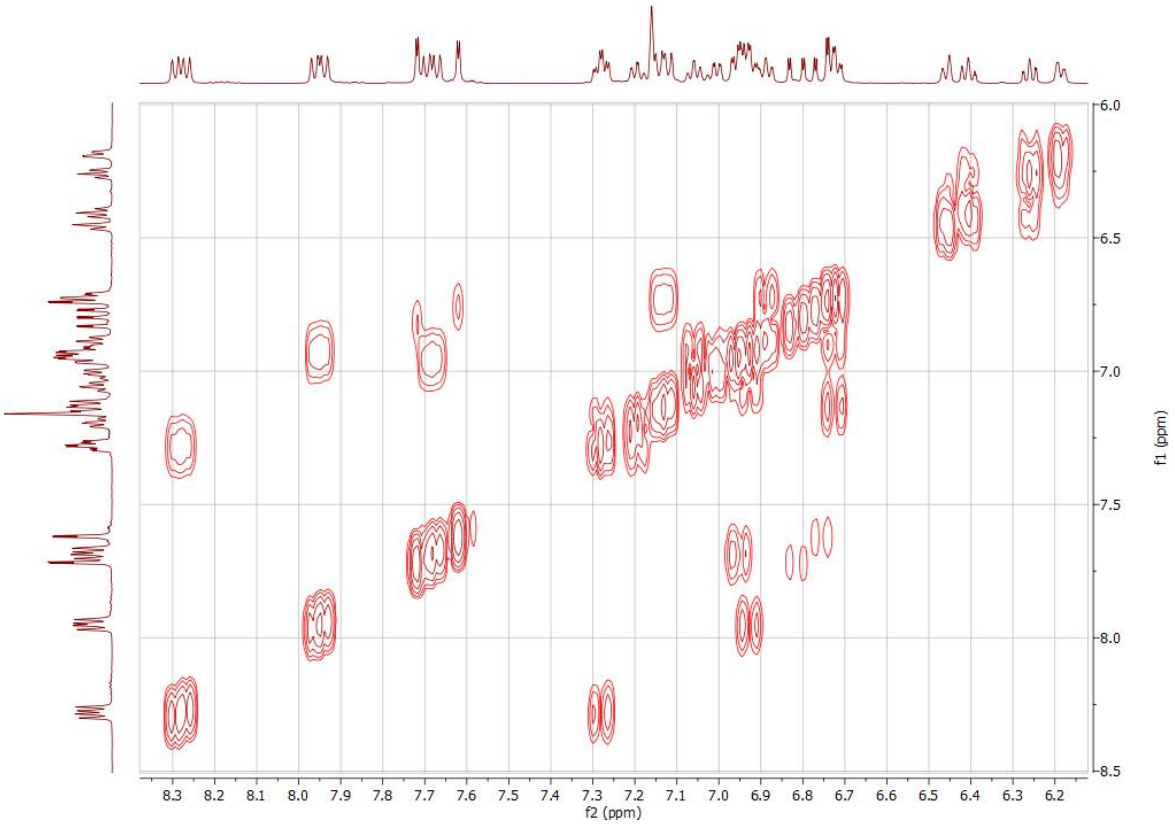

Figure S123: ^{1}H-^{1}H COSY (500 MHz, C_6D_6, 300 K)(zoom) of 7b

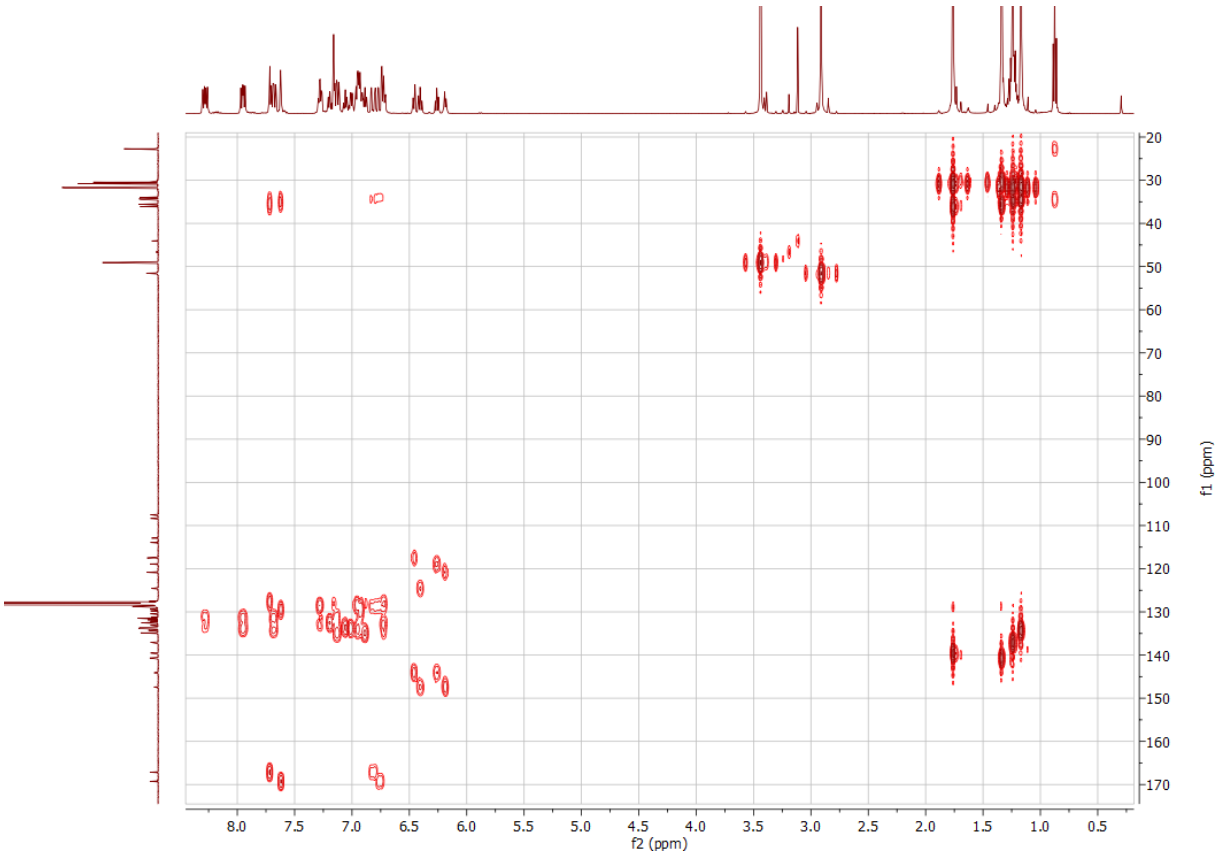

Figure S124: ^{1}H-^{13}C HMBC (500 MHz / 126 MHz, C_6D_6, 300 K)(whole spectrum) of 7b

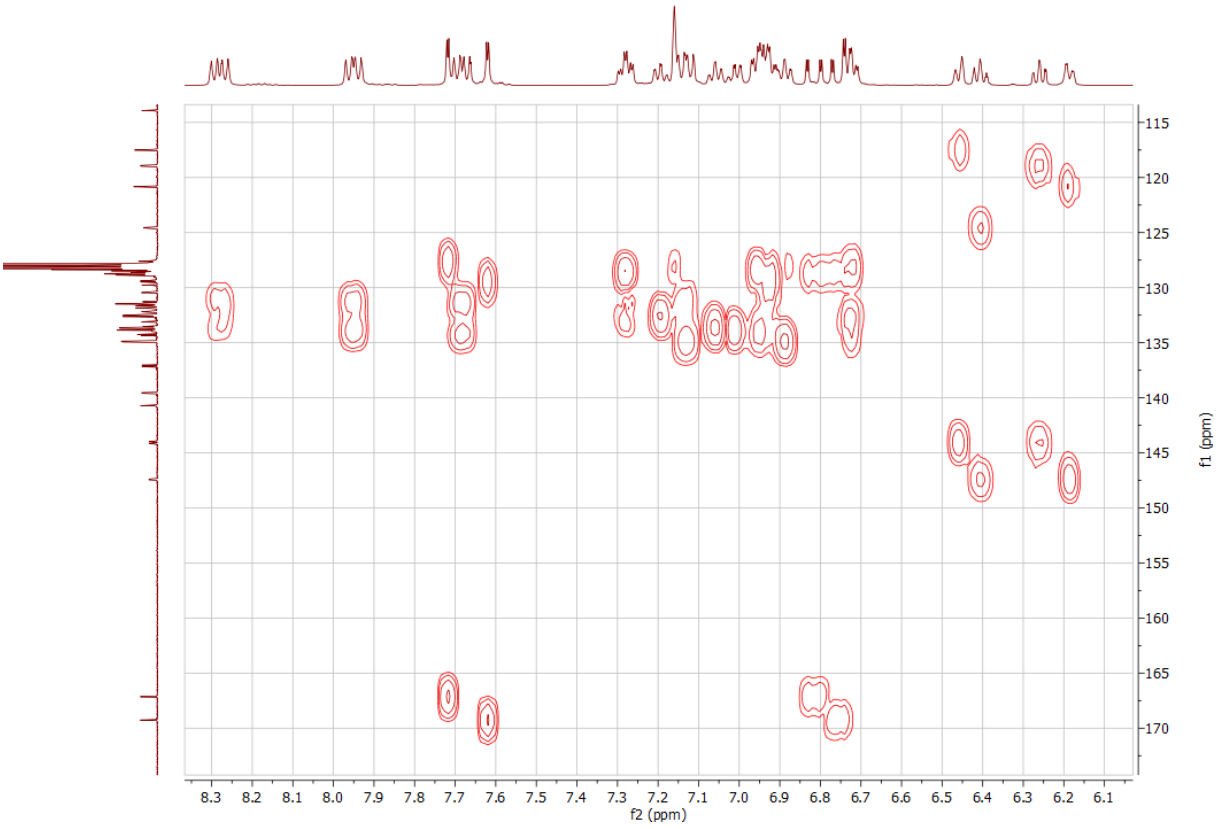

Figure S125: ^{1}H-^{13}C HMBC (500 MHz / 126 MHz, C_6D_6, 300 K)(zoom) of 7b

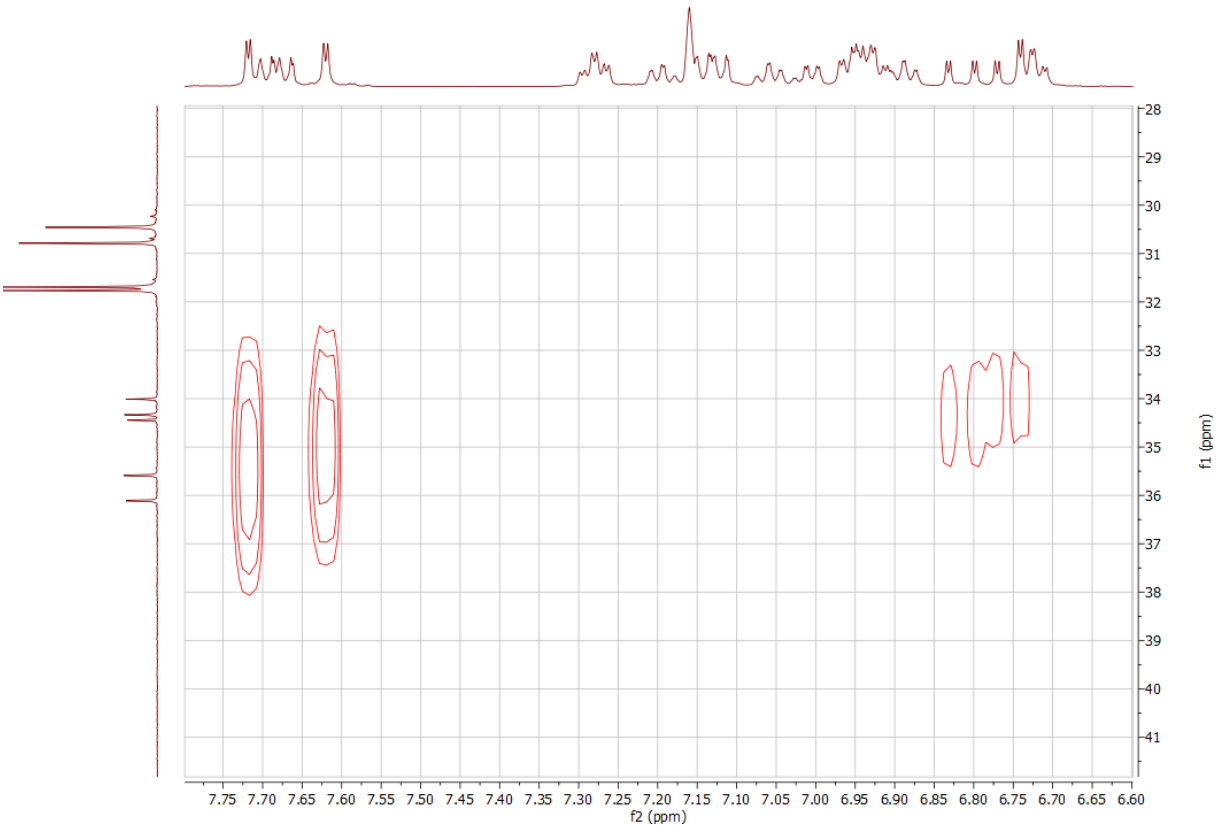

Figure S126: ^{1}H-^{13}C HMBC (500 MHz / 126 MHz, C_6D_6, 300 K)(zoom) of 7b

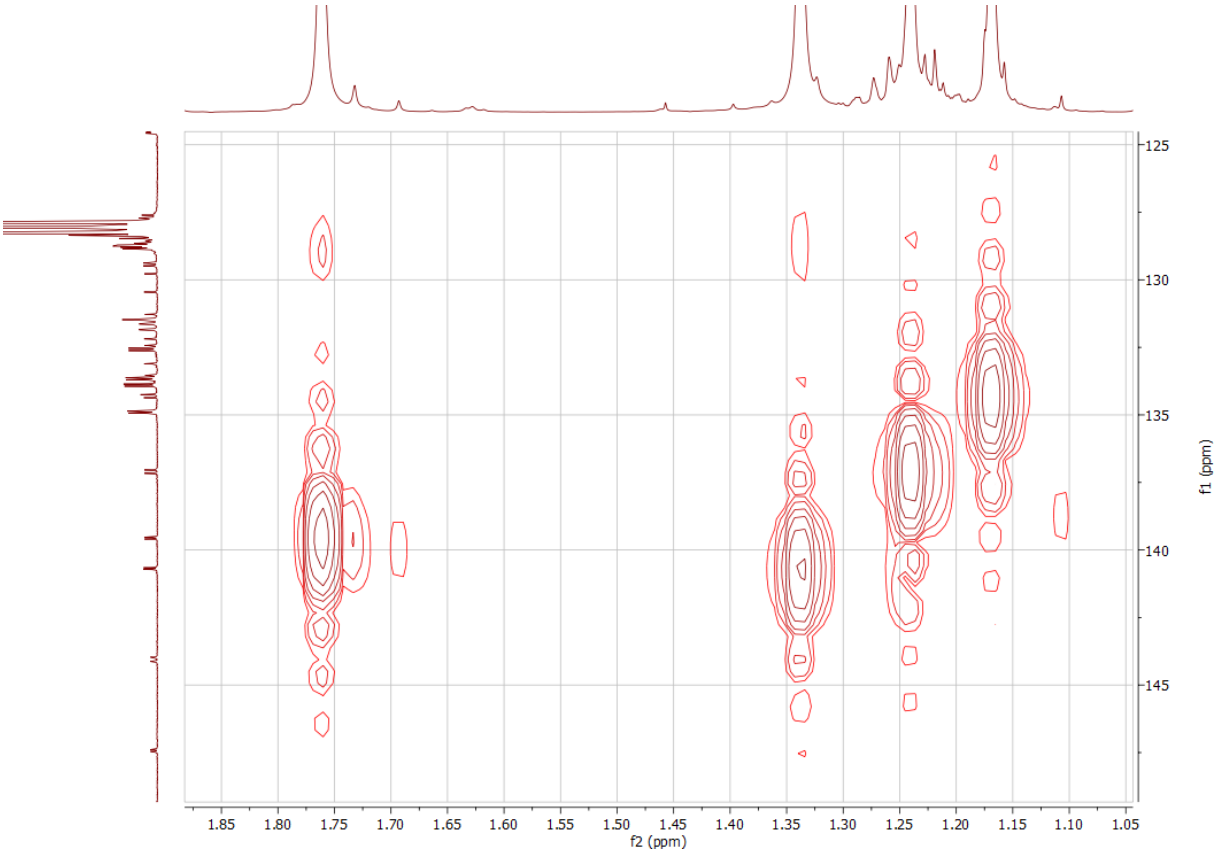

Figure S127: ^{1}H-^{13}C HMBC (500 MHz / 126 MHz, C_6D_6, 300 K)(zoom) of 7b

Figure S128: ^{1}H-^{13}C HMBC (500 MHz / 126 MHz, C_6D_6, 300 K)(zoom) of 7b

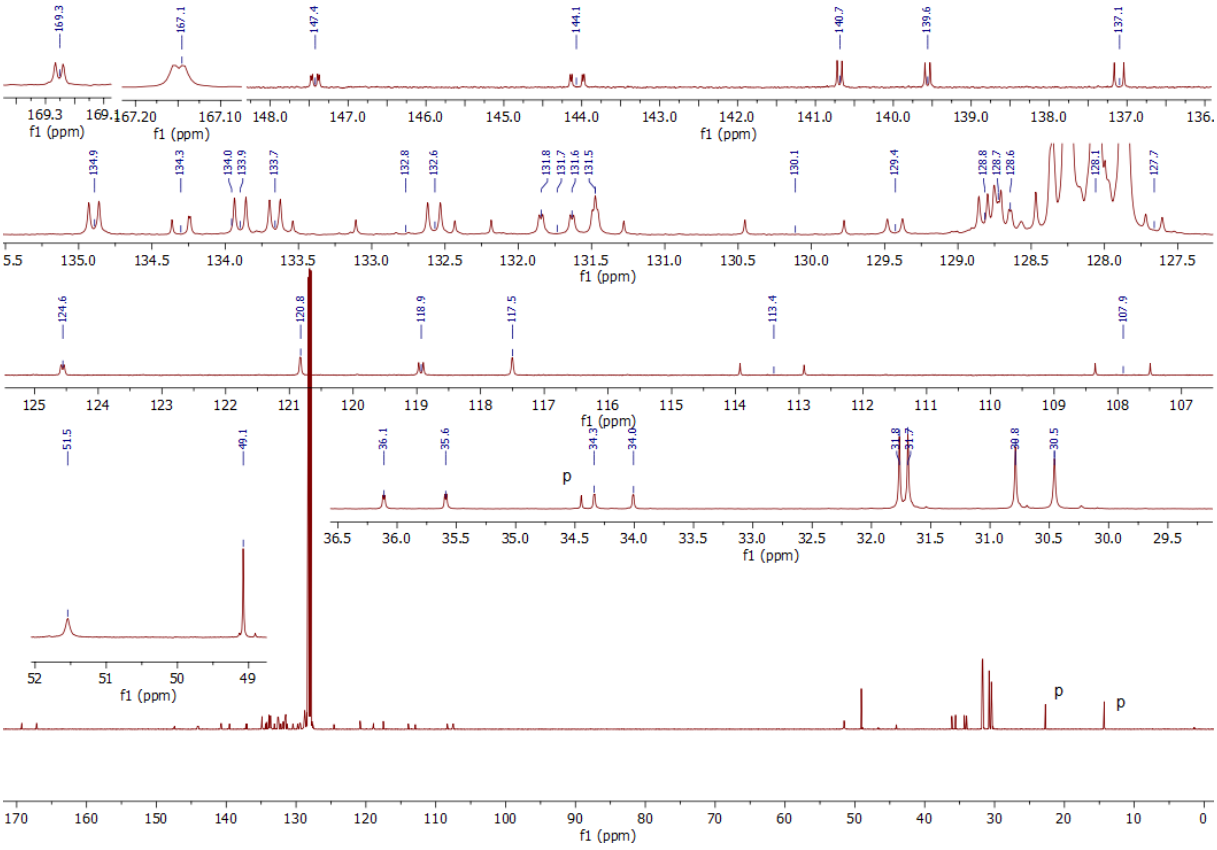

Figure S129: $^{13}C\{^{1}H\}$ NMR (126 MHz, C_6D_6, 300 K) of 7b

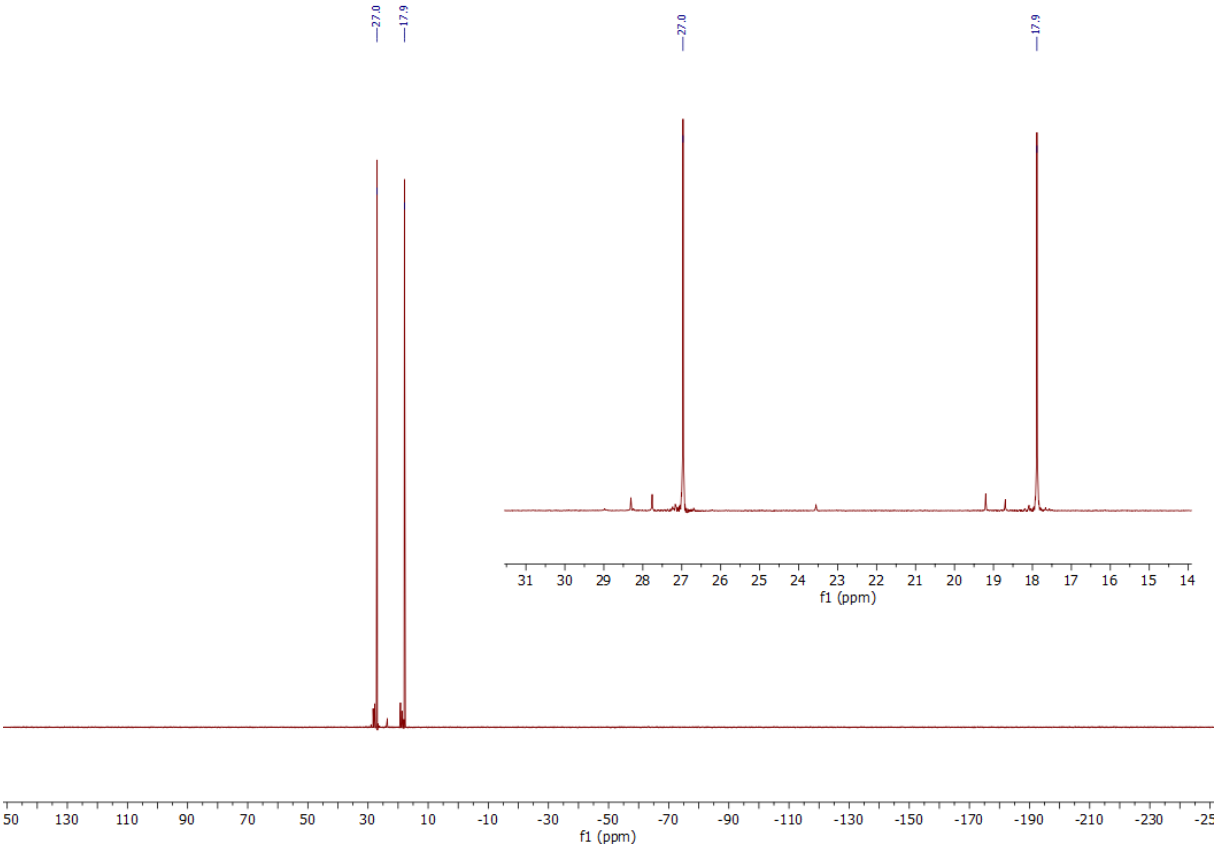

Figure S130: $^{31}P\{^{1}H\}$ NMR (202 MHz, C_6D_6, 300 K) of 7b

Complex 7c

^{1}H-^{1}H COSY (600.2 MHz, C_6D_6, 300 K) [selected cross-peaks]: 8.16/7.22 (*o* of PPh_2 / *m* of PPh_2), 7.82-7.77 / 7.14-7.07 (*o* of PPh_2 / *m* of PPh_2), 7.76 / 7.06-6.95 (*H*3 of PAr / *H*5 of PAr), 7.74 / 7.06-6.95 (*H*3 of PAr / *H*5 of PAr), 7.59 / 7.06-6.95 (*o* of PPh_2 / *m* of PPh_2), 7.49 / 6.91 (*o* of PPh_2 / *m* of PPh_2), 4.18-4.04 / 3.06 / 2.90 (1H, NCH_2 /1H, NCH_2), 3.63-3.51 / 2.77-2.67 (1H, NCH_2 / 1H, NCH_2).

^{1}H-^{13}C HMBC (600.2 MHz / 150.9 MHz, C_6D_6, 300 K) [selected cross-peaks]: 7.76 / 166.5 (*H*3 of PAr / *C*1 of PAr), 7.76 / 35.8 (*H*3 of PAr / C of tBu^2), 7.76 / 33.9 (*H*3 of PAr / C of tBu^4), 7.74 / 169.7 (*H*3 of PAr / *C*1 of PAr), 7.74/ 35.7 (*H*3 of PAr / C of tBu^2), 7.74/ 33.8 (*H*3 of PAr / C of tBu^4), 7.0 / 33.9 (*H*5 of PAr / C of ^{t}Bu^4), 7.0 / 33.8 (*H*5 of PAr / C of ^{t}Bu^4), 1.81 / 140.0 (H of ^{t}Bu^2 / *C*2 of PAr), 1.63 / 140.4 (H of ^{t}Bu^2 / *C*2 of PAr), 1.23 / 133.4 (H of ^{t}Bu^4 / *C*4 of PAr), 1.20 / 136.0 (H of ^{t}Bu^4 / *C*4 of PAr), 1.81 / 35.8 (H of ^{t}Bu^2 / C of tBu^2), 1.63 / 35.7 (H of ^{t}Bu^2 / C of tBu^2), 1.23 / 33.9 (H of ^{t}Bu^4 / C of tBu^4), 1.20 / 33.8 (H of ^{t}Bu^4 / C of tBu^4).

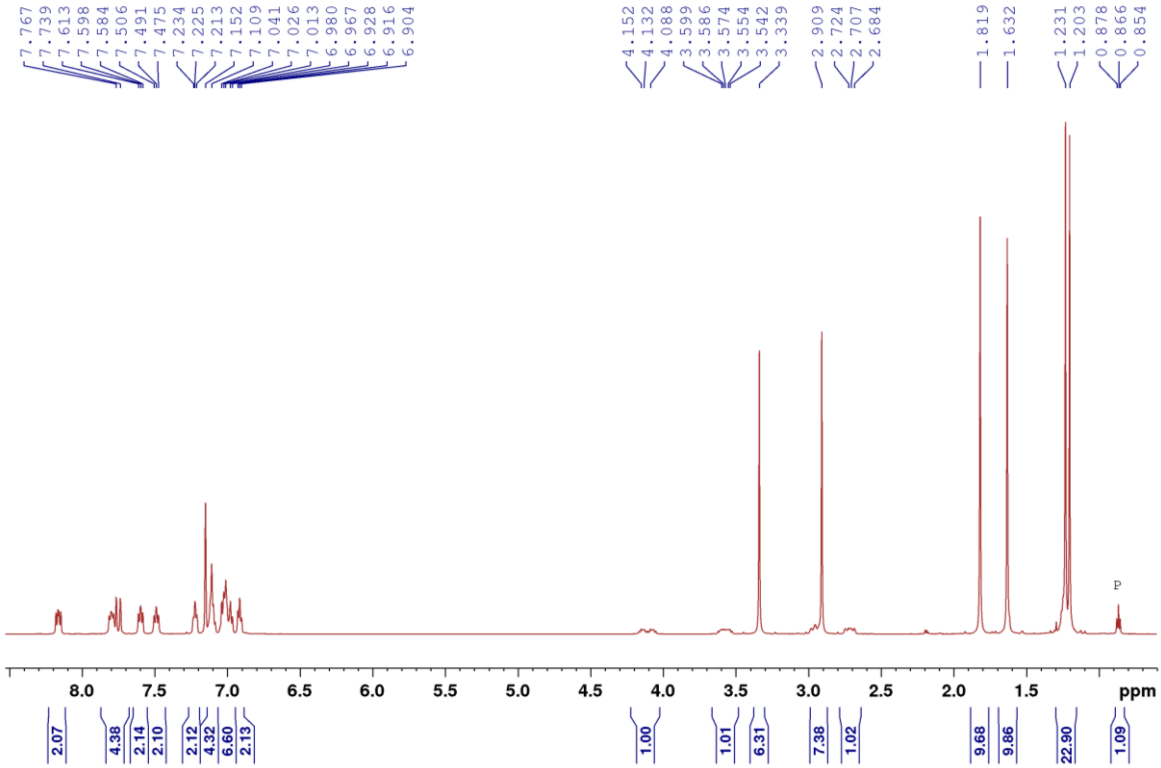

Figure S131: ^{1}H NMR (600.2 MHz, C_6D_6, 300 K) of 7c (p: pentane)

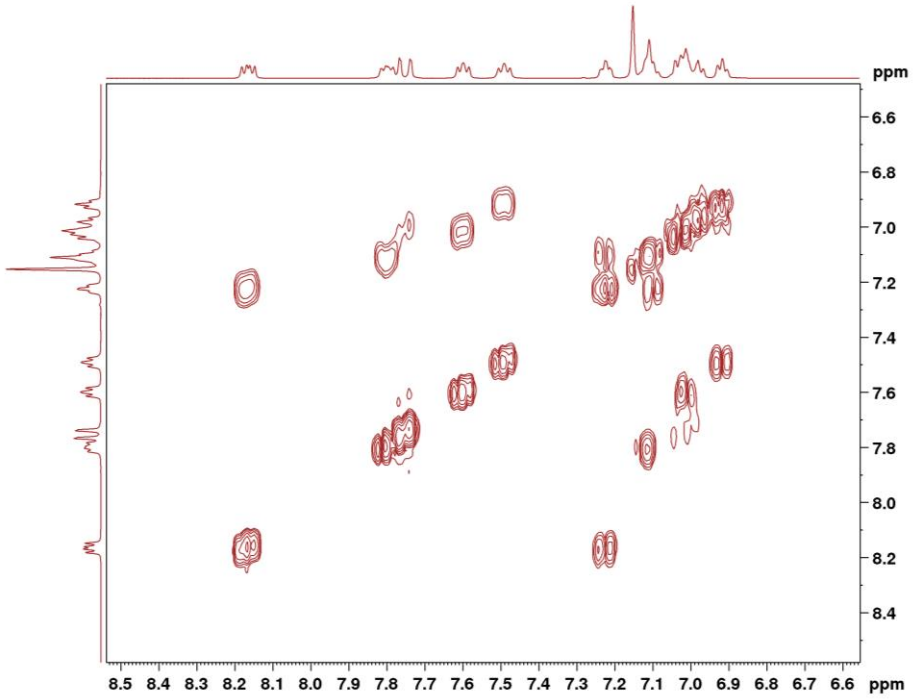

Figure S132: ^{1}H - ^{1}H COSY (600.2 MHz, C_6D_6, 300 K) (zoom) of 7c

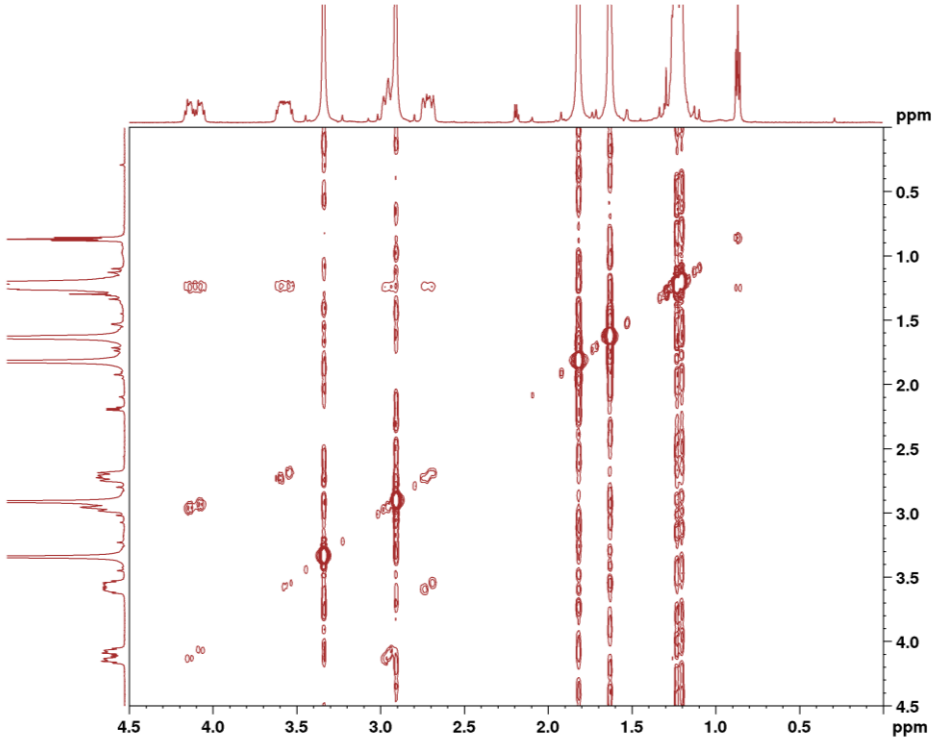

Figure S133: ^{1}H - ^{1}H COSY (600.2 MHz, C_6D_6, 300 K) (zoom) of 7c

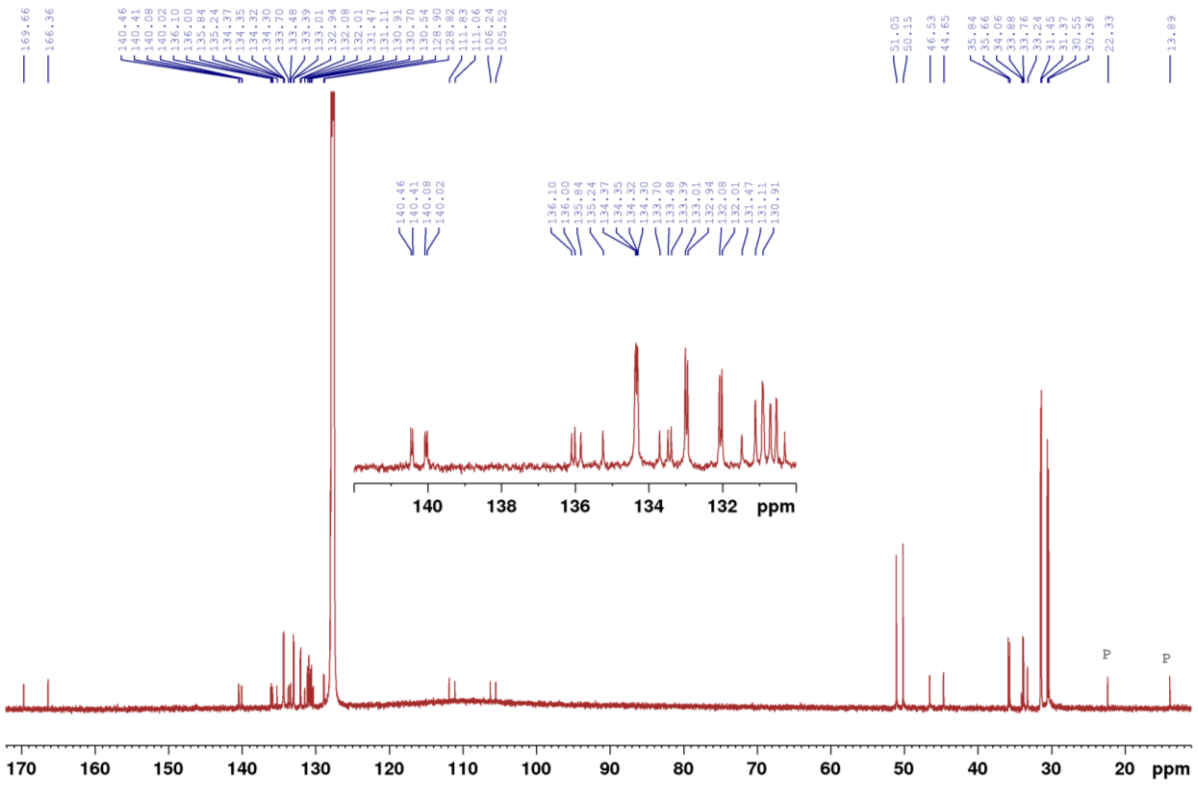

Figure S134: ^{13}C NMR (150.9 MHz, C_6D_6, 300 K) of 7c (p: pentane)

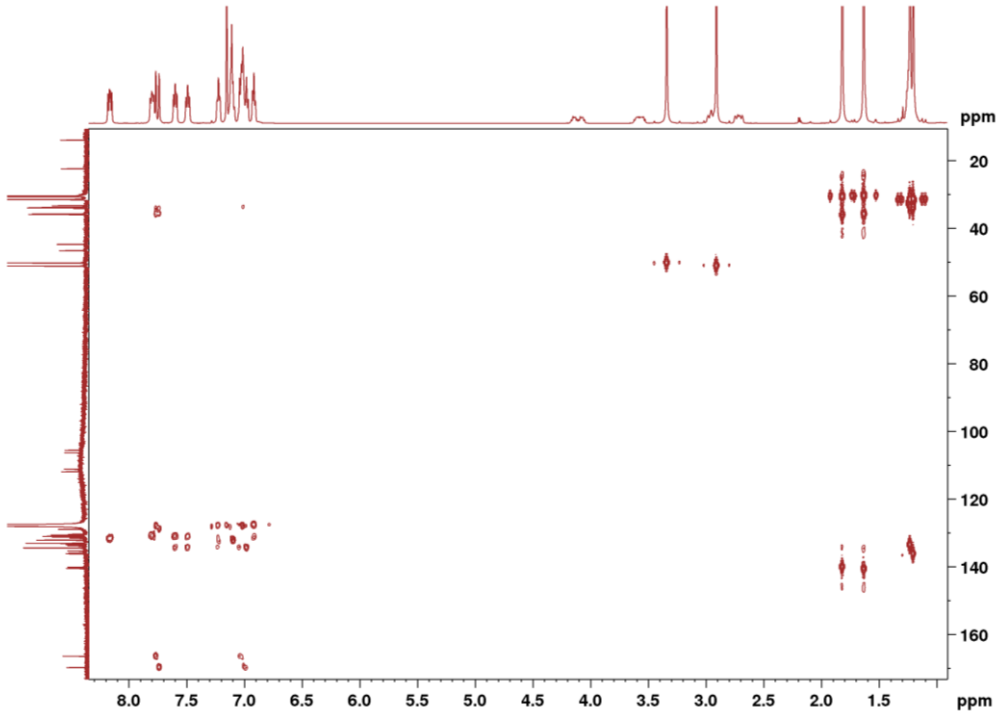

Figure S135: ^{1}H - ^{13}C HMBC (600.2 MHz / 150.9 MHz, C_6D_6, 300 K) (zoom) of 7c

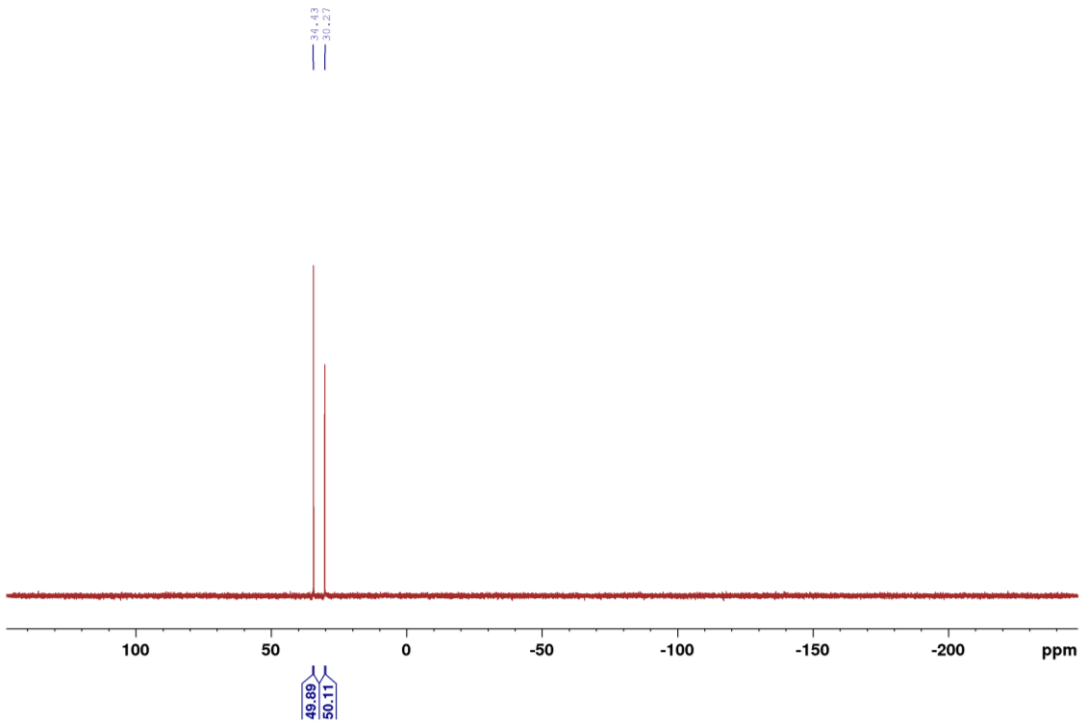

Figure S136: ^{31}P {^{1}H} NMR (243MHz, C_6D_6, 300 K) of 7c

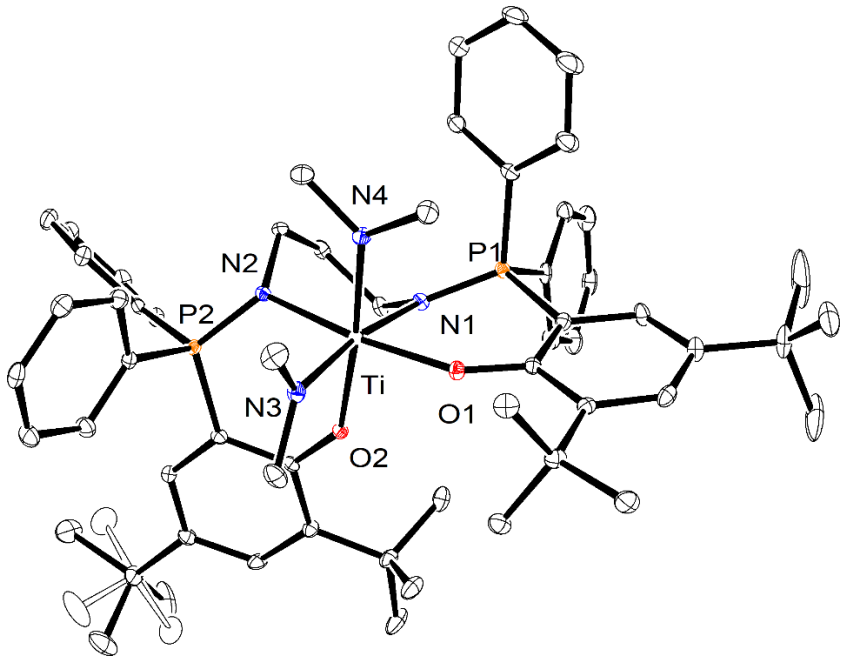

Figure S137: Crystal structure of 7c

Table S9: Crystal data and structure refinement of 7c

Identification code	7c
Internal reference	1809rm3_0m_a
Empirical formula	$C_{59}H_{78}N_4O_2P_2Ti$

Formula weight	985.09
Temperature/K	115.0
Crystal system	monoclinic
Space group	$P2_1/n$
a/Å	13.449(3)
b/Å	27.820(7)
c/Å	14.860(4)
α/°	90
β/°	97.910(4)
γ/°	90
Volume/Å^3	5507(2)
Z	4
ρ_{calc}g/cm^3	1.188
μ/mm^{-1}	0.258
F(000)	2112.0
Crystal size/mm^3	0.2 × 0.15 × 0.1
Radiation	MoKα (λ = 0.71073)
2Θ range for data collection/°	5.192 to 55.314
Index ranges	-13 ≤ h ≤ 17, -36 ≤ k ≤ 36, -19 ≤ l ≤ 19
Reflections collected	67556
Independent reflections	12796 [R_{int} = 0.0956, R_{sigma} = 0.0798]
Data/restraints/parameters	12796/0/660
Goodness-of-fit on F^2	1.044
Final R indexes [I>=2σ (I)]	R_1 = 0.0560, wR_2 = 0.1022
Final R indexes [all data]	R_1 = 0.1000, wR_2 = 0.1182
Largest diff. peak/hole / e Å^{-3}	0.62/-0.64
CCDC	1978295

Special refinement details for 7c

One of the tert-butyl groups was found disordered and anisotropically refined over two positions with occupation factors converging to 0.53/0.47.

ROP of *rac*-lactide studies

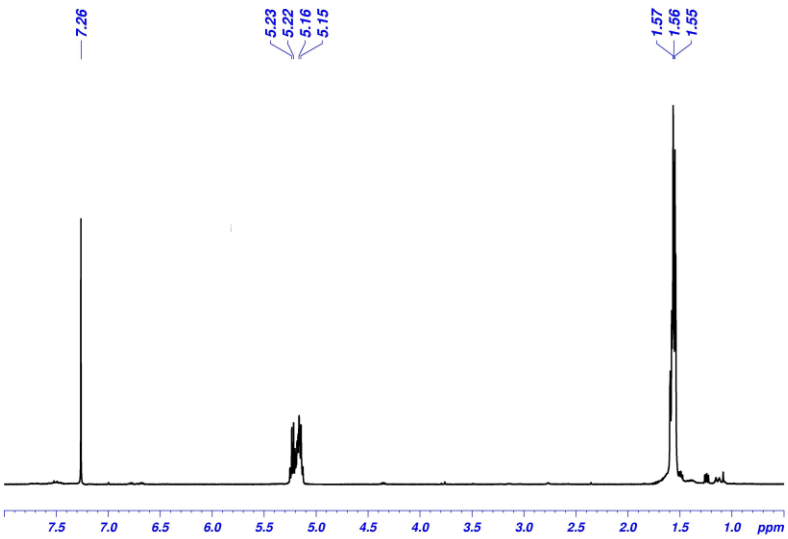

Figure S138: ^{1}H NMR ($CDCl_3$, 400 MHz) of isolated PLA from the ROP of *rac*-lactide (100 equiv) using initiator 4a in solution (toluene, 90 °C, 6 h, 86% conversion to PLA)

==== Shimadzu LCsolution GPC Analysis Report ====

Acquired by	: Admin
Sample Name	: rl 114
Sample ID	: rl 114
Vail#	:
Injection Volume	: 100 uL
Data Filename	: rl 114.lcd
Method Filename	: gpc.lcm
Batch Filename	:
Report Filename	: Report_template.lcr
Date Acquired	: 06/04/2017 16:59:20
Data Processed	: 06/04/2017 17:29:22

Chromatogram & Calibration Curve

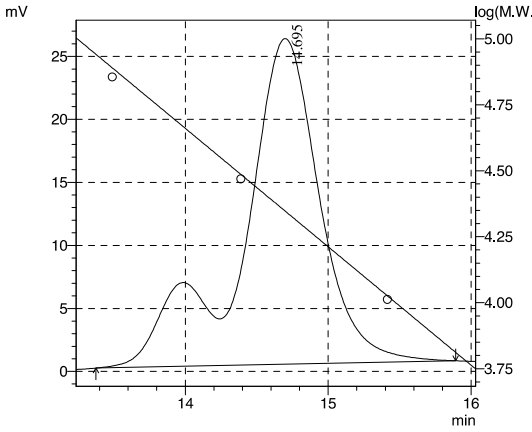

Molecular Weight Distribution Curve

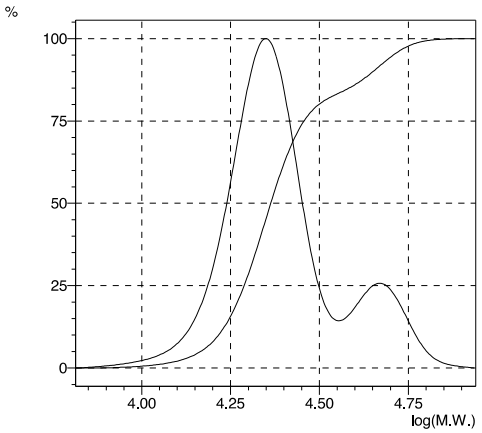

GPC Calculation Results

Peak#:1 (Detector A Ch1)
[Peak Information]

	Time(min)	Volume(mL)	Molecular Weight	Height
Start	13.375	13.375	87335	266
Top	14.695	14.695	22335	25840
End	15.892	15.892	6487	845

Area : 979897
Area% : 100.0000

[Average Molecular Weight]

Number Average Molecular Weight(Mn)	23056
Weight Average Molecular Weight(Mw)	26452
Z Average Molecular Weight(Mz)	31112
Z+1 Average Molecular Weight(Mz1)	36885
Mw/Mn	1.14730
Mv/Mn	1.12341
Mz/Mw	1.17618

Detector A Ch1
[Average Molecular Weight(Total)]

Number Average Molecular Weight(Mn)	23056
Weight Average Molecular Weight(Mw)	26452
Z Average Molecular Weight(Mz)	31112
Z+1 Average Molecular Weight(Mz1)	36885
Mw/Mn	1.14730
Mv/Mn	1.12341
Mz/Mw	1.17618

Figure S139: GPC data for isolated PLA from the ROP of lactide (100 equiv) using initiator 4a (toluene, 90 °C, 6 h, 86 % conversion to PLA)

==== Shimadzu LCsolution GPC Analysis Report ====

Acquired by	: Admin
Sample Name	: rl 129
Sample ID	: rl 129
Vail#	:
Injection Volume	: 100 uL
Data Filename	: rl 129.lcd
Method Filename	: gpc.lcm
Batch Filename	:
Report Filename	: Report_template.lcr
Date Acquired	: 08/04/2017 12:03:36
Data Processed	: 08/04/2017 12:33:38

Chromatogram & Calibration Curve

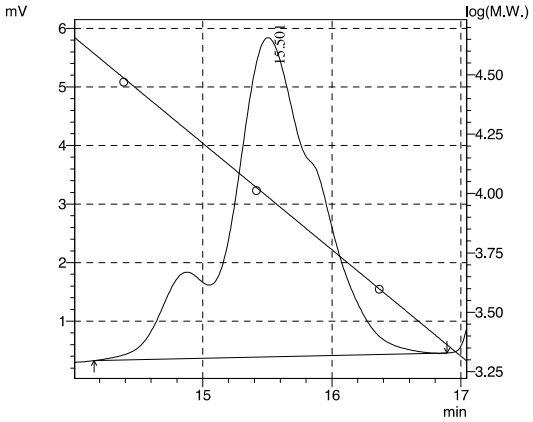

Molecular Weight Distribution Curve

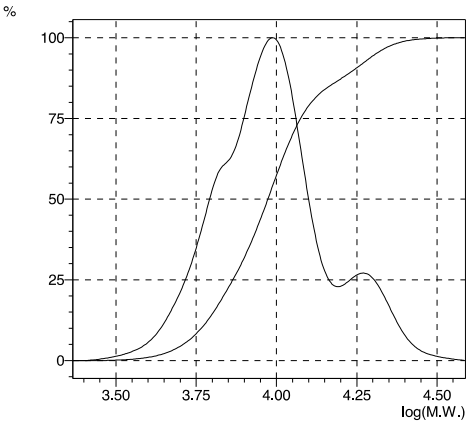

GPC Calculation Results

Peak#:1 (Detector A Ch1)
[Peak Information]

	Time(min)	Volume(mL)	Molecular Weight	Height
Start	14.158	14.158	38880	326
Top	15.501	15.501	9715	5451
End	16.892	16.892	2309	457

Area : 264618
Area% : 100.0000

[Average Molecular Weight]

Number Average Molecular Weight(Mn)	8887
Weight Average Molecular Weight(Mw)	10469
Z Average Molecular Weight(Mz)	12533
Z+1 Average Molecular Weight(Mz1)	15045
Mw/Mn	1.17800
Mv/Mn	1.15010
Mz/Mw	1.19715

Detector A Ch1
[Average Molecular Weight(Total)]

Number Average Molecular Weight(Mn)	8887
Weight Average Molecular Weight(Mw)	10469
Z Average Molecular Weight(Mz)	12533
Z+1 Average Molecular Weight(Mz1)	15045
Mw/Mn	1.17800
Mv/Mn	1.15010
Mz/Mw	1.19715

Figure S140: GPC data for isolated PLA from the ROP of lactide (100 equiv) using initiator 4b (toluene, 90 °C, 24 h, 60 % conversion to PLA)

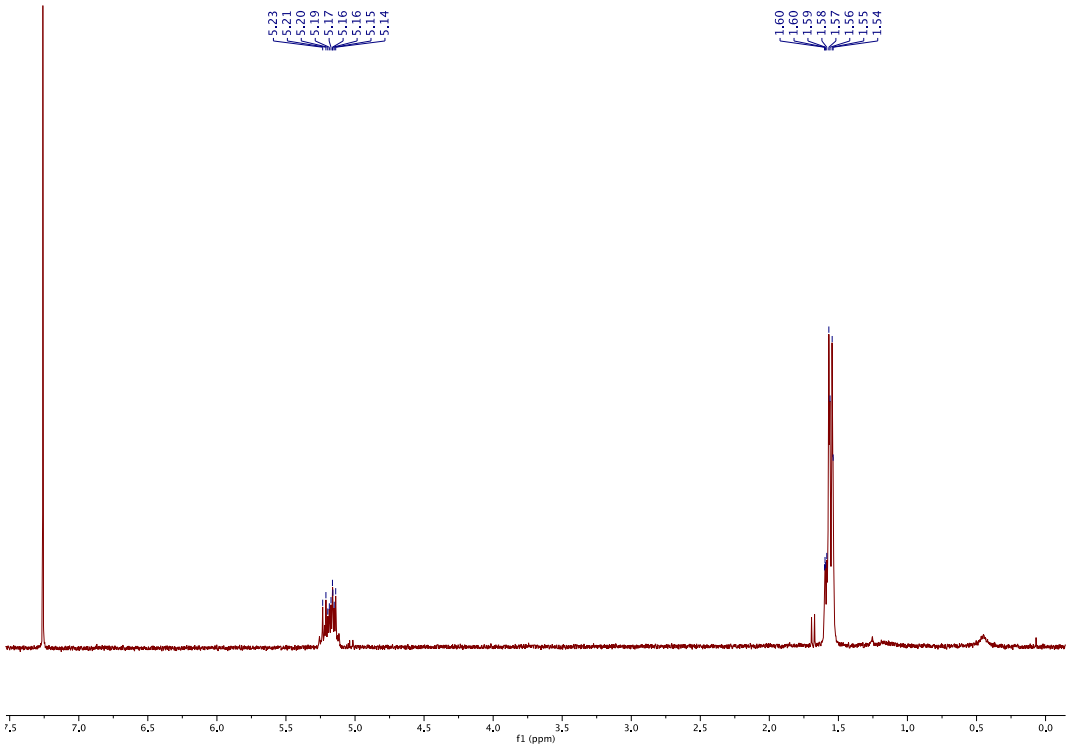

Figure S141: ^{1}H NMR ($CDCl_3$, 400 MHz) of isolated PLA from the ROP of *rac*-lactide (100 equiv) using initiator 4b under bulk conditions (130 °C, 4 h, 92% conversion to PLA)

==== Shimadzu LCsolution GPC Analysis Report ====

Acquired by	: Admin
Sample Name	: rl 127
Sample ID	: rl 127
Vail#	:
Injection Volume	: 100 uL
Data Filename	: rl 127.lcd
Method Filename	: gpc.lcm
Batch Filename	:
Report Filename	: Report_template.lcr
Date Acquired	: 08/04/2017 12:07:16
Data Processed	: 08/04/2017 11:34:38

Chromatogram & Calibration Curve

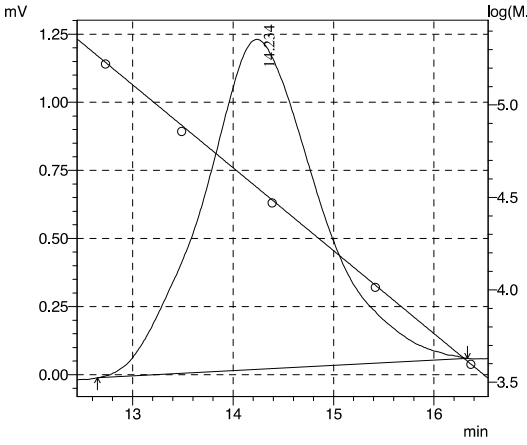

Molecular Weight Distribution Curve

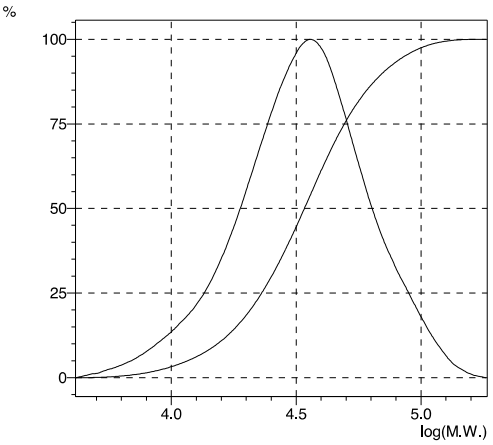

GPC Calculation Results

Peak#:1 (Detector A Ch1)
[Peak Information]

	Time(min)	Volume(mL)	Molecular Weight	Height
Start	12.650	12.650	184707	-11
Top	14.234	14.234	35974	1212
End	16.333	16.333	4110	60

Area : 96569
Area% : 100.0000

[Average Molecular Weight]

Number Average Molecular Weight(Mn)	27692
Weight Average Molecular Weight(Mw)	39370
Z Average Molecular Weight(Mz)	53118
Z+1 Average Molecular Weight(Mz1)	68218
Mw/Mn	1.42169
Mv/Mn	1.36042
Mz/Mw	1.34920

Detector A Ch1
[Average Molecular Weight(Total)]

Number Average Molecular Weight(Mn)	27692
Weight Average Molecular Weight(Mw)	39370
Z Average Molecular Weight(Mz)	53118
Z+1 Average Molecular Weight(Mz1)	68218
Mw/Mn	1.42169
Mv/Mn	1.36042
Mz/Mw	1.34920

Figure S142: GPC data for isolated PLA from the ROP of *rac*-lactide (100 equiv) using initiator 4b under bulk conditions (130 °C, 4 h, 92 % conversion to PLA)

.

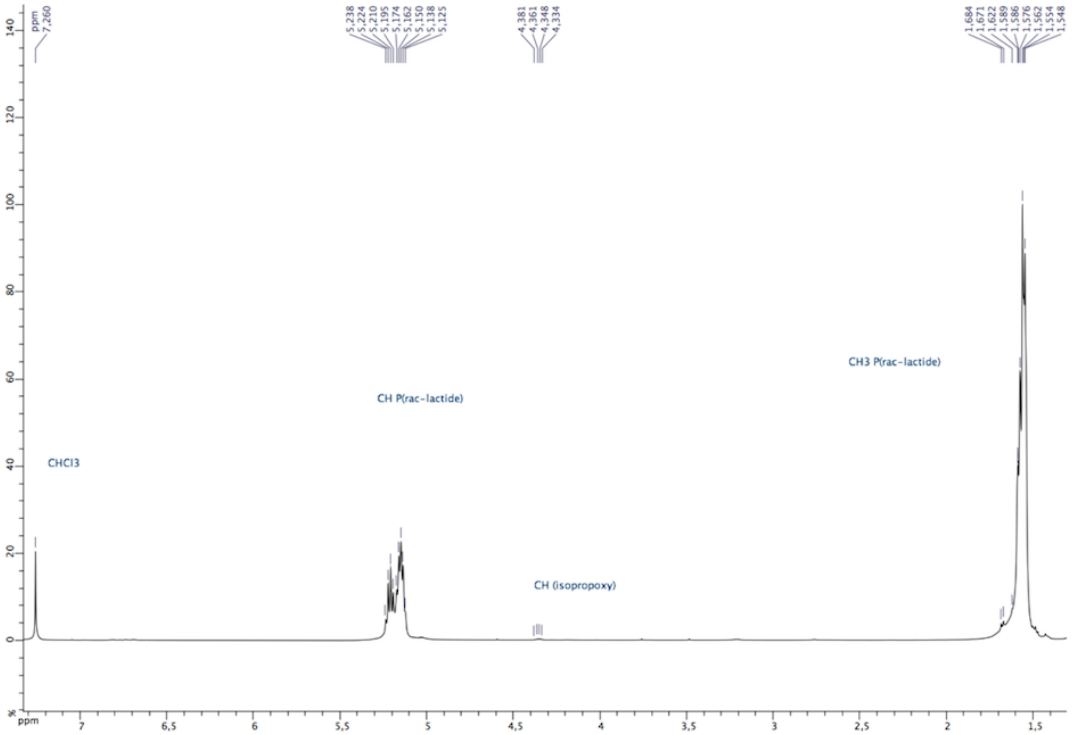

Figure S143: ^{1}H NMR ($CDCl_3$, 400 MHz) of isolated PLA from the ROP of *rac*-lactide (100 equiv) using Zr–O^{i}Pr cation 5a as initiator (toluene, 90 °C, 14 h, 98 % conversion to PLA)

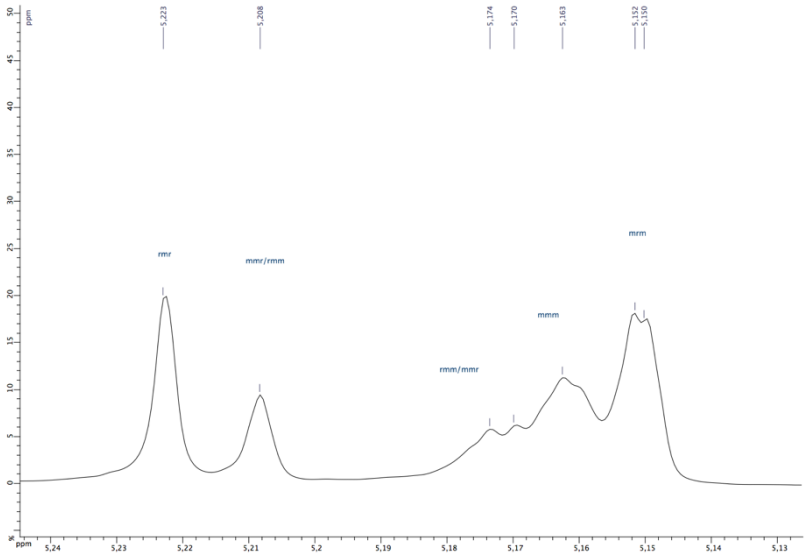

Figure S144: Homodecoupled ^{1}H NMR spectrum ($CDCl_3$, 500 Mhz) of isolated PLA from the ROP of *rac*-lactide (100 equiv) using Zr–O^{i}Pr cation 5a as initiator (toluene, 90 °C, 14 h, 98 % conversion to PLA). P_r = 0.63, as estimated according to literature.[3]

[3] B. M. Chamberlain, M. Cheng, D. R. Moore, T. M. Ovitt, E. B. Lobkovsky and G. W. Coates, *J. Am. Chem. Soc.*, 2001, **123**, 3229-3238.

==== Shimadzu LCsolution GPC Analysis Report ====

Acquired by	: Admin
Sample Name	: 97
Sample ID	: 97
Vail#	:
Injection Volume	: 100 uL
Data Filename	: rl 219.lcd
Method Filename	: gpc.lcm
Batch Filename	:
Report Filename	: Report_template.lcr
Date Acquired	: 22/03/2017 13:57:17
Data Processed	: 22/03/2017 14:27:20

Chromatogram & Calibration Curve

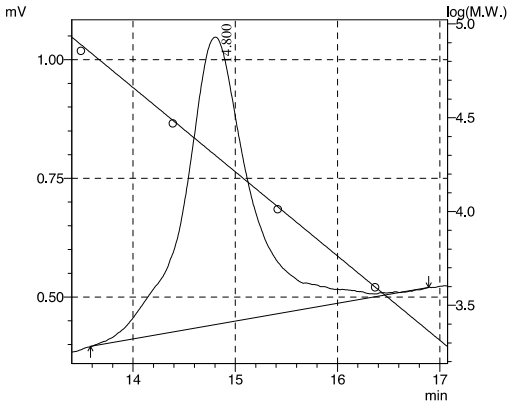

Molecular Weight Distribution Curve

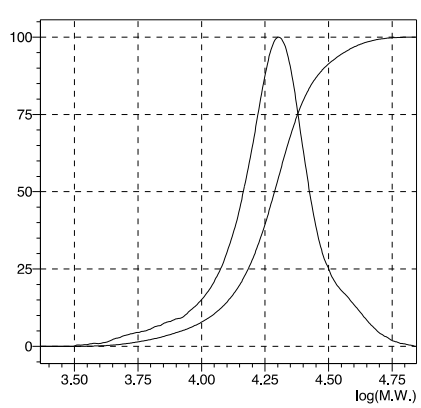

GPC Calculation Results

Peak#:1 (Detector A Ch1)
[Peak Information]

	Time(min)	Volume(mL)	Molecular Weight	Height
Start	13.583	13.583	70423	396
Top	14.800	14.800	20045	606
End	16.892	16.892	2309	520

Area : 27284
Area% : 100.0000

[Average Molecular Weight]

Number Average Molecular Weight(Mn)	16963
Weight Average Molecular Weight(Mw)	20407
Z Average Molecular Weight(Mz)	23809
Z+1 Average Molecular Weight(Mz1)	27585
Mw/Mn	1.20299
Mv/Mn	1.17662
Mz/Mw	1.16675

Detector A Ch1
[Average Molecular Weight(Total)]

Number Average Molecular Weight(Mn)	16963
Weight Average Molecular Weight(Mw)	20407
Z Average Molecular Weight(Mz)	23809
Z+1 Average Molecular Weight(Mz1)	27585
Mw/Mn	1.20299
Mv/Mn	1.17662
Mz/Mw	1.16675

Figure S145: GPC data for the ROP of *rac*-lactide (100 equiv) initiated by cationic Zr–O^{i}Pr^{+} species 5a. (toluene, 70 °C, 15 h, 93 % conversion to PLA

==== Shimadzu LCsolution GPC Analysis Report ====

Acquired by	: Admin
Sample Name	: ab311
Sample ID	: ab311
Vail#	:
Injection Volume	: 100 uL
Data Filename	: ab311.lcd
Method Filename	: Etalon PS 30.06.2017 8points.lcm
Batch Filename	:
Report Filename	: Report_template.lcr
Date Acquired	: 11/04/2018 11:27:48
Data Processed	: 11/04/2018 13:11:57

Chromatogram & Calibration Curve

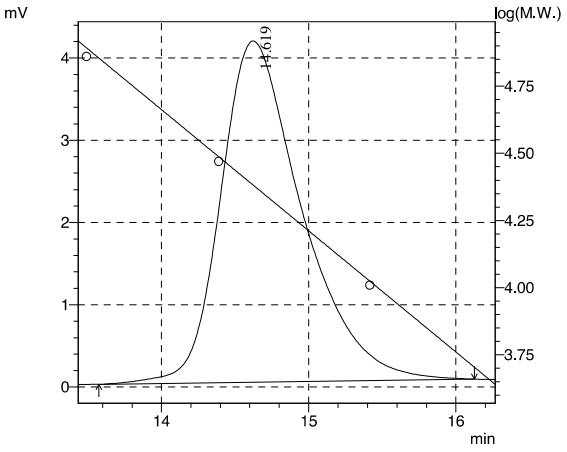

Molecular Weight Distribution Curve

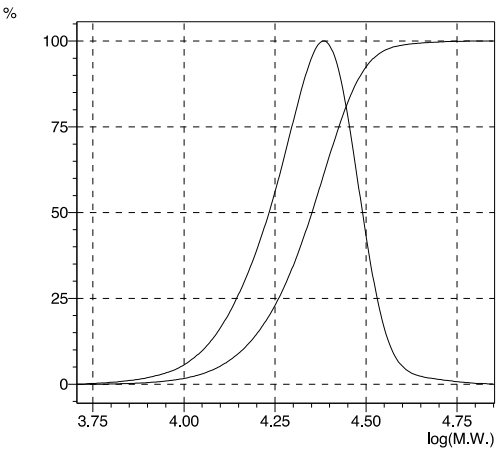

GPC Calculation Results

Peak#:1 (Detector A Ch1)
[Peak Information]

	Time(min)	Volume(mL)	Molecular Weight	Height
Start	13.575	13.575	71511	31
Top	14.619	14.619	24181	4151
End	16.125	16.125	5059	95

Area : 159664
Area% : 100.0000

[Average Molecular Weight]

Number Average Molecular Weight(Mn)	20685
Weight Average Molecular Weight(Mw)	22732
Z Average Molecular Weight(Mz)	24665
Z+1 Average Molecular Weight(Mz1)	26633
Mw/Mn	1.09895
Mv/Mn	1.08610
Mz/Mw	1.08505

Detector A Ch1
[Average Molecular Weight(Total)]

Number Average Molecular Weight(Mn)	20685
Weight Average Molecular Weight(Mw)	22732
Z Average Molecular Weight(Mz)	24665
Z+1 Average Molecular Weight(Mz1)	26633
Mw/Mn	1.09895
Mv/Mn	1.08610
Mz/Mw	1.08505

Figure S146: GPC data for the ROP of *rac*-lactide (100 equiv) initiated by cationic Zr–O^{i}Pr^{+} species 5a. (toluene, 90 °C, 14 h, 98 % conversion to PLA)

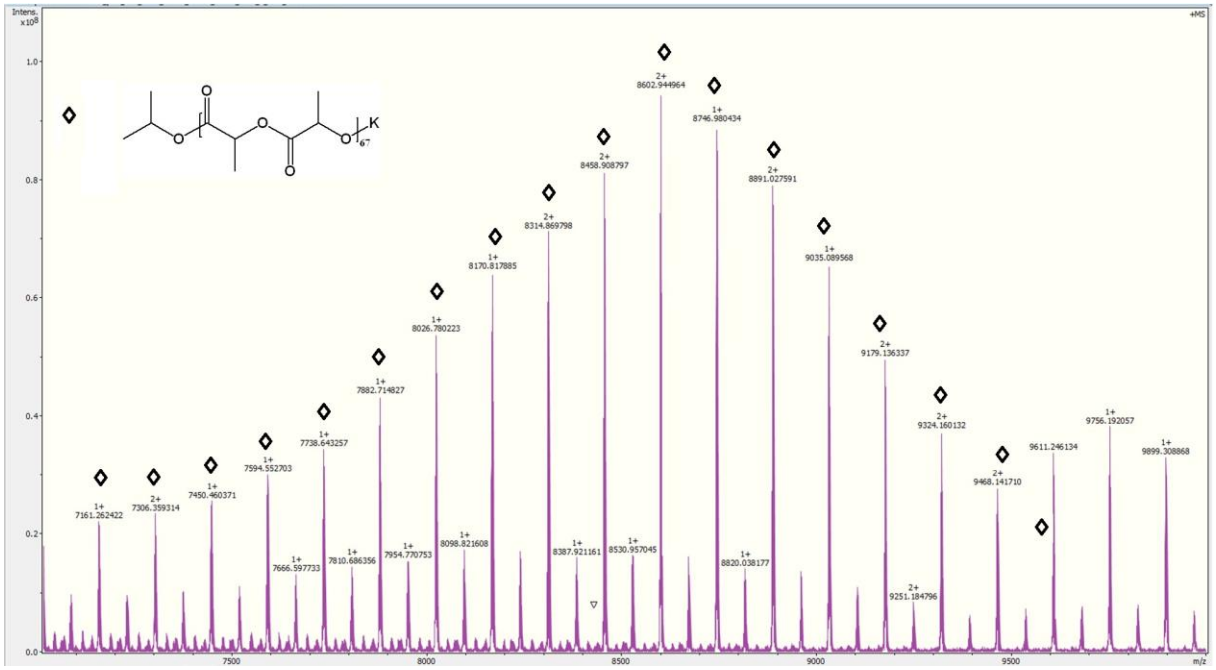

Figure S147: MALDI-TOF MS data of isolated PLA from the ROP of *rac*-lactide (100 equiv) initiated by cationic Zr–O^{i}Pr^{+} species 5a. (toluene, 70 °C, 15 h, 93 % conversion to PLA)

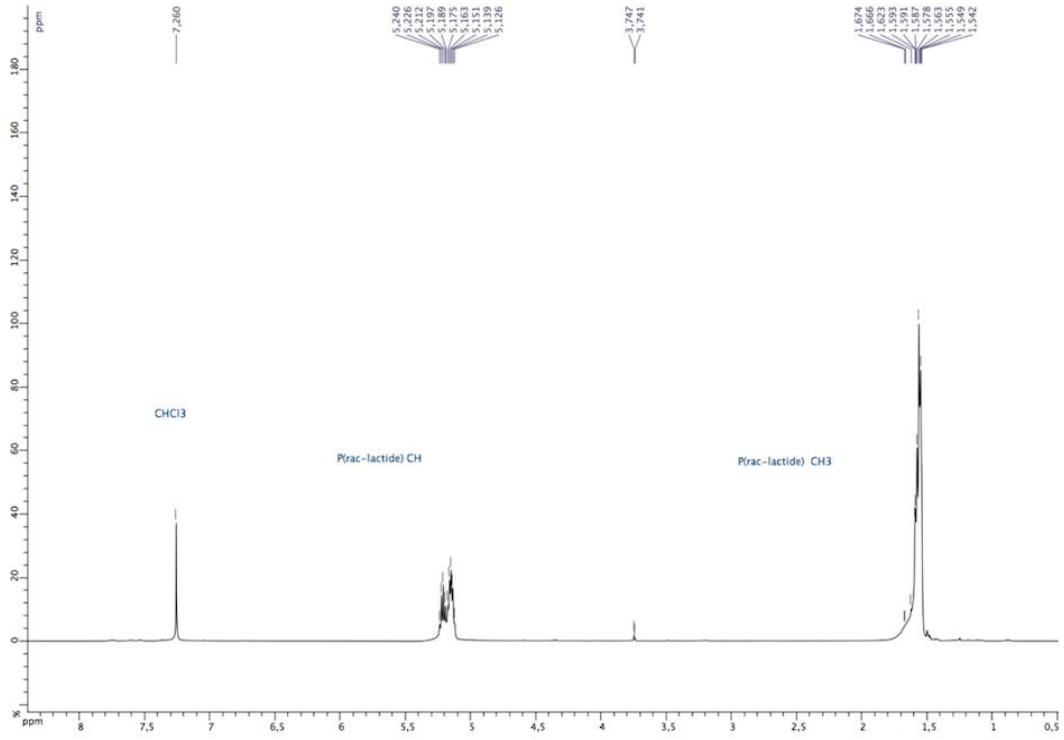

Figure S148: ^{1}H NMR ($CDCl_3$, 400 MHz) of isolated PLA from the ROP of *rac*-lactide (100 equiv) using Zr–lactate cation 6a as initiator (toluene, 90 °C, 14 h, 99 % conversion to PLA)

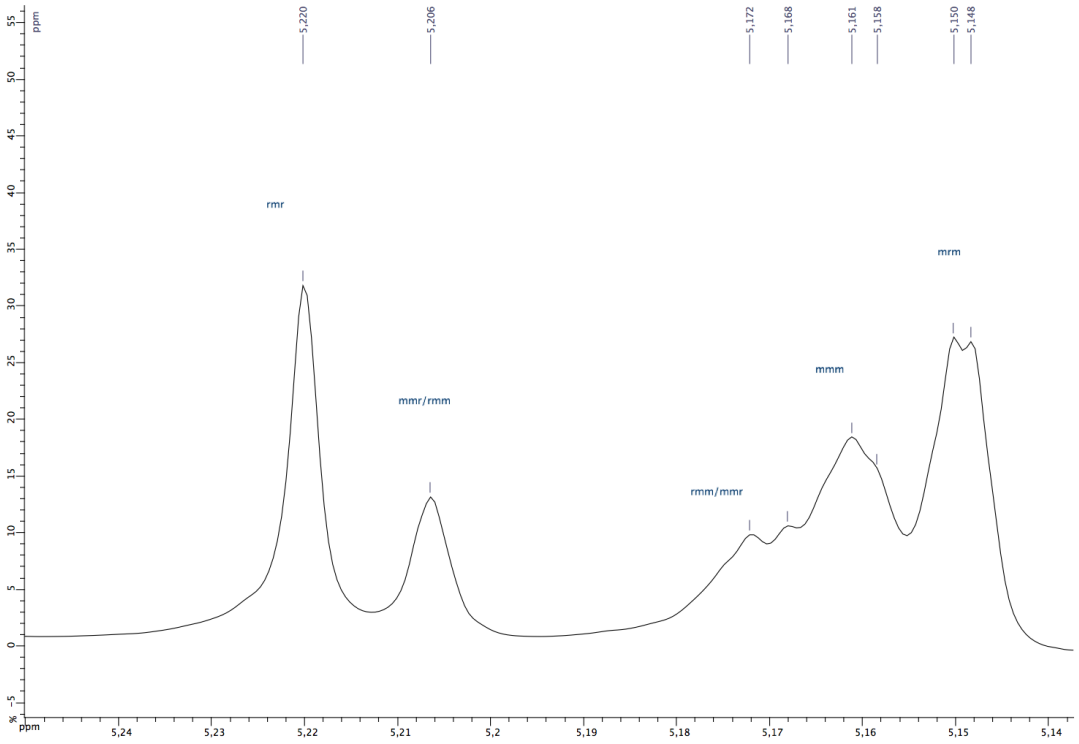

Figure S149: Homodecoupled ^{1}H NMR spectrum ($CDCl_3$, 500 MHz) of isolated PLA from the ROP of *rac*-lactide (100 equiv) using Zr–lactate cation 6a as initiator (toluene, 90 °C, 14 h, 99 % conversion to PLA). P_r = 0.71, as estimated according to literature.[3]

==== Shimadzu LCsolution GPC Analysis Report ====

Acquired by	: Admin
Sample Name	: ab312
Sample ID	: ab312
Vail#	:
Injection Volume	: 100 uL
Data Filename	: ab312.lcd
Method Filename	: gpc.lcm
Batch Filename	:
Report Filename	: Report_template.lcr
Date Acquired	: 11/04/2018 13:27:17
Data Processed	: 11/04/2018 13:57:19

Chromatogram & Calibration Curve

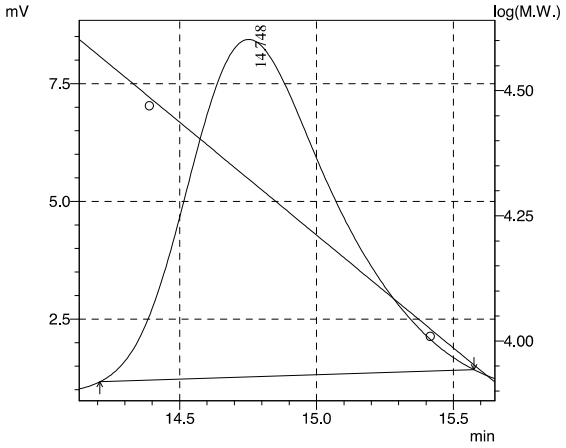

Molecular Weight Distribution Curve

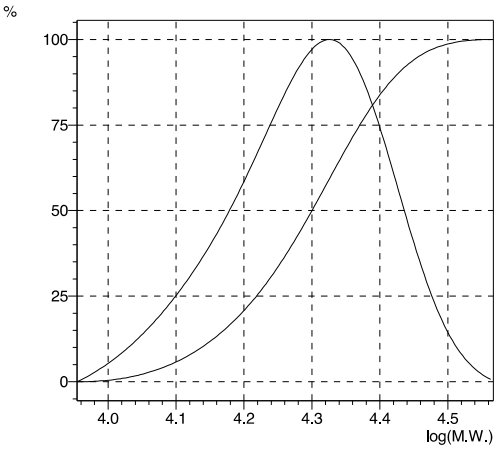

GPC Calculation Results

Peak#:1 (Detector A Ch1)
[Peak Information]

	Time(min)	Volume(mL)	Molecular Weight	Height
Start	14.208	14.208	37041	1171
Top	14.748	14.748	21138	7165
End	15.575	15.575	8957	1431

Area : 261567
Area% : 100.0000

[Average Molecular Weight]

Number Average Molecular Weight(Mn)	18968
Weight Average Molecular Weight(Mw)	20223
Z Average Molecular Weight(Mz)	21434
Z+1 Average Molecular Weight(Mz1)	22577
Mw/Mn	1.06617
Mv/Mn	1.05729
Mz/Mw	1.05987

Detector A Ch1
[Average Molecular Weight(Total)]

Number Average Molecular Weight(Mn)	18968
Weight Average Molecular Weight(Mw)	20223
Z Average Molecular Weight(Mz)	21434
Z+1 Average Molecular Weight(Mz1)	22577
Mw/Mn	1.06617
Mv/Mn	1.05729
Mz/Mw	1.05987

Figure S150: GPC data for the ROP of *rac*-lactide (100 equiv) initiated by Zr–lactate cation species 6a. (toluene, 90 °C, 14 h, 99 % conversion to PLA)

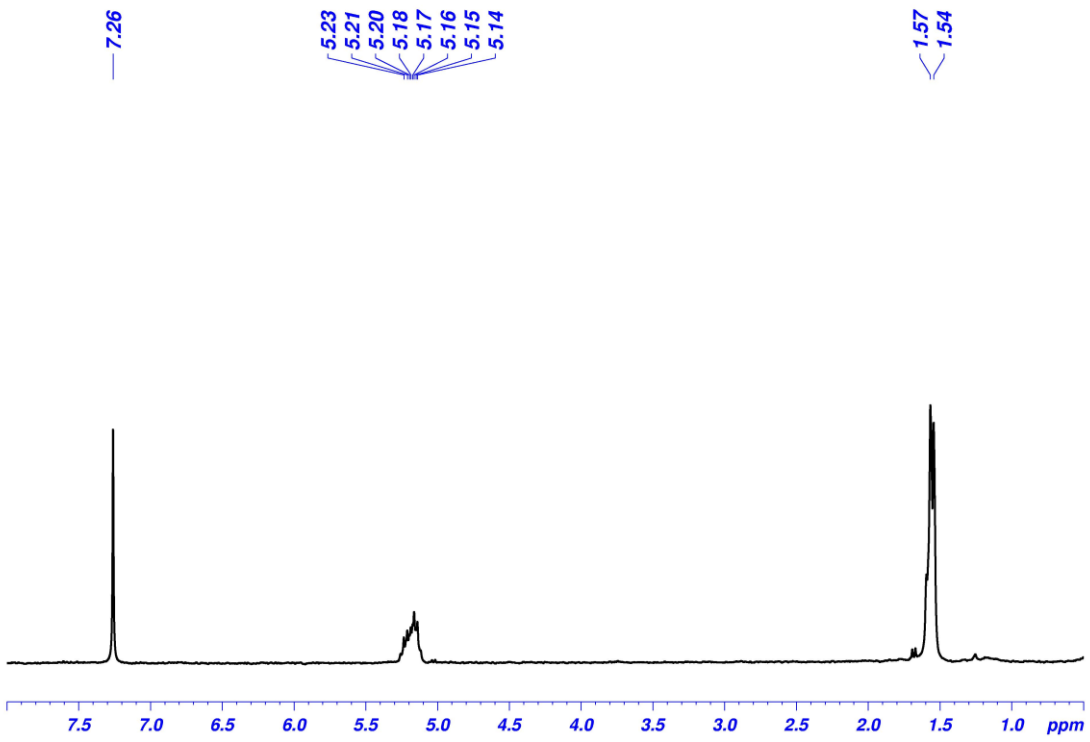

Figure S151: ^{1}H NMR ($CDCl_3$, 400 MHz) of isolated PLA from the ROP of *rac*-lactide (100 equiv) using Zr–lactate cation 6b as initiator (toluene, 70 °C, 15 h, 32 % conversion to PLA)

==== Shimadzu LCsolution GPC Analysis Report ====

Acquired by	: Admin
Sample Name	: rl 252_1
Sample ID	: rl 252_1
Vail#	:
Injection Volume	: 100 uL
Data Filename	: rl 252_1.lcd
Method Filename	: gpc.lcm
Batch Filename	:
Report Filename	: Report_template.lcr
Date Acquired	: 25/06/2017 15:33:15
Data Processed	: 25/06/2017 16:03:17

Chromatogram & Calibration Curve

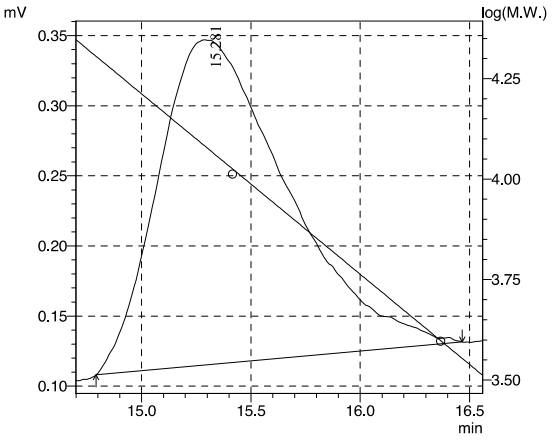

Molecular Weight Distribution Curve

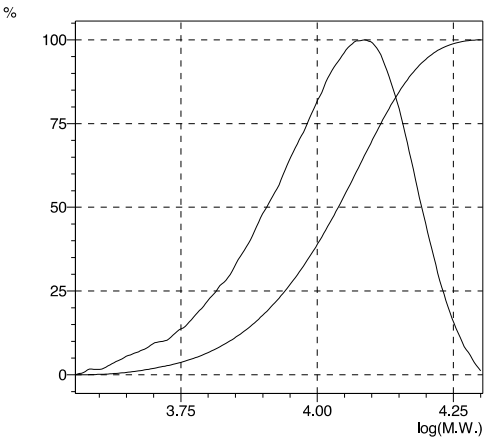

GPC Calculation Results

Peak#:1 (Detector A Ch1)
[Peak Information]

	Time(min)	Volume(mL)	Molecular Weight	Height
Start	14.792	14.792	20210	108
Top	15.281	15.281	12184	232
End	16.467	16.467	3581	132

Area : 9553
Area% : 100.0000

[Average Molecular Weight]

Number Average Molecular Weight(Mn)	10033
Weight Average Molecular Weight(Mw)	10989
Z Average Molecular Weight(Mz)	11843
Z+1 Average Molecular Weight(Mz1)	12594
Mw/Mn	1.09524
Mv/Mn	1.08305
Mz/Mw	1.07778

Detector A Ch1
[Average Molecular Weight(Total)]

Number Average Molecular Weight(Mn)	10033
Weight Average Molecular Weight(Mw)	10989
Z Average Molecular Weight(Mz)	11843
Z+1 Average Molecular Weight(Mz1)	12594
Mw/Mn	1.09524
Mv/Mn	1.08305
Mz/Mw	1.07778

Figure S152: GPC data for the ROP of *rac*-lactide (100 equiv) initiated by Zr–lactate cation species 6b (toluene, 90 °C, 15 h, 32 % conversion to PLA

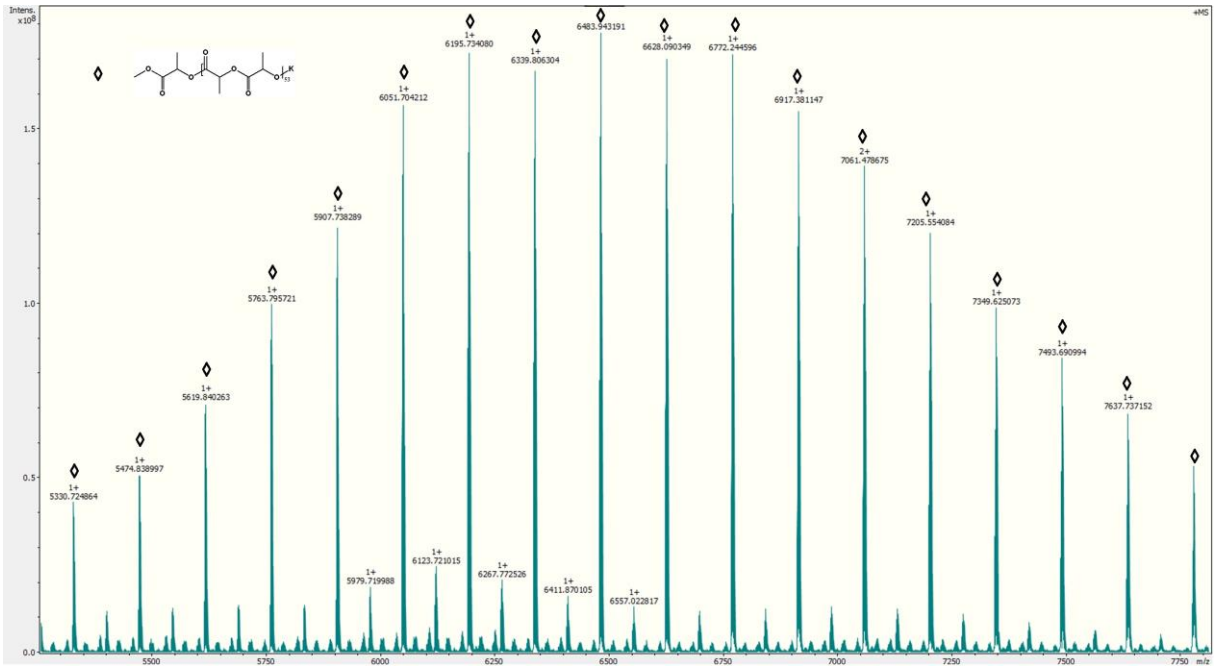

Figure S153: MALDI-TOF MS data of isolated PLA from the ROP of *rac*-lactide (100 equiv) initiated by cationic Zr–lactate cation species 6b. (toluene, 70 °C, 15 h, 32 % conversion to PLA)